

**A multilevel optimization framework for aircraft operations on near-airport communities  
Minimizing noise impact and fuel consumption**

Ho Huu, Vinh

**DOI**

[10.4233/uuid:6ed4204e-36b8-43d4-8541-3375df9312b8](https://doi.org/10.4233/uuid:6ed4204e-36b8-43d4-8541-3375df9312b8)

**Publication date**

2020

**Document Version**

Final published version

**Citation (APA)**

Ho Huu, V. (2020). *A multilevel optimization framework for aircraft operations on near-airport communities: Minimizing noise impact and fuel consumption*. [Dissertation (TU Delft), Delft University of Technology]. <https://doi.org/10.4233/uuid:6ed4204e-36b8-43d4-8541-3375df9312b8>

**Important note**

To cite this publication, please use the final published version (if applicable).  
Please check the document version above.

**Copyright**

Other than for strictly personal use, it is not permitted to download, forward or distribute the text or part of it, without the consent of the author(s) and/or copyright holder(s), unless the work is under an open content license such as Creative Commons.

**Takedown policy**

Please contact us and provide details if you believe this document breaches copyrights.  
We will remove access to the work immediately and investigate your claim.

**A MULTILEVEL OPTIMIZATION FRAMEWORK FOR  
AIRCRAFT OPERATIONS ON NEAR-AIRPORT  
COMMUNITIES**

MINIMIZING NOISE IMPACT AND FUEL CONSUMPTION



# **A MULTILEVEL OPTIMIZATION FRAMEWORK FOR AIRCRAFT OPERATIONS ON NEAR-AIRPORT COMMUNITIES**

MINIMIZING NOISE IMPACT AND FUEL CONSUMPTION

## **Dissertation**

for the purpose of obtaining the degree of doctor  
at Delft University of Technology  
by the authority of the Rector Magnificus, prof. dr. ir. T. H. J. J. van der Hagen,  
chair of the Board for Doctorates,  
to be defended publicly on  
Thursday 16 April 2020 at 15:00 o'clock

By

**Vinh HO-HUU**

Master of Engineering in Computational Science,  
Ho Chi Minh City University of Technology, Vietnam  
born in Binh Dinh, Vietnam.

This dissertation has been approved by the promotor.

Composition of the doctoral committee:

Rector Magnificus,	chairperson
Prof. dr. R. Curran,	Delft University of Technology, promotor
Dr. B. F. Santos,	Delft University of Technology, copromotor

*Independent members:*

Prof. dr. B. Van de Walle,	Delft University of Technology
Prof. dr. V. Gollnick,	Technische Universitat Hamburg, Germany
Prof. dr. T. Nguyen-Thoi,	Ton Duc Thang University, Vietnam
Assoc. prof. dr. X. Prats,	Universitat Politècnica de Catalunya, Spain
Prof. dr. J. M. Hoekstra,	Delft University of Technology, reserve member

*Other members:*

Dr. ir. S. Hartjes,	Dutch Ministry of Infrastructure and Water Management
---------------------	-------------------------------------------------------



*Keywords:* Aircraft noise, Airport noise, Community noise, Trajectory optimization, Route design, Aircraft allocation, Optimization framework

Copyright © 2019 by V. Ho-Huu

An electronic version of this dissertation is available at  
<http://repository.tudelft.nl/>.

# CONTENTS

<b>Summary</b>	<b>vii</b>
<b>Samenvatting</b>	<b>xi</b>
<b>Acknowledgements</b>	<b>xv</b>
<b>1 Introduction</b>	<b>1</b>
1.1 Research context . . . . .	1
1.2 Previous studies and research gaps . . . . .	3
1.2.1 Problem 1: Aircraft route design . . . . .	3
1.2.2 Problem 2: Flight allocation . . . . .	4
1.2.3 Problem 3: Route design and flight allocation in a linked manner . . . . .	5
1.3 Main aim and research objectives . . . . .	6
1.4 Research approach and thesis outline . . . . .	6
<b>2 Development of optimization methods</b>	<b>9</b>
2.1 Problem statement . . . . .	10
2.2 Contributions . . . . .	10
<b>3 Aircraft route design</b>	<b>41</b>
3.1 Problem statement . . . . .	42
3.2 Contributions . . . . .	42
<b>4 Flight allocation</b>	<b>77</b>
4.1 Problem statement . . . . .	78
4.2 Contributions . . . . .	78
<b>5 Linking aircraft route design and flight allocation</b>	<b>109</b>
5.1 Problem statement . . . . .	110
5.2 Contributions . . . . .	110
<b>6 A multilevel optimization framework with integrated operational requirements</b>	<b>127</b>
6.1 Problem statement . . . . .	128
6.2 Contributions . . . . .	128
<b>7 Conclusions</b>	<b>165</b>
7.1 Review of objectives . . . . .	165
7.2 Research novelty and contribution . . . . .	167
7.3 Limitations and recommendations for future research . . . . .	168

<b>References</b>	<b>171</b>
<b>Curriculum Vitæ</b>	<b>175</b>
<b>List of Publications</b>	<b>177</b>

# SUMMARY

With a significant impact on the development of the global economy and society, air transport is predicted to rapidly grow in the coming years. Unfortunately, while delivering positive global economic and social benefits, air transport has also generated an adverse influence on the environment, especially on the quality of life of communities around airports. Air transport is the main cause of noise nuisance in the vicinity of airports, which has been linked to various human health effects, such as cardiovascular diseases, sleep disturbance, hearing loss, and communication interference.

Over the years, significant efforts have been put into finding suitable options to support the continued growth of air transport, such as the design of optimal routes and the optimal allocation of flights to specific routes and runways. However, research on these topics is typically conducted separately, and hence studies that consider the link between these topics are still lacking. In an attempt to fulfill the mentioned research gap, an optimization framework has been developed in this thesis. The developed framework aims to exploit the advantages of considering the route design and flight allocation optimization problems in a linked manner to minimize aircraft noise impact and fuel consumption simultaneously. The outcome of the research is a framework that is able to determine suitable routes for given standard departure instrument (SID) routes, and the optimal number of flights of each aircraft type that should be assigned to these routes, while taking operational constraints related to aircraft sequencing and separation requirements into account.

In order to reach this goal successfully, the work in this research has been broken down into smaller steps. Due to the simultaneous consideration of two objectives, i.e., noise impact and fuel consumption, research to identify appropriate optimization approaches is carried out first in **Chapter 2**. Although different approaches have been proposed to deal with multi-objective optimization problems in previous studies, the research indicated that the multi-objective evolutionary algorithm based on decomposition (MOEA/D) is an effective method. Thanks to decomposing a multi-objective optimization problem into a set of single-objective optimization problems and searching their optimal solutions simultaneously, the MOEA/D method is able to deal with complicated multi-objective optimization problems and is able to provide optimal solutions with a fast convergence rate. In this chapter, besides studies to understand the searching principle of MOEA/D, some improvements on MOEA/D have also been carried out, which can help to improve the quality of Pareto solutions and the computational cost.

Secondly, research into the route design problem and the application of the MOEA/D algorithm to this type of problems are presented in **Chapter 3**. By employing the advantages of the MOEA/D algorithm and the characteristic of the route design problem, a new setting rule in the optimization procedure is also introduced. Several case studies at Amsterdam Airport Schiphol have been used to evaluate the performance of the proposed approach. The obtained results reveal that the proposed approach can gener-

ate better options for routes with a lower computational cost compared with alternative methods.

In addition to the route design problem, research into the allocation of flight movements is presented in **Chapter 4**. In this chapter, a new air traffic assignment model is proposed. Unlike models developed in previous studies, where optimization problems are typically formulated as single-objective nonlinear programming optimization problems, the model developed in this study considers each flight operation as a single design variable and optimizes two potentially conflicting objectives (i.e., noise impact and fuel consumption) concurrently. The model is applied to a case study at Belgrade Airport in Serbia. The obtained solutions indicate that the proposed model can provide optimal allocation of flights that can effectively balance between the two objectives at a modest computational cost.

After developing a good understanding of both the route design and flight allocation problems, the development of an optimization framework that considers both problems in a linked manner is presented in **Chapter 5**. The developed framework features two consecutive steps. In the first step, multi-objective trajectory optimization is used to compute and store a set of trajectories for each given route. These obtained sets then serve as input for the optimization problem in the second step. In this second step, the selection of routes from the set of optimal routes and the optimal allocation of flights to these routes are conducted simultaneously. To validate the proposed framework, an analysis involving an integrated (one-step) approach, in which both trajectory optimization and flight allocation are formulated as a single optimization problem, is also conducted. A comparison of both approaches applied to a small-scale problem is then performed. The obtained results show that the proposed two-step framework is effective and reliable. The comparison also indicates that the proposed two-step approach is more flexible to adapt to the changes in the number of flights when a reallocation of flights is demanded or new routes and runways are considered.

Finally, operational constraints related to aircraft sequencing and separation requirements are studied and integrated into the model developed in the previous chapter. Then, a completed multilevel optimization framework is proposed and presented in **Chapter 6**. To handle the operational constraints, a runway assignment model, a conflict detection algorithm, and a rerouting technique have been developed and integrated into the framework. The proposed framework is applied to a realistic case study at Amsterdam Airport Schiphol in the Netherlands, in which 599 departure flights and 13 different SID routes are considered. The optimization results show that the proposed model is reliable and effective. From the obtained Pareto front, a selected representative solution can offer a reduction in the number of people annoyed of up to 21%, and a reduction in fuel consumption of 8% relative to the reference case solution.

From the research carried out, it is emphatically concluded that the consideration of both types of problems (i.e., route design and flight allocation) in a linked manner may bring benefits to the management of aircraft and airport operations. Due to the consideration of the operational constraints, the developed framework is not only able to offer proper solutions with less noise impact and fuel burn, but can also bring them relatively close to real operations. Although many research issues have been addressed along the course of the thesis, there are still certain limitations. Firstly, the developed framework

does not take weather conditions into account, and it relies on a single specific noise criterion (i.e., noise annoyance). These concerns should be considered in future work. Moreover, since the research mainly focuses on departure operations, the extension of the framework to arrival operations and the combination of arrival and departure operations could be interesting research topics for future work.



# SAMENVATTING

Met een aanzienlijke impact op de ontwikkeling van de wereldeconomie en -maatschappij wordt voorspeld dat het luchtverkeer de komende jaren snel zal groeien. Helaas heeft het luchtverkeer, hoewel het positieve wereldwijde economische en sociale voordelen oplevert, ook een negatieve invloed op het milieu, met name op de kwaliteit van het leven van gemeenschappen rond luchthavens. Luchtverkeer is de belangrijkste oorzaak van geluidsoverlast in de nabijheid van luchthavens, en wordt in verband staat gebracht met verschillende effecten op de gezondheid van de mens, zoals hart- en vaatziekten, slaapstoornissen, gehoorverlies en communicatie-interferentie.

In de loop der jaren zijn aanzienlijke inspanningen geleverd om geschikte opties te vinden om de voortdurende groei van het luchtverkeer te ondersteunen, zoals het ontwerp van optimale routes en de optimale toewijzing van vluchten aan specifieke routes en start- en landingsbanen. Onderzoek naar deze onderwerpen wordt echter meestal afzonderlijk uitgevoerd, en er ontbreekt nog steeds onderzoek naar het verband tussen deze onderwerpen. In een poging om de genoemde onderzoekskloof te dichten, is in dit proefschrift een optimalisatieframework ontwikkeld. Het ontwikkelde framework wil de voordelen benutten van het overwegen van het routeontwerp en tegelijkertijd problemen op het gebied van allocatieoptimalisatie bestrijden om de impact van vliegtuiggeluid en brandstofverbruik allebei te minimaliseren. De uitkomst van het onderzoek is een framework dat in staat is om geschikte routes te bepalen voor bepaalde standard departure instrument (SID) routes, en het optimale aantal vluchten van elk vliegtuigtype dat aan deze routes moet worden toegewezen, terwijl operationele beperkingen met betrekking tot volgorde en minimale scheidingsafstanden van vliegtuigen worden meegenomen.

Om dit doel met succes te bereiken, is het werk in dit onderzoek opgedeeld in kleinere stappen. Vanwege de gelijktijdige afweging van twee doelstellingen, namelijk geluidsbelasting en brandstofverbruik, wordt allereerst onderzoek om geschikte optimalisatiebenaderingen te identificeren in hoofdstuk 2 beschreven. Hoewel in eerdere studies verschillende benaderingen zijn voorgesteld om multi-objective optimalisatieproblemen aan te pakken, wees onderzoek uit dat het multi-objective evolutionaire algoritme op basis van ontleding (MOEA/D) een effectieve methode is. Dankzij het ontbinden van een multi-objective optimalisatieprobleem in een set van single-objective optimalisatieproblemen en het gelijktijdig zoeken naar hun optimale oplossingen, is de MOEA/D-methode in staat om ingewikkelde multi-objective optimalisatieproblemen aan te pakken en is het in staat optimale oplossingen te bieden met een snelle convergentie. In dit hoofdstuk zijn naast onderzoeken om het zoekprincipe van MOEA/D te begrijpen, ook enkele verbeteringen aan MOEA/D voorgesteld, die kunnen helpen de kwaliteit van Pareto-oplossingen en de rekenkosten te verbeteren.

Ten tweede wordt onderzoek naar het routeontwerpprobleem en de toepassing van het MOEA/D-algoritme op dit soort problemen gepresenteerd in hoofdstuk 3. Door ge-

bruik te maken van de voordelen van het MOEA/D-algoritme en de karakteristieken van het routeontwerpprobleem, wordt er een nieuwe instellingsregel in de optimalisatieprocedure geïntroduceerd. Verschillende case studies op Amsterdam Airport Schiphol zijn gebruikt om de prestaties van de voorgestelde aanpak te evalueren. De verkregen resultaten laten zien dat de voorgestelde aanpak betere opties kan genereren voor routes, met lagere rekenkosten in vergelijking met alternatieve methoden.

Naast het routeontwerpprobleem van hoofdstuk 3, wordt onderzoek naar de toewijzing van vliegbewegingen gepresenteerd in hoofdstuk 4. In dit hoofdstuk wordt een nieuw toewijzingsmodel voor luchtverkeer voorgesteld. In tegenstelling tot modellen die in eerdere studies zijn ontwikkeld, waar optimalisatieproblemen meestal worden geformuleerd als niet-lineaire programmeringsoptimalisatieproblemen met één doelstelling, beschouwt het model dat in deze studie is ontwikkeld elke vluchtuitvoering als één ontwerpvariabele en optimaliseert het twee potentieel conflicterende doelstellingen (geluidseffect en brandstofconsumptie) tegelijkertijd. Het model wordt toegepast op een case study op Belgrado Airport in Servië. De verkregen oplossingen geven aan dat het voorgestelde model een optimale toewijzing van vluchten kan bieden die effectief tegen een bescheiden rekenkosten tussen de twee doelstellingen kan balanceren.

Na het ontwikkelen van een goed begrip van zowel het routeontwerp als de vluchttoewijzingsproblemen, wordt de ontwikkeling van een optimalisatieframework dat beide problemen op een gekoppelde manier beschouwt, gepresenteerd in hoofdstuk 5. Het ontwikkelde framework bestaat uit twee opeenvolgende stappen. In de eerste stap wordt multi-objective trajectoptimalisatie gebruikt om een reeks trajecten voor elke gegeven route te berekenen en op te slaan. Deze verkregen sets dienen dan als input voor het optimalisatieprobleem in de tweede stap. In deze tweede stap wordt de selectie van routes uit de set van optimale routes en de optimale toewijzing van vluchten aan deze routes tegelijkertijd uitgevoerd. Om het voorgestelde framework te valideren, wordt een analyse uitgevoerd met een geïntegreerde (eenstaps) aanpak, waarbij zowel trajectoptimalisatie als vluchttoewijzing worden geformuleerd als één optimalisatieprobleem. Een vergelijking van beide benaderingen toegepast op een kleinschalig probleem wordt vervolgens uitgevoerd. De verkregen resultaten tonen aan dat het voorgestelde tweestapsframework effectief en betrouwbaar is. De vergelijking geeft ook aan dat de voorgestelde tweestapsbenadering flexibeler is om zich aan te passen aan veranderingen in het aantal vluchten wanneer een nieuwe toewijzing van vluchten wordt geëist, of nieuwe routes en start- en landingsbanen worden overwogen.

Ten slotte worden operationele beperkingen met betrekking tot volgorde van en scheidingseisen voor vliegtuigen bestudeerd en geïntegreerd in het model dat in het vorige hoofdstuk is ontwikkeld. Vervolgens wordt een compleet multilevel optimalisatieframework voorgesteld en gepresenteerd in hoofdstuk 6. Om de operationele beperkingen aan te pakken, zijn een baantoewijzingsmodel, een conflictdetectie-algoritme en een herrouteringstechniek ontwikkeld en geïntegreerd in het framework. Het voorgestelde framework wordt toegepast op een realistische case study op Amsterdam Airport Schiphol in Nederland, waarbij 599 vertrekvluchten en 13 verschillende SID-routes worden overwogen. De optimalisatieresultaten tonen aan dat het voorgestelde model betrouwbaar en effectief is. Vanuit het verkregen Pareto-front kan een geselecteerde representatieve oplossing een vermindering van het aantal geïrriteerde personen tot 21% en een vermin-

dering van het brandstofverbruik van 8% ten opzichte van de referentiecasi-oplossing worden bewerkstelligd.

Uit het uitgevoerde onderzoek wordt nadrukkelijk geconcludeerd dat de gekoppelde aanpak van beide problemen (routeontwerp en vluchtoewijzing) voordelen kan opleveren voor het management van vliegtuigen en luchthavenactiviteiten. Door operationele beperkingen in overweging te nemen, is het ontwikkelde framework niet alleen in staat om goede oplossingen te bieden met minder geluidsimpact en brandstofverbranding, maar kan het ook relatief dichtbij echte operaties komen. Hoewel veel onderzoeksproblemen in de loop van het proefschrift zijn aangepakt, zijn er nog beperkingen. Ten eerste houdt het ontwikkelde framework geen rekening met weersomstandigheden en vertrouwt het op één specifiek geluidscriterium (namelijk geluidsoverlast). Met deze problemen moet in toekomstig onderzoek rekening worden gehouden. Aangezien het onderzoek vooral gericht is op vertrekoperaties, kan de uitbreiding van het framework tot aankomstoperaties en de combinatie van aankomst- en vertrekoperaties interessant zijn voor toekomstig onderzoek.



# ACKNOWLEDGEMENTS

Growing up in a poor countryside with a farming family background, I was convinced that without self-effort, I could not have reached the level I am now. Although I can go wherever I want, without the right guidance and support, my desired destination could remain very far away! Therefore, reaching this point would not have been easy for me without the guidance and support from people to whom I would like to express my appreciation and gratitude.

First and foremost, I would like to express my deep gratitude to my daily supervisor, Dr. ir. **Sander Hartjes**. To Sander, thank you so much for continuously supporting me not only in my research but also in my personal life. You have been a great supervisor with helpful feedback, challenging questions, full of encouragements, and a solid technical background. I really appreciate your willingness to help me out whenever I need.

Together with Sander, I would like to thank my promoter, Prof. dr. **Richard Curran (Ricky)**, for accepting me as a PhD candidate and giving me a great opportunity to carry out research at the Air Transport and Operations (ATO) group. I still remember the first day I had an interview with you, where you have inspired me with friendly talks and questions, and your football question has been one of the memorable moments in my life.

I would like to give special thanks to Dr. ir. **Hendrikus G. Visser (Dries)** for his patient guidance and genuine support during my PhD time at ATO. Although you had no obligation to supervise me, you were always available and said yes whenever I needed. Thank you for your time and effort to give me ideas, correct my opinions, review my papers, check English, and finally and especially provide "rocket" feedback. Your knowledge and enthusiasm have been a great addition to the success of my PhD thesis.

I would like to acknowledge my previous supervisor, Prof. dr. **Trung Nguyen-Thoi** who has influenced my life after my Bachelor graduation. It has been a great honour for me to have you as a teacher. You have taught me a lot from work to life, from how to live positively and actively to how to do research. Your help and support will be carried with me wherever I go. Great appreciation also goes to anh **Lam Phat Thuan** who has helped me out both in education and personal life during the last year of my Bachelor. Advice and support given by anh **Phung Van Phuc** are also highly appreciated.

I would like to thank anh **Le The Hai** and anh **Ta Quoc Bao** in motivating and encouraging me to go abroad for doing my PhD. Particular thanks to anh Hai for helping me from the PhD application process until obtaining a PhD position at TUDelft. You are always the first person who motivates me to overcome from challenge upon challenge during my PhD period with a simple quote "*keep striving and dedicating*".

I would like to thank my colleagues at the ATO group for sharing their knowledge, resources and funny moments. I am particularly grateful for the help and support given by **Stef** during my time at ATO and Delft. You have been one of my closest friends in Delft. My thanks also go to Dr. **Emir Ganic** from University of Belgrade for his friendship

and effective collaboration. To Emir, Thank you for accompanying me during my trip to Serbia.

Many thanks go to my friends from the Vietnamese community at Delft, specially **VDFC** and **VCiD thu nho**. Thank you all for making me and my family feel at home. I would like to thank anh **Hung** and anh **Hieu** for building up a strong football team at Delft, where I can play football and enjoy fun time after hard working hours. I wish to thank the family of **Minh-Vinh-Dau** for helping my tiny family from the time Cherry was growing in her mom's belly until the day she was born. Thanks also go to the family of **Linh-Thu-BinhPhu-BinhMinh** for sharing fun talks and lovely food almost every week-end. Support and advice given by chi **Hoang Anh**, anh **Nghi**, and **Chi** are greatly appreciated. For those who are not listed here, your help and support are also acknowledged and highly appreciated.

Deeply from my heart, I would like to thank my parents and family for their unconditional love, support, and continuous encouragement. I would like to express my deepest gratitude to my deceased father, who has always believed in me and suffered from my unknowledgeable game when I was a child. I wish you can see who I am and where I am now, and I can tell you that "*Daddy, no one can despise and ridicule our family anymore!*"

Last but definitely not least, I would like to thank my wife **Nguyen Thi Diem** and my daughter **Cherry** for their boundless love that have been the strongest motivation for me to reach this point successfully. **Diem** and **Cherry**, you both are always the biggest part of my life! **Diem**, you are a wonderful mom and wife! **Cherry**, you will always be an angel in my life!

**Vinh Ho-Huu**

Delft, 28 October, 2019

# 1

## INTRODUCTION

### 1.1. RESEARCH CONTEXT

AVIATION has been playing an irreplaceable role in the development of global economy and society. Air transport carried nearly 4.4 billion passengers, created over 65 million jobs worldwide, and contributed roughly \$704.4 billion to the world's gross domestic product (GDP) in 2018<sup>1</sup>. As a consequence of its benefits, the aviation industry is predicted to rapidly grow in the coming decades<sup>2</sup>.

However, while delivering positive global economic and social benefits, the aviation industry has also generated an adverse influence on the environment. Air transport produces around 2% of global human-made carbon dioxide emissions (CO<sub>2</sub>) and is responsible for 12% of CO<sub>2</sub> emissions from all transport sources<sup>1</sup>. Air transport is also the main cause of noise nuisance which significantly impacts the quality of life of communities in the vicinity of airports<sup>3</sup>. Aircraft noise annoyance has been linked to various human health effects such as cardiovascular diseases, sleep disturbance, hearing loss, and communication interference [1, 2]. The continued growth of air transport has led to the aircraft noise exposure of millions of Europeans<sup>3</sup>. Consequently, aircraft noise has been well recognized as one of the most significant factors leading to restrictions on the expansion of flight and airport operations [2].

In an attempt to support the sustainable development of the aviation industry, a series of research initiatives have been launched in recent years. For example, Clean Sky<sup>4</sup>, one of the largest European research programs, has been established since 2008 with the aim of reducing CO<sub>2</sub>, gas emissions and noise levels produced by aircraft; and the Asia and South Pacific Initiative to Reduce Emissions (ASPIRE)<sup>5</sup> was formed in 2008 and aimed to develop operational procedures that reduce the environmental footprint of all phases of flight, from terminal to terminal. Apart from these research initiatives, various

<sup>1</sup><https://www.atag.org/facts-figures.html>

<sup>2</sup>[https://aviationbenefits.org/media/166344/abbb18\\_full-report\\_web.pdf](https://aviationbenefits.org/media/166344/abbb18_full-report_web.pdf)

<sup>3</sup><https://www.easa.europa.eu/eaer/topics/adapting-changing-climate/noise>

<sup>4</sup><http://www.cleansky.eu/no-back>

<sup>5</sup><http://www.aspire-green.com/>

strategies have also been proposed and are currently being implemented, such as setting new rules and regulations (e.g., limiting aircraft operations at airports during the night), developing new engine/aircraft models and renewable fuels, and varying operational procedures at airports (e.g., applying noise abatement departure and arrival procedures) [3]. While new technologies and sustainable fuels may provide a significant reduction in environmental impact, they require much effort and time to develop and implement. In contrast, despite having smaller mitigation potential, operational changes can be carried out in the short-term period [3]. From a practical implementation and economic point of view, it can be observed that the variation of aircraft/airport operational procedures emerges as a reasonable option that can result in short term improvements and could prove less costly in comparison with the other options. As promising options in this category, the design of optimal routes and the assignment of aircraft (flights) to specific runways and routes with the aim of minimizing aircraft noise impact and fuel consumption have been well recognized and have shown encouraging results over the years [4, 5].

Although a significant effort has been put into finding suitable options to support the continued growth of air transport, there is still a lack of studies that consider different aspects of flight and airport operations in a combined manner. Particularly, research on the design of optimal routes has identified a significant potential reduction in noise impact and fuel burn, as reported in [5–18]. However, these studies typically considered only one standard route at a time, and its interaction with other routes was ignored. Therefore, from an operational perspective, the obtained results might be rather difficult to implement when other factors, such as airspace capacity or aircraft separation, are not taken into account. Similarly, research on the allocation of flight to current runways and routes has also significantly contributed to the reduction of aircraft noise impact and fuel consumption, as reported in [19–24]. These studies, however, only considered existing routes instead of optimized routes. Thus, the potential noise and fuel reduction benefits were not fully explored. Moreover, these studies relied on the assumption that the acquired solutions satisfy operational requirements, such as aircraft sequencing and separation requirements. As a result, the true influence of optimal allocation solutions to these issues has not yet been adequately investigated.

From the above considerations, it is realized that solutions that properly address the aforementioned research gaps of both types of problems (i.e., route design and flight allocation) are very important. Such solutions are not only able to deal with aircraft noise concerns and fuel burn, but also are capable of handling operations-related issues. Unfortunately, research to develop frameworks that concurrently consider these types of problems and are able to provide such kinds of solutions is still missing. In order to aid the continued growth of air transport sustainably, the need for developing such a framework becomes more and more crucial. To address this urgent need, an optimization framework that can efficiently support the operations of aircraft and airports in terms of noise impact and fuel consumption is developed in this study. The developed framework will be able to effectively address the existing research gap, which is to formulate and solve the optimization problems of route design and flight allocation in a linked manner, while taking operational constraints related to aircraft sequencing and separation into account.

## 1.2. PREVIOUS STUDIES AND RESEARCH GAPS

This section provides a brief overview of previous research on three problems of route design, flight allocation, and the integration between them. These problems are illustrated in Fig. 1.1, in which questions 1 and 2 constitute the main research questions relating to the first two problems, respectively, whereas the consideration of all 3 questions in a linked manner is the main research question relating to the third problem. The review is, therefore, organized into three different categories corresponding to the three distinct problems. For each category, limitations and research gaps are identified.

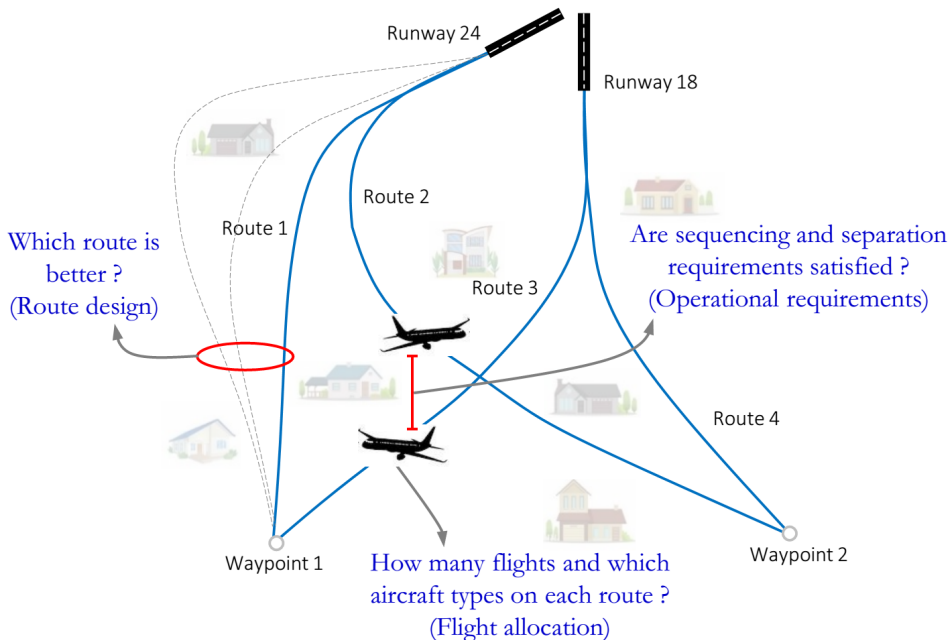


Figure 1.1: Illustration of research problems considered in the thesis

### 1.2.1. PROBLEM 1: AIRCRAFT ROUTE DESIGN

Over the years, significant attention has been given to the problem of designing environmentally friendly aircraft routes, and various approaches have been proposed. Visser and Wijnen [15, 16] developed an optimization tool called NOISHHH – which is a combination of a noise model, an emissions inventory model, a geographic information system, and a dynamic trajectory optimization algorithm – to generate environmentally optimal departure and arrival trajectories. This tool was later also adapted to optimize noise abatement routes based on area navigation [6, 9, 25]. Prats et al. [10, 11] employed a lexicographic optimization technique to deal with aircraft departure trajectories for minimizing noise annoyance. Khardi and Abdallah [26] studied a comparison of direct and indirect methods in solving an ordinary differential equation system (ODEs) to opti-

mize aircraft flight paths for noise reduction. Matthes et al. [27] presented a concept for multi-criteria environmental assessment of aircraft trajectories, where the mathematical framework for environmental assessment and optimization of aircraft trajectories were developed.

Despite being quite efficient in searching optimal trajectories, the techniques mentioned in the above studies belong to the group of gradient-based methods, which contain certain limitations in solving optimization problems. In particular, due to using gradient information for searching an optimal solution, these methods are often only suitable for optimization problems whose objective and constraint functions are differentiable, and whose decision variables are continuous. Moreover, their solutions are often trapped in local optima if the considered problems are nonlinear and contain more than one local optimal solution.

As an alternative to gradient-based algorithms, different gradient-free optimization techniques have also been applied in recent years. Torres et al. [13] proposed a non-gradient optimizer, namely multi-objective mesh adaptive direct search (multi-MADS), to synthesize optimal departure trajectories for NO<sub>x</sub> emissions and noise at a single measurement point. Hartjes and Visser [8] applied an elitist non-dominated sorting genetic algorithm (NSGA-II) combined with a novel trajectory parameterization technique for the optimal design of departure trajectories to minimize environmental impact. This method was then also applied by Zhang et al. [18] and Kim et al. [28] to optimize departure routes at Manchester airport and Gimpo international airport, respectively. McEntegart et al. [29] proposed a combination of inverse dynamics in a virtual domain method and a multi-objective differential evolution to design optimal departure routes for a case study at London Luton Airport.

In terms of the utilization of optimization techniques, from the results reported in [8, 13, 18, 28, 29], it is indicated that the use of non-gradient multi-objective optimization methods is a potential approach for designing optimal routes. These methods do not only readily overcome the limitations of gradient-based methods in dealing with discontinuous problems and integer or/and discrete design variables, but also can identify a set of non-dominated optimal solutions and hence bring more choices for policymakers and authorities. Unfortunately, the computational cost for solving an optimization problem using these methods is still quite high, which has limited their application to larger problems. Due to the searching mechanism with multiple design points at the same time, these methods require many evaluations of the objective and constraint functions, which are time-consuming. This restriction again has motivated researchers to develop computationally efficient approaches that can effectively balance expected results and computation cost, and hence has been one of the focuses of the thesis.

### 1.2.2. PROBLEM 2: FLIGHT ALLOCATION

Besides the attempts to design environmentally friendly routes, the allocation of aircraft to specific routes and runways has also attracted significant attention, and several approaches have been proposed over the years. Frair [19] developed an integer optimization model to find the optimal allocation of flight among available approach and departure routes with the aim of minimizing community annoyance. Kuiper et al. [22] developed a linear programming model to maximize the number of aircraft movements

operating at an airport within an allotted annual noise budget by optimally assigning annual flights to available routes and runways. Kim et al. [30] presented a mixed integer programming model to minimize airport surface emissions by concurrently allocating aircraft among runways and scheduling departure and arrival flights on these runways. Zachary et al. [20] formulated and solved an optimization problem to minimize noise and pollutant emissions by simultaneously considering operational procedures, arrival and departure routes, and fleet combination. In this research, a multi-objective nonlinear optimization problem was formulated, and linearization and weighting approaches were employed to solve the formulated problem. Using a similar approach, Zachary et al. [21] also evaluated the potential reduction in operational cost that could be gained by optimal solutions. Ganic et al. [23] developed an integer optimization model to allocate flights among available departure and arrival routes with the aim of reducing the population noise exposure while taking into account daily migrating populations.

Although significant achievements in terms of noise and fuel reduction have been reported, there are still certain gaps in this type of study. Specifically, the above-mentioned studies typically considered only one objective at a time (i.e., either fuel consumption or noise impact), while there is a potential conflict between these two objectives. Also, optimization problems were formulated as nonlinear programming models, which contain a large number of decision variables. Though such a model can be extended to multi-objective problems by applying weighting approaches [20, 21], it is normally difficult to obtain solutions in which conflicting objectives are well balanced. Furthermore, these studies relied on the assumption that the obtained optimal solutions satisfy all operational requirements, such as aircraft sequencing and separation. However, it can be expected that, in reality, not all these requirements are met. Therefore, the actual influence of optimal allocation solutions on operational requirements is not yet adequately studied. In addition, since these models only considered standard routes instead of optimized routes, the benefits of noise and fuel reduction were not effectively explored.

### 1.2.3. PROBLEM 3: ROUTE DESIGN AND FLIGHT ALLOCATION IN A LINKED MANNER

As already seen in Fig. 1.1, there is a strong connection between the route design and flight allocation problems, and therefore, these problems should be considered in a linked manner. Unfortunately, due to the high complexity and huge computational cost of considering an integrated problem, research on this type of problem is limited. So far, only Heblj [31] considered this problem in his thesis. However, this study still contained significant limitations. As also acknowledged in [31], the optimized departure profiles derived from aircraft route design problems are based on a single-event noise criterion, which is most likely not a perfect proxy for the allocation phase where multi noise events are considered [31]. It should be noted that the optimal routes derived from single-event and multi-event noise criteria are likely different.

Moreover, the allocation model in [31] only considered runway capacity, whereas actual aircraft separation on the runways and along noise-optimized routes is not considered. Additionally, even though a multi-objective optimization approach is used in the framework in [31], it is based on a weighting approach, and, consequently, only a single solution was obtained at a time. Since the determination of a suitable weighting vector

for the objectives is difficult, it is challenging to obtain a well-balanced solution between conflicting objectives. Therefore, there is a clear opportunity for the development of an effective optimization framework that addresses the problems of route design and flight allocation in conjunction.

### 1.3. MAIN AIM AND RESEARCH OBJECTIVES

In an effort to address the crucial gap identified above, the aim of this thesis is to develop an optimization framework that is able to *effectively address the optimization problems of route design and flight allocation in a linked manner, while taking into account operational constraints related to aircraft sequencing and separation requirements to minimize noise impact and fuel consumption.*

Essentially, the aim of the thesis is to find a shared answer to all three questions given in Fig. 1.1 in a linked manner. In particular, the final goal of the thesis is to determine, *for each given standard instrument departure (SID) route, which route is optimal, and how many movements of each aircraft type should be assigned to this route while taking into account operational constraints related to aircraft sequencing and separation requirements*

Solving the individual problems discussed above individually has proven not to be a trivial task. Consequently, considering both problems simultaneously is even more challenging, which is one of the main reasons for the apparent lack of previous research on the topic. Therefore, without having a good understanding of each problem itself, it will be challenging to be able to develop a generic framework.

To systematically address the above concerns, this research has been broken down into smaller steps. In each step, a particular research problem is considered, and a specific objective is addressed. In each of these steps existing research gaps in these sub-problems are also addressed. The individual objectives are:

1. *To select or develop (a) suitable and efficient optimization method(s) capable of addressing the specific problems of route design and flight allocation for multiple objectives.*
2. *To improve the performance of solving aircraft route design problems based on the application of the developed method.*
3. *To develop a flight allocation problem formulation that allows to address noise impact and fuel consumption concurrently.*
4. *To establish a suitable approach that is capable of solving the problems of route design and flight allocation in a linked manner.*
5. *To develop an optimization framework that can effectively address the former points simultaneously.*

### 1.4. RESEARCH APPROACH AND THESIS OUTLINE

Following the five objectives defined above, the thesis has been structured into five main content sections (i.e., Chapters 2 to 6), relating to objectives 1 to 5, respectively. The overview of the thesis is illustrated in Fig. 1.2.

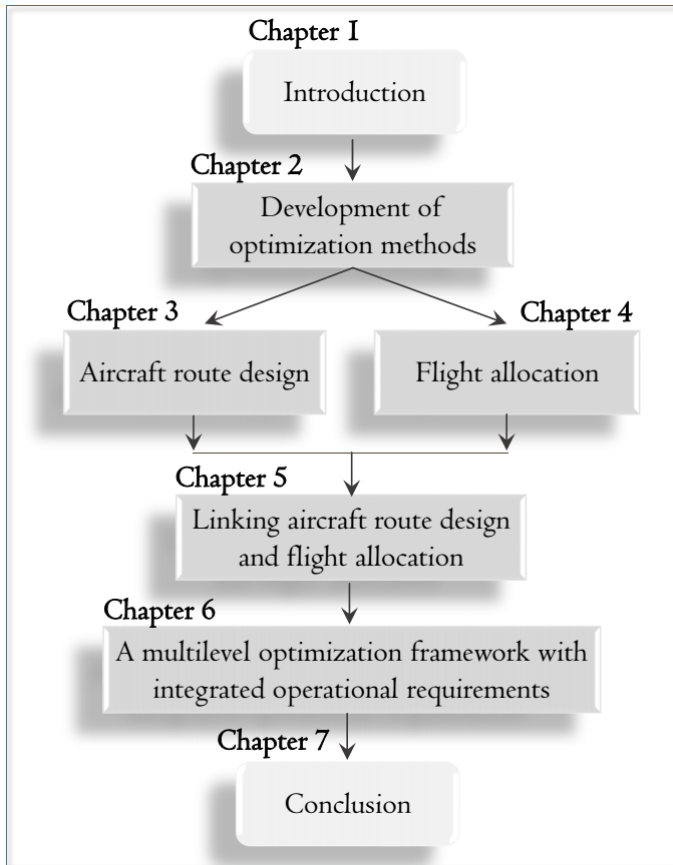


Figure 1.2: Overview of the thesis

Because aircraft noise impact and fuel consumption are the two main objectives considered through the developed framework, research to identify a suitable approach for effectively dealing with multi-objective optimization problems is therefore the first aim of the thesis. Due to its advantages, such as having a good convergence rate and providing high-quality solutions, the multi-objective evolutionary algorithm based on decomposition (MOEA/D) is selected as one of the main algorithms to address most multi-objective optimization problems formulated in the thesis.

Since the MOEA/D method has not yet been applied to the field of aircraft and airport operations, a study on this method is carried out in **Chapter 2**. The study is first to understand its searching principle and to integrate recent developments in the field of evolutionary optimization into the algorithm to increase its performance. Thereafter, the potential of the developed method to solve aircraft route design problems is investigated.

Based on the obtained initial results of designing optimal routes, the features of the MOEA/D algorithm, and the characteristics of the route design problem are further stud-

ied in **Chapter 3**. The main aim of this chapter is to increase the performance of the optimization process by formulating the optimization problems such that it best exploits the characteristics of the MOEA/D algorithm. Furthermore, the simultaneous integration of route design and aircraft allocation for a given route is executed in this chapter. This case study aims to provide a view on the complexity of the integrated problem and hence provides guidance for further steps.

Next, research on flight allocation problems (which are also referred to as air traffic assignment problems in this thesis) is presented in **Chapter 4**. This chapter aims to give a good understanding of the air traffic assignment problems, which plays a vital role in the integration of this type of problem into the developed framework. The study also helps to develop a suitable air traffic assignment model that is able to effectively consider two potentially conflicting objectives, i.e., noise impact and fuel consumption, at the same time.

After both sub-problems (i.e., route design and flight allocation) have been studied, research on the link between them is considered in **Chapter 5**. In this chapter, a two-step optimization framework that links the problems of route design and flight allocation together is proposed. Thereafter, operational constraints related to aircraft sequencing and separation requirements are studied and integrated into the developed model. Consequently, a completed model that is able to consider the design of optimal routes and the allocation of aircraft in a linked manner while taking aircraft sequencing and separation constraints into account is proposed in **Chapter 6**.

Finally, **Chapter 7** summarizes the research findings of the thesis and provides recommendations for future work in this field.

# 2

## DEVELOPMENT OF OPTIMIZATION METHODS

*The aim of the study in this chapter is to select or develop (a) suitable and efficient optimization method(s) capable of addressing the specific problems of route design and flight allocation for multiple objectives. The resulting method is called the multi-objective evolutionary algorithm based on decomposition (MOEA/D). In addition to studies to understand the searching principle of the MOEA/D method, research to improve its performance related to the computational cost and the quality of Pareto front solutions has also been carried out in this chapter. Furthermore, to make the algorithm more efficient, recent developments in the field of evolutionary optimization are integrated. The performance of the developed method is first validated through benchmark test functions and structural optimization problems, and then applied to the aircraft route design problem.*

---

The content of this chapter is based on the following research articles:

- [1]. **V. Ho-Huu**, S. Hartjes, H. G. Visser, and R. Curran, *An improved MOEA/D algorithm for bi-objective optimization problems with complex Pareto fronts and its application to structural optimization*, Expert Systems with Applications, vol. 92, pp. 430-446, 2018. -> Paper 2.1.
- [2]. **V. Ho-Huu**, S. Hartjes, L. H. Geijselaers, H. G. Visser, and R. Curran, *Optimization of noise abatement aircraft terminal routes using a multi-objective evolutionary algorithm based on decomposition*, Transportation Research Procedia, vol. 29, pp. 157-168, 2018. -> Paper 2.2.

## 2.1. PROBLEM STATEMENT

With the concurrent consideration of two objectives, i.e., noise impact and fuel consumption, the research presented in this thesis mainly deals with multi-objective optimization problems. As pointed out in previous studies [8, 13, 19, 20, 25], the problems in this field are highly nonlinear optimization problems and contain different types of design variables, such as continuous, integer, or mixed continuous/integer variables. Therefore, it is crucial to first determine a reasonable algorithm that is able to solve such kinds of problems effectively.

In this chapter, the MOEA/D, initially proposed by Zhang and Li [32], is chosen as the main algorithm to deal with most multi-objective optimization problems formulated in the framework. The reason for this selection is that MOEA/D has been realized as one of the most powerful methods in the field of multi-objective optimization [33]. Compared with other methods, MOEA/D has been demonstrated to be more effective both in terms of convergence rate and computational cost [34], which are promising features for solving large-scale real-world problems. However, the application of MOEA/D to real-world problems is still limited, especially in the field of aerospace engineering.

Before applying the MOEA/D algorithm to solve problems in the field of aircraft and airport operations, certain efforts have been put into understanding and adapting the searching principle, specifically aimed at the intended application. For this reason, a study on the MOEA/D method has been carried out in Ho-Huu et al. [35]. In this study, some improvements to increase its performance regarding the computational cost and the quality of solutions have been proposed. In addition, recent developments in the field of evolutionary optimization are integrated into the developed algorithm to make it more efficient. The performance and reliability of the developed algorithm are evaluated on well-known benchmark test functions and structural optimization problems.

Later, the developed method is applied to the problem of designing departure and arrival routes at Rotterdam The Hague Airport in The Netherlands, which is presented in detail in Ho-Huu et al. [36]. The study aims to explore whether or not the method is suitable for solving such kinds of problems.

## 2.2. CONTRIBUTIONS

The main contributions of this chapter are as follows:

1. In Ho-Huu et al. [35], an improved version of the MOEA/D algorithm is proposed, which is capable of handling multi-objective optimization problems with complicated Pareto fronts. Thanks to the integration of new developments, the performance of the algorithm has been significantly improved both in terms of computational cost and the quality of solutions. Compared with other approaches, the proposed method offers a saving of more than 20% in the computational cost while providing slightly better results.
2. In Ho-Huu et al. [36], the MOEA/D method has been successfully applied to the design of optimal routes with less noise impact and fuel consumption. In comparison with the reference scenario, MOEA/D provides better route options relative to both the noise and fuel objectives. From the obtained Pareto front, a selected

representative solution can offer a reduction of up to 55% in the number of awakenings and savings of 10% in fuel. Compared with another approach, namely the Non-dominated Sorting Genetic Algorithm II (NSGA-II), MOEA/D provides comparable or slightly better solutions with a significantly lower computational cost. For both case studies of designing departure and arrival routes, MOEA/D can save up to 20% in CPU time.



# An improved MOEA/D algorithm for bi-objective optimization problems with complex Pareto fronts and its application to structural optimization



V. Ho-Huu\*, S. Hartjes, H.G. Visser, R. Curran

Faculty of Aerospace Engineering, Delft University of Technology, Delft, The Netherlands

## ARTICLE INFO

### Article history:

Received 8 June 2017

Revised 22 September 2017

Accepted 23 September 2017

Available online 28 September 2017

### Keywords:

Multi-objective evolutionary algorithm (MOEA)

Multi-objective evolutionary algorithm based on decomposition (MOEA/D)

Complicated Pareto fronts (PFs)

Structural optimization

Truss structures

## ABSTRACT

The multi-objective evolutionary algorithm based on decomposition (MOEA/D) has been recognized as a promising method for solving multi-objective optimization problems (MOPs), receiving a lot of attention from researchers in recent years. However, its performance in handling MOPs with complicated Pareto fronts (PFs) is still limited, especially for real-world applications whose PFs are often complex featuring, e.g., a long tail or a sharp peak. To deal with this problem, an improved MOEA/D (named iMOEA/D) that mainly focuses on bi-objective optimization problems (BOPs) is therefore proposed in this paper. To demonstrate the capabilities of iMOEA/D, it is applied to design optimization problems of truss structures. In iMOEA/D, the set of the weight vectors defined in MOEA/D is numbered and divided into two subsets: one set with odd-weight vectors and the other with even-weight vectors. Then, a two-phase search strategy based on the MOEA/D framework is proposed to optimize their corresponding populations. Furthermore, in order to enhance the total performance of iMOEA/D, some recent developments for MOEA/D, including an adaptive replacement strategy and a stopping criterion, are also incorporated. The reliability, efficiency and applicability of iMOEA/D are investigated through seven existing benchmark test functions with complex PFs and three optimal design problems of truss structures. The obtained results reveal that iMOEA/D generally outperforms MOEA/D and NSGA-II in both benchmark test functions and real-world applications.

© 2017 Elsevier Ltd. All rights reserved.

## 1. Introduction

In many real-world engineering applications, for example, structural optimization (Cai & Aref, 2015; Vo-Duy, Duong-Gia, Ho-Huu, Vu-Do, & Nguyen-Thoi, 2017), aircraft trajectory optimization (Hartjes & Visser, 2016; Hartjes, Visser, & Hebly, 2010; Visser & Hartjes, 2014), optimal design problems often have multiple conflicting objectives and are known as multi-objective optimization problems (MOPs) (Deb, 2001). By solving these problems, a set of trade-off solutions between objectives can be found. From this set, decision makers can select the most suitable solutions, which may help them save much time and/or money. Solving real-world MOPs, however, is usually a challenging task for the decision makers because of their complexities such as high nonlinearity, non-convexity and discontinuity (Grandhi, 1993). Therefore, the development of efficient optimization methods for coping with these

problems becomes more important and attracts much attention from researchers (Trivedi, Srinivasan, Sanyal, & Ghosh, 2016).

Among different approaches, multi-objective evolutionary algorithms (MOEAs) have been recognized as well-suited methods for solving such MOPs since they are capable of approximating multiple non-dominated solutions in a single run (Deb, 2001; Li, Kwong, Zhang, & Deb, 2015). One of the recent effective methods is the multi-objective evolutionary algorithm based on decomposition (MOEA/D) (Zhang & Li, 2007). In MOEA/D, an MOP is decomposed into a set of scalar optimization sub-problems, and these sub-problems are solved simultaneously in a collaborative manner. Owing to the diversity maintenance of sub-problems and the information sharing between individuals dwelling in a neighborhood, MOEA/D may acquire well-distributed solutions over a Pareto front (PF). In a comparative study with the non-dominated sorting genetic algorithm (NSGA-II) (Li & Zhang, 2009), the obtained results showed that MOEA/D outperforms NSGA-II in terms of both the quality of solutions and convergence rate. In addition, the efficiency of MOEA/D is also proven through real-world applications such as wireless sensor networks (Konstantinidis & Yang, 2012), route planning (Waldock & Corne, 2011), and economic emission

\* Corresponding author.

E-mail addresses: [vhohuu@tudelft.nl](mailto:vhohuu@tudelft.nl) (V. Ho-Huu), [s.hartjes@tudelft.nl](mailto:s.hartjes@tudelft.nl) (S. Hartjes), [h.g.visser@tudelft.nl](mailto:h.g.visser@tudelft.nl) (H.G. Visser), [r.curran@tudelft.nl](mailto:r.curran@tudelft.nl) (R. Curran).

dispatch (Zhu, Wang, & Qu, 2014). Nevertheless, recent research in (Jiang & Yang, 2016; Qi et al., 2013; Wang, Zhang, Li, Ishibuchi, & Jiao, 2017; Yang, Jiang, & Jiang, 2016) indicated that MOEA/D often only effectively handles MOPs with simple PFs, while it is not good at solving MOPs with complex PFs exhibiting features such as a long tail or a sharp peak.

To enhance the capability of MOEA/D in solving MOPs with complicated PFs, some different approaches have been proposed in recent literature. Qi et al. (2013) proposed an improved MOEA/D with an adaptive weight adjustment. In this version, a new weight vector initialization method is introduced for generating the set of initial weight vectors, and an adaptive weight vector adjustment strategy is developed to detect the overcrowded solutions on a PF and create new candidates to replace them. Yang et al. (2016) investigated the impact of penalty factors in the penalty boundary intersection (PBI) on the spread of a PF, and then proposed a new variant of MOEA/D with two different penalty schemes. Jiang and Yang (2016) developed an improved MOEA/D with a new search strategy, namely MOEA/D-TPN, where the optimization procedure is divided into two phases. The solving process of an MOP is started with the first phase, and after this phase terminates, the crowded information of obtained solutions is evaluated to decide whether or not the second phase is continued. Wang et al. (2017) examined, for the first time, the influence of the ideal point and the nadir point in the Tchebycheff function on the distribution of optimal solutions over a PF and then developed a new improved MOEA/D, in which both these points are integrated into the Tchebycheff function to decompose an MOP into a number of scalar optimization sub-problems. Through the evaluations on benchmark test functions in Jiang and Yang (2016), Qi et al. (2013), Wang et al. (2017) and Yang et al. (2016), it was shown that most of these developed methods outperform MOEA/D and some other available methods. They, however, often require more computational procedures or have more control parameters than MOEA/D, which may lead to certain limitations for engineering designers in applying them to real-world applications. For example, the method in Qi et al. (2013) has an extra algorithm for detecting and replacing overcrowded sub-problems during the optimization process, while the method in Jiang and Yang (2016) requires a pre-defined reasonable number of evaluations for the distribution of computational resources for both phases.

From the review of the above methods and motivated by the desire to solve complex real-world problems, e.g. structural optimization problems, an improved MOEA/D (iMOEA/D) which mainly focuses on bi-objective optimization problems (BOPs) is proposed in this paper. The iMOEA/D algorithm is developed based on the studies in Jiang and Yang (2016) and Wang et al. (2017), where the advantages of using the ideal point and the nadir point, and the benefits of solving an MOP based on two phases are exploited. In iMOEA/D, the solving process of a bi-objective optimization problem (BOP) is separated into two parts, and for each part the general framework of MOEA/D is applied. Firstly, the set of weight vectors of MOEA/D is numbered and divided into two subsets: one set with odd-weight vectors and the other with even-weight vectors. Then, a simple two-phase search strategy is developed to optimize the corresponding populations of each set. In the proposed search strategy, the optimization process of the two phases is almost the same except for the use of the Tchebycheff function type (Miettinen, 1999) in which either the ideal point or the nadir point is utilized. The search of iMOEA/D is started at the first phase with the set of odd-weight vectors. In this phase, the Tchebycheff function with the ideal point is utilized. After that, the second phase is continued with the set of even-weight vectors, and the Tchebycheff function with the nadir point  $\mathbf{z}^{\text{nad}}$  is used.

Furthermore, to enhance the overall performance of the algorithm, some recent developments related to MOEA/D consisting

of an adaptive replacement strategy (Wang, Zhang, Zhou, Gong, & Jiao, 2016) and a stopping criterion (Abdul Kadhar & Baskar, 2016) are also integrated into iMOEA/D. To estimate the performance of the proposed algorithm, seven existing benchmark test functions with complicated PFs are tested first, and then three structural optimization problems of truss structures are solved. The efficiency and reliability of iMOEA/D are also compared with those of MOEA/D, MOEA/D-TPN and NSGA-II.

The rest of the paper is structured as follows. Section 2 provides some basic backgrounds of an MOP and the Tchebycheff decomposition method. Section 3 presents a general framework of the MOEA/D algorithm, in which some recent developments are also included. The iMOEA/D algorithm is described in Section 4. Experimental studies are presented in Section 5, and some conclusions are drawn in Section 6.

## 2. Backgrounds

### 2.1. Basic definitions

A multi-objective optimization problem (MOP) can be stated as follows:

$$\begin{aligned} \min \quad & F(\mathbf{x}) = (f_1(\mathbf{x}), \dots, f_m(\mathbf{x}))^T \\ \text{s.t.} \quad & \mathbf{x} \in \Omega \end{aligned} \quad (1)$$

where  $\mathbf{x} = (x_1, \dots, x_n)^T \in \mathbf{R}^n$  is the vector of design variables,  $\Omega$  is the feasible search domain,  $f_j(\mathbf{x})$  is the  $j$ th objective function, and  $m$  is the number of objective functions.

In multi-objective optimization, some basic definitions in the context of minimization problems are given as follows:

- Let  $\mathbf{x}_1, \mathbf{x}_2 \in \Omega$  be two solutions of an MOP,  $\mathbf{x}_1$  is said to *dominate*  $\mathbf{x}_2$  (denoted  $\mathbf{x}_1 \prec \mathbf{x}_2$ ), if and only if  $f_j(\mathbf{x}_1) \leq f_j(\mathbf{x}_2), \forall j \in \{1, \dots, m\}$ , and  $f_j(\mathbf{x}_1) < f_j(\mathbf{x}_2)$  for at least one index  $j \in \{1, \dots, m\}$ .
- Let  $\mathbf{x}^* \in \Omega$  be called *Pareto optimal* if there is no other solution in  $\Omega$  which dominates  $\mathbf{x}^*$ .
- The set of Pareto optimal solutions in  $\Omega$  are called the *Pareto set* (PS), which is determined by  $PS = \{\mathbf{x}^* | \exists \mathbf{x} \in \Omega, \mathbf{x} \prec \mathbf{x}^*\}$ . The corresponding objective vectors of the solutions in PS is called the *Pareto front* (PF) and defined as  $PF = \{F(\mathbf{x}) | \mathbf{x} \in PS\}$ .
- A point  $\mathbf{z}^* = (z_1^*, \dots, z_m^*)^T$  is called the *ideal point* if  $z_j^* < \min\{f_j(\mathbf{x}) | \mathbf{x} \in \Omega, j = 1, \dots, m\}$ .
- A point  $\mathbf{z}^{\text{nad}} = (z_1^{\text{nad}}, \dots, z_m^{\text{nad}})^T$  is called the *nadir point* if  $z_j^{\text{nad}} > \max\{f_j(\mathbf{x}) | \mathbf{x} \in \Omega, j = 1, \dots, m\}$ .

### 2.2. Tchebycheff decomposition approach

Over the past decades, many approaches have been proposed for decomposing an MOP into a set of scalar optimization sub-problems and can be found in Das and Dennis (1998) and Messac, Ismail-Yahaya, and Mattson (2003). Among these approaches, the weighted Tchebycheff approach is the most widely utilized because of its capability of handling multi-objective optimization problems with non-convex Pareto fronts (Zhang & Li, 2007). A scalar optimization subproblem based on the weighted Tchebycheff approach with the ideal point is determined by

$$\begin{aligned} \min \quad & g^{\text{te}}(\mathbf{x} | \mathbf{w}, \mathbf{z}^*) = \max_{1 \leq j \leq m} \{w_j |f_j(\mathbf{x}) - z_j^*|\} \\ \text{s.t.} \quad & \mathbf{x} \in \Omega \end{aligned} \quad (2)$$

where  $\mathbf{w} = (w_1, \dots, w_m)^T, (w_j \geq 0, \sum_{j=1}^m w_j = 1, j = 1, \dots, m)$  is the weight vector of the scalar optimization subproblem, and  $\mathbf{z}^*$  is the ideal point.

The Tchebycheff approach in Eq. (2) is often only suitable for MOPs with normalized objective functions. Thus, when the ranges

of the objectives are on very different scales, the Tchebycheff function is defined as follows (Zhang & Li, 2007):

$$\min_{\mathbf{x} \in \Omega} g^{te}(\mathbf{x}|\mathbf{w}, \mathbf{z}^*) = \max_{1 \leq j \leq m} \left\{ w_j \left| \frac{f_j(\mathbf{x}) - z_j^*}{z_j^{\text{nad}} - z_j^*} \right| \right\} \quad (3)$$

According to Jiang and Yang (2016), the scalar optimization sub-problem may also be formulated by using the nadir point as follows:

$$\max_{\mathbf{x} \in \Omega} g^{te}(\mathbf{x}|\mathbf{w}, \mathbf{z}^{\text{nad}}) = \min_{1 \leq j \leq m} \left\{ w_j |z_j^{\text{nad}} - f_j(\mathbf{x})| \right\} \quad (4)$$

Similarly, to deal with MOPs whose objectives are on very different scales, the sub-problem in Eq. (4) is defined in the following form:

$$\max_{\mathbf{x} \in \Omega} g^{te}(\mathbf{x}|\mathbf{w}, \mathbf{z}^{\text{nad}}) = \min_{1 \leq j \leq m} \left\{ w_j \left| \frac{z_j^{\text{nad}} - f_j(\mathbf{x})}{z_j^{\text{nad}} - \mathbf{z}^*} \right| \right\} \quad (5)$$

**3. MOEA/D algorithm**

The multi-objective evolutionary algorithm based on decomposition (MOEA/D), firstly developed by Zhang and Li (2007), has been recognized as one of the most popular multi-objective evolutionary algorithms to date (Trivedi et al., 2016). In MOEA/D, MOPs are decomposed into a number of scalar optimization sub-problems by applying decomposition approaches, and these sub-problems are optimized concurrently by mean of using evolutionary algorithms. By employing different decomposition methods and different evolutionary algorithms, various versions of MOEA/D have been developed in recent years such as MOEA/D-DE (Li & Zhang, 2009), MOEA/D-DRA (Zhang, Liu, & Li, 2009), MOEA/D-XBS (Zhang & Li, 2007), and MOEA/D-GR (Wang et al., 2016). Although different variants of MOEA/D are available in the literature, there is no single MOEA/D version that combines the many distinct advantages of the various versions. With the aim of developing an efficient version of MOEA/D for real-life problems, a MOEA/D version is therefore developed in this study which is a combination of MOEA/D-DE (Li & Zhang, 2009), an adaptive replacement strategy (Wang et al., 2016), and a stopping condition criterion (Abdul Kadhar & Baskar, 2016). The general framework of MOEA/D is presented in Algorithm 1.

In Step 2.2, each element  $\tilde{y}_k$  of solution  $\tilde{\mathbf{y}} = (\tilde{y}_1, \dots, \tilde{y}_n)^T$  is generated by using “DE/rand/1” operator (Storn & Price, 1997) as follows:

$$\tilde{y}_k = \begin{cases} x_k^{r_1} + F(x_k^{r_2} - x_k^{r_3}) & \text{with probability } CR, \\ x_k^{r_1} & \text{with probability } (1 - CR) \end{cases} \quad (6)$$

where  $F$  and  $CR$  are two control parameters. The polynomial mutation operator used to create the new solution  $\mathbf{y}$  is defined as follows:

$$y_k = \begin{cases} \tilde{y}_k + \sigma_k \times (x_{ub_k} - x_{lb_k}) & \text{with probability } p_m, \\ \tilde{y}_k & \text{with probability } (1 - p_m) \end{cases} \quad (7)$$

where

$$\sigma_k = \begin{cases} (2 \times rand)^{\frac{1}{\eta}} - 1 & \text{if } rand < 0.5, \\ 1 - (2 - 2 \times rand)^{\frac{1}{\eta}} & \text{otherwise} \end{cases} \quad (8)$$

where  $rand$  is the uniformly distributed random number from [0, 1]. The distribution index  $\eta$  and the mutation rate  $p_m$  are two control parameters, and  $x_{lb}$  and  $x_{ub}$  are the lower and upper bounds of the  $k$ th design variable, respectively.

In Step 3, the stopping criterion named maximum Tchebycheff objective error (MTOE) (Abdul Kadhar & Baskar, 2016) is utilized. The method uses the information of the Tchebycheff objectives of

all sub-problems to set a stopping condition for the algorithm. Firstly, the maximum value of Tchebycheff objective error (TOE) is computed based on the absolute difference between the current and previous generation’s Tchebycheff objectives. Then, the maximum value in the set of TOE (MTOE) at the current generation is determined.

$$MTOE_{gen} = \max_{1 \leq i \leq N} \{TOE_i\} \quad (9)$$

Finally, a  $\chi^2$  test is applied for statistical evaluation of the variations in the MTOE values during previous  $g$  generations (Sharma & Rangaiah, 2013; Wagner & Trautmann, 2010). If the variation of MTOE is smaller than a pre-defined tolerance value ( $\epsilon$ ), then the search process of the algorithm is terminated.

$$Chi(MTOE) = \frac{\text{variance}[MTOE_1, MTOE_2, \dots, MTOE_g](g - 1)}{\epsilon^2} \quad (10)$$

$$p(MTOE) = \chi^2 \text{test}[Chi(MTOE), (g - 1)] \quad (11)$$

where  $MTOE_1, \dots, MTOE_g$  are the MTOE values of the previous  $g$  generations,  $\epsilon$  is the expected tolerance value for the standard deviation of MTOE,  $Chi(MTOE)$  is the test statistic, and  $p(MTOE)$  is the probability of which the  $\chi^2$  test supports the hypothesis that the variance of MTOE is lower than the pre-defined tolerance  $\epsilon$ . If the probability  $p$  is equal to or larger than 99%, the algorithm terminates its search process. The probability  $p$  is defined by referring to the lookup table of  $\chi^2$  distribution for  $(g - 1)$  degrees of freedom, where  $g$  is the number of generations. For instance, if the number of generation  $g$  is set to be 10, to get a probability  $p$  of 99%, then  $Chi(MTOE)$  must be smaller than or equal to 2.088.

**4. iMOEA/D algorithm**

As pointed out by Wang et al. (2017), the use of the ideal point  $\mathbf{z}^*$  and the nadir point  $\mathbf{z}^{\text{nad}}$  in the Tchebycheff function has a significant influence on the distribution of optimal solutions over a PF. Particularly, in the case of using  $\mathbf{z}^*$  as the reference point, the optimal solutions of sub-problems for a convex PF and a concave PF are shown in Fig. 1a and b, respectively. From the figures, it is clear that the optimal solution density in the central part of the convex PF is much larger than those of the concave PF, while it is opposite on the boundaries of the PFs. In contrast with the use of  $\mathbf{z}^*$ , the distribution of optimal solutions on these PFs is in a contrary direction if  $\mathbf{z}^{\text{nad}}$  is used as the reference point, which is depicted as in Fig. 1c and d, respectively.

From the obtained results of the investigation in Wang et al. (2017), it is evident that the idea of combining both the ideal point  $\mathbf{z}^*$  and the nadir point  $\mathbf{z}^{\text{nad}}$  in the Tchebycheff function can be an efficient way to handle MOPs with complicated PFs. To take this advantage, Jiang and Yang (2016) have also developed a search strategy with two phases for MOEA/D, in which the Tchebycheff function with  $\mathbf{z}^*$  is used in the first phase, and the Tchebycheff function with  $\mathbf{z}^{\text{nad}}$  is employed in the second phase. The search of the algorithm is started with the first phase; and after this phase, the crowded information of obtained solutions is estimated. If the crowded information shows that there is a significant difference between the solutions at the boundary/extreme and the intermediate of the PF, the second phase will be continued which aims to supplement more solutions on the boundary/extreme regions of the PF; otherwise, the second phase is not applied, and the search of the algorithm is completed. Through benchmark test functions with complex PFs, the method has been demonstrated to be able to deal effectively with MOPs with complicated PFs. The method, however, also has two limitations which may be described as follows: 1) the algorithm uses a pre-defined number of evaluations to switch from Phase 1 to Phase 2. It is very difficult to set this in

**Algorithm 1** Pseudo-code of MOEA/D algorithm.

```

Input:

- A multi-objective optimization problem as Eq. (1);
- A stopping criterion;
- $N$ : number of sub-problems;
- $\mathbf{w}^i = (w_1^i, \dots, w_m^i)^T, i = 1, \dots, N$ : a set of  $N$  weight vectors;
- $T_m$ : size of mating neighborhood;
- $T_{rmax}$ : maximum size of replacement neighborhood;
- $\delta$ : the probability that mating parents are selected from the neighborhood;
- $MaxIter$ : maximum iteration;
- $FES = 0$ : the number of function evaluations;

Step 1. Initialization

- 1.1. Find the  $T_m$  closest weight vectors to each weight vector based on the Euclidean distances of any two weight vectors. For each sub-problem  $i = 1, \dots, N$  set  $\mathbf{B}^i = \{i_1, \dots, i_{T_m}\}$  where  $\mathbf{w}^{i_1}, \dots, \mathbf{w}^{i_{T_m}}$  are the closest weight vectors to  $\mathbf{w}^i$ ;
- 1.2. Create an initial population  $\mathbf{P} = \{\mathbf{x}^1, \dots, \mathbf{x}^N\}$  by uniformly randomly sampling from  $\Omega$ . Evaluate the fitness value  $FV^i$  of each solution  $\mathbf{x}^i$ , i.e.  $FV^i = (f_1(\mathbf{x}^i), \dots, f_m(\mathbf{x}^i))$  and set  $\mathbf{FV} = \{FV^1(\mathbf{x}^1), \dots, FV^N(\mathbf{x}^N)\}$ ;
- 1.3. Initialize ideal point  $\mathbf{z}^* = (z_1^*, \dots, z_m^*)^T$  by setting  $z_j^* = \min\{f_j(\mathbf{x}) | \mathbf{x} \in \Omega, j = 1, \dots, m\}$  and nadir point  $\mathbf{z}^{nad} = (z_1^{nad}, \dots, z_m^{nad})^T$  by setting  $z_j^{nad} = \max\{f_j(\mathbf{x}) | \mathbf{x} \in \Omega, j = 1, \dots, m\}$ ;
- 1.4. Set  $FES = FES + N$ , and generation:  $gen = 1$ ;

Step 2. Update
while (the stopping conditions are not satisfied)
    for  $i = 1, \dots, N$ ; do

- 2.1. Selection of mating/update range
            
Set  $\mathbf{B}_m = \begin{cases} \mathbf{B}^i & \text{if } rand < \delta \\ \{1, \dots, N\} & \text{otherwise} \end{cases}$ 
  
where  $rand$  is a uniformly distributed random number in  $[0, 1]$ ;
- 2.2. Reproduction: randomly select three parent individuals  $r_1, r_2, r_3$  ( $r_1 \neq r_2 \neq r_3 \neq i$ ) from  $\mathbf{B}_m$  and generate a solution  $\tilde{\mathbf{y}}$  by applying "DE/rand/1" operator, and then perform a mutation operator on  $\tilde{\mathbf{y}}$  to create a new solution  $\mathbf{y}$ ;
- 2.3. Repair: if any element of  $\mathbf{y}$  is out of  $\Omega$ , its value will be randomly regenerated inside  $\Omega$ ;
- 2.4. Evaluate the fitness value of new solution  $\mathbf{y}$ ;
- 2.5. Update of  $\mathbf{z}^*, \mathbf{z}^{nad}$ : for each  $j = 1, \dots, m$  if  $z_j^* \leq f_j(\mathbf{x}^i)$  then set  $z_j^* = f_j(\mathbf{x}^i)$ , and if  $z_j^{nad} \geq f_j(\mathbf{x}^i)$  then set  $z_j^{nad} = f_j(\mathbf{x}^i)$ ;
- 2.6. Update of solution: use an adaptive replacement strategy in Wang et al. (2016):
  - 2.6.1. Find the most suitable sub-problem  $k$  for the new solution  $\mathbf{y}$  by  $k = \arg \min_{1 \leq l \leq N} |g_l^{ns}(\mathbf{y})|$ ;
  - 2.6.2. Define the maximum numbers of solutions which may be replaced by the new solution  $\mathbf{y}$  in the neighborhood set of the sub-problem  $k$  by  $T_r = \lceil \frac{T_{rmax}}{1 + \exp(-20 \times (\frac{z_j^{nad} - f_j(\mathbf{y})}{z_j^{nad} - z_j^*})^2)} \rceil$ , where  $\lceil \cdot \rceil$  is the ceiling function,  $\gamma$  is the control parameter in  $[0, 1]$ ;
  - 2.6.3. Set  $\mathbf{B}_r = \mathbf{B}^k \setminus \{l\}, l = 1, \dots, T_r$  to be the set of solutions in the neighborhood set of the sub-problem  $k$  which can be replaced by the new solution  $\mathbf{y}$ ;
  - 2.6.4. For each solution  $\mathbf{x}^l$  in  $\mathbf{B}_r$ , replace  $\mathbf{x}^l$  by  $\mathbf{y}$  if  $g^{ns}(\mathbf{y}) \leq g^{ns}(\mathbf{x}^l)$ ;

end for
  
Set  $FES = FES + N$ , and  $gen = gen + 1$ ;
    Step 3. Stopping condition
  
Use a stopping criterion in Abdul Kadhar and Baskar (2016).
    if (the stopping criterion is satisfied or  $MaxIter$  is reached)
      Stop the algorithm;
    end if
end while
Output:

- Pareto set  $\mathbf{PS} = \{\mathbf{x}^1, \dots, \mathbf{x}^N\}$ ;
- Pareto front  $\mathbf{PF} = \{FV^1(\mathbf{x}^1), \dots, FV^N(\mathbf{x}^N)\}$ .

```

advance without any knowledge about a problem, while it has a significant influence on the performance of the algorithm (Jiang & Yang, 2016); and 2) the computational cost of solving an MOP will increase significantly compared with available versions of MOEA/D if Phase 2 of the algorithm is executed.

Motivated by solving complex real-world problems and in an effort to overcome the limitations of the algorithm in Jiang and Yang (2016), this paper attempts to develop a newly improved MOEA/D (iMOEA/D) and applies it to solving bi-objective optimization problems (BOPs) of truss structures. In iMOEA/D, firstly, in order to surmount the first limitation in Jiang and Yang (2016), the stopping criterion recently proposed in Abdul Kadhar and Baskar (2016) is applied. This method will help automatically stop the algorithm if there is no considerable improvement on the optimal solutions instead of using the number of evaluations. The details of this approach have been presented in Section 3. Secondly, to improve the distribution of optimum solutions over a complex PF while the computational cost of the algorithm does not increase, a new two-phase search strategy is proposed. The idea behind this approach is depicted in Fig. 2, and it includes the following steps. First, the set of the weight vectors of MOEA/D is num-

bered and split into two subsets: one set with odd-weight vectors and the other with even-weight vectors. Then, the optimization process is started with the set of odd-weight vectors in the first phase. In this phase, the general framework of MOEA/D as shown in Algorithm 1 is applied, in which the Tchebycheff function with the ideal point  $\mathbf{z}^*$  as Eq. (2) is utilized. After this phase has been completed, the nadir point  $\mathbf{z}^{nad}$  is determined from the obtained set of solutions, and the Tchebycheff function as Eq. (4) is employed for the second phase with the set of even-weight vectors.

As shown in Fig. 2, it can be observed that by dividing the set of weight vectors into two subsets and applying different types of the Tchebycheff function, the distribution of optimal points over a complicated PF obtained by the algorithm becomes better. Fig. 2 also shows that this approach can work efficiently for a simple PF. Moreover, the computational cost of the algorithm will not increase because the total population size is equal to the population size of MOEA/D. The framework of iMOEA/D is summarized in Algorithm 2.

In Algorithm 2, it should be noted that the set of odd-weight vectors in the first phase should include the weight vectors of  $(1,0)^T$  and  $(0,1)^T$ . This setting aims to ensure that a nadir point  $\mathbf{z}^{nad}$ ,

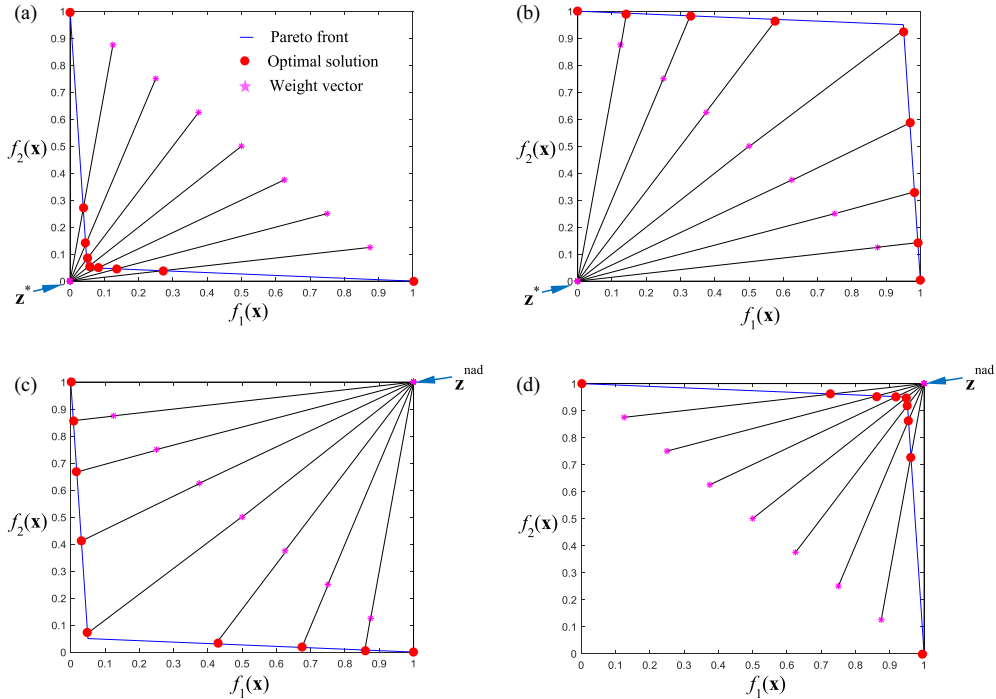


Fig. 1. The distribution of optimal solutions on Pareto fronts by using  $z^*$  point and  $z^{nad}$  point.

**Algorithm 2** Pseudo-code of iMOEA/D algorithm.

**Input:**

- A multi-objective optimization problem Eq. (1);
- A stopping criterion;
- $N$ : number of sub-problems;
- $w^{odd} = (w_1^i, \dots, w_m^i)^T, i = 1, 3, \dots, N$ : a set of odd-weight vectors;
- $w^{even} = (w_1^i, \dots, w_m^i)^T, i = 2, 4, \dots, N - 1$ : a set of even-weight vectors;
- $T_m$ : size of mating neighborhood;
- $T_{rmax}$ : maximum size of replacement neighborhood;
- $\delta$ : the probability that mating parents are selected from the neighborhood;
- $MaxIter$ : maximum iteration;

**Phase 1:**

- 1.1. Apply Step 1 to Step 3 in Algorithm 1 for the set of odd-weight vectors  $w^{odd} = (w_1^i, \dots, w_m^i)^T, i = 1, 3, \dots, N$ ;
- 1.2. Obtain  $PS_1 = \{x^1, \dots, x^i, \dots, x^N\}$ ,  $PF_1 = \{FV^1(x^1), \dots, FV^i(x^i), \dots, FV^N(x^N)\}, i = 1, 3, \dots, N$ ;

**Phase 2:**

- 2.1. Define  $z^{nad} = (z_1^{nad}, \dots, z_m^{nad})^T$  with  $z_j^{nad} = \max\{f_j(x) | x \in \Omega, f_j(x) \in PF_1\}$ ;
- 2.2. Set the initial population  $P = PS_1$  and  $FV = FV_1$ ;
- 2.3. Apply Step 1 to Step 3 in Algorithm 1 for the set of even-weight vectors  $w^{even} = (w_1^i, \dots, w_m^i)^T, i = 2, 4, \dots, N - 1$ , where Steps 1.2, 1.3, 2.5 are ignored; Step 2.6.4 is changed by "for each current solution  $x^i$  in  $B_i$ , replace  $x^i$  by  $y$  if  $g^{ev}(y) \geq g^{ev}(x^i)$ ";
- 2.4. Obtain  $PS_2 = \{x^2, \dots, x^i, \dots, x^{N-1}\}$ ,  $PF_2 = \{FV^2(x^2), \dots, FV^i(x^i), \dots, FV^{N-1}(x^{N-1})\}, i = 2, 4, \dots, N - 1$ ;

**Output:**

- Pareto set  $PS = \{PS_1; PS_2\}$ ;
- Pareto front  $PF = \{PF_1; PF_2\}$ .

which is obtained after finishing Phase 1, can fully cover the range of a Pareto front.

With the new two-phase search strategy and the integration of some recent developments, iMOEA/D possesses some advantages as follows:

- 1) It is able to handle BOPs with complicated Pareto fronts;
- 2) It does not require extra computational procedures; and the algorithm structure is almost the same with MOEA/D except for

using it for both phases, which is not too difficult for engineering designers to implement.

- 3) The computational cost for solving BOPs can be reduced significantly, which is quite crucial for solving real engineering applications.

These benefits are verified and evaluated in Section 5 through seven benchmark test functions and three practical applications of the optimal design of truss structures.

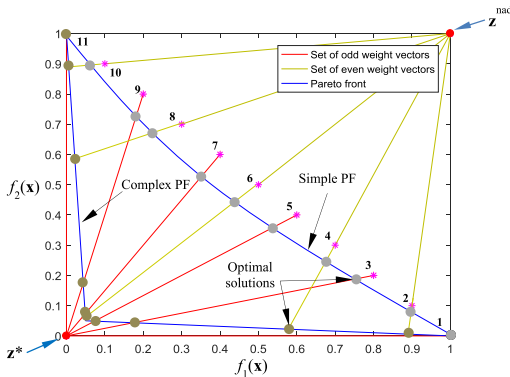


Fig. 2. The distribution of optimal solutions on a complex Pareto front acquired by iMOEA/D.

5. Experimental study

This section is divided into two parts. The first part is to examine the performance of the proposed method through benchmark test functions with complicated Pareto fronts. The second part is to evaluate the applicability of iMOEA/D for solving structural optimization problems. The performance of iMOEA/D is compared with MOEA/D in Algorithm 1, MOEA/D-TPN (Jiang & Yang, 2016), and NSGA-II (K Deb, Pratab, Agarwal, & Meyarivan, 2002). To make a fair comparison regarding the computational cost of NSGA-II, a stopping criterion which is proposed for NSGA-II in Roudenko and Schoenauer (2004) is also utilized. All algorithms are implemented in Matlab 2016b on a Core i7, 8 GB ram laptop.

5.1. Benchmark test functions

In order to evaluate the performance of iMOEA/D, a set of seven test instances as shown in Table 1 is used. In Table 1, F1-F3, F4-F6, and F7 are taken from Wang et al. (2017), Yang et al. (2016), and Jiang and Yang (2016), respectively. As mentioned in Jiang and Yang (2016), Wang et al. (2017) and Yang et al. (2016), the Pareto fronts of these problems are very complicated which are very difficult for MOEA/D to obtain a proper distribution of optimal solutions over the Pareto fronts.

5.1.1. Performance metrics

The performance of the algorithms is assessed by two widely-used performance metrics including the Hypervolume indicator (HV) (Zitzler & Thiele, 1999) and the inverted generational distance (IGD) (Zitzler, Thiele, Laumanns, Fonseca, & Da Fonseca, 2003). These indicators are defined as follows:

- HV (Zitzler & Thiele, 1999): Let  $z^* = (z_1^*, \dots, z_m^*)$  be a reference point in the objective space which satisfies  $z_j^* \geq \max(f_j)$ . Let  $P$  be an approximate set to the PF gained by an algorithm. The HV of  $P$  is the volume of the region dominated by  $P$  and bounded by  $z^*$  and is computed by

$$HV(P, z^*) = volume(\cup [f_1(x), z_1^*] \times \dots [f_m(x), z_m^*]) \quad (12)$$

where  $volume(\cdot)$  is the Lebesgue measure. In this study,  $z^*$  is set to (2.0, 2.0) for all test instances (Jiang & Yang, 2016). It is noted that the method with a larger HV metric is better.

- IGD (Zitzler et al., 2003): Let  $P^*$  be a set of uniformly distributed points over the PF in the objective space. Suppose  $P$

be an approximate set to the PF gained by an algorithm. The inverted generational distance from  $P^*$  to  $P$  is defined by

$$IGD(P^*, P) = \frac{\sum_{p \in P} d(v, P^*)}{|P|} \quad (13)$$

where  $d(v, P^*)$  is the Euclidean distance between the member  $v$  of  $P$  and the nearest member of  $P^*$ . In this paper, 500 representative points created from the true PF are used for all the benchmark test problems. It is noted that the method with a lower IGD metric is better.

5.1.2. Parameter settings

For all test instances, the parameter settings are the same. The parameters of NSGA-II are set according to Song (2011). For MOEA/D, MOEA/D-TPN, and iMOEA/D, their parameters are set as follows:

- Population size  $N$ :  $N = 100$ .
- Reproduction operators: CR and  $F = [0.4, 0.6]$ ,  $\delta = 0.9$ , and  $p_m = 1/n$  ( $n$  is the number of decision variables);
- Neighborhood size: In MOEA/D,  $T_m$  and  $T_{rmax} = 0.2N$ . In iMOEA/D and MOEA/D-TPN  $T_m$  and  $T_{rmax} = 0.1N$ .
- Stopping condition: In MOEA/D, MOEA/D-TPN and iMOEA/D,  $\epsilon = 10^{-6}$ ,  $g = 10$ , and  $MaxIter = 1000$ . The algorithms terminated when their stopping conditions are satisfied or the maximum number of iterations ( $MaxIter$ ) is reached.
- Number of runs: Each algorithm is independently run 30 times on each test instance.

It should be noted that the above parameters are set either based on the literature or on the experience obtained by running simulations with different settings. More specifically,  $N$ ,  $\epsilon$  and  $g$  are derived from Yang et al. (2016) and Abdul Kadhar and Baskar (2016) respectively, while the others are based on empirical results.

5.1.3. Evaluation of the new improvements

In order to demonstrate the ability of iMOEA/D to solve BOPs with the two-phase search strategy and to establish its advantages compared to the method (denoted as MOEA/D-TPN) in Jiang and Yang (2016), the benchmark tests F5 and F6 are used for investigation.

The performance of iMOEA/D in solving BOPs with complex PFs is evaluated by F5 and illustrated in Fig. 3. As shown in Fig. 3, the optimal solutions are densely populated in the central part of the PF and sparsely near the boundary of the PF in Phase 1 (Fig. 3a), and vice versa in Phase 2 (Fig. 3b). By combining the obtained results in both phases, the distribution of the solutions on the final PF has significantly improved as shown in Fig. 3c.

As mentioned in Section 4, iMOEA/D is developed based on MOEA/D-TP (Jiang & Yang, 2016), where the two improvements are integrated: 1) the incorporation of two recently developed features (i.e. an adaptive replacement strategy and a stopping criterion), and 2) the division of the initial weight vectors into two subsets. For the first improvement, it is easy to recognize that the computational cost of MOEA/D-TPN will be significantly larger than that of iMOEA/D if this improvement is not integrated into MOEA/D-TPN. This is because MOEA/D-TPN uses a conventional replacement scheme which has been demonstrated to be more costly than the adaptive replacement strategy (Wang et al., 2016), and a maximum number of iterations which do not allow to stop the algorithm until this number is reached. Therefore, the remaining comparison between iMOEA/D and MOEA/D-TPN will focus on the second improvement. For this comparison, the first improvement is also incorporated into MOEA/D-TPN. In this version, however, the niche scheme introduced in Jiang and Yang (2016) is not included because it is not employed in iMOEA/D. It should also be noted that the HV-metric values can be better if the obtained results

**Table 1**  
Benchmark test functions.

Instance	Objective function	Domain	$n$	PF characteristic
F1	$f_1 = 1 - \cos(0.5\pi x_1) + \frac{2}{ I_1 } \sum_{i \in I_1}  g_i ^{0.7}$ $f_2 = 10 - 10 \sin(0.5\pi x_1) + \frac{2}{ I_2 } \sum_{i \in I_2}  g_i ^{0.7}$ $g_i = x_i - 0.9 \sin(\frac{i\pi}{n}), i \in 2, \dots, n$ where $I_1 = \{i  i \text{ is odd and } 2 \leq i \leq n\}$ , and $I_2 = \{i  i \text{ is even and } 2 \leq i \leq n\}$ Pareto Front : $f_2 = (1 - \sqrt{f_1})^2$	$[0, 1] \times [-1, 1]^{n-1}$	30	Convex
F2	$f_1 = x_1 + \frac{2}{ I_1 } \sum_{i \in I_1}  g_i + \frac{\sin(\pi g_i)}{\pi} $ $f_2 = \frac{1 - 19x_1}{19} + \frac{2}{ I_2 } \sum_{i \in I_2}  g_i + \frac{\sin(\pi g_i)}{\pi} $ if $x_1 \leq 0.005$ $\frac{1}{19} - \frac{x_1}{19} + \frac{2}{ I_2 } \sum_{i \in I_2}  g_i + \frac{\sin(\pi g_i)}{\pi} $ otherwise $g_i = x_i - 0.9 \sin(\frac{i\pi}{n}), i \in 2, \dots, n$ where $I_1 = \{i  i \text{ is odd and } 2 \leq i \leq n\}$ , and $I_2 = \{i  i \text{ is even and } 2 \leq i \leq n\}$ Pareto Front : $f_2 = \sqrt{(1 - f_1^2)}$	$[0, 1] \times [-1, 1]^{n-1}$	30	Piecewise, convex
F3	$f_1 = x_1 + \frac{2}{ I_1 } \sum_{i \in I_1} (1 - e^{- g_i })$ $f_2 = \frac{1 - 8x_1^4}{8(1 - x_1)^4} + \frac{2}{ I_2 } \sum_{i \in I_2} (1 - e^{- g_i })$ if $x_1 \leq 0.5$ $\frac{1}{8}(1 - x_1)^4 + \frac{2}{ I_2 } \sum_{i \in I_2} (1 - e^{- g_i })$ otherwise $g_i = x_i - 0.9 \sin(\frac{i\pi}{n}), i \in 2, \dots, n$ where $I_1 = \{i  i \text{ is odd and } 2 \leq i \leq n\}$ , and $I_2 = \{i  i \text{ is even and } 2 \leq i \leq n\}$ Pareto Front : $f_2 = 0.5(1 - f_1 + \sqrt{1 - f_1}) \cos^2(4\pi(1 - f_1))$	$[0, 1] \times [-1, 1]^{n-1}$	30	Separable, convex, concave
F4	$f_1 = (1 + g)x_1$ $f_2 = (1 + g)(1 - \sqrt{x_1})^3$ $g = 2 \sin(0.5\pi x_1)(n - 1 + \sum_{i=2}^n (y_i^2 - \cos(2\pi y_i)))$ where $y_{i=2:n} = x_i - \sin(0.5\pi x_i)$ Pareto Front : $f_2 = (1 - \sqrt{f_1})^3$	$[0, 1]^n$	30	Convex
F5	$f_1 = (1 + g)(x_1 + 0.05 \sin(6\pi x_1))^2$ $f_2 = (1 + g)(1 - x_1 + 0.05 \sin(6\pi x_1))^2$ $g = 2 \sin(0.5\pi x_1)(n - 1 + \sum_{i=2}^n (y_i^2 - \cos(2\pi y_i)))$ where $y_{i=2:n} = x_i - \sin(0.5\pi x_i)$ Pareto Front : $f_1^{0.5} + f_2^{0.5} = 1 + 0.1 \sin(3\pi(f_1^{0.5} - f_2^{0.5} + 1))$	$[0, 1]^n$	30	Nonconvex
F6	$f_1 = (1 + g)(x_1 + 0.05 \sin(6\pi x_1))^{0.2}$ $f_2 = (1 + g)(1 - x_1 + 0.05 \sin(6\pi x_1))^{10}$ $g = 2 \sin(0.5\pi x_1)(n - 1 + \sum_{i=2}^n (y_i^2 - \cos(2\pi y_i)))$ where $y_{i=2:n} = x_i - \sin(0.5\pi x_i)$ Pareto Front : $f_1^2 + f_2^{0.1} = 1 + 0.1 \sin(3\pi(f_1^2 - f_2^{0.1} + 1))$	$[0, 1]^n$	30	Nonconvex
F7	$f_1 = (1 + g)(1 - x_1)$ $f_2 = 0.5(1 + g)(x_1 + \sqrt{x_1} \cos^2(4\pi x_1))$ $g = 2 \sin(0.5\pi x_1)(n - 1 + \sum_{i=2}^n (y_i^2 - \cos(2\pi y_i)))$ where $y_{i=2:n} = x_i - \sin(0.5\pi x_i)$ Pareto Front : $f_2 = 0.5(1 - f_1 + \sqrt{1 - f_1}) \cos^2(4\pi(1 - f_1))$	$[0, 1]^n$	30	Nonconvex, disconnected

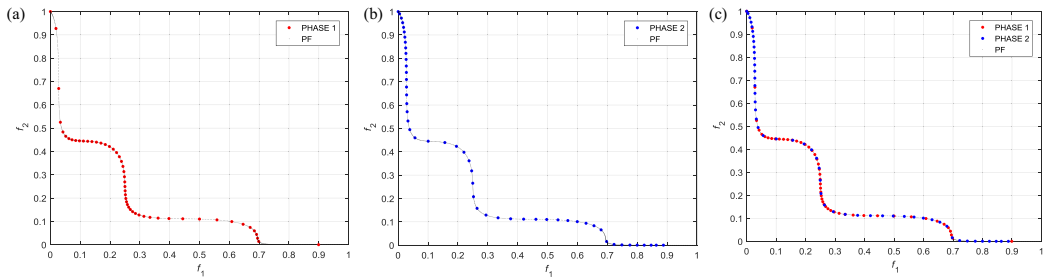


**Fig. 3.** Illustration of the Pareto front obtained by iMOEA/D for F5 relative to Phases 1, 2 and their combination.

have more Pareto solutions, which depend on the initial population size ( $N$ ). Thus, if the same  $N$  is applied for both the methods, the HV-metric values of MOEA/D-TPN may be better than those of iMOEA/D. This is because MOEA/D-TPN will use the same  $N$  in both phases if the crowded information of obtained solutions in Phase 1 is satisfied, and Phase II is executed, while iMOEA/D always uses half of  $N$  for both phases. For this evaluation, therefore, two different sizes of  $N$  ( $N=50, 100$ ) are investigated for MOEA/D-TPN, and only one size of  $N$  ( $N=100$ ) is used for iMOEA/D.

The statistical results of F5 and F6 gained by iMOEA/D and MOEA/D-TPN are provided in Table 2. A comparison of results ob-

tained by iMOEA/D and MOEA/D-TPN with  $N=50$  indicates that iMOEA/D outperforms MOEA/D-TPN. Specifically, all the comparative quantities obtained by iMOEA/D are better than those of MOEA/D-TPN, except for the computational cost in F6. However, the reason for the reduction of the computation cost in F6 is because the crowded information of obtained results in Phase 1 is unsatisfied, and Phase 2 of MOEA/D-TPN is not executed. This explains why its HV-metric values of F6 is much worse than those of iMOEA/D. This is also reflected in Fig. 4a. Moreover, the diversity of weight vectors with  $N=50$  is often less than that with  $N=100$ ,

**Table 2**  
Comparison of statistical results of iMOEA/D and MOEA/D-TPN for F5 and F6.

Metric	Method		F5	F6
HV	MOEA/D-TPN (N = 50)	Mean	3.8259	3.3190
		Worst	3.8259	3.3188
		Best	3.8260	3.3191
		Std.	0.0000	0.0001
	MOEA/D-TPN (N = 100)	Mean	3.8271	3.3221
		Worst	3.8271	3.3219
		Best	3.8272	3.3223
		Std.	0.0000	0.0001
	iMOEA/D	Mean	3.8261	3.3233
		Worst	3.8260	3.3232
		Best	3.8261	3.3233
		Std.	0.0000	0.0000
IGD	MOEA/D-TPN (N = 50)	Mean	0.0010	0.0212
		Worst	0.0011	0.0221
		Best	0.0009	0.0207
		Std.	0.0001	0.0004
	MOEA/D-TPN (N = 100)	Mean	0.0009	0.0216
		Worst	0.0010	0.0220
		Best	0.0009	0.0201
		Std.	0.0000	0.0004
	iMOEA/D	Mean	0.0009	0.0118
		Worst	0.0010	0.0125
		Best	0.0008	0.0111
		Std.	0.0000	0.0004
Computational cost	MOEA/D-TPN (N = 50)	FEs	22,337	13,667
		Time (min)	0.3382	0.1697
	MOEA/D-TPN (N = 100)	FEs	39,524	21,512
		Time (min)	0.6755	0.2671
	iMOEA/D	FEs	19,067	19,537
		Time (min)	0.2641	0.2426

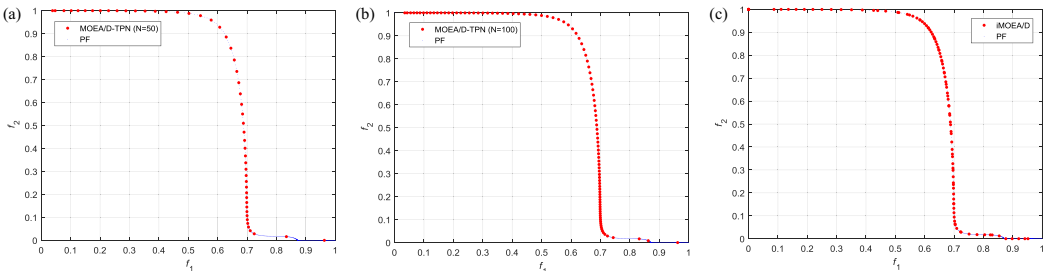


**Fig. 4.** Illustration of the Pareto fronts obtained by MOEA/D-TPN (N=50,100) and iMOEA/D for F6.

which can lead to the reduction of the quality of solutions obtained by MOEA/D-TPN.

In contrast to MOEA/D-TPN with  $N=50$ , for the test F5, the HV-metric values obtained by MOEA/D-TPN with  $N=100$  are much better than those of iMOEA/D, which is as an obvious result of the increased number of Pareto solutions. Nevertheless, the computational cost is mostly doubled because of the double growth of the population when both phases are executed. Like the case of  $N=50$ , for the test F6, MOEA/D-TPN with  $N=100$  also terminates at Phase 1. Thus, its HV-metric values are still worse than those of iMOEA/D. In addition, the computational cost in this case is still higher compared to those of iMOEA/D. Also, for the test F6, although the diversity of weight vectors is the same, the quality of IGD-metric values of MOEA/D-TPN is still bigger than those of iMOEA/D. This may be due to the efficiency of using the nadir point  $z^{nad}$  in the second phase of iMOEA/D.

From the above evaluation results, it can be concluded that the incorporation of the two recent features (i.e. an adaptive replacement strategy and a stopping criterion), and the idea of using two different subsets of weight vectors are helpful and meaningful

compared to MOEA/D-TPN. To further evaluate the performance of iMOEA/D, MOEA/D-TPN is also used to solve the remaining test instances together with NSGA-II and MOEA/D, and for a consistent comparison, the initial populations ( $N$ ) of all the methods are set to be the same.

5.1.4. Experimental results

In this part, iMOEA/D is tested on all the remaining functions, and the obtained statistical results are presented in Table 3 in comparison with those gained by NSGA-II, MOEA/D and MOEA/D-TPN. By taking a close look at the HV-metric values in Table 3, it can be seen that MOEA/D-TPN is the best method, except for the F6 metrics. However, it should be noted that for F1-F5 and F7, both phases of MOEA/D-TPN are carried out with the same  $N$ . Thus, the obtained optimal solutions are mostly doubled, and as a result, the HV-metric values are obviously much better. The HV-metric values for F6 are almost the same with those of MOEA/D and worse than those of iMOEA/D and NSGA-II, which are because only the first phase of MOEA/D-TPN is executed. The comparison between iMOEA/D, MOEA/D and NSGA-II indicates that iMOEA/D outper-

**Table 3**  
Statistical results for the benchmark tests.

Metric	Method		F1	F2	F3	F4	F5	F6	F7	
HV	NSGA-II	Mean	1.6317	3.9422	3.4820	3.8957	3.8250	3.3226	3.6787	
		Worst	1.5441	3.9334	3.4739	3.8950	3.8245	3.3223	3.6783	
		Best	1.6833	3.9446	3.4855	3.8962	3.8254	3.3230	3.6789	
	MOEA/D	Std.	0.0388	0.0027	0.0035	0.0003	0.0003	0.0002	0.0001	
		Mean	1.6123	3.9462	3.4925	3.8949	3.8247	3.3221	3.6787	
		Worst	1.6076	3.9458	3.4906	3.8948	3.8246	3.3221	3.6786	
	MOEA/D-TPN	Best	1.6199	3.9464	3.4933	3.8949	3.8249	3.3222	3.6787	
		Std.	0.0029	0.0002	0.0007	0.0000	0.0001	0.0000	0.0000	
		Mean	1.8055	3.9486	3.4958	3.8985	3.8271	3.3221	3.6798	
	iMOEA/D	Worst	1.7919	3.9484	3.4937	3.8985	3.8271	3.3219	3.6798	
		Best	1.8111	3.9488	3.4966	3.8986	3.8272	3.3223	3.6799	
		Std.	0.0041	0.0001	0.0008	0.0000	0.0000	0.0001	0.0000	
	IGD	NSGA-II	Mean	1.7793	3.9480	3.4926	3.8969	3.8261	3.3233	3.6784
			Worst	1.7720	3.9475	3.4901	3.8968	3.8260	3.3232	3.6783
			Best	1.7877	3.9481	3.4934	3.8970	3.8261	3.3233	3.6784
MOEA/D		Std.	0.0039	0.0001	0.0009	0.0000	0.0000	0.0000	0.0000	
		Mean	0.0308	0.0069	0.0105	0.0042	0.0012	0.0126	0.0007	
		Worst	0.0446	0.0114	0.0157	0.0053	0.0014	0.0177	0.0009	
MOEA/D-TPN		Best	0.0201	0.0041	0.0075	0.0027	0.0009	0.0034	0.0005	
		Std.	0.0064	0.0023	0.0023	0.0005	0.0001	0.0037	0.0001	
		Mean	0.0047	0.0011	0.0018	0.0011	0.0008	0.0217	0.0005	
iMOEA/D		Worst	0.0056	0.0016	0.0022	0.0012	0.0009	0.0222	0.0006	
		Best	0.0041	0.0010	0.0015	0.0011	0.0007	0.0213	0.0004	
		Std.	0.0004	0.0002	0.0002	0.0000	0.0000	0.0002	0.0000	
Computational cost		NSGA-II	Mean	0.0065	0.0014	0.0016	0.0035	0.0009	0.0216	0.0006
			Worst	0.0077	0.0027	0.0020	0.0035	0.0010	0.0220	0.0006
			Best	0.0056	0.0010	0.0014	0.0034	0.0009	0.0201	0.0005
	MOEA/D	Std.	0.0005	0.0004	0.0001	0.0000	0.0000	0.0004	0.0000	
		Mean	0.0065	0.0010	0.0020	0.0035	0.0009	0.0118	0.0005	
		Worst	0.0073	0.0012	0.0033	0.0037	0.0010	0.0125	0.0006	
	MOEA/D-TPN	Best	0.0057	0.0010	0.0017	0.0034	0.0008	0.0111	0.0004	
		Std.	0.0004	0.0001	0.0003	0.0001	0.0000	0.0004	0.0000	
		FES	71,417	88,443	83,253	44,483	75,247	57,287	57,033	
	MOEA/D	Time (min)	0.8427	1.2515	0.8603	0.4196	0.7851	0.8631	0.5931	
		FES	101,000	101,000	101,000	32,151	24,997	27,421	25,434	
		Time (min)	1.2167	1.2667	1.0667	0.3342	0.2887	0.3394	0.2728	
	MOEA/D-TPN	FES	170,191	88,845	162,596	42,621	39,524	21,512	54,068	
		Time (min)	2.2804	1.1034	1.7003	0.6545	0.6755	0.2671	0.5831	
		FES	82,597	63,950	82,700	20,557	19,067	19,537	24,572	
iMOEA/D	Time (min)	1.1067	0.7942	0.8648	0.3157	0.2641	0.2426	0.2650		

forms NSGA-II and MOEA/D on F1-F6, while NSGA-II and MOEA/D are better on F7. From the comparison of IGD-metric values, it can be seen that iMOEA/D performs slightly better than MOEA/D-TPN and both somewhat worse than MOEA/D, but all three methods are significantly better than NSGA-II. Regarding the computational cost (in terms of time in minute (min) and the number of function evaluations (FEs)), however, it can be observed that iMOEA/D is the best method with the smallest amount of FEs for all the tests. The total FEs of iMOEA/D for F1-F7 is 312,980 which is almost 46% less than those of MOEA/D-TPN (579,357), nearly 25% less than those of MOEA/D (413,003), approximately 35% less than those of NSGA-II (477,163). By looking at the standard deviation (Std.), it is observed that for all the investigated benchmark tests the standard deviations of iMOEA/D, MOEA/D-TPN and MOEA/D are quite small, while those of NSGA-II are often larger.

Based on the obtained statistical results, it can be concluded that iMOEA/D is more effective than NSGA-II and MOEA/D in terms of the distribution of optimal solutions over the PFs and the computational cost. Compared with MOEA/D-TPN, iMOEA/D performs worse with respect to HV-metric values, but significantly better in terms of the computational cost and slightly better concerning IGD-metric values. From the results, it can also be recognized that iMOEA/D is a proper method that can balance effectively between the quality of solutions and the computational cost.

Corresponding to the results given in Table 3, the PFs acquired by the methods are plotted in Fig. 5. From the figures, it can be seen that NSGA-II, MOEA/D-TPN and iMOEA/D have the ability to

give a better distribution of solutions on complicated PFs compared to MOEA/D. However, when taking a closer look at the figures, it can be observed that the quality of the solutions on the PFs obtained by MOEA/D, MOEA/D-TPN and iMOEA/D is much better than those obtained by NSGA-II. Here, it is also recognized that MOEA/D-TPN has more optimal solutions on the PFs at F1-F5 and F7, while those of F6 are almost the same with those of MOEA/D. These illustrations again reflect the HV- and IGD-metric values provided in Table 3.

### 5.2. Structural optimization problems

In this section, iMOEA/D is applied to deal with three optimal design problems of truss structures. Since the computational cost of MOEA/D-TPN has been demonstrated to be huge in the previous section, which is a large restriction for real-world engineering applications, only MOEA/D and NSGA-II are applied to solve these problems for comparison purposes. The problems include a 15-bar planar truss (Tang, Tong, & Gu, 2005), a 72-bar space truss (Wu & Chow, 1995), and a 160-bar space truss (Groenwold & Stander, 1997) as shown in Figs. 6–8, respectively. These are structural optimization problems which are widely used to measure the applicability of single-objective optimization methods in the literature.

In this study, the above problems are reformulated as bi-objective design optimization problems. For all of the problem-cases considered, the aim of the objective functions is to minimize

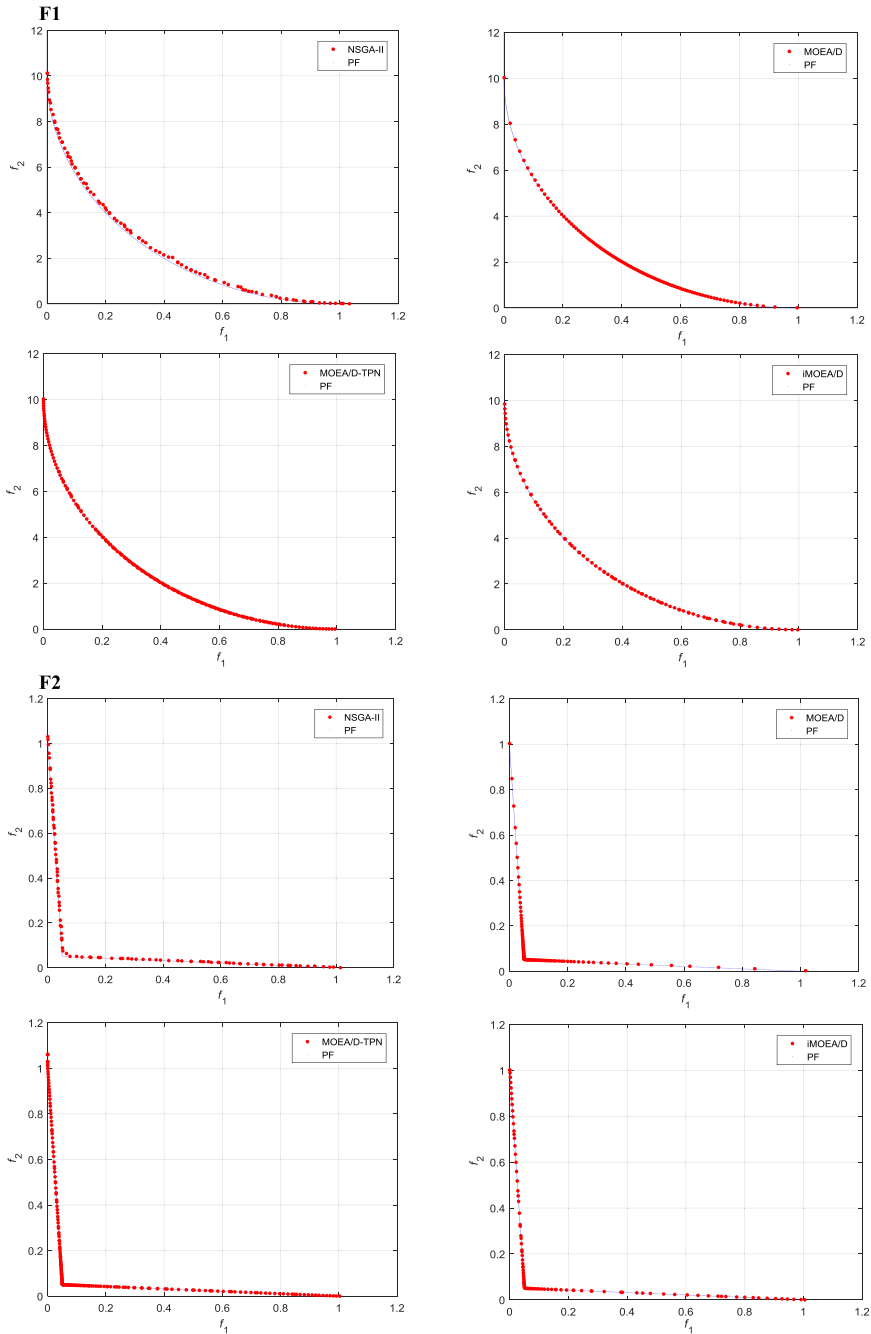


Fig. 5. Pareto fronts obtained by NSGA-II, MOEA/D, MOEA/D-TPN and iMOEA/D for F1-F7.

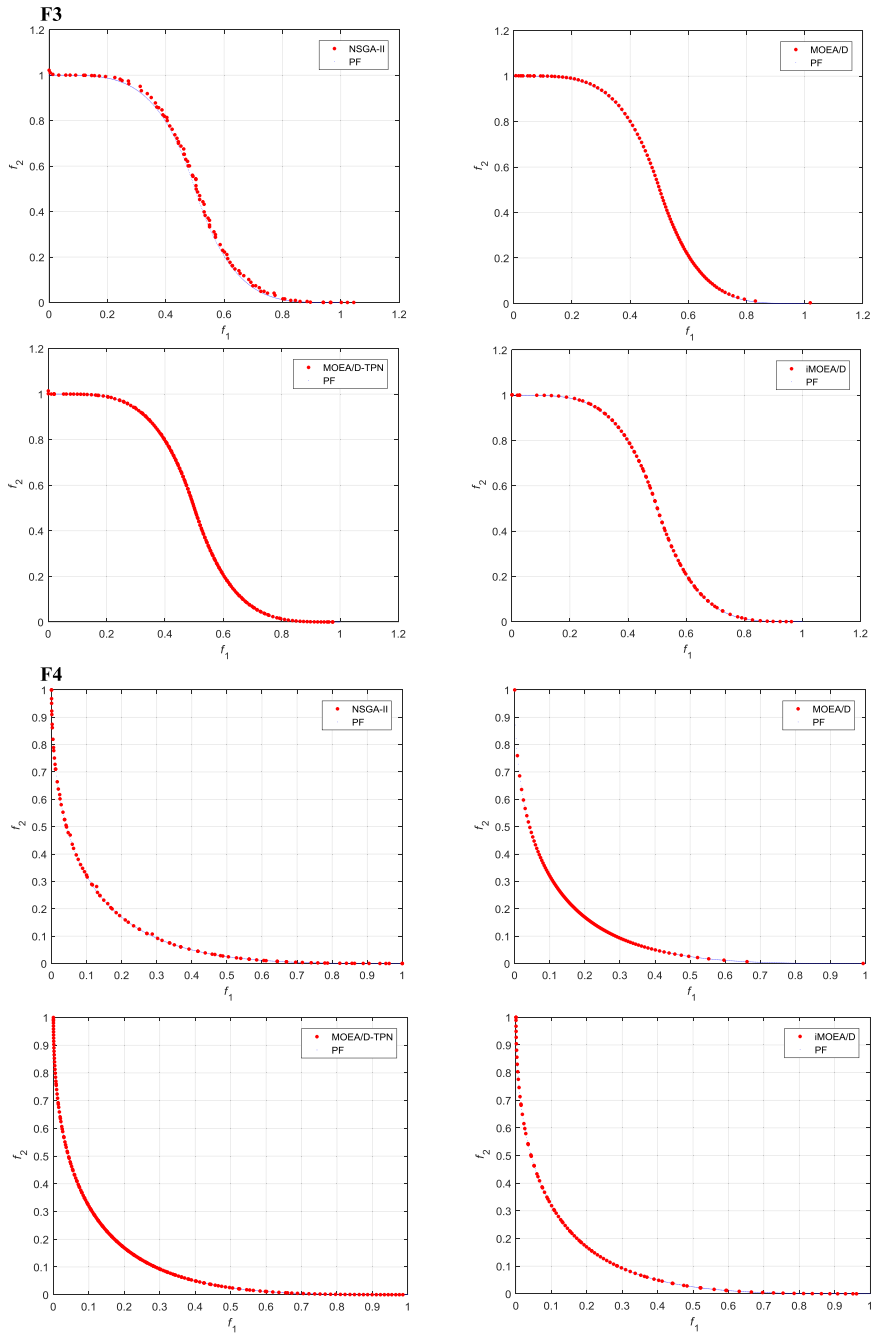


Fig. 5. Continued

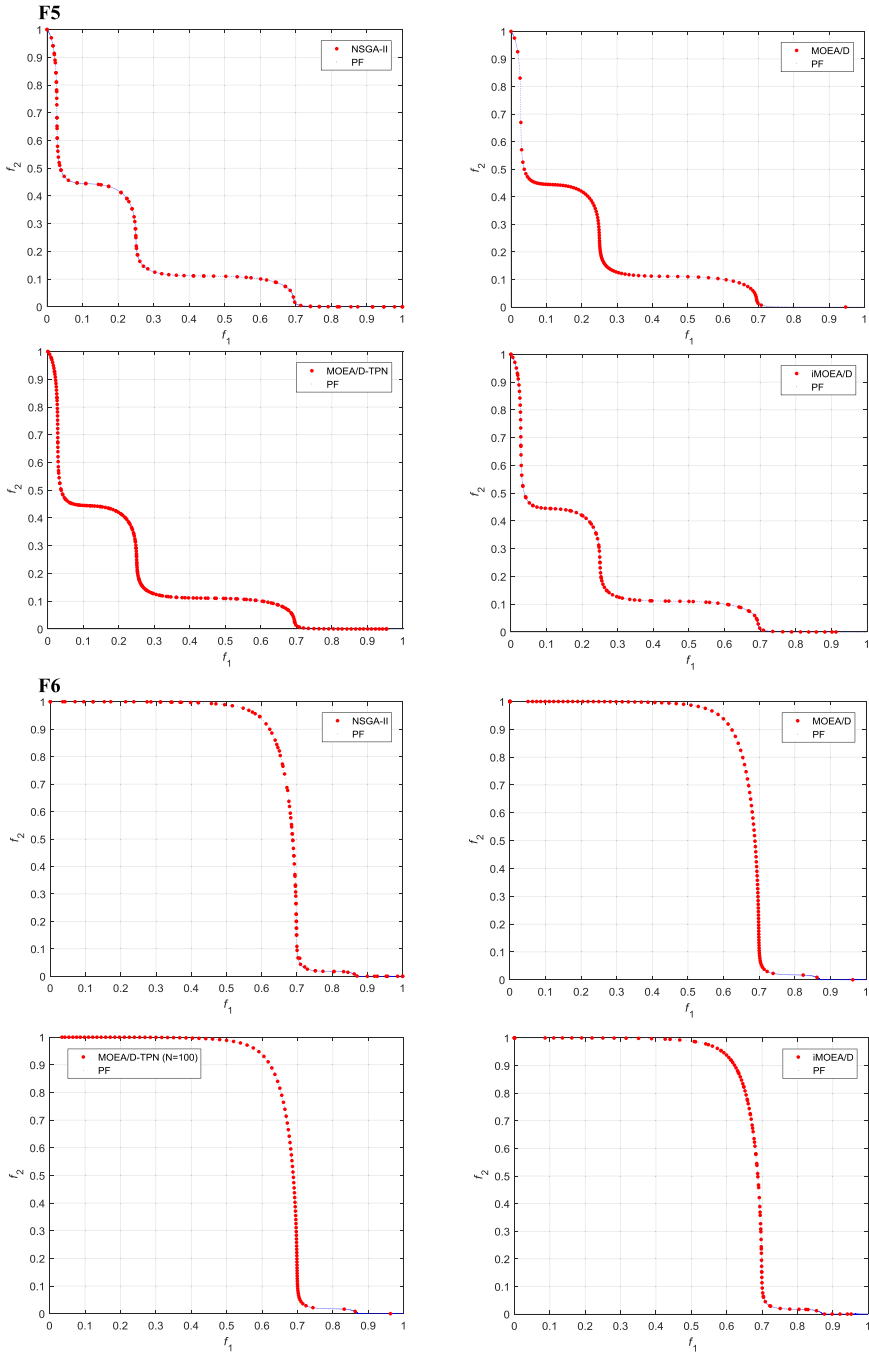


Fig. 5. Continued

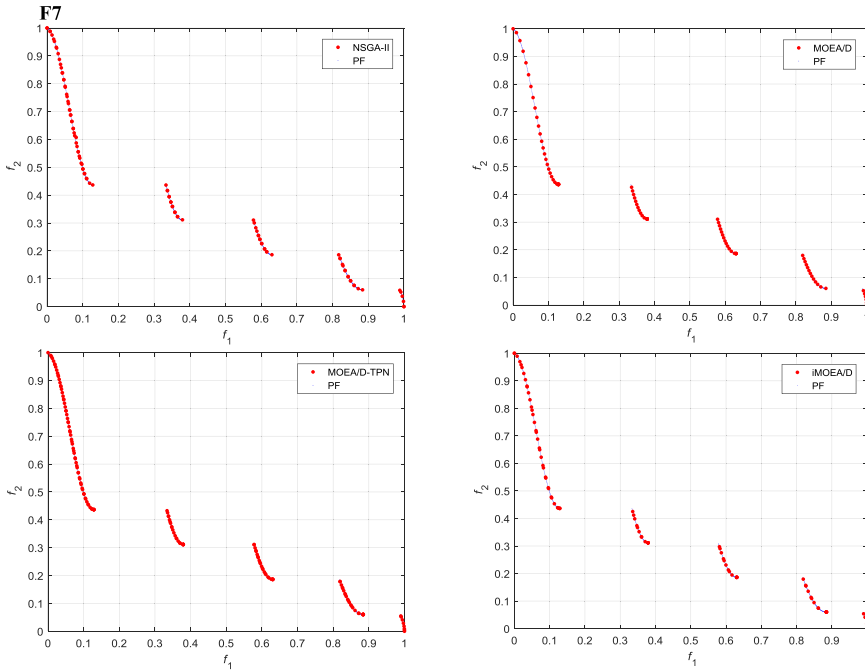


Fig. 5. Continued

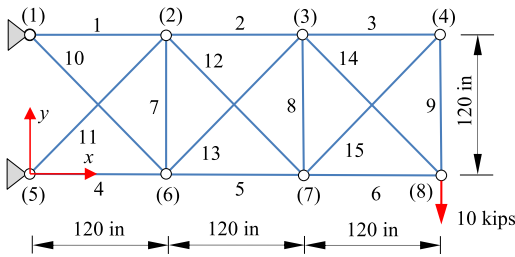


Fig. 6. The 15-bar planar truss.

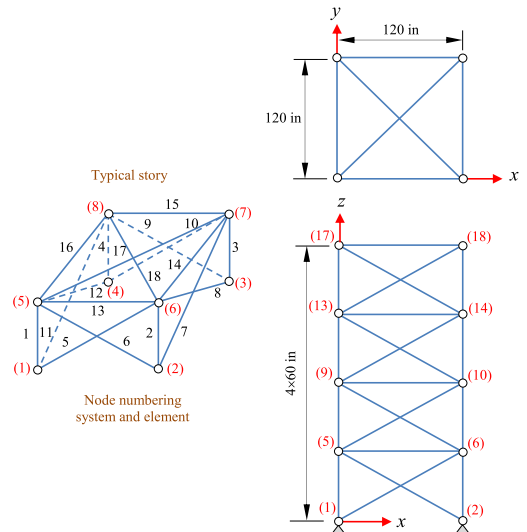


Fig. 7. The 72-bar space truss.

the overall weight of the structures and the maximum displacement at the truss nodes. The design variables and the constraints for each problem are described as follows:

- The 15-bar planar truss: The design problem has 8 continuous design variables of node coordinates and 15 discrete design variables of cross-sectional areas. All members are subjected to the stress limitation of  $\pm 25$  (ksi). The details of the input data for this problem can be found in Ho-Huu, Nguyen-Thoi, Nguyen-Thoi, and Le-Anh (2015) and Rahami, Kaveh, and Gholipour (2008).
- The 72-bar space truss: The structure has 72 members that are divided into 16 groups corresponding to 16 design variables. The design variables are discrete values and selected from an available set. This structure was designed for two separate loading conditions and subjected to design constraints which consist of the stress limitations of  $\pm 25,000$  psi and a restric-

tion for all nodal displacements of  $\pm 0.25$  in. The input data for the problem is available in Ho-Huu, Nguyen-Thoi, Vo-Duy, and Nguyen-Trang (2016) and Kaveh and Mahdavi (2014).

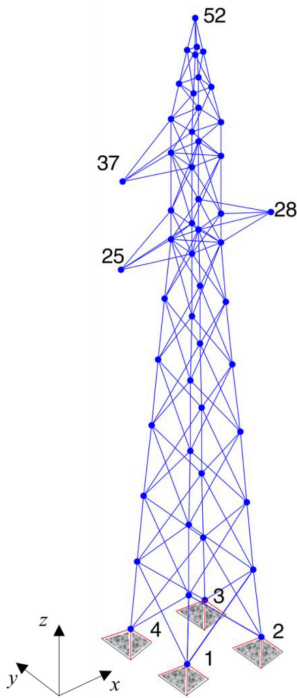


Fig. 8. The 160-bar space truss.

- The 160-bar space truss: The 160 bars of the truss are connected to 38 independent discrete design variables. The structure is designed for eight independent load cases, and the design constraints are considered for compression members. The details for these input data are given in [Groenwold and Stander \(1997\)](#) and [Ho-Huu et al. \(2016\)](#).

In order to handle constraints and discrete design variables for the problems in this section, a constraint-handling technique recently proposed in [Jan and Khanum \(2013\)](#), and a rounding technique in [Kaveh and Mahdavi \(2014\)](#) are utilized, respectively. All three problems are run 20 independent times with a population size of 80. Due to the exact solutions for these problems not being available, a set of all non-dominated solutions obtained by three methods after 20 independent runs is used as an approximate PF for evaluating the IGD metric. To validate the reliability of the used methods, some obtained solutions on PFs are also compared to those acquired by single-objective optimization methods in the literature.

Table 4 provides the statistical results obtained by the methods. At first glance, it can be seen that the acquired results show the same trend for all the problems. Specifically, in a comparison of the HV-metric values, it is observed that iMOEA/D is the best method in all statistical indices including the worst, best and standard deviation (Std.) values, and NSGA-II is the second one. This implies that iMOEA/D shows a considerable improvement on the distribution of solutions over a PF compared with MOEA/D and NSGA-II. Nevertheless, this order is slightly changed in terms of the IGD-metric values, where the order rank is MOEA/D, iMOEA/D and

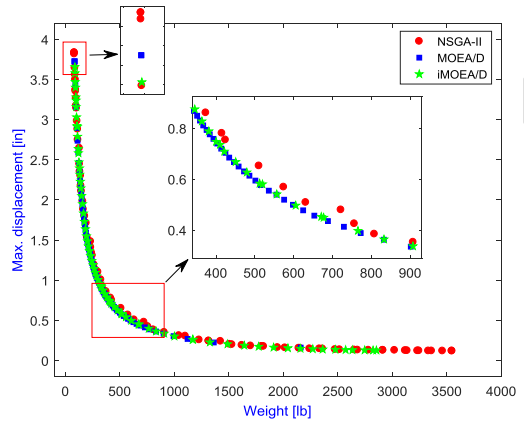


Fig. 9. Pareto fronts with the largest HV among 20 runs for the 15-bar planar truss.

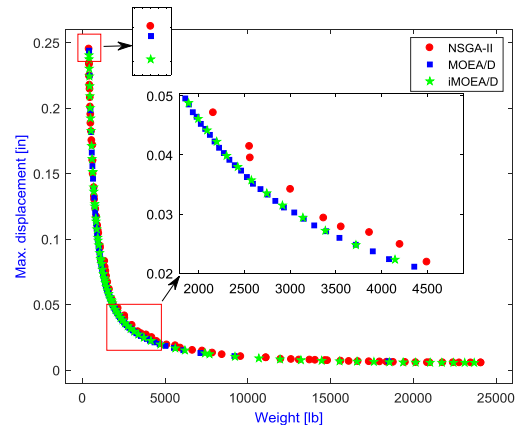


Fig. 10. Pareto fronts with the largest HV among 20 runs for the 72-bar space truss.

NSGA-II for all the statistical indexes. This means that the quality of solutions gained by MOEA/D is often better than those of iMOEA/D and NSGA-II. However, this difference between MOEA/D and iMOEA/D is small, while it is quite large when comparing with those of NSGA-II.

In terms of computational cost, again iMOEA/D is the best method with the lowest values of time and FEs, while MOEA/D is better than NSGA-II. The FEs of iMOEA/D is around half to three-quarters of those of NSGA-II, and around three-quarters of those of MOEA/D.

From the above results, it can be concluded that with the new features on MOEA/D, iMOEA/D has a significant improvement on the performance of the algorithm, particularly in the distribution of solutions over PFs and the computational cost.

The PFs obtained by the methods for all considered problems are illustrated in [Figs. 9–11](#), respectively. As shown in the figures, the design problems have complicated PFs with a long tail at both ends, and the distributions of solutions acquired by the methods are quite different. The PFs of NSGA-II are often wider than those of MOEA/D and iMOEA/D. Their solution quality, however, is not as good as those of MOEA/D and iMOEA/D. A comparison between

**Table 4**  
Statistical results for the structural optimization problems.

Metric	Method		15-bar truss	72-bar truss	160-bar truss
HV	NSGA-II	Mean	1.3909	0.6413	5.2517
		Worst	1.3880	0.6405	5.2352
		Best	1.3929	0.6419	5.2623
		Std.	0.0012	0.0004	0.0066
	MOEA/D	Mean	1.3901	0.6399	5.2434
		Worst	1.3875	0.6380	5.2109
		Best	1.3920	0.6411	5.2664
		Std.	0.0015	0.0009	0.0186
	iMOEA/D	Mean	1.3981	0.6442	5.3039
		Worst	1.3970	0.6439	5.2914
		Best	1.3989	0.6445	5.3115
		Std.	0.0006	0.0002	0.0054
IGD	NSGA-II	Mean	4.5106	14.4666	12.2144
		Worst	14.6534	20.6656	17.8192
		Best	1.8665	9.2638	8.3395
		Std.	3.1474	2.1842	3.0719
	MOEA/D	Mean	0.3284	2.5892	1.2162
		Worst	0.6924	4.4179	2.0974
		Best	0.2259	1.3245	0.3566
		Std.	0.1097	0.9183	0.5282
	iMOEA/D	Mean	1.2766	6.1325	5.1365
		Worst	2.1820	12.3974	10.1472
		Best	0.3817	2.5065	1.5691
		Std.	0.4866	2.4370	2.2344
Computational cost	NSGA-II	FES	80,000	80,000	80,000
		Time (min)	1.6533	4.5233	65.5117
	MOEA/D	FES	68,351	57,371	72,300
		Time (min)	1.1636	3.5033	38.1137
	iMOEA/D	FES	40,035	40,803	64,397
		Time (min)	0.8434	2.2558	32.3817

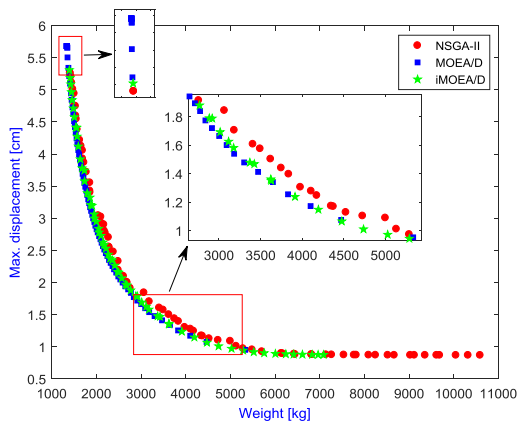


**Fig. 11.** Pareto fronts with the largest HV among 20 runs for the 160-bar space truss.

MOEA/D and iMOEA/D shows that iMOEA/D always offers a better enhancement on the spread of solutions over the PFs.

The comparison of the obtained solutions with those of single-objective optimization approaches in the literature is presented in Table 5, where the results of iMOEA/D, MOEA/D, and NSGA-II are extracted from the end of the second objective, i.e. maximum displacement as shown in Figs. 9–11, respectively. From the table, the results indicate that the obtained solutions are reasonable and reliable. Although there is a difference between solutions, this can be due to the different purposes of the employed optimization methods. In fact, the single-objective optimization methods only focus

on one objective, while the multi-objective optimization methods concentrate on the trade-off between two objectives. This is also shown by particular values of the objectives in the table. For example, in the 15-bar truss problem, the method in Ho-Huu et al. (2015) gives a weight of 74,6818 (lb) with a corresponding maximum displacement of 4.2044 (in), whilst iMOEA/D gives a larger weight of 87,0909 (lb), but with a smaller maximum displacement of 3.6568 (in).

## 6. Conclusion

In this work, a newly improved version of MOEA/D named iMOEA/D is developed for solving BOPs with complicated PFs. In iMOEA/D, the set of the weight vectors of MOEA/D is numbered and partitioned into two subsets: one set with odd-weight vectors and the other with even ones. Then, a two-phase search strategy based on the MOEA/D framework is developed to optimize their corresponding populations. In the first phase, the population of the set of odd-weight vectors is optimized by using the Tchebycheff function with the ideal point  $z^*$ . After that, from the set of obtained solutions, the nadir point  $z^{\text{had}}$  is determined, and the Tchebycheff function with this point is applied for the set of even-weight vectors in the second phase. Moreover, the performance of the iMOEA/D is also further improved by the integration of two recent developments consisting of an adaptive replacement strategy and a stopping criterion.

The reliability, efficiency and the applicability of iMOEA/D are evaluated through the seven existing benchmark test functions with complicated PFs and three optimal design problems of truss structures. The obtained results from the benchmark test functions indicate that iMOEA/D is more competitive than MOEA/D, MOEA/D-TPN and NSGA-II. Although MOEA/D-TPN and NSGA-II provide PFs with better spread compared with iMOEA/D and MOEA/D, the computational cost of MOEA/D-TPN is significantly larger than that of iMOEA/D and MOEA/D, while the quality of op-

**Table 5**  
Comparison with single objective optimization designs.

Problem	Method	Weight	Maximum displacement
15-bar truss	Tang et al. (2005)	79.820 (lb)	4.2314 (in)
	Rahami et al. (2008)	76.685 (lb)	4.1161 (in)
	Ho-Huu et al. (2015)	74.681 (lb)	4.2044 (in)
	NSGA-II	82.159 (lb)	3.8358 (in)
	MOEA/D	84.163 (lb)	3.7259 (in)
	iMOEA/D	87.090 (lb)	3.6568 (in)
72-bar truss	Wu and Chow (1995)	427.203 (lb)	0.5996 (in)
	Kaveh et al. (2009)	393.380 (lb)	0.2501 (in)
	Ho-Huu et al. (2016)	389.334 (lb)	0.2496 (in)
	NSGA-II	401.830 (lb)	0.2452 (in)
	MOEA/D	409.254 (lb)	0.2437 (in)
	iMOEA/D	402.486 (lb)	0.2404 (in)
160-bar truss	Groenwold et al. (1997)	1359.781 (kg)	5.6092 (cm)
	Capriles, Fonseca, Barbosa, and Lemonge (2007)	1348.905 (kg)	5.6525 (cm)
	Ho-Huu et al. (2016)	1336.634 (kg)	5.6814 (cm)
	NSGA-II	1412.365 (kg)	5.2638 (cm)
	MOEA/D	1336.794 (kg)	5.6814 (cm)
	iMOEA/D	1396.266 (kg)	5.3089 (cm)

timal solutions of NSGA-II is not as good as that of iMOEA/D and MOEA/D. The obtained results from the practical applications show that iMOEA/D outperforms MOEA/D and NSGA-II, and is a good candidate for solving these kinds of problems.

Although iMOEA/D has shown a considerable improvement in the performance of the algorithm, it is currently still limited to bi-objective optimization problems. For future work, therefore, the idea of the division of weight vectors into two subsets (i.e. even and odd set) should be investigated and extended for optimization problems with more than two objectives. However, to implement this, it should be noted that the distribution of the divided sets should be equal over the weight space, which calls for considerable research efforts in the future. Moreover, although iMOEA/D obtains significant achievements in terms of computational cost compared to the compared methods, its total number of function evaluations is still high. This will be a major restriction when it is extended and applied to different large problems in civil engineering like frames, composite beams and plates, and for various applications in aerospace engineering, such as the optimal design of departure/arrival routes of aircraft and runway allocations, where the computational cost for each function evaluation is often quite large. Thus, in the future, approximate models like artificial neural network (ANN), adaptive neuro fuzzy inference system (ANFIS) (Ramasamy & Rajasekaran, 1996; Rodger, 2014a, 2014b) can also be developed and applied for approximating objective functions to assist iMOEA/D in solving large scale optimization problems in reality.

Furthermore, although the multi-objective optimization problems of truss structures have been solved, suitable criteria for selecting a good candidate from PFs are still an open question. Therefore, studies which aim to help engineering designers to pick a reasonable solution from PFs will also be a potential research direction for researchers in the future.

## Acknowledgment

The authors would like to thank the anonymous reviewers for their constructive, helpful and valuable comments and suggestions.

## Appendix

The Matlab source codes of MOEA/D, iMOEA/D and the truss optimization problems are available on the website: [https://www.researchgate.net/profile/V\\_Ho-Huu](https://www.researchgate.net/profile/V_Ho-Huu).

## References

- Abdul Kadhar, K. M., & Baskar, S. (2016). A stopping criterion for decomposition-based multi-objective evolutionary algorithms. *Soft Computing*, 1–20. <https://doi.org/10.1007/s00500-016-2331-7>.
- Cai, H., & Aref, A. J. (2015). A genetic algorithm-based multi-objective optimization for hybrid fiber reinforced polymeric deck and cable system of cable-stayed bridges. *Structural and Multidisciplinary Optimization*, 52(3), 583–594. <https://doi.org/10.1007/s00158-015-1266-4>.
- Capriles, P. V. S. Z., Fonseca, L. G., Barbosa, H. J. C., & Lemonge, A. C. C. (2007). Rank-based ant colony algorithms for truss weight minimization with discrete variables. *Communications in Numerical Methods in Engineering*, 23(6), 553–575. <https://doi.org/10.1002/cnm.912>.
- Das, I., & Dennis, J. (1998). Normal-boundary intersection: A new method for generating the pareto surface in nonlinear multicriteria optimization problems. *SIAM Journal on Optimization*, 8(3), 631–657. <https://doi.org/10.1137/S1052623496307510>.
- Deb, K. (2001). *Multi-objective optimization using evolutionary algorithms*. Wiley.
- Deb, K., Pratap, S., Agarwal, S., & Meyarivan, T. (2002). A fast and elitist multiobjective genetic algorithm: NSGA-II. *IEEE Transactions on Evolutionary Computing*, 6(2), 182–197. <https://doi.org/10.1109/4235.996017>.
- Grandhi, R. (1993). Structural optimization with frequency constraints – A review. *AIAA Journal*, 31(12), 2296–2303. <https://doi.org/10.2514/3.11928>.
- Groenwold, A. A., & Stander, N. (1997). Optimal discrete sizing of truss structures subject to buckling constraints. *Structural Optimization*, 14(2–3), 71–80. <https://doi.org/10.1007/BF01812508>.
- Hartjes, S., & Visser, H. (2016). Efficient trajectory parameterization for environmental optimization of departure flight paths using a genetic algorithm. *Proceedings of the Institution of Mechanical Engineers, Part G: Journal of Aerospace Engineering*, 0(0), 1–9. <https://doi.org/10.1177/0954410016648980>.
- Hartjes, S., Visser, H. G., & Heblly, S. J. (2010). Optimisation of RNAV noise and emission abatement standard instrument departures. *Aeronautical Journal*, 114(1162), 757–767. <https://doi.org/10.1017/CBO9781107415324.004>.
- Ho-Huu, V., Nguyen-Thoi, T., Nguyen-Thoi, M. H., & Le-Anh, L. (2015). An improved constrained differential evolution using discrete variables (D-ICDE) for layout optimization of truss structures. *Expert Systems with Applications*, 42(20), 7057–7069. <https://doi.org/10.1016/j.eswa.2015.04.072>.
- Ho-Huu, V., Nguyen-Thoi, T., Vo-Duy, T., & Nguyen-Trang, T. (2016). An adaptive elitist differential evolution for truss optimization with discrete variables. *Computer & Structures*, 165, 59–75. <https://doi.org/10.1016/j.compstruc.2015.11.014>.
- Jan, M. A., & Khanum, R. A. (2013). A study of two penalty-parameterless constraint handling techniques in the framework of MOEA/D. *Applied Soft Computing Journal*, 13(1), 128–148. <https://doi.org/10.1016/j.asoc.2012.07.027>.
- Jiang, S., & Yang, S. (2016). An improved multiobjective optimization evolutionary algorithm based on decomposition for complex pareto fronts. *IEEE Transactions on Cybernetics*, 46(2), 421–437. <https://doi.org/10.1109/TCYB.2015.2403131>.
- Kaveh, A., & Mahdavi, V. R. (2014). Colliding bodies optimization method for optimum discrete design of truss structures. *Computer & Structures*, 139, 43–53. <https://doi.org/10.1016/j.advengsoft.2014.01.002>.
- Kaveh, A., & Talatahari, S. (2009). A particle swarm ant colony optimization for truss structures with discrete variables. *Journal of Constructional Steel Research*, 65(8–9), 1558–1568. <https://doi.org/10.1016/j.jcsr.2009.04.021>.
- Konstantinidis, A., & Yang, K. (2012). Multi-objective energy-efficient dense deployment in wireless sensor networks using a hybrid problem-specific MOEA/D. *Applied Soft Computing Journal*, 12(7), 1847–1864. <https://doi.org/10.1016/j.asoc.2012.04.017>.

- Li, H., & Zhang, Q. (2009). Multiobjective optimization problems with complicated pareto sets, MOEA/D and NSGA-II. *IEEE Transactions on Evolutionary Computation*, 13(2), 284–302. <https://doi.org/10.1109/TEVC.2008.925798>.
- Li, K., Kwong, S., Zhang, Q., & Deb, K. (2015). Interrelationship-based selection for decomposition multiobjective optimization. *IEEE Transactions on Cybernetics*, 45(10), 2076–2088. <https://doi.org/10.1109/TCYB.2014.2365354>.
- Messac, A., Ismail-Yahaya, A., & Mattson, C. A. (2003). The normalized normal constraint method for generating the Pareto frontier. *Structural and Multidisciplinary Optimization*, 25(2), 86–98. <https://doi.org/10.1007/s00158-002-0276-1>.
- Miettinen, K. (1999). *Nonlinear multiobjective optimization*. Norwell, MA: Kluwer.
- Qi, Y., Ma, X., Liu, F., Jiao, L., Sun, J., & Wu, J. (2013). MOEA/D with adaptive weight adjustment. *Evolutionary Computation*, 22(3), 231–264. <https://doi.org/10.1162/EVC0>.
- Rahami, H., Kaveh, A., & Gholipour, Y. (2008). Sizing, geometry and topology optimization of trusses via force method and genetic algorithm. *Engineering Structures*, 30(9), 2360–2369. <https://doi.org/10.1016/j.engstruct.2008.01.012>.
- Ramasamy, J. V., & Rajasekaran, S. (1996). Artificial neural network and genetic algorithm for the design optimization of industrial roofs – A comparison. *Computers & Structures*, 58(4), 747–755. [https://doi.org/http://dx.doi.org/10.1016/0045-7949\(95\)00179-K](https://doi.org/http://dx.doi.org/10.1016/0045-7949(95)00179-K).
- Rodger, J. A. (2014a). A fuzzy nearest neighbor neural network statistical model for predicting demand for natural gas and energy cost savings in public buildings. *Expert Systems With Applications*, 41(4), 1813–1829. <https://doi.org/10.1016/j.eswa.2013.08.080>.
- Rodger, J. A. (2014b). Application of a fuzzy feasibility bayesian probabilistic estimation of supply chain backorder aging, unfilled backorders, and customer wait time using stochastic simulation with Markov blankets. *Expert Systems With Applications*, 41(16), 7005–7022. <https://doi.org/10.1016/j.eswa.2014.05.012>.
- Roudenko, O., & Schoenauer, M. (2004). A steady performance stopping criterion for pareto-based evolutionary algorithms. In Proceedings of the 6th international multi-objective programming and goal programming conference, Hammamet, Tunisia.
- Sharma, S., & Rangaiah, G. P. (2013). An improved multi-objective differential evolution with a termination criterion for optimizing chemical processes. *Computers and Chemical Engineering*, 56, 155–173. <https://doi.org/10.1016/j.compchemeng.2013.05.004>.
- Song, L. (2011). NGPM – A NSGA-II program in matlab, college of astronautics, Northwestern Polytechnica. <https://doi.org/Aerospace Structural Dynamics Research Laboratory College of Astronautics, Northwestern Polytechnical University, China>.
- Storn, R., & Price, K. (1997). Differential evolution - A simple and efficient heuristic for global optimization over continuous spaces. *Journal of Global Optimization*, 11(4), 341–359. <https://doi.org/10.1023/A:1008202821328>.
- Tang, W., Tong, L., & Gu, Y. (2005). Improved genetic algorithm for design optimization of truss structures with sizing, shape and topology variables. *International Journal for Numerical Methods in Engineering*, 62(13), 1737–1762. <https://doi.org/10.1002/nme.1244>.
- Trivedi, A., Srinivasan, D., Sanyal, K., & Ghosh, A. (2016). A survey of multiobjective evolutionary algorithms based on decomposition. *IEEE Transactions on Evolutionary Computation* (c), 1–1. <https://doi.org/10.1109/TEVC.2016.2608507>.
- Visser, H. G., & Hartjes, S. (2014). Economic and environmental optimization of flight trajectories connecting a city-pair. *Proceedings of the Institution of Mechanical Engineers, Part G: Journal of Aerospace Engineering*, 228(6), 980–993. <https://doi.org/10.1177/0954410013485348>.
- Vo-Duy, T., Duong-Gia, D., Ho-Huu, V., Vu-Do, H. C., & Nguyen-Thoi, T. (2017). Multi-objective optimization of laminated composite beam structures using NSGA-II algorithm. *Composite Structures*, 168. <https://doi.org/http://dx.doi.org/10.1016/j.comstruct.2017.02.038>.
- Wagner, T., & Trautmann, H. (2010). Online convergence detection for evolutionary multi-objective algorithms revisited. In 2010 IEEE congress on evolutionary computation (CEC2010) (pp. 3554–3561). <https://doi.org/10.1109/CEC.2010.5586474>.
- Wallock, A., & Corne, D. (2011). Multiple objective optimisation applied to route planning. In Proceedings of the 13th annual conference on genetic and evolutionary computation (pp. 1827–1834). New York, NY, USA: ACM. <https://doi.org/10.1145/2001576.2001821>.
- Wang, Z., Zhang, Q., Li, H., Ishibuchi, H., & Jiao, L. (2017). On the use of two reference points in decomposition based multiobjective evolutionary algorithms. *Swarm and Evolutionary Computation*, 0–1 (January). <https://doi.org/10.1016/j.swevo.2017.01.002>.
- Wang, Z., Zhang, Q., Zhou, A., Gong, M., & Jiao, L. (2016). Adaptive replacement strategies for MOEA/D. *IEEE Transactions on Cybernetics*, 46(2), 474–486. <https://doi.org/10.1109/TCYB.2015.2403849>.
- Wu, S.-J., & Chow, P.-T. (1995). Steady-state genetic algorithms for discrete optimization of trusses. *Computers & Structures*, 56(6), 979–991. [https://doi.org/10.1016/0045-7949\(94\)00551-D](https://doi.org/10.1016/0045-7949(94)00551-D).
- Yang, S., Jiang, S., & Jiang, Y. (2016). Improving the multiobjective evolutionary algorithm based on decomposition with new penalty schemes. *Soft Computing*. <https://doi.org/10.1007/s00500-016-2076-3>.
- Zhang, Q., & Li, H. (2007). MOEA/D: A multiobjective evolutionary algorithm based on decomposition. *IEEE Transactions on Evolutionary Computation*, 11(6), 712–731. <https://doi.org/10.1109/TEVC.2007.892759>.
- Zhang, Q., Liu, W., & Li, H. (2009). The performance of a new version of MOEA/D on CEC09 unconstrained MOP test instances. 2009 IEEE congress on evolutionary computation. <https://doi.org/10.1109/CEC.2009.4982949>.
- Zhu, Y., Wang, J., & Qu, B. (2014). Multi-objective economic emission dispatch considering wind power using evolutionary algorithm based on decomposition. *International Journal of Electrical Power & Energy Systems*, 63, 434–445. <https://doi.org/10.1016/j.ijepes.2014.06.027>.
- Zitzler, E., & Thiele, L. (1999). Multiobjective evolutionary algorithms: A comparative case study and the strength Pareto approach. *IEEE Transactions on Evolutionary Computation*, 3(4), 257–271. <https://doi.org/10.1109/4235.797969>.
- Zitzler, E., Thiele, L., Laumanns, M., Fonseca, C. M., & Da Fonseca, V. G. (2003). Performance assessment of multiobjective optimizers: An analysis and review. *IEEE Transactions on Evolutionary Computation*, 7(2), 117–132. <https://doi.org/10.1109/TEVC.2003.810758>.

Available online at [www.sciencedirect.com](http://www.sciencedirect.com)**ScienceDirect**

Transportation Research Procedia 29 (2018) 157–168

---

---

**Transportation  
Research  
Procedia**  
[www.elsevier.com/locate/procedia](http://www.elsevier.com/locate/procedia)**2**

6th CEAS AIR & SPACE CONFERENCE AEROSPACE EUROPE 2017, CEAS 2017, 16-20  
October 2017, Bucharest, Romania

## Optimization of noise abatement aircraft terminal routes using a multi-objective evolutionary algorithm based on decomposition

V. Ho-Huu<sup>\*</sup>, S. Hartjes, L. H. Geijselaers, H. G. Visser, R. Curran

*Faculty of Aerospace Engineering, Delft University of Technology, Delft, The Netherlands*

---

### Abstract

Recently, a multi-objective evolutionary algorithm based on decomposition (MOEA/D) has emerged as a potential method for solving multi-objective optimization problems (MOPs) and attracted much attention from researchers. In MOEA/D, the MOPs are decomposed into a number of scalar optimization sub-problems, and these sub-problems are optimized concurrently by only utilizing the information from their neighboring sub-problems. Thanks to these advantages, MOEA/D has demonstrated to be more efficient than the non-dominated sorting genetic algorithm II (NSGA-II) and other methods. However, its applications to practical problems are still limited, especially in the domain of aerospace engineering. Therefore, this paper aims to present a new application of MOEA/D for the optimal design of noise abatement aircraft terminal routes. First, in order to optimize aircraft noise for aircraft terminal routes while taking into account the interests of various stakeholders, bi-objective optimization problems including noise and fuel consumption are formulated, in which both the ground track and vertical profile of a terminal route are optimized simultaneously. Then, MOEA/D is applied to solve these problems. Furthermore, to ensure the design space of vertical profiles is always feasible during the optimization process, a trajectory parameterization technique recently proposed is also used. This technique aims at reducing the number of model evaluations of MOEA/D and hence the computational cost will decrease significantly. The efficiency and reliability of the developed method are evaluated through case studies for departure and arrival routes at Rotterdam The Hague Airport in the Netherlands.

© 2018 The Authors. Published by Elsevier B.V.

Peer-review under responsibility of the scientific committee of the 6th CEAS Air & Space Conference Aerospace Europe 2017.

*Keywords:* Terminal routes; trajectory optimization; noise abatement; fuel consumption; MOEA/D.

---

<sup>\*</sup> Corresponding author. Tel.: +31 633902729.

E-mail address: [v.hohuu@tudelft.nl](mailto:v.hohuu@tudelft.nl), [vinh.ho.h@gmail.com](mailto:vinh.ho.h@gmail.com)

## 1. Introduction

2

With the substantial contribution of aviation to the development of business, communication and tourism globally, the air transport industry is expected to grow rapidly in the coming years. However, one of the considerable concerns which policymakers are facing with the extension of aircraft and airport operations is the protest of near-airport communities. This is because of the significant increase in negative impacts on the environment such as noise and pollutant emissions (Hartjes et al., 2014), which directly affect the daily life of communities surrounding airports. Therefore, to grow the air transport sustainably, it is crucial to figure out feasible solutions for decreasing its adverse influences. One of the potential options is the optimal design of new terminal routes (i.e. departure and arrival routes), which has been widely studied during the past few years (Visser and Wijnen, 2001).

Research on optimization of environmentally friendly terminal routes has obtained significant achievements, and different approaches have been proposed in recent years. Hartjes et al. (2010) developed a trajectory optimisation tool NOISHHH including a noise model, an emissions inventory model, a geographic information system and a dynamic trajectory optimisation algorithm to generate environmentally optimal departure trajectories based on area navigation. Later, this tool was also used for the optimal design of area navigation noise abatement approach trajectories (Braakenburg et al., 2011; Hogenhuis et al., 2011). Prats et al. (2010a, 2010b) applied a lexicographic optimization technique to deal with aircraft departure trajectories for minimizing noise annoyance. Torres et al. (2011) proposed a non-gradient optimizer called multi-objective mesh adaptive direct search (multi-MADS) to optimize departure trajectories for NOx emissions and noise at a single measurement point. Recently, Hartjes and Visser (2016) employed an elitist non-dominated sorting genetic algorithm (NSGA-II) combined with a novel trajectory parameterization technique for the optimal design of departure trajectories with environmental criteria.

Based on the obtained results from Hartjes and Visser (2016); and Torres et al. (2011), it is evident that the use of non-gradient multi-objective optimization methods is one of the efficient approaches for the optimal design of terminal routes. These methods do not only help find out a set of non-dominate optimal solutions, but also help avoid the limitations of gradient methods in coping with discontinuous problems and integer or/and discrete design variables. Up to now, besides multi-MADS and NSGA-II, there are various multi-objective optimization algorithms available in literature, which may also be potential candidates for solving these kinds of problems. However, as yet, they have not been properly investigated. Among them, MOEA/D recently emerged as a powerful method, and has received much attention from researchers. Compared to NSGA-II, MOEA/D is better in terms of both the quality of solutions and the convergence rate (Li and Zhang, 2009), which are promising features for solving large-scale real-world problems. Nevertheless, the application of MOEA/D for real engineering problems is still limited, especially in the domain of aerospace engineering. This paper, therefore, aims to apply MOEA/D to the optimization of noise abatement aircraft terminal routes. In order to make the applied algorithm more efficient, advantageous features recently developed for MOEA/D are also integrated into the proposed version. They include an adaptive replacement strategy (Wang et al., 2016), a stopping condition criterion (Abdul Kadhar and Baskar, 2016), and a constraint-handling technique (Jan and Khanum, 2013). Moreover, to reduce redundant evaluations of infeasible solutions derived from operational constraints during different flight phases, the new trajectory parameterization technique in Hartjes and Visser (2016) is also employed. The robustness and reliability of the proposed approach are validated through two numerical examples comprising of a departure route and an arrival route at Rotterdam The Hague Airport.

### Nomenclature

$D$	drag force
$ff$	fuel flow
$g_0$	gravitational acceleration
$h$	altitude
$s$	along-track distance
$T$	thrust
$V_{EAS}$	equivalent airspeed
$V_{TAS}$	true airspeed

$W$	aircraft weight
$\gamma$	flight path angle
$\rho$	ambient air density
$\rho_0$	air density at sea level

## 2. Aircraft model

In this study, an intermediate point-mass model is used. This model relies on several assumptions (Hartjes and Visser, 2016): 1) there is no wind present, 2) the Earth is flat and non-rotating, 3) the flight is coordinated. Furthermore, the flight path angle is considered sufficiently small ( $\gamma < 15^\circ$ ). With these assumptions, the equations of motion can be written as:

$$\begin{aligned}\dot{V}_{TAS} &= g_0 \cdot ((T - D)/W - \sin\gamma) \\ \dot{s} &= V_{TAS} \cdot \cos\gamma \\ \dot{h} &= V_{TAS} \cdot \sin\gamma \\ \dot{W} &= -ff \cdot g_0\end{aligned}\quad (1)$$

where  $\dot{V}_{TAS}$ ,  $\dot{s}$ ,  $\dot{h}$  and  $\dot{W}$  are the derivatives of true airspeed, distance flown, altitude and aircraft weight, respectively; and  $T$ ,  $D$ , and  $ff$  are, respectively, thrust, drag, and fuel flow.

At a condition of low altitude and speed, equivalent airspeed  $V_{EAS}$  can serve as a proxy for an indicated airspeed, and can be derived from the true airspeed by the following relationship:

$$V_{EAS} = V_{TAS} \cdot \sqrt{\rho/\rho_0}\quad (2)$$

where  $\rho$  is the ambient air density, and  $\rho_0$  is the air density at sea level.

By applying Eq. (2), the first equation in Eq. (1) can be rewritten as follows:

$$\dot{V}_{EAS} = [g_0 \cdot ((T - D)/W - \sin\gamma) + 1/(2\rho) \cdot d\rho/dh \cdot V_{TAS}^2 \cdot \sin\gamma] \cdot \sqrt{\rho/\rho_0}\quad (3)$$

where  $d\rho/dh$  is the derivative of the ambient air density with respect to altitude.

The aircraft performance model has two control variables, viz. the flight path angle  $\gamma$  and thrust  $T$ , and four state variables  $\mathbf{x} = [V_{EAS} \ h \ s \ W]$ .

## 3. Trajectory parameterization

With the effort of reducing the number of model evaluations of infeasible solutions during the optimization process, Hartjes and Visser (2016) proposed a novel trajectory parameterization which can diminish significantly the number of operational constraints in the problem formulation. The technique divides a trajectory into two separate parts, a ground track and a vertical path.

For the ground track generation, a modern navigation technology known as required navigation performance (RNP) is employed. In the RNP, track-to-a-fix (TF) and radius-to-a-fix (RF) leg types are often used for constructing a flight path between waypoints. This is because of their abilities in avoiding noise-sensitive areas and minimizing flight track dispersion. By using these two segment types, the ground track can be generated by using only straight legs, and constant radius turns as shown in Fig. 1. In this figure, the optimal design variables include  $L_1, L_2, L_3, R_1, R_2, R_3, \Delta\chi_1$ , and  $\Delta\chi_2$ , while  $L_4$  and  $\Delta\chi_3$  are defined based on geometric relationships.

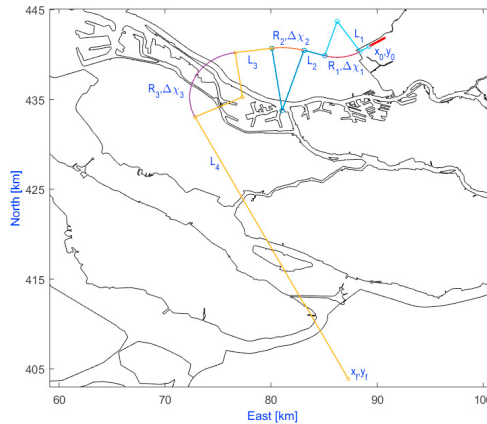


Fig. 1. Ground track parameterization.

For the vertical path, the vertical profile is synthesized based on flight procedures derived from ICAO (2006). For instance, aircraft are not allowed to descend and/or decelerate during departure and ascend and/or accelerate during arrival. In order to parameterize this part, the trajectory is split into a number of segments. In each segment, two control inputs (i.e. flight path angle setting  $\gamma_{n,i}$  and throttle setting  $T$ ) are kept constant, and they are either directly assigned based on operational requirements or designated as optimal design variables. For each segment, the flight path angle  $\gamma_i$  and thrust  $T_i$  are set by adjusting their normalized control optimization parameters  $\gamma_{n,i}$  ( $0 \leq \gamma_{n,i} \leq 1$ ), and  $T_{n,i}$  ( $0 \leq T_{n,i} \leq 1$ ), respectively, as follows:

$$\gamma_i = (\gamma_{\max,i} - \gamma_{\min,i})\gamma_{n,i} + \gamma_{\min,i} \quad (4)$$

$$T_i = (T_{\max,i} - T_{\min,i})T_{n,i} + T_{\min,i} \quad (5)$$

where the subscript  $n$  presents a normalized control optimization parameter. The subscripts  $\max, i$  and  $\min, i$  indicate the maximum and minimum allowable values of the flight path angle and thrust for  $i$ th segment, which are specified based on the features of flight procedures.

In the departure procedure,  $T_{\max}$  is set to be either maximum take-off thrust (TO) or maximum climb thrust (TCL), depending on the flight stage. In addition, since descending is not permitted in this phase ( $\dot{h} \geq 0$ ), the minimum flight path angle is set to zero ( $\gamma_{\min} = 0$ ). Furthermore,  $\gamma_{\max}$  can be defined from the first equation in Eq. (3) based on an assumption that an aircraft is flying with a maximum thrust at a constant speed ( $\dot{V}_{EAS} = 0$ ). From this equation,  $T_{\min}$  can also be determined when a minimum thrust is required to maintain the aircraft at constant speed ( $\dot{V}_{EAS} = 0$ ). These formulas are derived as follows:

$$\gamma_{\max} = \sin^{-1} [(-2 \cdot \rho \cdot g_0 \cdot (T_{\max} - D)) / (W(d\rho/dh \cdot V_{TAS}^2 - 2 \cdot \rho \cdot g_0))] \quad (6)$$

$$T_{\min} = D - (W / (2 \cdot \rho \cdot g_0)) \cdot d\rho/dh \cdot V_{TAS}^2 \cdot \sin\gamma + W \cdot \sin\gamma \quad (7)$$

In the arrival procedure, the minimum thrust  $T_{\min}$ , called an idle thrust is derived for each specific aircraft model, whilst the maximum flight path angle is set to zero ( $\gamma_{\max} = 0$ ) because ascending is not allowed in this phase ( $\dot{h} \leq 0$ ). In addition, by assuming that the aircraft can only maintain its speed during descending when the maximum thrust is applied,  $T_{\max}$  can be determined by the same formula in Eq. (7) with a replacement of  $T_{\min}$  by  $T_{\max}$ . The minimum flight path angle  $\gamma_{\min}$  is evaluated with respect to the minimum thrust  $T_{\min}$  by the same formula in Eq. (6) with a replacement of  $T_{\max}$  and  $\gamma_{\max}$  by  $T_{\min}$  and  $\gamma_{\min}$ .

#### 4. Problem statement

The aim of the study is to optimally design terminal routes which can help to reduce the negative impact of

aircraft noise in near-airport communities. However, purely focussing on noise impact may lead to a considerable increase in fuel consumption which is against the interests of stakeholders like airline companies. To take into account this issue, two conflicting objectives (one related to noise and the other related to fuel consumption) are therefore considered in this study.

While the fuel consumption can easily be measured by the change of the aircraft weight from Eq. (1), noise impact is more difficult to quantify. To assess the influence of aircraft noise on near-airport communities, the percentage of people who are likely to be awakened due to aircraft noise exposure is employed in this paper. This criterion was proposed by the Federal Interagency Committee on Aviation Noise (FICAN) in 1997 and defined as follows (FICAN, 1997):

$$\%Awakening = 0.0087 \cdot (SEL_{\text{indoor}} - 30)^{1.79} \quad (8)$$

where  $\%Awakening$  is the maximum percentage of awakened people owing to noise of an aircraft.  $SEL_{\text{indoor}}$  is the indoor sound exposure level (dBA) and is evaluated by using a replica of the integrated noise model (INM) (Hartjes and Visser, 2016). Because  $SEL$  calculated from INM represents an outdoor value, an amount of 20.5 dB is subtracted to obtain  $SEL_{\text{indoor}}$ , accounting for the sound absorption of an average house (Visser and Wijnen, 2001).

With the above definitions of two objectives, the optimization problem is formulated as follows:

$$\begin{aligned} \min_{\mathbf{x}, \boldsymbol{\gamma}_n, \boldsymbol{\Gamma}_n} \quad & \{ \text{number of awakening, fuel burn} \} \\ \text{s. t.} \quad & h = h_{\text{final}}, \quad V_{\text{EAS}} = V_{\text{EAS\_final}} \end{aligned} \quad (9)$$

where  $\mathbf{x}$  is the vector of ground track variables.  $\boldsymbol{\gamma}_n$  and  $\boldsymbol{\Gamma}_n$  are the vectors of the flight path angle setting and throttle setting variables on segments. The parameters  $h_{\text{final}}$  and  $V_{\text{EAS\_final}}$  are, respectively, the final altitude and equivalent airspeed of the flight procedures.

## 5. MOEA/D algorithm

Many real-world problems present themselves as complex optimization problems with more than two conflicting objectives and this has given rise to the birth of various multi-objective optimization methods. Among the various different algorithms, the MOEA/D method, firstly developed by Zhang and Li (2007), has been emerged as a promising, potential method for solving complicated multi-objective optimization problems (MOPs) (Trivedi et al., 2016). In MOEA/D, the MOPs are transformed into a set of single optimization sub-problems by applying decomposition approaches, and then evolutionary optimization methods are applied to optimize these sub-problems simultaneously. In recent years, MOEA/D has been applied in different fields such as power system transmission and distribution networks (Biswas et al., 2017), and wireless sensor networks (Konstantinidis and Yang, 2012); and various versions have been developed such as MOEA/D-DE (Li and Zhang, 2009), MOEA/D-DRA (Zhang et al., 2009), and MOEA/D-GR (Wang et al., 2016). Although there are many variants of MOEA/D available in literature, a powerful single version of MOEA/D that combines different advantages of current versions is not yet in place. With the aim of developing an efficient algorithm for the presented problem, therefore, an MOEA/D version which is the combination of MOEA/D-DE (Li and Zhang, 2009) with an adaptive replacement strategy (Wang et al., 2016), a stopping condition criterion (Abdul Kadhar and Baskar, 2016) and a constraint-handling technique (Jan and Khanum, 2013) is developed in this study. The general framework of the algorithm is presented in Algorithm 1. For more detail, readers are encouraged to refer to Refs. (Abdul Kadhar and Baskar, 2016; Ho-Huu et al., 2018; Jan and Khanum, 2013; Li and Zhang, 2009; Wang et al., 2016).

---

### Algorithm 1. Pseudo-code of MOEA/D algorithm

---

#### Input:

- A multi-objective optimization problem as Eq. (9);
- A stopping criterion;
- $N$ : number of sub-problems;
- $\mathbf{w}^i = (w_1^i, \dots, w_m^i), i = 1, \dots, N$ : a set of  $N$  weight vectors;
- $T_m$ : size of mating neighbourhood;
- $T_{r\text{max}}$ : maximum size of replacement neighbourhood;
- $\delta$ : the probability that mating parents are selected from the neighbourhood;

- *MaxIter*: maximum iteration;
- *FES* = 0: the number of function evaluations;

**Step 1. Initialization**

- 1.1. Find the  $T_m$  closest weight vectors to each weight vector based on the Euclidean distances of any two weight vectors. For each sub-problem  $i = 1, \dots, N$  set  $\mathbf{B}^i = (i_1, \dots, i_{T_m})$  where  $\mathbf{w}^{i_1}, \dots, \mathbf{w}^{i_{T_m}}$  are the closest weight vectors to  $\mathbf{w}^i$ ;
- 1.2. Create an initial population  $\mathbf{P} = \{\mathbf{x}^1, \dots, \mathbf{x}^N\}$  by uniformly randomly sampling from design space  $\Omega$ . Evaluate the fitness value  $FV^i$  of each solution  $\mathbf{x}^i$ , i.e.  $FV^i = (f_1(\mathbf{x}^i), \dots, f_m(\mathbf{x}^i))$  and set  $\mathbf{FV} = \{FV^1(\mathbf{x}^1), \dots, FV^N(\mathbf{x}^N)\}$ ;
- 1.3. Initialize ideal point  $\mathbf{z}^* = (z_1^*, \dots, z_m^*)^T$  by setting  $z_j^* = \min\{f_j(\mathbf{x}) | \mathbf{x} \in \Omega, j = 1, \dots, m\}$  and nadir point  $\mathbf{z}^{\text{nad}} = (z_1^{\text{nad}}, \dots, z_m^{\text{nad}})^T$  by setting  $z_j^{\text{nad}} = \max\{f_j(\mathbf{x}) | \mathbf{x} \in \Omega, j = 1, \dots, m\}$ ;
- 1.4. Set  $FES = FES + N$ , and generation:  $gen = 1$ ;

**Step 2. Update**

**while** (the stopping condition is not satisfied)

**for**  $i = 1, \dots, N$ ; **do**

    2.1. Selection of mating/update range

      Set  $\mathbf{B}_m = \begin{cases} \mathbf{B}^i & \text{if } rand < \delta \\ \{1, \dots, N\} & \text{otherwise} \end{cases}$

      where *rand* is a uniformly distributed random number in  $[0, 1]$ ;

    2.2. Reproduction: randomly select three parent individuals  $r_1, r_2$  and  $r_3$  ( $r_1 \neq r_2 \neq r_3 \neq i$ ) from  $\mathbf{B}_m$  and generate a solution  $\bar{\mathbf{y}}$  by applying “DE/rand/1” operator, and then perform a mutation operator on  $\bar{\mathbf{y}}$  to create a new solution  $\mathbf{y}$ ;

    2.3. Repair: if any element of  $\mathbf{y}$  is out of  $\Omega$ , its value will be randomly regenerated inside  $\Omega$ ;

    2.4. Evaluate the fitness value of new solution  $\mathbf{y}$ ;

    2.5. Update of  $\mathbf{z}^*$  and  $\mathbf{z}^{\text{nad}}$ : for each  $j = 1, \dots, m$  if  $z_j^* \leq f_j(\mathbf{x}^i)$  then set  $z_j^* = f_j(\mathbf{x}^i)$ , and if  $z_j^{\text{nad}} \geq f_j(\mathbf{x}^i)$  then set  $z_j^{\text{nad}} = f_j(\mathbf{x}^i)$ ;

    2.6. Update of solutions: use an adaptive replacement strategy in Wang et al. (2016):

**end for**

  Set  $FES = FES + N$ , and  $gen = gen + 1$ ;

**Step 3. Stopping condition**

  Use a stopping criterion in Abdul Kadhar and Baskar (2016).

**if** (stopping criterion is satisfied or *MaxIter* is reached)

    Stop the algorithm;

**end if**

**end while**

**Output:** Pareto set  $\mathbf{PS} = \{\mathbf{x}^1, \dots, \mathbf{x}^N\}$ ; Pareto front  $\mathbf{PF} = \{FV^1(\mathbf{x}^1), \dots, FV^N(\mathbf{x}^N)\}$ .

## 6. Numerical example

To evaluate the applicability and effectiveness of MOEA/D for dealing with optimization of noise abatement terminal routes, two scenarios including departure and arrival at Rotterdam The Hague Airport are considered in this section. The airport is located in the north of Rotterdam city, The Netherlands, and is surrounded by densely populated regions such as The Hague, Rotterdam, and Utrecht. It has one runway which can be operated in both directions, labelled as 06 and 24. The investigated cases include a standard instrument departure (SID) named WOODY1B starting from runway 24 and finishing at waypoint EH162, and a standard terminal arrival route (STAR) named STD starting at a ground based beacon STD and finishing at way point EH252 as shown in Fig. 2. The population density data with a grid size of 500m×500m is utilised and illustrated in Fig. 2 as well. An aircraft model of a Boeing 737 with twin engines is used. To compare the performance of MOEA/D, the well-known NSGA-II (Deb et al., 2002) is also applied to solve these problems. A population size of 50 is used for both methods, and the algorithms will stop when either their convergence criteria are satisfied, or the maximum number of iterations (*MaxIter*) is reached, where *MaxIter* is set to 1000. All algorithms are implemented in Matlab 2016b on a Core i7, 8GB ram laptop.

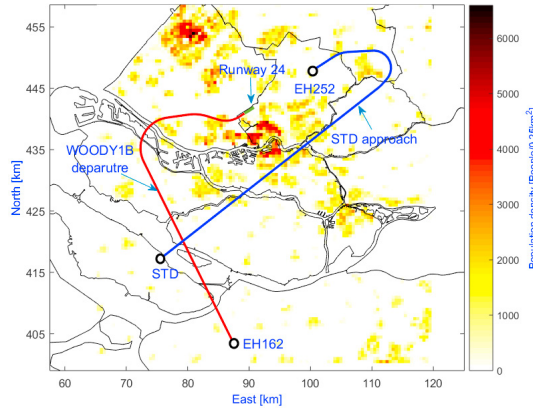


Fig. 2. Departure and arrival scenarios.

6.1. Departure route

The simulation of this problem is started at an altitude of 35 ft and a take-off safety speed  $V_2 + 10$  kts with the landing gear retracted and departure flaps selected, and is terminated at an altitude of 6,000 ft and an equivalent airspeed (EAS) of 250 kts. The ground track is constructed by four straight legs and three turns as shown in Fig. 1, while the vertical path is subdivided into 10 segments. The vertical profile parameters including both the optimal and reference cases are derived from Hartjes and Visser (2016).

The Pareto-optimal solutions obtained by the methods are shown in Fig. 3, and their corresponding ground tracks are illustrated in Fig. 4. From a perspective of solution methods, it can be seen from Fig. 3 that MOEA/D gives more dominating solutions of awakening, whilst NSGA-II has more solutions regarding fuel burn. In general, however, it can be observed that MOEA/D is better than NSGA-II. Moreover, to get these results, MOEA/D only requires 39,371 model evaluations in 6.45 hours, whilst NSGA-II required 50,000 evaluations in 8.17 hours. From an engineering point of view, it can be observed that the obtained ground tracks in Fig. 4 appear to be reasonable and appropriate. There are four different groups of ground tracks obtained by MOEA/D and three groups obtained by NSGA-II, and all of them try to avoid densely populated regions. This helps to explain why there are some gaps on the Pareto fronts. Compared to the reference case, all solutions feature a shorter ground track and better environmental performance.

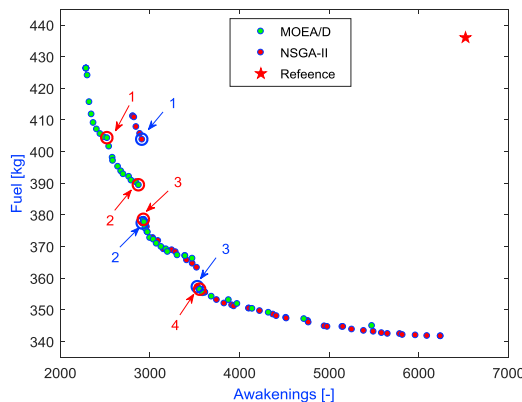


Fig. 3. Comparison of Pareto-optimal solutions obtained by NSGA-II and MOEA/D and the result of the reference case.

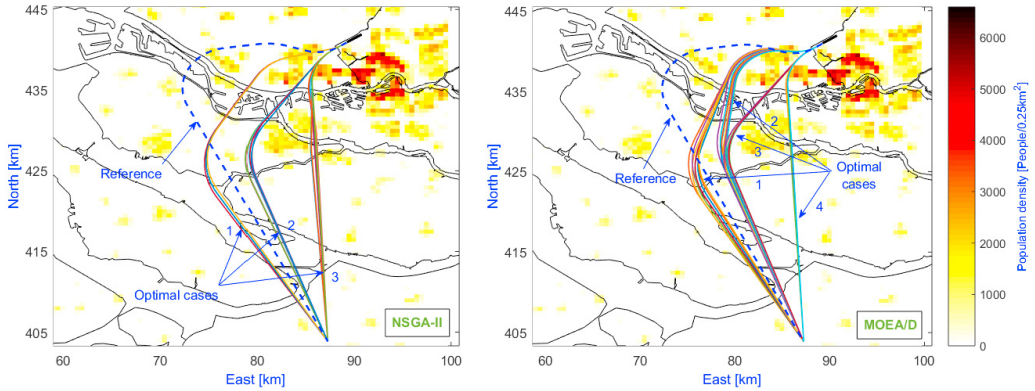


Fig. 4. Optimal ground tracks obtained by NSGA-II and MOEA/D.

For a comparison of performances, the expected number of awakenings and fuel burn of four representative cases extracted from the Pareto fronts (numbered as shown in Fig. 3) and those of the reference case are presented in Table 1. Their corresponding vertical profiles are also given in Fig. 5. It is seen from the table that all optimal cases give a better solution for time, fuel and awakenings. It is also observed that the cases with shorter routes (i.e. 2 and 3) have less fuel burn but more awakenings, which are the results of directly flying over areas with dense population. When looking at the vertical profiles in Fig. 5, it is indicated that all four optimal cases prefer a low altitude, which is because the spread of aircraft noise at a low altitude is smaller than that at a higher altitude due to increased lateral attenuation; and hence it may lead to a significant reduction of awakenings. For the airspeed shapes, there are some distinct levels which may be due to either the constraints of a bank angle or reducing thrust when flying over populated areas.

Table 1. Comparison of objectives of cases 1-4 and the reference case.

Case number	Time (s)	Fuel (kg)	Awakening
Reference	420.90	436.02	6519
1 MOEA/D	383.40	404.28	2523
2 NSGA-II	385.29	403.80	2912
3 MOEA/D	360.46	389.39	2875
4 NSGA-II	343.33	377.31	2918
1 MOEA/D	344.38	378.47	2930
2 NSGA-II	311.07	357.19	3532
3 MOEA/D	308.60	356.39	3558

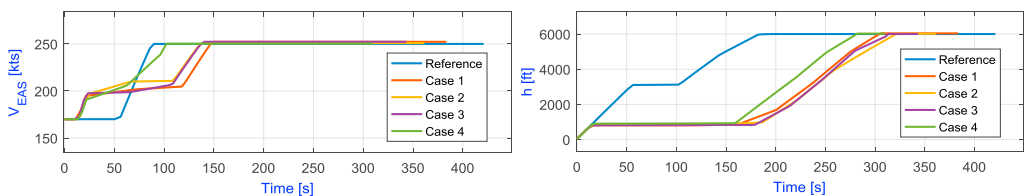


Fig. 5. Vertical profiles of cases 1-4 and the reference case.

Although the obtained solutions are better than the reference case, from a practical perspective, they may not be accepted in reality because of flying at a low altitude for a long time. Thus, to make optimal solutions more applicable, an additional constraint on the flight path angle is applied, where the normalized control parameter  $\gamma_{n,i}$  is set to be larger than 0.2 from an altitude of 35 ft to 1,500 ft i.e. if  $h \leq 1,500$  ft,  $(0.2 \leq \gamma_{n,i} \leq 1)$ , otherwise  $(0 \leq \gamma_{n,i} \leq 1)$ . With this new constraint, the optimal results obtained by MOEA/D are given in Fig. 6a in relation to the previous situation, their ground tracks are provided in Fig. 6b, and the vertical profiles of two representative cases (1 and 4) are indicated in Fig. 7. It can be observed that all new solutions have larger values for the objectives, especially in the number of awakenings which can be due to increasing the dispersion of aircraft noise at a higher altitude. This may also be the cause of slight changes in the ground tracks. The shapes of the airspeed and altitude histories have not changed much, except for an increase in altitude.

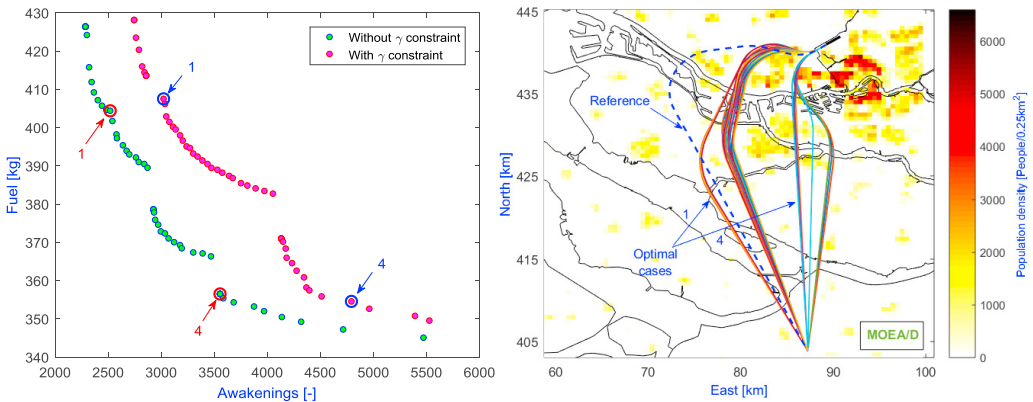


Fig. 6. a) Optimal objectives with and without the new constraint of  $\gamma_{n,i}$ ; b) Optimal ground tracks.

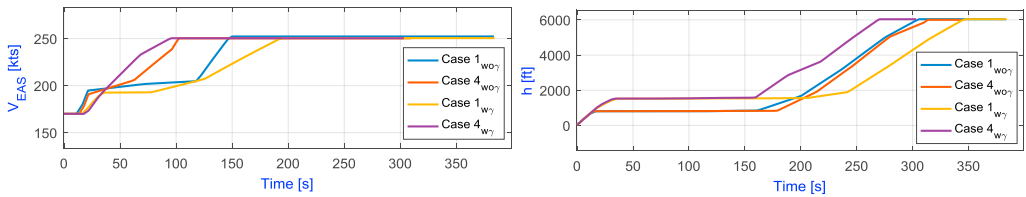


Fig. 7. Comparison of vertical profiles of cases 1 and 4 with and without the new constraint of  $\gamma_{n,i}$ .

6.2. Arrival route

For this problem, the simulation is started at an altitude of 6,000 ft and an equivalent airspeed of 250 kts, and is finished at an altitude of 2,000 ft and an equivalent airspeed of 170 kts. Similar to the departure problem, the ground track is also constructed by four straight legs and three turns, and the vertical path is also subdivided into 10 segments. The problem has 28 design variables consisting of 8 ground track variables and 20 parameters defining the vertical profile. To make a fair comparison for the reference case, a composite objective of awakenings and fuel burn with an equal weight vector of [0.5 0.5] is used for optimizing the vertical profiles.

The Pareto-optimal solutions obtained by both methods are illustrated in Fig. 8, and the ground tracks are provided in Fig. 9. To acquire these results, NSGA-II spends 50,000 model evaluations in 9.92 hours, while MOEA/D converges after 37,331 model evaluations in 7.95 hours. The resulting ground tracks are reasonable. In a comparison with the reference case, it can be seen that most of the optimal cases dominate the reference case.

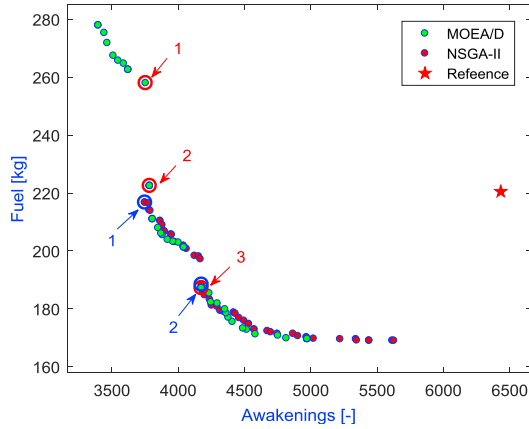


Fig. 8. Comparison of Pareto-optimal solutions obtained by NSGA-II and MOEA/D and the result of the reference case.

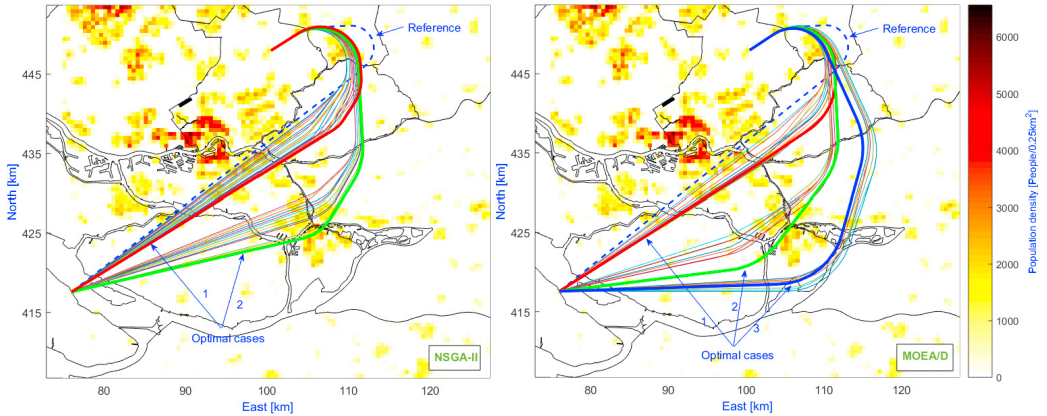


Fig. 9. Optimal ground tracks obtained by NSGA-II and MOEA/D.

For a comparison of specific values, the number of awakenings and fuel burn of the representative cases extracted from the Pareto-solution solutions (as numbered in Fig. 8) are presented Table 2. Their vertical profiles are provided in Fig. 10. It seems that even the ground track of the reference case is shorter than cases 2 of MOEA/D and NSGA-II; its flight time is still higher though. This can be due to the trade-off of two objectives of fuel burn and awakenings with an equal priority.

Table 2. Comparison of objectives of the representative cases and the reference case.

Case no.	Time (s)	Fuel (kg)	Awakening
Reference	570.09	220.49	6432
1 MOEA/D	489.64	187.19	4175
1 NSGA-II	480.47	188.39	4176
2 MOEA/D	530.02	222.48	3785
2 NSGA-II	527.43	216.74	3749
3 MOEA/D	594.03	257.98	3754

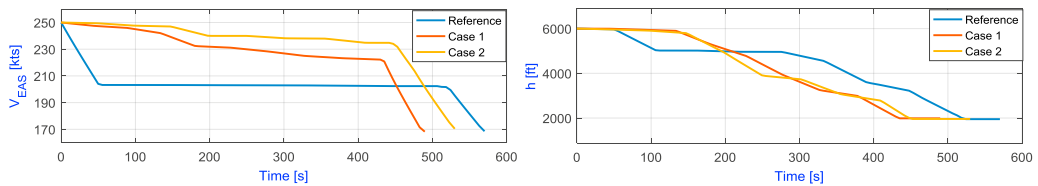


Fig. 10. Vertical profiles of cases 1 and 2 and the reference case.

Summarily, based on the obtained results, it can be concluded that MOEA/D is an effective method for handling the optimal design of noise abatement terminal routes. Compared to NSGA-II, MOEA/D generally outperforms NSGA-II in terms of both the quality of solutions and computation time.

## 7. Conclusion

In this paper, a new application of a well-known method named MOEA/D for solving the optimization problems of noise abatement terminal routes is presented. In MOEA/D, besides its typical advantages, its performance is also improved significantly by the integration of new features recently developed, which consist of an adaptive replacement strategy, a stopping condition criterion and a constraint-handling technique. The applicability and effectiveness of MOEA/D are demonstrated through two example scenarios related to Rotterdam The Hague Airport, including a standard instrument departure route, i.e. WOODY1B and a standard terminal arrival route, i.e. STD. The results obtained by MOEA/D are also compared to those of NSGA-II. The comparative results reveal that MOEA/D is generally better than NSGA-II in both the quality of solutions and the convergence rate, and hence it is an adequate algorithm for solving these kinds of problems.

In future work, MOEA/D will be extended for different routes at other airports, and its performance will also be investigated in different problems like route and runway allocations. Furthermore, the performance of the algorithm will also be enhanced further to deal with large and complex problems, especially in the distribution of solutions and the convergence rate.

## References

- Abdul Kadhar, K.M., Baskar, S., 2016. A stopping criterion for decomposition-based multi-objective evolutionary algorithms. *Soft Comput.* 1–20. doi:10.1007/s00500-016-2331-7
- Biswas, P.P., Mallipeddi, R., Suganthan, P.N., Amaratunga, G.A.J., 2017. A multiobjective approach for optimal placement and sizing of distributed generators and capacitors in distribution network. *Appl. Soft Comput.* 60, 268–280. doi:https://doi.org/10.1016/j.asoc.2017.07.004
- Braakenburg, M.L., Hartjes, S., Visser, H.G., 2011. Development of a Multi-Event Trajectory Optimization Tool for Noise-Optimized Approach Route Design. *AIAA J.* 1–13. doi:10.2514/6.2011-6929
- Deb, K., Pratab, S., Agarwal, S., Meyarivan, T., 2002. A Fast and Elitist Multiobjective Genetic Algorithm: NSGA-II. *IEEE Trans. Evol. Comput.* 6, 182–197. doi:10.1109/4235.996017
- Federal Interagency Committee on Aviation Noise. Effects of aviation noise on awakenings from sleep. March 1997.
- Hartjes, S., Dons, J., Visser, H.G., 2014. Optimization of Area Navigation Arrival Routes for Cumulative Noise Exposure. *J. Aircr.* 51, 1432–1438. doi:10.2514/1.C032302
- Hartjes, S., Visser, H., 2016. Efficient trajectory parameterization for environmental optimization of departure flight paths using a genetic algorithm. *Proc. Inst. Mech. Eng. Part G J. Aerosp. Eng.* 0, 1–9. doi:10.1177/0954410016648980
- Hartjes, S., Visser, H.G., Hebly, S.J., 2010. Optimisation of RNAV noise and emission abatement standard instrument departures. *Aeronaut. J.* 114, 757–767. doi:10.1017/CBO9781107415324.004
- Ho-Huu, V., Hartjes, S., Visser, H.G., Curran, R., 2018. An improved MOEA / D algorithm for bi-objective optimization problems with complex Pareto fronts and its application to structural optimization. *Expert Syst. Appl.* 92, 430–446. doi:10.1016/j.eswa.2017.09.051
- Hogenhuis, R.H., Hebly, S.J., Visser, H.G., 2011. Optimization of area navigation noise abatement approach trajectories. *Proc. Inst. Mech. Eng. Part G-Journal Aerosp. Eng.* 225, 513–521. doi:10.1177/09544100JAERO840

- International Civil Aviation Organization, 2006. Procedures for air navigation services – Aircraft operations. Vol. I, Flight Procedures.
- Jan, M.A., Khanum, R.A., 2013. A study of two penalty-parameterless constraint handling techniques in the framework of MOEA/D. *Appl. Soft Comput. J.* 13, 128–148. doi:10.1016/j.asoc.2012.07.027
- Konstantinidis, A., Yang, K., 2012. Multi-objective energy-efficient dense deployment in Wireless Sensor Networks using a hybrid problem-specific MOEA/D. *Appl. Soft Comput. J.* 12, 1847–1864. doi:10.1016/j.asoc.2012.04.017
- Li, H., Zhang, Q., 2009. Multiobjective Optimization Problems With Complicated Pareto Sets, MOEA/D and NSGA-II. *IEEE Trans. Evol. Comput.* 13, 284–302. doi:10.1109/TEVC.2008.925798
- Prats, X., Puig, V., Quevedo, J., Nejjari, F., 2010a. Lexicographic optimisation for optimal departure aircraft trajectories. *Aerosp. Sci. Technol.* 14, 26–37. doi:10.1016/j.ast.2009.11.003
- Prats, X., Puig, V., Quevedo, J., Nejjari, F., 2010b. Multi-objective optimisation for aircraft departure trajectories minimising noise annoyance. *Transp. Res. Part C Emerg. Technol.* 18, 975–989. doi:10.1016/j.trc.2010.03.001
- Torres, R., Chaptal, J., Bès, C., Hiriart-Urruty, J.-B., 2011. Optimal , Environmentally Friendly Departure Procedures for Civil Aircraft. *J. Aircr.* 48, 11–23. doi:10.2514/1.C031012
- Trivedi, A., Srinivasan, D., Sanyal, K., Ghosh, A., 2016. A Survey of Multiobjective Evolutionary Algorithms based on Decomposition. *IEEE Trans. Evol. Comput.* 1–1. doi:10.1109/TEVC.2016.2608507
- Visser, H.G., Wijnen, R.A.A., 2001. Optimization of Noise Abatement Departure Trajectories. *J. Aircr.* 38, 620–627. doi:10.2514/2.2838
- Wang, Z., Zhang, Q., Zhou, A., Gong, M., Jiao, L., 2016. Adaptive Replacement Strategies for MOEA/D. *IEEE Trans. Cybern.* 46, 474–486. doi:10.1109/TCYB.2015.2403849
- Zhang, Q., Li, H., 2007. MOEA/D: A Multiobjective Evolutionary Algorithm Based on Decomposition. *IEEE Trans. Evol. Comput.* 11, 712–731. doi:10.1109/TEVC.2007.892759
- Zhang, Q., Liu, W., Li, H., 2009. The performance of a new version of MOEA/D on CEC09 unconstrained MOP test instances. 2009 IEEE Congr. Evol. Comput. doi:10.1109/CEC.2009.4982949

# 3

## AIRCRAFT ROUTE DESIGN

*In the previous chapter, the selection and development of a multi-objective optimization method, namely MOEA/D, have been performed, and its capability of solving the aircraft route design problem has been validated. In this chapter, the application of the developed algorithm to the route design problem is studied in more detail. In order to increase the performance of the optimization process, a new setting rule in the optimization procedure is implemented. This implementation aims to exploit the characteristics of the algorithm and the optimization problem to eliminate unnecessary computational steps, which can help to reduce the computational cost significantly. The proposed approach is first tested on a case study at Amsterdam Airport Schiphol in The Netherlands. Then, it is applied to simultaneously optimize the route design and allocation problem for a case study at the same airport. The study also aims to establish whether or not the simultaneous solving of route design and flight allocation will be applicable for the concurrent consideration of multiple routes. Furthermore, a new criterion that can help to make a fair distribution of noise over communities is studied in this study.*

---

The content of this chapter is based on the following research articles:

- [1]. **V. Ho-Huu**, S. Hartjes, H. G. Visser, and R. Curran, *An efficient application of the MOEA/D algorithm for designing noise abatement departure trajectories*, Aerospace, vol. 4, pp. 54, 2017. -> Paper 3.1.
- [2]. **V. Ho-Huu**, S. Hartjes, H. G. Visser, and R. Curran, *Integrated design and allocation of optimal aircraft departure routes*, Transportation Research Part D: Transport and Environment, vol. 63, pp. 689-705, 2018. -> Paper 3.2.

### 3.1. PROBLEM STATEMENT

In the previous chapter, the study on the development of an efficient optimization technique, namely MOEA/D, has been carried out. Although the developed method has shown promising potential to deal with the route design problem, its computational cost of solving such problems is still high. The aim of this chapter is, therefore, to study the potential capability of the developed algorithm in more detail and to develop new techniques to increase the performance of the optimization process, specifically aimed at the trajectory optimization process.

In this chapter, a new setting rule in the optimization procedure has been introduced. This setting aims to exploit the characteristics of the applied algorithm and the optimization problem to eliminate unnecessary computational steps. To determine whether a new candidate solution is better than other solutions in the previous iteration or not, its performance on objective and constraint functions is calculated during the optimization process. Unfortunately, this process is carried out in many calculation steps and is therefore time-consuming. However, based on the characteristics of the applied algorithm and the route design problem, the comparison between these solutions can, for many cases, be ignored. Consequently, the computational cost can be significantly reduced. The details of this study and its performance on the route design problem are presented in Ho-Huu et al. [37].

In order to further assess the capability of the proposed approach, the method is then applied to a more complicated problem. In this problem, both the design of optimal routes and the allocation of flights to these routes are considered simultaneously. In addition, a new noise criterion that aims to make a fair distribution of aircraft noise events over communities is introduced. The aim of the study is to provide options for routes that do not only effectively balance between the number of peopled annoyed and fuel consumption, but also offer a fair distribution of aircraft noise events among the population. This study is presented in detail in Ho-Huu et al. [38].

### 3.2. CONTRIBUTIONS

The main contributions of this chapter are as follows:

1. In Ho-Huu et al. [37], the computational cost of solving the optimal route design problems has been significantly decreased thanks to the new implementation on the optimization procedure. For example, as given in the first case study in [37], the computational cost to solve the problem with a considered area of 66 km x 59 km is only 2.2 hours, while that of the problem with a smaller considered area of 35 km x 40 km in the previous chapter [36] is 6.45 hours.
2. In Ho-Huu et al. [38], the developed model has been successfully applied to a complex problem, in which both the route design and flight allocation problems are addressed simultaneously. A new criterion that aims to fairly distribute noise events over communities is also considered in this study. By considering three objectives concurrently, the obtained results do not only create good options of routes with less noise impact and fuel consumption, but also offer a fair distribution of noise among communities.

3. Based on the results obtained in [38], it is also indicated that although the proposed approach is capable of handling the integrated problem, it is only suitable for designing one given SID route at a time. In case of considering multiple routes concurrently, the complexity of the problem will dramatically increase, and hence the computational cost will increase as well. As a result, it will be difficult to extend this approach for the developed framework, when both the problems of route design and flight allocation for multiple routes are considered simultaneously. Therefore, a new approach has been developed, which will be presented in Chapter 5.



Article

# An Efficient Application of the MOEA/D Algorithm for Designing Noise Abatement Departure Trajectories

Vinh Ho-Huu <sup>†</sup>, Sander Hartjes <sup>\*,†</sup>, Hendrikus G. Visser <sup>id</sup> and Richard Curran

Faculty of Aerospace Engineering, Delft University of Technology, 2629 HS Delft, The Netherlands; v.hohuu@tudelft.nl (V.H.-H.); h.g.visser@tudelft.nl (H.G.V.); r.curran@tudelft.nl (R.C.)

\* Correspondence: s.hartjes@tudelft.nl; Tel.: +31-15-27-88925

† These authors contributed equally to this work.

Received: 2 October 2017; Accepted: 27 October 2017; Published: 1 November 2017

**Abstract:** In an effort to allow to increase the number of aircraft and airport operations while mitigating their negative impacts (e.g., noise and pollutant emission) on near-airport communities, the optimal design of new departure routes with less noise and fuel consumption becomes more important. In this paper, a multi-objective evolutionary algorithm based on decomposition (MOEA/D), which recently emerged as a potential method for solving multi-objective optimization problems (MOPs), is developed for this kind of problem. First, to minimize aircraft noise for departure routes while taking into account the interests of various stakeholders, bi-objective optimization problems involving noise and fuel consumption are formulated where both the ground track and vertical profile of a departure route are optimized simultaneously. Second, in order to make the design space of vertical profiles feasible during the optimization process, a trajectory parameterization technique recently proposed is employed. Furthermore, some modifications to MOEA/D that are aimed at significantly reducing the computational cost are also introduced. Two different examples of departure routes at Schiphol Airport in the Netherlands are shown to demonstrate the applicability and reliability of the proposed method. The simulation results reveal that the proposed method is an effective and efficient approach for solving this kind of problem.

**Keywords:** departure routes; trajectory optimization; noise abatement; fuel consumption; MOEA/D

## 1. Introduction

Due to the high demand of air transport, the aviation industry is expected to develop rapidly in the coming years [1]. To adapt to this requirement, the increase of aircraft and airport operations is necessary and important. However, the increase in these operations often results in negative impacts on the quality of life of near-airport communities, such as noise and pollutant emissions [2]. As a result, the protest of communities surrounding airports becomes a major restriction that policymakers have to deal with when accommodating additional operations. In order to develop air transport sustainably, it is important to investigate potential solutions for decreasing its adverse influences. In recent years, a series of projects aiming to develop the aviation sector sustainably have been launched by European and national authorities, including CleanSky [3], the Atlantic Interoperability Initiative to Reduce Emission (AIRE) [4], and the Asia and South Pacific Initiative to Reduce Emission (ASPIRE) [5]. Various strategies have been proposed, such as making new policies and standards, developing advanced aircraft technologies and sustainable alternative fuels, and changing aircraft/airport operational procedures [6]. Among them, the change of aircraft/airport operational procedures may be a potential option in the short-term as it can be adapted more quickly and often at less cost as compared to the

other options [6]. The optimal design of new routes for departures and arrivals is one of the possible solutions that has been broadly studied in the past few years [7,8].

In order to design optimal environmentally friendly terminal routes, different approaches have been proposed in recent years. Visser and Wijnen [9,10] developed an optimization tool called NOISHHH that combines a noise model, an emissions inventory model, a geographic information system, and a dynamic trajectory optimization algorithm to generate environmentally optimal departure and arrival trajectories. Later, this tool was also adapted to optimize noise abatement terminal routes based on area navigation [11–13]. Prats et al. [14,15] employed a lexicographic optimization technique to deal with aircraft departure trajectories for minimizing noise annoyance. Khardi and Abdallah [16] studied a comparison of direct and indirect methods in solving a system of ordinary differential equations (ODEs) to optimize aircraft flight paths to reduce noise. Recently, Matthes et al. [17] presented a concept for multi-criteria environmental assessment of aircraft trajectories where the mathematical framework for environmental assessment and optimization of aircraft trajectories was developed. Despite being quite efficient in searching optimal trajectories, these techniques belong to the group of gradient-based methods that have certain limitations in solving optimization problems. For example, due to the use of gradient information to search for an optimal solution, these methods are often only suitable for optimization problems whose objective and constraint functions are differentiable and whose decision variables are continuous. Moreover, their solutions are often trapped in local optima if the considered problems are nonlinear and contain more than one local optimal solution. Nevertheless, current optimization problems become more and more complex due to the integration of operational constraints in realistic scenarios. It is therefore quite difficult to construct differentiable optimization problems. Also, these techniques are single-optimization methods, which means that only a single optimal solution is obtained after each time the optimization problem is solved.

By considering the above research gaps, different gradient-free optimization techniques have also been applied. Torres et al. [18] proposed a non-gradient optimizer called multi-objective mesh adaptive direct search (multi-MADS) to synthesize optimal departure trajectories for NO<sub>x</sub>-emissions and noise at a single measurement point. Recently, Hartjes and Visser [19] employed an elitist non-dominated sorting genetic algorithm (NSGA-II) combined with a novel trajectory parameterization technique for the optimal design of departure trajectories with environmental criteria. This approach was then also applied by Zhang et al. [20] to optimize departure routes at Manchester Airport. From the obtained results in [18–20], it is clear that the use of non-gradient multi-objective optimization methods is a potential approach for designing new routes. These methods readily overcome the limitations of gradient-based methods in dealing with discontinuous problems and integer or discrete design variables and can find out a set of non-dominated optimal solutions, which helps to present more options to policymakers and authorities. However, one of the major limitations of the methods in this group is their computational cost. Because they feature random searches with multiple design points at the same time, these methods require many evaluations of the objective and constraint functions which are quite time-consuming. These restrictions again have motivated researchers to develop computationally efficient approaches that can balance the expected results and computation cost effectively.

Until now, besides multi-MADS and NSGA-II, there are various multi-objective optimization algorithms available in the literature that may be considered potential candidates for solving these kinds of problems. However, they have not yet been properly investigated. Among them, the multi-objective evolutionary algorithm based on decomposition (MOEA/D) [21] has recently emerged as a powerful method and has received much attention from researchers. According to recent studies [21,22], MOEA/D has been demonstrated to be more efficient than NSGA-II and some other methods regarding both the quality of solutions and the convergence rate, which are promising features for solving large-scale real-world problems. Nonetheless, the application of MOEA/D to real engineering problems is still somewhat limited, especially in the field of aerospace engineering.

In this paper, MOEA/D is considered for the optimal design of aircraft noise abatement departure routes. As mentioned before, however, MOEA/D is a gradient-free optimization method, and hence its computation cost is still significant. In order to make the applied algorithm more efficient, a new implementation in the definition of the optimization problem for MOEA/D is introduced that can help to reduce the computational cost significantly. Furthermore, the efficiency of the MOEA/D version in this paper is also considerably enhanced by the integration of some recently developed advantageous features. These include an adaptive replacement strategy [23], a stopping condition criterion [24], and a constraint-handling technique [25]. Also, to reduce redundant evaluations of infeasible solutions derived from operational constraints during different flight phases, the new trajectory parameterization technique recently proposed in [19] is also applied. The robustness and reliability of the proposed method are validated through two numerical examples at Schiphol Airport in The Netherlands.

## 2. Aircraft Model and Trajectory Parameterization Technique

### 2.1. Aircraft Model

To model an aircraft during departure operations, an intermediate point-mass model [19] is used in this paper. The model is based on several assumptions: (1) there is no wind present; (2) the Earth is flat and non-rotating; and (3) the flight is coordinated. In addition, the flight path angle is considered sufficiently small ( $\gamma < 15^\circ$ ). The underlying assumption for the intermediate model is the equilibrium of forces normal to the flight path. The implication of this simplifying assumption is that the aerodynamic drag is slightly underestimated since it is evaluated as if the aircraft performs a quasi-linear flight. With these assumptions, the equations of motion can be stated as follows:

$$\dot{V}_{TAS} = g_0 \left[ \frac{(T - D)}{W} - \sin \gamma \right], \quad (1)$$

$$\dot{s} = V_{TAS} \cos \gamma, \quad (2)$$

$$\dot{h} = V_{TAS} \sin \gamma, \quad (3)$$

$$\dot{W} = -\dot{m}_f g_0, \quad (4)$$

where  $\dot{V}_{TAS}$ ,  $\dot{s}$ ,  $\dot{h}$ , and  $\dot{W}$  are the time derivatives of the true airspeed, ground distance flown, altitude, and aircraft weight, respectively;  $g_0$  is the gravitational acceleration, and  $T$ ,  $D$ , and  $\dot{m}_f$  are the thrust, drag, and fuel mass flow, respectively.

At low altitudes and airspeeds, the equivalent airspeed,  $V_{EAS}$ , can serve as a proxy for the indicated airspeed, and from the relationship with true airspeed, the following expression can be derived:

$$V_{EAS} = V_{TAS} \sqrt{\rho / \rho_0}, \quad (5)$$

where  $\rho$  is the ambient air density, and  $\rho_0$  is the air density at sea level.

By combining Equations (1)–(4) with Equation (5), the equations of motion can be rewritten as follows:

$$\dot{V}_{EAS} = \left\{ g_0 \left[ \frac{(T - D)}{W} - \sin \gamma \right] + \frac{1}{2\rho} \frac{\partial \rho}{\partial h} V_{TAS}^2 \sin \gamma \right\} \sqrt{\rho / \rho_0}, \quad (6)$$

$$\dot{s} = V_{EAS} \sqrt{\rho_0 / \rho} \cos \gamma, \quad (7)$$

$$\dot{h} = V_{EAS} \sqrt{\rho_0 / \rho} \sin \gamma, \quad (8)$$

$$\dot{W} = -\dot{m}_f g_0, \quad (9)$$

where,  $\frac{\partial \rho}{\partial h}$  is the derivative of the ambient air density with respect to altitude.

With the use of Equations (6)–(9), the aircraft performance model has two control variables, *viz.* the flight path angle  $\gamma$  and thrust  $T$ , and four state variables  $x = [V_{EAS}, h, s, W]$ .

2.2. The Trajectory Parameterization Technique

As pointed out in Section 1, although the use of gradient-free optimization methods has many advantages, their computational cost is still quite large, notably spent on evaluating the objective function or constraints (or model evaluations). Therefore, one of the most efficient approaches to reduce the computational cost for these methods is to decrease the number of model evaluations as much as possible, especially by avoiding the evaluation of infeasible solutions during the optimization process. In trajectory optimization problems, operational constraints in different flight phases can cause the violation of new solutions found by an optimization algorithm, and hence there will be a large amount of computation time for evaluating these solutions while they are not potential candidates for an optimal solution. Recognizing this problem, Hartjes and Visser [19] introduced a novel trajectory parameterization that can handle operational constraints in the problem formulation, thus reducing the computational cost significantly. This technique aims to decompose a trajectory into a separate vertical path and ground track. The main advantage of this decomposition is that events in the vertical and horizontal plane can be decoupled, and that the overall number of optimization parameters can be reduced significantly without compromising the accuracy or degrees of freedom of the final solutions.

For ground track generation, a modern navigation technology known as required navigation performance (RNP) is applied. In RNP, track-to-a-fix (TF) and radius-to-a-fix (RF) leg types are often used to construct flight paths between waypoints. This is because of their ability to avoid noise-sensitive areas and minimizing flight track dispersion. By using these two segment types, the ground track can be generated using only straight legs and constant radius turns. An example of this is given in Figure 1, where the optimal design variables comprise of  $L_1, L_2, R_1, R_2,$  and  $\Delta\chi_1$ . When the initial and final position is known, the remaining parameters  $L_3$  and  $\Delta\chi_2$  can be determined analytically through a geometric relationship.

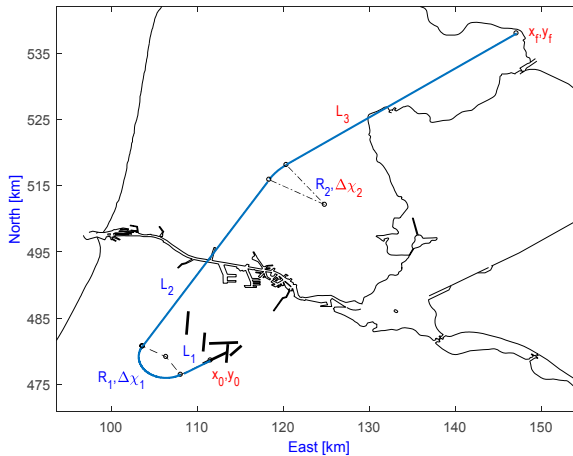


Figure 1. Ground track parameterization.

For the vertical path generation, the vertical profile is synthesized based on flight procedures derived from ICAO [26]. For instance, aircraft are not allowed to descend and/or decelerate during departure and ascend and/or accelerate during arrival. In order to parameterize this part, the trajectory is split into a number of segments. In each segment, two control inputs (i.e., flight path angle setting  $\gamma_{n,i}$  and throttle setting  $\Gamma_{n,i}$ ) are kept constant and are either directly assigned based on operational

requirements or designated as optimal design variables. For each segment, the flight path angle  $\gamma_i$  and thrust  $T_i$  are set by adjusting their normalized control optimization parameters  $\gamma_{n,i}$  ( $0 \leq \gamma_{n,i} \leq 1$ ), and  $\Gamma_{n,i}$  ( $0 \leq \Gamma_{n,i} \leq 1$ ), respectively, as follows:

$$\gamma_i = (\gamma_{\max,i} - \gamma_{\min,i})\gamma_{n,i} + \gamma_{\min,i}, \quad (10)$$

$$T_i = (T_{\max,i} - T_{\min,i})\Gamma_{n,i} + T_{\min,i}, \quad (11)$$

where the subscript  $n$  presents a normalized control optimization parameter. The subscripts  $\max, i$  and  $\min, i$  indicate the maximum and minimum allowable values of the flight path angle and thrust for the  $i$ th segment, which are specified based on the features of flight procedures.

In the departure procedure,  $T_{\max}$  is set to be either maximum take-off thrust (TO) or maximum climb thrust (TCL) depending on the flight stage. In addition, because descending is not permitted in this phase ( $\dot{h} \geq 0$ ), the minimum flight path angle is set to zero ( $\gamma_{\min}$ ). In addition, with the assumption that  $T_{\max}$  is selected and that the airspeed is maintained constant,  $\gamma_{\max}$  can be determined from Equation (6). Finally,  $T_{\min}$  can be determined as well from Equation (6), but now assuming level flight at constant speed is maintained. This yields the following equations:

$$\gamma_{\max} = \sin^{-1} \left[ \frac{-2\rho g_0 \cdot (T_{\max} - D)}{W \left( \frac{\partial \rho}{\partial h} V_{TAS}^2 - 2\rho g_0 \right)} \right], \quad (12)$$

$$T_{\min} = D - \frac{W}{2\rho g_0} \frac{\partial \rho}{\partial h} V_{TAS}^2 \sin \gamma_{\min} + W \sin \gamma_{\min}. \quad (13)$$

In the arrival procedure, the process is reversed. The minimum thrust  $T_{\min}$  is set equal to the idle thrust derived from the aircraft engine model, while the maximum flight path angle is set to be zero ( $\gamma_{\max} = 0$ ), as ascending is not allowed in the approach. In addition, by assuming that the aircraft is not allowed to accelerate during descending,  $T_{\max}$  can be determined by the same formula in Equation (13), replacing  $T_{\min}$  by  $T_{\max}$ . The minimum flight path angle  $\gamma_{\min}$  is evaluated with respect to the minimum thrust  $T_{\min}$  by the same formula in Equation (12), replacing  $T_{\max}$  and  $\gamma_{\max}$  by  $T_{\min}$  and  $\gamma_{\min}$ .

### 3. Formulation of the Optimization Problem

The main objective of the study is to design optimal departure routes which can help reduce considerably the adverse impact of aircraft noise on people living in the vicinity of airports. However, purely focusing on noise impact may result in a significant increase in fuel consumption, which is against the interests of stakeholders like airline companies. To balance this conflict, therefore, fuel consumption is also taken into account as the second objective.

While fuel consumption can readily be evaluated by the change of the aircraft weight from Equations (6)–(9), noise impact is harder to quantify. In order to measure the influence of aircraft noise on communities surrounding airports, the percentage of people who are likely to be awakened due to aircraft noise exposure is utilized in this paper. This criterion was proposed by the American National Standards Institute (ANSI) in 2008 and is defined as follows [27]:

$$\%Awakening = \frac{1}{1 + e^{-(-6.8884 + 0.04444SEL_{\text{indoor}})}}, \quad (14)$$

where %Awakening is the percentage of awakened people owing to the noise of an aircraft.  $SEL_{\text{indoor}}$  is the indoor sound exposure level in decibel (dB) and is evaluated by using a replica of the integrated noise model (INM) that has been the Federal Aviation Authorities' (FAA) standard regulatory noise model since the late 1970s [19]. Because SEL obtained from INM represents an outdoor value, an amount of 15 dB is subtracted to obtain  $SEL_{\text{indoor}}$ , accounting for the sound absorption of an average

house with an open window [28]. It should be noted that only SEL values that are larger than or equal to 50 dB are taken into account, while those that are less than 50 dB are ignored, and their probabilities are set to zero [29].

By considering two objectives (noise and fuel) at the same time, a bi-objective optimization problem is formulated as follows:

$$\begin{aligned}
 & \min_{x, \gamma_n, \Gamma_n} \quad \{\text{number of awakenings, fuel burn}\} \\
 & \text{s.t.} \quad \begin{aligned}
 & \mu \leq \mu_{\max} \\
 & h_f = h_{\text{final}} \\
 & V_{\text{EAS}, f} = V_{\text{EAS}, \text{final}}
 \end{aligned}
 \end{aligned} \tag{15}$$

where  $x$  is the vector of ground track variables.  $\gamma_n$  and  $\Gamma_n$  are the vectors of the flight path angle setting and throttle setting variables for each segment. The variable  $\mu$  is the bank angle, which is defined by  $\mu = \pm \tan^{-1} \left( \frac{V_{\text{IAS}}^2}{g0K} \right)$ . The parameter  $\mu_{\max}$  is the allowable value of  $\mu$ , which is dependent on altitude as specified by ICAO [26]. The parameters  $h_{\text{final}}$  and  $V_{\text{EAS}, \text{final}}$  are, respectively, the prescribed final altitude and equivalent airspeed of the flight procedures.

**4. MOEA/D Algorithm and New Implementations**

*4.1. MOEA/D Algorithm*

The multi-objective evolutionary algorithm based on decomposition (MOEA/D), first proposed by Zhang and Li [21], has been recognized as one of the most popular multi-objective evolutionary algorithms to date [30]. In MOEA/D, a multi-objective optimization problem (MOP) is transformed into a set of single optimization sub-problems by applying decomposition approaches, and then evolutionary algorithms are utilized to optimize these sub-problems simultaneously. With the use of different decomposition methods and different evolutionary algorithms, various versions of MOEA/D have been developed in recent years, e.g., MOEA/D-DE [22], MOEA/D-DRA [31], MOEA/D-XBS [21], and MOEA/D-GR [23]. Although different variants of MOEA/D are available in literature, a powerful single version of MOEA/D that integrates different advantages of the current versions is not yet in place. With the aim of developing an efficient version of MOEA/D for real-life problems, a powerful MOEA/D version is therefore developed in this study that is a combination of MOEA/D-DE [22], an adaptive replacement strategy [23], a stopping condition criterion [24], and a constraint-handling technique [25]. The general framework of MOEA/D is presented in Algorithm 1. For more details, readers are encouraged to refer to [22–25,32].

*4.2. New Implementations*

Although MOEA/D has been demonstrated to be more efficient than NSGA-II and other methods, and in this study, its performance has also been strongly supported by the integration of the powerful features recently developed, like other population-based optimization methods, MOEA/D is still time-consuming, requiring a significant amount of model evaluations. Since the considered problem is a constrained optimization problem, there could be many trial solutions evaluated by MOEA/D during the optimization process that violate the constraints (or are infeasible). The evaluations of these solutions may lead to a significant increase in the computational cost of the algorithm, while they may not provide helpful information for searching an optimal solution.

**Algorithm 1.** MOEA/D algorithm**Input:**

- A multi-objective optimization problem as Equation (15);
- A stopping criterion;
- $N$ : number of sub-problems;
- $w^i = (w_1^i, \dots, w_m^i)$ ,  $i = 1, \dots, N$ : a set of  $N$  weight vectors;
- $T_m$ : size of mating neighbourhood;
- $T_{max}$ : maximum size of replacement neighbourhood;
- $\delta$ : the probability that mating parents are selected from the neighborhoods;
- $MaxIter$ : maximum iteration;
- $FES = 0$ : the number of function evaluations;

**Step 1. Initialization**

- 1.1. Find the  $T_m$  closest weight vectors to each weight vector based on the Euclidean distances of any two weight vectors. For each sub-problem  $i = 1, \dots, N$  set  $B^i = (i_1, \dots, i_{T_m})$  where  $w^{i_1}, \dots, w^{i_{T_m}}$  are the closest weight vectors to  $w^i$ ;
- 1.2. Create an initial population  $P = \{x^1, \dots, x^N\}$  by uniformly randomly sampling from design space  $\Omega$ . Evaluate the fitness value  $FV^i$  of each solution  $x^i$ , i.e.,  $FV^i = (f_1(x^i), \dots, f_m(x^i))$  and set  $FV = \{FV^1(x^1), \dots, FV^N(x^N)\}$ ;
- 1.3. Initialize ideal point  $z^* = (z_1^*, \dots, z_m^*)^T$  by setting  $z_j^* = \min\{f_j(x) \mid x \in \Omega, j = 1, \dots, m\}^T$  and nadir point  $z^{nad} = (z_1^{nad}, \dots, z_m^{nad})^T$  by setting  $z_j^{nad} = \max\{f_j(x) \mid x \in \Omega, j = 1, \dots, m\}^T$ ;
- 1.4. Set  $FES = FES + N$ , and generation:  $gen = 1$ ;

**Step 2. Update**

**while** (the stopping condition is not satisfied)

**for**  $i = 1, \dots, N$ ; **do**

- 2.1. Selection of mating/update range

$$\text{Set } B_m \begin{cases} B^i & \text{if } rand < \delta \\ \{1, \dots, N\} & \text{otherwise} \end{cases}$$

where  $rand$  is a uniformly distributed random number in  $[0, 1]$ ;

- 2.2. Reproduction: randomly select three parent individuals  $r_1, r_2$  and  $r_3$  ( $r_1 \neq r_2 \neq r_3 \neq i$ ) from  $B_m$  and generate a solution  $\bar{y}$  by applying "DE/rand/1" operator, and then perform a mutation operator on  $\bar{y}$  to create a new solution  $y$ ;
- 2.3. Repair: if any element of  $y$  is out of  $\Omega$ , its value will be randomly regenerated inside  $\Omega$ ;
- 2.4. Evaluate the fitness value of new solution  $y$ ;
- 2.5. Update of  $z^*$  and  $z^{nad}$ : for each  $j = 1, \dots, m$  if  $z_j^* \leq f_j(x^i)$  then set  $z_j^* = f_j(x^i)$ , and if  $z_j^{nad} \geq f_j(x^i)$  then set  $z_j^{nad} = f_j(x^i)$ ;
- 2.6. Update of solutions: use an adaptive replacement strategy in [23];

**end for**

Set  $FES = FES + N$ , and  $gen = gen + 1$ ;

**Step 3. Stopping condition**

Use a stopping criterion in [24].

**if** (stopping criterion is satisfied or  $MaxIter$  is reached)

  Stop the algorithm;

**end if**

**end while**

**Output:** Pareto set  $PS = \{x^1, \dots, x^N\}$ ; Pareto front  $PF = \{FV^1(x^1), \dots, FV^1(x^N)\}$ .

In an effort to avoid the above problem, a new implementation on the setting of the optimization problem and MOEA/D is introduced. More specifically, for the considered problem, the computational cost is mainly spent on two main tasks: one for solving the ODEs to obtain the fuel objective and the necessary inputs for calculating noise and to evaluate the constraints of the optimization problem (for example, the final conditions of velocity and altitude, and the bank angle constraints), and the other for computing the noise objective. While the computational cost of the first task is not so significant, the computational expense of the second task is quite considerable. In MOEA/D, after a new solution is found, its objectives and constraints are measured and compared with those of previous solutions. The solutions with the better objectives and/or the better level of constraint violation will be selected for the next generation. It is readily clear that if there is a comparison between a feasible solution and an infeasible solution, the feasible one will be selected, and in the case of comparing two infeasible solutions, the solution with the lowest level of constraint violation will be chosen. By recognizing this feature, a new decision has been made for the algorithm to decide whether or not the noise calculation of a new solution is executed. Particularly, after the fuel objective and constraints of a new solution are assessed, a quick check and comparison of the level of constraint violation between them are executed first. If the new solution violates the constraints or has a higher level of constraint violation compared to, respectively, a feasible solution or an infeasible solution at the previous generation, its noise calculation will not be executed. In that case, the update procedures 2.5 and 2.6 of MOEA/D in Algorithm 1 are ignored as well.

With the above new implementation, the computational cost of noise calculation only is spent on either feasible solutions or on the infeasible solution with the lowest level of constraint violation, and hence the computational cost of the whole optimization process will be significantly reduced.

## 5. Numerical Example

In order to demonstrate the capabilities and efficiencies of MOEA/D for conducting the optimal design of noise abatement departure routes, two standard instrument departures (SID) currently in use at Schiphol Airport are considered in this section. The first SID is called SPIJKERBOOR2K, which starts at runway 24 and finishes at the ANDIK intersection, and the other one is ARNEM2N, which starts at runway 09 and terminates at the IVLUT intersection, as shown in Figure 2. These routes pass closely by the communities of Hoofddorp, Haarlem, and Amstelveen, where most of the noise nuisance occurs. For both departures, the optimized trajectory starts at 35 ft, a take-off safety speed of  $V_2 + 10$  kts, with the landing gear retracted and departure flaps selected and is terminated at an altitude of 6000 ft and an equivalent airspeed (EAS) of 250 kts. The ground tracks are constructed by three straight legs and two turns, as shown in Figure 2, which results in five design variables, while the vertical path is subdivided into 10 segments and parameterized as the study in [19], which results in an additional 18 design variables. For the reference case, the ground track is fixed to conform to the current SID, while the vertical path is optimized for fuel burn after finishing the NADP-1. The details of the parameterization can be found in Hartjes and Visser [19]. Two noise-exposed regions of  $66 \text{ km} \times 59 \text{ km}$  and  $36.5 \text{ km} \times 20 \text{ km}$  with a population grid cell size of  $500 \text{ m} \times 500 \text{ m}$  [33] are used for the SPIJKERBOOR2K and ARNEM2N SIDs, respectively. A Boeing 737-800 with two engines is used as the aircraft model, based on the Base of Aircraft Data (BADA), with an initial mass of 68 tons (85% of the maximum take-off weight) as a representative take-off mass.

To compare the performance of MOEA/D, the well-known NSGA-II [34] is also applied to solve these problems. A population size of 50 is used for both methods, and the algorithms will stop when either their convergence criteria are satisfied or the maximum number of iterations (*MaxIter*) is reached, where *MaxIter* is set at 1000. All algorithms are implemented in Matlab 2016b on a Core i5, 8 GB RAM desktop.

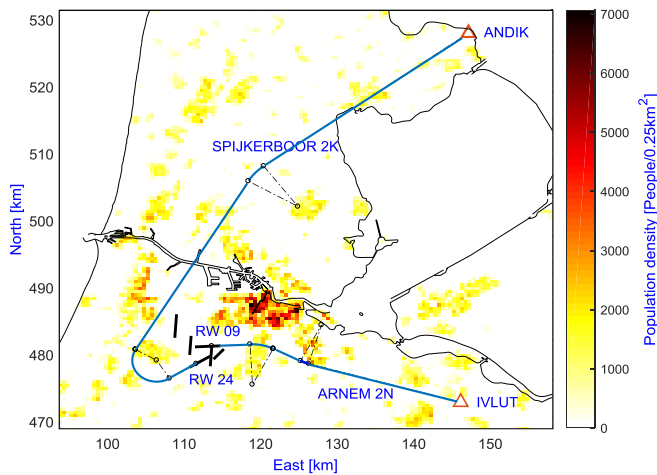


Figure 2. Departure scenarios.

### 5.1. Departure Route SPIJKERBOOR2K

The Pareto-optimal solutions obtained by the methods are shown in Figure 3, and their corresponding ground tracks are illustrated in Figure 4. The cases highlighted in Figure 3 by a yellow star and red circle are also highlighted in Figure 4 and further discussed in the text. From a comparison of solution methods in Figure 3, it can be seen that the quality of solutions obtained by MOEA/D is generally better than those achieved by NSGA-II. Specifically, MOEA/D provides many solutions that dominate those of NSGA-II with a significantly lower computational effort. In order to achieve these results, MOEA/D requires 23,357 model evaluations, in which only 8399 involve a noise calculation. Hence, the total computation time is only 2.2 h, while NSGA-II requires 50,500 evaluations resulting in 9.59 h computation time for a full evaluation.

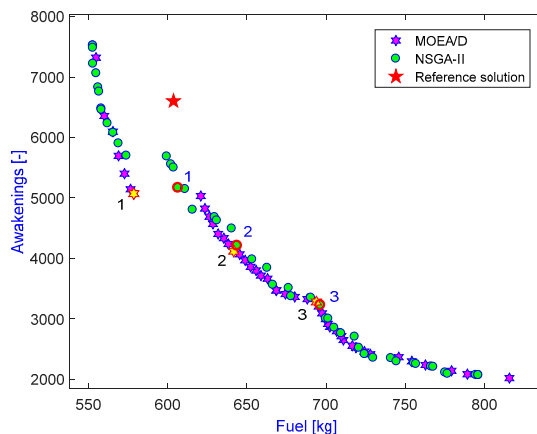


Figure 3. Comparison of optimal solutions obtained by NSGA-II, MOEA/D, and the reference case.

From an engineering point of view, it can be seen that the obtained ground tracks in Figure 4 are quite reasonable and appropriate. There are three different groups of ground tracks generated by MOEA/D and four groups by NSGA-II, all of them trying to avoid noise-sensitive communities.

These results also help to explain why there are some gaps in the Pareto fronts. In comparison to the reference case, it can be observed that most of the optimal solutions offer a better environmental performance. In particular, as shown in the left of Figure 3, there are some cases that perform better for both objectives, whereas the remaining solutions on the right are much better regarding awakenings, although there is a slight increase in fuel burn.

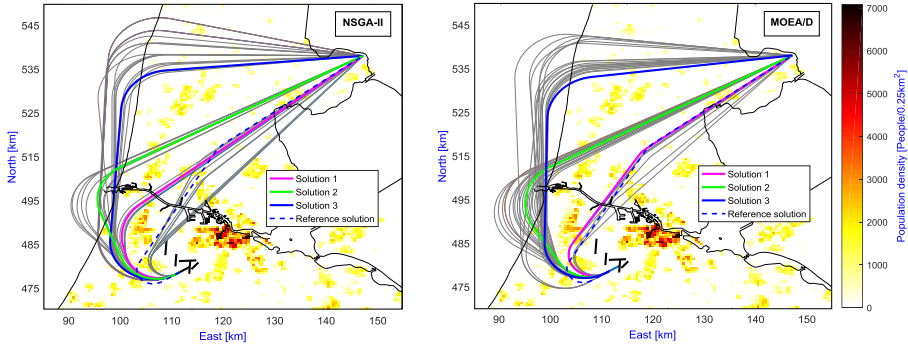
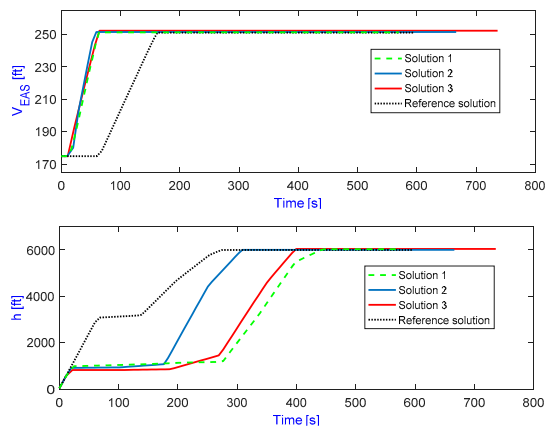
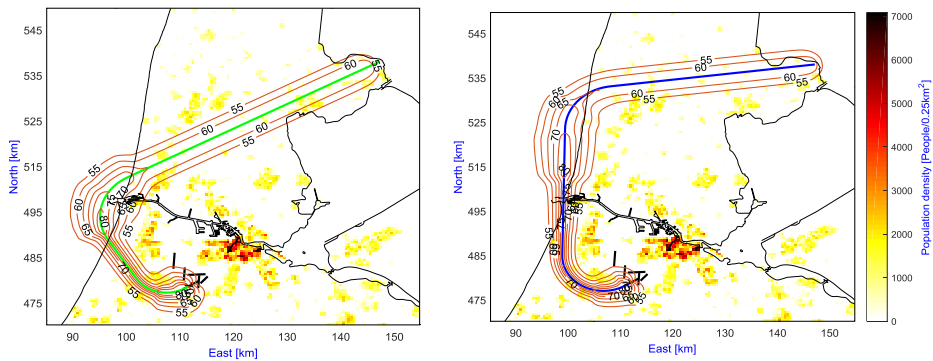


Figure 4. Optimal ground tracks obtained by NSGA-II (left) and MOEA/D (right).

For a performance comparison, the number of people expected to be awakened and the fuel burn of the three representative cases are extracted from the Pareto fronts (numbered as shown in Figures 3 and 4) and listed in Table 1 along with the results of the reference case. The vertical profiles of the MOEA/D computed cases are given in Figure 5. Compared to the reference case, it can be seen that all solutions are non-dominated, either better at awakenings and worse at fuel burn or vice versa, except for case 1. Despite having almost the same ground track length with an optimal combination of the ground track and vertical profile, case 1 offers much better performance in terms of all three criteria. From Table 1, it can also be seen that the difference between the objective values of the three representative cases is significant, especially in terms of the number of awakenings. A relatively small detour allows a significant part of the communities surrounding the airport to be avoided, and, considering the exponential relationship between noise and awakenings, consequently leads to a significant reduction in the noise criterion. By taking a closer look at Figure 5, it can be seen that in the first phase of flight, for all optimal cases, the aircraft prefers to fly at a low altitude with a high speed to pass over populated regions. This is because the spread of aircraft noise at a low altitude is smaller than that at a higher altitude due to increased lateral attenuation, and hence it leads to a significant reduction of awakenings. Also, maintaining a low altitude allows the aircraft to accelerate to a high airspeed sooner, which leads to lower exposure times and hence to lower SEL-values, while the source noise levels do not increase significantly. From Figure 5, it also becomes clear that the time during which the aircraft stays at a low altitude is dependent on the population density distribution underneath the flight path. This is also clearly depicted in Figure 6, where the noise level contours of cases 2 and 3 are illustrated.

**Table 1.** Comparison of objectives of cases 1–3 and the reference case.

Case Number		Time (s)	Fuel (kg)	Awakening
1	MOEA/D	569.69	578.66	5072
	NSGA-II	612.68	607.91	5199
2	MOEA/D	666.38	641.81	4121
	NSGA-II	668.63	643.76	4213
3	MOEA/D	736.27	693.90	3280
	NSGA-II	747.17	696.35	3232
Reference solution		595.11	603.69	6602

**Figure 5.** Vertical profiles of cases 1–3, and the reference case.**Figure 6.** Noise level contours for cases 2 (left) and 3 (right).

## 5.2. Departure Route ARNEM2N

The Pareto-optimal solutions obtained by MOEA/D and NSGA-II for this example are illustrated in Figure 7, while the ground tracks are provided in Figure 8. Again, some representative cases are highlighted in the figures. To acquire these results, NSGA-II requires 45,000 model evaluations in 4.36 h, while MOEA/D converges after 24,122 model evaluations in 1.99 h, with only 17,010 requiring a noise calculation. Compared to the previous example, the obtained ground tracks, in this case, are more divergent. This is because there is no area with a high concentration of population within the

investigated region except for a small area close to runway 09. However, this region has been avoided by most of the optimal solutions. It can also be seen from Figure 7 that all optimal solutions dominate the reference case.

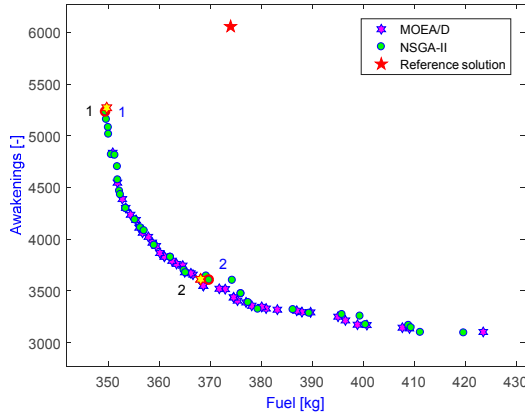


Figure 7. Comparison of optimal solutions obtained by NSGA-II and MOEA/D and the reference case.

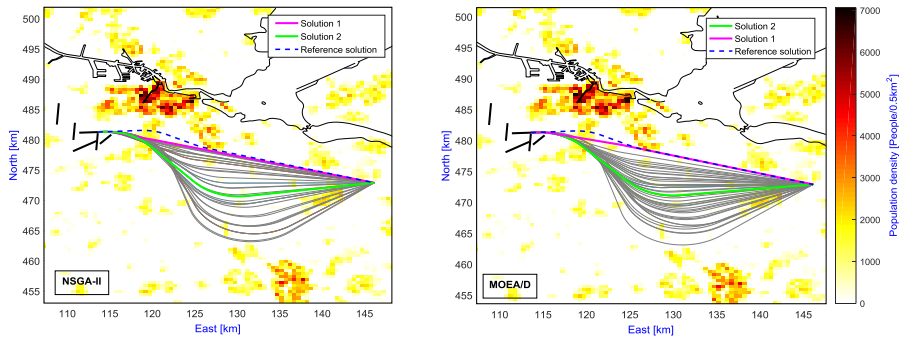


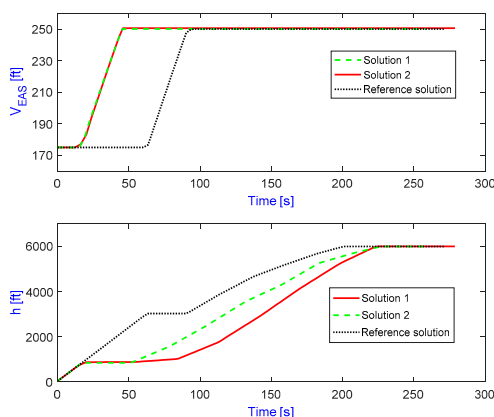
Figure 8. Optimal ground tracks obtained by NSGA-II (left) and MOEA/D (right).

For a comparison of specific values, the number of awakenings and fuel burn of the representative cases extracted from the Pareto-optimal solutions (as highlighted in Figure 7) are given in Table 2. The vertical profiles of the MOEA/D cases are also provided in Figure 9. From the table, it can be seen that all optimal cases have better results regarding fuel burn and awakenings compared to the reference case, while case 1 significantly outperforms the reference case on all considered criteria (i.e., fuel burn, awakenings, and time). As the airspeed and altitude histories are concerned, their behavior is almost the same as in the previous example. The aircraft often fly at a low altitude with a relatively high speed when passing over densely populated areas in the first phases, while the time during which an aircraft flies at a low attitude depends on the population distribution underneath a flight path.

Summarizing, based on the obtained results, it can be concluded that MOEA/D is an effective method for solving the optimal design problem of noise abatement departure routes. Compared to NSGA-II, MOEA/D generally outperforms NSGA-II in terms of both the quality of solutions and computation time.

**Table 2.** Comparison of objectives of cases 1–2 and the reference case.

Case Number		Time (s)	Fuel (kg)	Awakening
1	MOEA/D	257.51	349.71	5271
	NSGA-II	256.29	349.46	5232
2	MOEA/D	278.81	368.14	3613
	NSGA-II	281.19	370.28	3634
Reference solution		271.14	374.01	6058

**Figure 9.** Vertical profiles of cases 1–2, and the reference solution.

## 6. Conclusions

In this study, a novel and efficient application of MOEA/D for the optimal design of noise abatement departure routes is presented. Besides the typical advantages, the performance of MOEA/D is also considerably enhanced by the integration of recently developed features, which include an adaptive replacement strategy, a stopping condition criterion, and a constraint-handling technique. Also, the performance of the entire optimization process is significantly improved by the implementation on the setting of the optimization problem and the MOEA/D algorithm. Owing to this implementation, the computational cost of solving the optimization problems is sharply reduced.

The applicability and effectiveness of MOEA/D and the new implementations are demonstrated through two example scenarios of departure routes at Schiphol Airport in the Netherlands: SPIJKERBOOR2K and ARNEM2N. For comparison purposes, NSGA-II is also applied to solve these problems. The comparative results show that MOEA/D is generally better than NSGA-II when considering the quality of solutions and much better regarding the convergence rate and overall computational cost.

With these promising results, in future work, MOEA/D will be extended to consider different routes at other airports, and its performance will also be investigated in different associated problems like route and runway allocations. Furthermore, the performance of the algorithm will also be further enhanced to deal with large and complex problems, especially in the distribution of solutions and the convergence rate.

**Author Contributions:** Vinh Ho-Huu developed the optimization algorithm, performed the numerical examples, and wrote the manuscript. Sander Hartjes proposed the idea and analyzed the results. Hendrikus G. Visser and Richard Curran provided important feedback on the proposed approach and contributed to the review of the paper.

**Conflicts of Interest:** The authors declare no conflict of interest.

## References

1. Boeing. Current Market Outlook 2016–2035. Available online: [http://www.boeing.com/resources/boeingdotcom/commercial/about-our-market/assets/downloads/cmo\\_print\\_2016\\_final\\_updated.pdf](http://www.boeing.com/resources/boeingdotcom/commercial/about-our-market/assets/downloads/cmo_print_2016_final_updated.pdf) (accessed on 12 July 2017).
2. Hartjes, S.; Dons, J.; Visser, H.G. Optimization of Area Navigation Arrival Routes for Cumulative Noise Exposure. *J. Aircr.* **2014**, *51*, 1432–1438. [CrossRef]
3. Clean Sky. Available online: <http://www.cleansky.eu/#no-back> (accessed on 23 October 2017).
4. Atlantic Interoperability Initiative to Reduce Emissions (AIRE). Available online: [https://ec.europa.eu/transport/modes/air/environment/aire\\_en](https://ec.europa.eu/transport/modes/air/environment/aire_en) (accessed on 23 October 2017).
5. Asia and South Pacific Initiative to Reduce Emissions (ASPIRE). Available online: <http://www.aspire-green.com/> (accessed on 23 October 2017).
6. Marais, K.B.; Reynolds, T.G.; Uday, P.; Muller, D.; Lovegren, J.; Dumont, J.-M.; Hansman, R.J. Evaluation of potential near-term operational changes to mitigate environmental impacts of aviation. *Proc. Inst. Mech. Eng. Part G J. Aerosp. Eng.* **2013**, *227*, 1277–1299. [CrossRef]
7. Visser, H.G. Generic and site-specific criteria in the optimization of noise abatement trajectories. *Transp. Res. Part D Transp. Environ.* **2005**, *10*, 405–419. [CrossRef]
8. Green, J.E. Air Travel-Greener by Design Mitigating the environmental impact of aviation: Opportunities and priorities. *Aeronaut. J.* **2005**, *109*, 361–416.
9. Visser, H.G.; Wijnen, R.A.A. Optimization of Noise Abatement Departure Trajectories. *J. Aircr.* **2001**, *38*, 620–627. [CrossRef]
10. Visser, H.G.; Wijnen, R.A.A. Optimisation of noise abatement arrival trajectories. *Aeronaut. J.* **2003**, *107*, 607–615.
11. Hartjes, S.; Visser, H.G.; Hebly, S.J. Optimisation of RNAV noise and emission abatement standard instrument departures. *Aeronaut. J.* **2010**, *114*, 757–767. [CrossRef]
12. Hogenhuis, R.H.; Hebly, S.J.; Visser, H.G. Optimization of area navigation noise abatement approach trajectories. *Proc. Inst. Mech. Eng. Part G J. Aerosp. Eng.* **2011**, *225*, 513–521. [CrossRef]
13. Braakenburg, M.L.; Hartjes, S.; Visser, H.G. Development of a Multi-Event Trajectory Optimization Tool for Noise-Optimized Approach Route Design. *AIAA* **2011**, 1–13. [CrossRef]
14. Prats, X.; Puig, V.; Quevedo, J.; Nejari, F. Lexicographic optimisation for optimal departure aircraft trajectories. *Aerosp. Sci. Technol.* **2010**, *14*, 26–37. [CrossRef]
15. Prats, X.; Puig, V.; Quevedo, J.; Nejari, F. Multi-objective optimisation for aircraft departure trajectories minimising noise annoyance. *Transp. Res. Part C Emerg. Technol.* **2010**, *18*, 975–989. [CrossRef]
16. Khardi, S.; Abdallah, L. Optimization approaches of aircraft flight path reducing noise: Comparison of modeling methods. *Appl. Acoust.* **2012**, *73*, 291–301. [CrossRef]
17. Matthes, S.; Grewe, V.; Dahlmann, K.; Frömming, C.; Irvine, E.; Lim, L.; Linke, F.; Lühns, B.; Owen, B.; Shine, K.; et al. A Concept for Multi-Criteria Environmental Assessment of Aircraft Trajectories. *Aerospace* **2017**, *4*, 42. [CrossRef]
18. Torres, R.; Chaptal, J.; Bès, C.; Hiriart-Urruty, J.-B. Optimal, Environmentally Friendly Departure Procedures for Civil Aircraft. *J. Aircr.* **2011**, *48*, 11–23. [CrossRef]
19. Hartjes, S.; Visser, H. Efficient trajectory parameterization for environmental optimization of departure flight paths using a genetic algorithm. *Proc. Inst. Mech. Eng. Part G J. Aerosp. Eng.* **2016**, *231*, 1115–1123. [CrossRef]
20. Zhang, M.; Filippone, A.; Bojdo, N. Multi-objective departure trajectory optimisation of commercial aircraft on environmental impacts. In Proceedings of the Greener Aviation Conference, Brussels, Belgium, 11–13 October 2016.
21. Zhang, Q.; Li, H. MOEA/D: A Multiobjective Evolutionary Algorithm Based on Decomposition. *IEEE Trans. Evol. Comput.* **2007**, *11*, 712–731. [CrossRef]
22. Li, H.; Zhang, Q. Multiobjective Optimization Problems with Complicated Pareto Sets, MOEA/D and NSGA-II. *IEEE Trans. Evol. Comput.* **2009**, *13*, 284–302. [CrossRef]
23. Wang, Z.; Zhang, Q.; Zhou, A.; Gong, M.; Jiao, L. Adaptive Replacement Strategies for MOEA/D. *IEEE Trans. Cybern.* **2016**, *46*, 474–486. [CrossRef] [PubMed]
24. Abdul Kadhar, K.M.; Baskar, S. A stopping criterion for decomposition-based multi-objective evolutionary algorithms. *Soft Comput.* **2016**, 1–20. [CrossRef]

25. Jan, M.A.; Khanum, R.A. A study of two penalty-parameterless constraint handling techniques in the framework of MOEA/D. *Appl. Soft Comput. J.* **2013**, *13*, 128–148. [[CrossRef](#)]
26. International Civil Aviation Organization. *Procedures for Air Navigation Services—Aircraft Operations; Flight Procedures*, ICAO Document Number 8168; International Civil Aviation Organization: Montreal, QC, Canada, 2006; Volume I.
27. ANSI/ASA. *Quantities and Procedures for Description and Measurement of Environmental Sound—Part 6: Methods for Estimation of Awakenings Associated with Outdoor Noise Events Heard in Homes*; ANSI/ASA: Washington, DC, USA, 2008.
28. Miller, N.P.; Schomer, P.D. How many people will be awakened by noise tonight? *Acoust. Today* **2009**, *5*, 26–31. [[CrossRef](#)]
29. Yu, H.; Van Kampen, E.-J.; Mulder, J.A. An Optimization Paradigm for Arrival Trajectories using Trajectory Segmentation and State Parameterization. *AIAA Guid. Navig. Control Conf.* **2016**, 1–17. [[CrossRef](#)]
30. Trivedi, A.; Srinivasan, D.; Sanyal, K.; Ghosh, A. A Survey of Multiobjective Evolutionary Algorithms based on Decomposition. *IEEE Trans. Evol. Comput.* **2016**, 440–462. [[CrossRef](#)]
31. Zhang, Q.; Liu, W.; Li, H. The performance of a new version of MOEA/D on CEC09 unconstrained MOP test instances. *IEEE Congr. Evol. Comput.* **2009**, 203–208.
32. Ho-Huu, V.; Hartjes, S.; Visser, H.G.; Curran, R. An improved MOEA/D algorithm for bi-objective optimization problems with complex Pareto fronts and its application to structural optimization. *Expert Syst. Appl.* **2017**. [[CrossRef](#)]
33. Xue, M.; Zelinski, S. Integrated Arrival- and Departure-Schedule Optimization Under Uncertainty. *J. Aircr.* **2015**, *52*, 1437–1443. [[CrossRef](#)]
34. Deb, K.; Pratab, S.; Agarwal, S.; Meyarivan, T. A Fast and Elitist Multiobjective Genetic Algorithm: NSGA-II. *IEEE Trans. Evol. Comput.* **2002**, *6*, 182–197. [[CrossRef](#)]



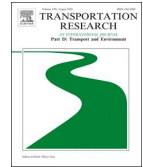
© 2017 by the authors. Licensee MDPI, Basel, Switzerland. This article is an open access article distributed under the terms and conditions of the Creative Commons Attribution (CC BY) license (<http://creativecommons.org/licenses/by/4.0/>).



Contents lists available at ScienceDirect

## Transportation Research Part D

journal homepage: [www.elsevier.com/locate/trd](http://www.elsevier.com/locate/trd)



# Integrated design and allocation of optimal aircraft departure routes

V. Ho-Huu\*, S. Hartjes, H.G. Visser, R. Curran

Faculty of Aerospace Engineering, Delft University of Technology, Delft, The Netherlands



3

### ARTICLE INFO

#### Keywords:

Departure routes  
Trajectory optimization  
Aircraft allocation  
Noise abatement  
Noise events  
Fuel consumption

### ABSTRACT

This paper presents a new multi-objective optimization formulation for the design and allocation of optimal aircraft departure routes. In the considered problem – besides two conventional objectives based on cumulative noise criteria and fuel burn – a new objective considering the flight frequency is introduced. Moreover, to take advantage of the combination of designing new routes and allocating flights to these routes, two different routes are considered simultaneously, and the distribution of flights over these two routes is addressed in parallel. Then, a new version of the so-called MOEA/D optimization algorithm is developed to solve the formulated optimization problem. Two different case studies, one at Rotterdam The Hague Airport and one at Amsterdam Airport Schiphol in The Netherlands, are carried out to evaluate the reliability and applicability of the proposed approach. The obtained results reveal that the proposed approach can provide solutions which can balance more effectively the concerned metrics such as the number of annoyed people, fuel burn, number of people exposed to certain noise levels, and number of aircraft movements which people are subjected to.

## 1. Introduction

With a significant impact on economic development, communication, tourism and job creation, aviation is predicted to grow quickly in the coming years (Boeing, 2016). In response to this trend, airports are forced to increase their operations, and hence a significantly increasing amount of aircraft movements needs to be handled every day. Nevertheless, the expansion of these activities often causes harmful effects on local communities such as noise and pollutant emissions (Hartjes et al., 2014). This leads to an adverse community reaction to authorities and policymakers, resulting in opposition to the extension of airport and aircraft operations. Thus, it is crucial to identify solutions to aid the sustainable development of the aviation industry, while minimizing its adverse impact as much as possible.

In an effort to overcome the above issues, a series of research initiatives has been launched in recent years, e.g. Clean Sky\*, AIRE†, and ASPIRE‡. Apart from these research initiatives, a number of different approaches have also been proposed – and are currently being implemented – such as creating new criteria and regulations, advancing new engine/aircraft models and replaceable fuels, and

\* Corresponding author.

E-mail addresses: [v.hohuu@tudelft.nl](mailto:v.hohuu@tudelft.nl) (V. Ho-Huu), [s.hartjes@tudelft.nl](mailto:s.hartjes@tudelft.nl) (S. Hartjes), [h.g.visser@tudelft.nl](mailto:h.g.visser@tudelft.nl) (H.G. Visser), [r.curran@tudelft.nl](mailto:r.curran@tudelft.nl) (R. Curran).

† Clean Sky. <http://www.cleansky.eu/#no-back>. (accessed 23 October 2017).

‡ Atlantic Interoperability Initiative to Reduce Emissions (AIRE). [https://ec.europa.eu/-transport/modes/air/environment/aire\\_en](https://ec.europa.eu/-transport/modes/air/environment/aire_en), (accessed 23 October 2017).

\* Asia and South Pacific Initiative to Reduce Emissions (ASPIRE). <http://www.aspire-green.com/>, (accessed 23 October 2017).

<https://doi.org/10.1016/j.trd.2018.07.006>

varying operational procedures of aircraft and airports (Marais et al., 2013). From a practical implementation point of view, it can be observed that the variation of aircraft/airport operational procedures emerges as a suitable option that can result in short term improvements and could be less costly in comparison with the other options. For this approach, the optimal design of routes for departures and arrivals, and the allocation of aircraft to these routes are considered as the most promising options (Green, 2005).

The literature shows that efforts to design optimal departure and arrival routes with less noise and fuel burn have been well studied over the past decades, and various strategies have been proposed. For example, the optimization tool NOISHHH, a combination of a dynamic trajectory optimization method, a noise model, an inventory model of emissions and a Geographic Information System (GIS), was developed by Visser and Wijnen (2003, 2001) to create environmentally optimal departure and arrival trajectories. This tool was extended over the years for amongst others the design of optimal terminal routes based on area navigation (Braakenburg et al., 2011; Hartjes et al., 2010; Hogenhuis et al., 2011). A lexicographic optimization approach was utilized by Prats et al. (2011, 2010a, 2010b) to optimize aircraft departure trajectories with noise annoyance criteria. In an effort to reduce noise impact, Khardi and Abdallah (2012) carried out a comparison study of direct and indirect approaches for solving the system of ordinary differential equations (ODEs) to generate optimal aircraft flight paths. Torres et al. (2011) applied a gradient-free optimization method called multi-objective mesh adaptive direct search (multi-MADS) to create optimal departure trajectories with less noise and  $\text{NO}_x$ -emissions at a single measurement point. Hartjes and Visser (2016) proposed a novel trajectory parameterization technique, and then applied the elitist non-dominated sorting genetic algorithm (NSGA-II) to design environmentally friendly departure trajectories. Later, this technique was also utilized to design departure routes at Manchester Airport by Zhang et al. (2016). Recently, a multi-objective evolutionary algorithm based on decomposition (MOEA/D) was developed by Ho-Huu et al. (2017, 2018a) to design optimal departure routes with less noise and fuel burn.

Besides the attempts to design environmentally friendly departure/arrival routes, the allocation of aircraft and operational procedures to specific routes could also help to considerably diminish the environmental impacts. For instance, Frair (1984) proposed a nonlinear integer programming model to minimize community annoyance at an airport by allocating aircraft to the existing arrival and departure trajectories. Zachary et al. (2010) investigated the optimization problem which aims at finding an optimal combination of approach and departure routes, operational procedures and fleet composition to optimize noise and pollutant emissions. Kuiper et al. (2012) developed an optimization tool for allocating and distributing the annual aircraft movements over available runways and routes to maximize the allowable number of flight operations into and out of an airport within a given annual noise budget. Kim et al. (2014) built an optimization model to minimize the total emissions on the airport surface and in the terminal area by allotting aircraft to runways and scheduling the arrival and departure operations on these runways concurrently.

Looking at the above literature review on the design of arrival and departure routes, the studies can be generally categorized into two different groups: those using single-event noise criteria (Hartjes et al., 2010; Ho-Huu et al., 2017; Hogenhuis et al., 2011; Prats et al., 2010a, 2010b; Torres et al., 2011; Visser and Wijnen, 2001, 2003) and those using multi-event or cumulative noise criteria (Braakenburg et al., 2011; Hartjes et al., 2014). For the first group, the most widely used criterion is to minimize the number of people awakened, which is derived from either the Federal Interagency Committee on Aviation Noise (FICAN, 1997) or later the American National Standards Institute (ANSI, 2008). Although results can be obtained for different types of aircraft, the resulting optimal routes are most likely only suitable for those specific aircraft. This is because the noise criteria are evaluated based on a specific aircraft model. From an airport operations or Air Traffic Control point of view, however, it is not feasible to manage individual routes for individual aircraft types. For the second group, the most broadly used criterion is to minimize the number of people annoyed, where dose-response relationships based on the day-evening-night noise level ( $L_{den}$ ) or night noise level ( $L_{night}$ ) are often employed (Braakenburg et al., 2011; Hartjes et al., 2014). Unlike the first approach, these noise criteria are determined based on the aggregation of noise caused by different aircraft types, where the number of aircraft movements is also taken into account. Therefore, the optimal routes obtained can be applied for different aircraft types and depend on an assumed fleet mix. Though the optimal solutions do not fully exploit the potential noise reduction for each individual aircraft type because of the requirements to follow a common path, from an operational perspective this approach is easier to implement.

From the studies using the second approach, it is also identified that all studies design only one optimal route at a time, and all aircraft movements have to follow the same common path. Although the multi-event noise metrics have already included the influence of the number of aircraft movements, they do not explicitly take into account the frequency of those events. Though noise levels will increase with increasing aircraft movements, and consequently the number of people highly annoyed will increase as well, it is conceivable that an increase in the number of movements above a certain level may lead to more resistance in local communities than the common dose-response relationships would predict. This issue has recently been recognized as one of the emerging concerns that should be investigated and taken into account in noise regulations and policies (Brown, 2014; Fields, 1984; Janssen et al., 2014). In addition, recent studies have also pointed out that despite playing an important role in noise assessment, the above metrics contain certain limitations (Porter et al., 2014; Southgate, 2011). Most importantly, these metrics do not represent the actual experience of communities who are not noise experts, and hence it is difficult for authorities and decision makers to communicate related policies to the local communities. As a consequence, they have been regularly considered as unhelpful and lacking transparency (Porter et al., 2014; Southgate, 2011). In order to address this issue, the Australian Government developed supplementary noise descriptor concepts that can help the general public to understand and communicate with the authorities (DOTARS, 2000). They include the numbers of events above certain noise levels (N70s, N65s), Person Event Index (PEI) and Average Individual Exposure (AIE), which are helpful to provide simple information on the location of flight paths, the number of aircraft movements and the time of day of the movements. Nowadays, these metrics have been recognized and widely used in many countries in the world such as Austria, Sweden and the United Kingdom (Porter et al., 2014). So far, these metrics are, however, rarely considered for designing new aircraft routes.

In an attempt to generate optimal departure routes which can balance the above concerns more effectively, in this paper we have

developed a new approach for the optimum design and allocation of departure routes. In the formulation of optimization problems, besides a conventional noise objective derived from cumulative noise criteria (i.e., the number of people annoyed) and fuel burn, a new objective considering the frequency of noise events is developed. While the first and second objectives can be obtained by designing only one route as in traditional approaches (Braakenburg et al., 2011; Hartjes et al., 2014), to minimize the third objective and essentially to distribute the noise impact, evidently at least two alternative routes are needed. For this reason, in the proposed optimization problem two alternative routes will be considered at the same time, and the allocation of flights to these two routes will be optimized concurrently. Furthermore, to make the approach more generic, two different departure procedures currently in use, namely, Noise Abatement Departure Procedure 1 and 2 (NADP1, NADP2) (ICAO, 2006) are utilized and considered as design variables as well.

With the above considerations, a multi-objective optimization problem with three objectives is formulated. It can be recognized that this is a nonlinear multi-objective optimization problem with mixed discrete-continuous design variables, where the continuous variables relate to the coordinates of the two routes, based on the regulations of the International Civil Aviation Organization (ICAO, 2006), while the discrete variables are the number of flights on each route and the selection of one of the two noise abatement departure procedures, i.e. NADP1 or NADP2. In addition, the optimization problem has both equality and inequality constraints, which are the restrictions on the total number of flights and on aircraft performance, such as bank angle constraints. Generally, this is a complicated optimization problem that needs a specific algorithm for resolution. In this study, a new version of the algorithm called multi-objective optimization based on decomposition (MOEA/D), which has been developed recently by the authors in Ho-Huu et al. (2017, 2018a) is extended to address this problem. Nevertheless, compared with the problems in Ho-Huu et al. (2017), besides the inequality constraints the problem in this study contains both equality constraints and mixed discrete-continuous design variables. Therefore, to increase the performance of the algorithm, techniques for handling these issues are also proposed.

The reliability, effectiveness and applicability of the proposed approach are demonstrated through two different case studies in The Netherlands. The first one is a scenario at a regional airport, viz. Rotterdam The Hague Airport (RTM), and the second example is a case study at one of the busiest airports in the world, viz. Amsterdam Airport Schiphol (AAS). The obtained simulation results indicate that the proposed approach can provide optimal solutions which offer a good trade-off between the concerned metrics.

The rest of the paper is structured as follows. Section 2 presents the formulation of the multi-objective optimization problem. Section 3 gives a brief overview of the trajectory parameterization technique and aircraft performance modeling. Section 4 describes the optimization algorithm and two techniques for handling the equality constraints and mixed discrete-continuous design variables. The numerical examples are presented in Section 5, and finally some conclusions and are stated in Section 6.

**2. Multi-objective optimization problem formulation**

As discussed above, to generate optimal departure routes which can effectively handle the concerns of policymakers, airlines and communities, besides the traditional objectives like the number of people annoyed and fuel burn, it is relevant to include objectives which can take into account the frequency of aircraft noise events. Therefore, a new optimization objective which considers this concern is developed in this study. In general, the mathematical model of an optimization problem with three objectives is stated as follows:

$$\begin{aligned} & \min_{\mathbf{d}} \quad (f_1(\mathbf{d}), f_2(\mathbf{d}), f_3(\mathbf{d})) \\ & \text{s.t.} \quad \sum_{j=1}^2 a_{ij} = T_{at,i}, \quad i = 1, \dots, N_{at} \\ & \quad \quad \mu_i(t) \leq \mu_{\max}(h) \end{aligned} \tag{1}$$

where  $\mathbf{d} = \{\mathbf{g}, \mathbf{a}, \mathbf{p}\}$  is the design variable vector of the optimization problem, in which  $\mathbf{g}$  is the vector of variables defining the geometric parameters of two departure routes,  $\mathbf{a}$  is the vector of aircraft allocation to each route (in which  $a_{ij}$  is the number of aircraft type  $i$  on route  $j$ ) and  $\mathbf{p}$  is the vector of noise abatement departure procedures of aircraft type  $i$  on route  $j$ . The parameters  $N_{at}$  and  $T_{at,i}$  are, respectively, the number of aircraft types and the total number of aircraft of type  $i$ . The variable  $\mu_i(t)$  is the bank angle of aircraft type  $i$  and denoted by  $\mu_i(t) = \pm \tan^{-1} \left( \frac{V_{T,i}^2}{g_0 R} \right)$ , where  $V_{T,i}$  is the true airspeed of aircraft type  $i$ ,  $g_0$  is the gravitational acceleration,  $R$  is the turn radius of the departure route, and  $t$  is the time at the turns. The parameter  $\mu_{\max}(h)$  is the maximum allowable value of  $\mu$ , which is stipulated for different altitudes  $h$  by ICAO (2006). It should be noted that the calculation of  $\mu_i(t)$  has been simplified based on the assumptions given in Section 3.2.

In the optimization problem in Eq. (1), the first objective  $f_1(\mathbf{d})$  is the total number of people annoyed, which is evaluated based on a criterion defined within the European Union (EEA, 2010). According to EEA (2010), the percentage of people annoyed (%PA) caused by a certain  $L_{den}$  value is determined as follows:

$$\%PA(\mathbf{r}, \mathbf{d}) = 8.588 \times 10^{-6} (L_{den}(\mathbf{r}, \mathbf{d}) - 37)^3 + 1.777 \times 10^{-2} (L_{den}(\mathbf{r}, \mathbf{d}) - 37)^2 + 1.221 (L_{den}(\mathbf{r}, \mathbf{d}) - 37) \tag{2}$$

in which  $L_{den}(\mathbf{r}, \mathbf{d})$  is the day-evening-night noise level defined by

$$L_{den}(\mathbf{r}, \mathbf{d}) = 10 \log_{10} \left[ \sum_{j=1}^2 \sum_{i=1}^{N_{at}} a_{ij} 10^{\frac{SE_{Eij}(\mathbf{r}, \mathbf{d}) + w_{den}}{10}} \right] - 10 \log_{10} T \text{ (dBA)}, \tag{3}$$

where  $\mathbf{r} = (x, y)$  is the vector of the center coordinates of a grid cell in the investigated area. The metric  $SEL_{ij}(\mathbf{r}, \mathbf{d})$  is the sound exposure level caused by aircraft type  $i$  on route  $j$  at the grid cells. This metric is calculated by employing a tool implemented in FORTRAN that uses an exact replication of the noise model described in the technical manual of the Integrated Noise Model (INM) (FAA, 2008). The parameters  $w_{den} = \{0, 5, 10\}$  are the weighting factors for day, evening and night time operations. By using a Geographic Information System (GIS), the objective  $f_1(\mathbf{d})$  can be determined by taking the sum of the multiplication of %PA in each grid cell with the population in that cell. The second objective  $f_2(\mathbf{d})$  is the total fuel burn which aircraft consume during departure and is denoted as follows:

$$f_2(\mathbf{d}) = \sum_{j=1}^2 \sum_{i=1}^{N_{at}} a_{ij} fuel_{ij}(\mathbf{d}), \quad (4)$$

where  $fuel_{ij}(\mathbf{d})$  is the fuel burn of aircraft type  $i$  on route  $j$ , which is evaluated based on the change of the aircraft weight during departure. The third objective  $f_3(\mathbf{d})$  is a composite objective based on the Person Event Index (PEI), which is the number of noise events above 65 dBA  $L_{A,max}(\mathbf{r}, \mathbf{d})$  (so-called N65) multiplied by the population in each grid cell. Note that  $L_{A,max}$  is also computed by using the same tool that is used to calculate  $SEL_{ij}(\mathbf{r}, \mathbf{d})$ . It is recalled that the main objective is to distribute the noise impact whilst still minimizing the number of people annoyed as defined in objective  $f_1(\mathbf{d})$ . Thus, the third objective function is formulated as follows:

$$f_3(\mathbf{d}) = \sum_{j=1}^2 \left( \prod_{i=1: N65}^{N_{at}} N_{p,j} \sum_{i=1}^{N_{at}} a_{ij} k_j \right) + \sum_{j=1}^2 \prod_{i=1: N65}^{N_{at}} S_{p,j} \quad (5)$$

where the term  $\prod_{i=1: N65}^{N_{at}} N_{p,j}$  is the total number of people enclosed in the intersection of the N65 contours caused by all aircraft types on route  $j$ , while the term  $\prod_{i=1: N65}^{N_{at}} S_{p,j}$  is the total number of people enclosed in the intersection of N65 contours caused by all aircraft types on both routes. The parameter  $k_j$  is a real number, which is equal to 1 if route  $j$  accommodates more than or equal to 50% of the total aircraft movements, and 0 otherwise. It should be noted that the number of flights on each route is determined in advance for any individual aircraft type based on the information of the design variables of aircraft allocation, and hence the value  $k_j$  in Eq. (5) is known.

In Eq. (5), the first component of the sum is essentially the PEI metric. Nevertheless, to avoid the trajectories converging at the same path, the PEI metric is only taken into account if the number of flights on a route is greater than or equal to 50%. This is controlled by the parameter  $k_j$ . Close to the runway, however, all departing aircraft still share the same ground track. People living in this area will be exposed to all aircraft movements regardless of the ground tracks of these routes or the allocation of flights to them. To ensure the trajectories are split up as soon as possible, and consequently to minimize the number of people exposed to all aircraft movements, the second component of Eq. (5) is taken into account. When minimized, this composite objective ensures that two distinct routes will be created that diverge as soon as possible within the limits of trajectory design and aircraft performance.

### 3. Trajectory parameterization and aircraft performance modeling

#### 3.1. Trajectory parameterization

In order to parameterize a trajectory in both the lateral and vertical plane, a trajectory parameterization technique developed recently by Hartjes and Visser (2016) is employed. This approach divides a trajectory into two isolated parts: a vertical path and a ground track. For the creation of the ground track, navigation based on required navigation performance (RNP) is assumed. In RNP, the flight path can be constructed by connecting waypoints through track-to-a-fix (TF) and radius-to-a-fix (RF) leg types. The advantages of using these leg types are that they can generate routes which can keep aircraft away from noise-sensitive areas and reduce flight track dispersion as well. Fig. 1 shows an example of a ground track generated using a sequence of TF and RF legs. From this figure, it can be observed that the design variable vector  $\mathbf{g}$  of a departure route consisting of four straight legs and three turns comprises  $L_1, L_2, L_3, R_1, R_2, R_3, \Delta\chi_1$  and  $\Delta\chi_2$ , while  $L_4$  and  $\Delta\chi_3$  are determined through the geometric relationship assuming the initial and final position are fixed. In this work, two different routes with the same definition, i.e. the same number of leg types, are considered and optimized simultaneously. Therefore, the number of design variables for generating routes is doubled.

For the vertical path, the vertical profile is created based on flight procedures derived from ICAO (2006), where two standard departure procedures, namely, Noise Abatement Departure Procedure 1 and 2 (NAPD1 and NAPD2), as shown Fig. 2, are used. In this study, the vertical procedure is fixed and complies with either NAPD1 or NAPD2. Therefore, there are no design variables considered in this part. Instead, the selection between NAPD1 and NAPD2 is included as a design variable for each aircraft type on each route. This aims to explore the advantage of these procedures for different aircraft types on different routes as well as to ensure that the optimal routes can be applied to all aircraft types.

#### 3.2. Aircraft performance modeling

In this study, an intermediate point-mass model is used (Hartjes and Visser, 2016). The model is based on some assumptions including: (1) no wind present, (2) a flat and non-rotating Earth, (3) coordinated flight, and (4) a sufficiently small flight path angle ( $\gamma < 15^\circ$ ). With the given assumptions, the equations of motion can be written by

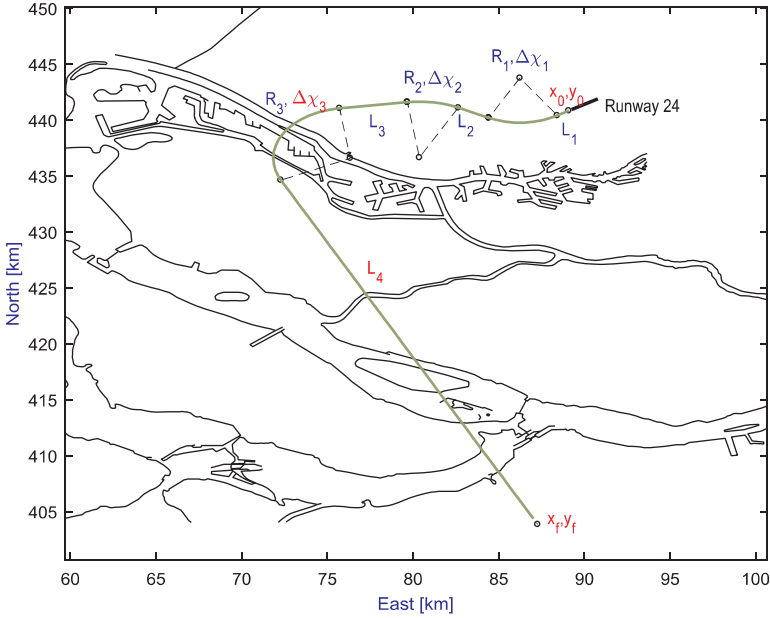


Fig. 1. Illustration of ground track parameterization.

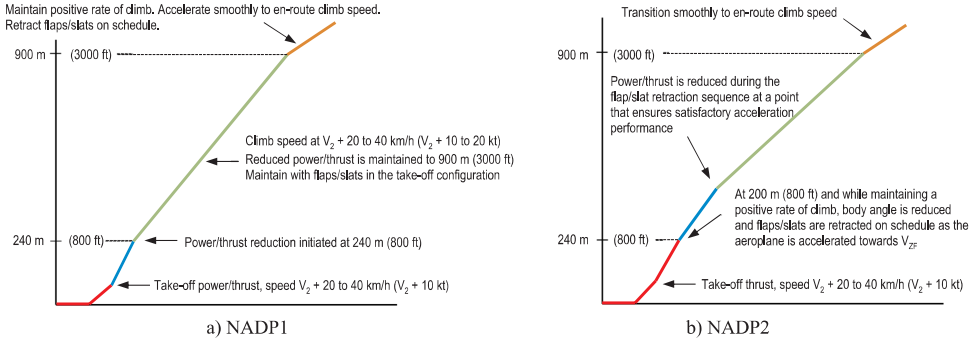


Fig. 2. Noise abatement departure procedure 1 and 2 (ICAO, 2006).

$$\begin{aligned}
 \dot{V}_T &= g_0 \left( \frac{T-D}{W} - \sin \gamma \right), \\
 \dot{s} &= V_T \cos \gamma, \\
 \dot{h} &= V_T \sin \gamma, \\
 \dot{W} &= -ff g_0,
 \end{aligned}
 \tag{6}$$

in which,  $V_T$ ,  $s$ ,  $h$  and  $W$  are the true airspeed, ground distance flown, altitude and aircraft weight, respectively. The parameters  $T$ ,  $D$  and  $ff$  are, respectively, thrust, drag and fuel flow.

In case of low altitudes and airspeeds, the indicated airspeed can be approximated by the equivalent airspeed  $V_E$ , and expressed as:

$$V_E = V_T \sqrt{\rho/\rho_0},
 \tag{7}$$

where  $\rho$  is the ambient air density, and  $\rho_0$  is the air density at sea level.

Based on the relationship in Eq. (7), the equations of motion in Eq. (6) can be rewritten as follows:

$$\begin{aligned}
 \dot{V}_E &= \left[ g_0 \left( \frac{T-D}{W} - \sin \gamma \right) + \frac{1}{2\rho^2} \frac{\partial \rho}{\partial h} V_E^2 \rho_0 \sin \gamma \right] \sqrt{\rho/\rho_0}, \\
 \dot{s} &= V_E \sqrt{\rho_0/\rho} \cos \gamma, \\
 \dot{h} &= V_E \sqrt{\rho_0/\rho} \sin \gamma, \\
 \dot{W} &= -ff g_0,
 \end{aligned} \tag{8}$$

where  $\frac{\partial \rho}{\partial h}$  is the derivative of the ambient air density with respect to altitude.

By integrating Eq. (8) along the trajectory defined in Section 3.1, the input parameters for the calculation of  $SEL$  and  $L_{A,\max}$  are acquired. By using the tool to calculate noise, the values of  $SEL_{ij}(\mathbf{r}, \mathbf{d})$  and  $L_{A,\max}(\mathbf{r}, \mathbf{d})$  at each grid cell are determined. When the velocity  $V_T$ , altitude  $h$  and the geometry of the route are known, the bank angle constraints in Eq. (1) are also evaluated for each aircraft type.

3

#### 4. Optimization algorithm

In this article, a new version of an optimization method called the multi-objective evolutionary algorithm based on decomposition (MOEA/D), which has been developed for the optimal design of departure routes in Ho-Huu et al. (2017) is employed. The method is a variant of the original MOEA/D algorithm proposed by Zhang and Li (2007), which has been demonstrated to be a potential candidate for solving complicated multi-objective optimization problems in the field of aerospace engineering (Ho-Huu et al., 2017). Therefore, it is again applied to solve the optimization problem stated in Section 2 in this study. However, compared with the problem in Ho-Huu et al. (2017), the considered optimization problem in this study is more complicated as it features three objectives and contains both continuous and discrete design variables, and equality constraints originating from the allocation of aircraft to different routes. To make the algorithm more efficient two techniques for handling these issues have also been developed. Since details of the algorithm have been given in Ho-Huu et al. (2017, 2018b) and Zhang and Li (2007), interested readers are encouraged to refer to these references, while the new techniques are presented in the next subsections.

##### 4.1. Handling mixed discrete-continuous variables

As pointed out in Section 2, the optimization problem has two different types of design variables, *viz.* continuous and discrete variables. The continuous variables are a set of geometric parameters to construct flight paths such as  $L_1, L_2, L_3, R_1, R_2$ , and  $\Delta\chi_1$  as given in Section 3. The discrete variables are integer numbers, including the number of each aircraft type on each departure route, and variables to select between the two possible departure procedures (NADP1 or NADP2, which are labeled as 1 and 2, respectively). Since the original MOEA/D algorithm has been developed mainly for optimization problems with continuous design variables, to deal with these kinds of variables during the optimization process a simple rounding technique is applied to the set of discrete design variables. Specifically, whenever the optimization algorithm creates a new candidate for optimal solutions, all real-valued solutions indicated for discrete variables will be rounded to the nearest discrete values in their permissible sets, while there are no additional steps for the continuous variables. By applying this technique, it is ensured that all candidate solutions found by the algorithm satisfy the requirements of the optimization problem, and hence the unnecessary computational burden of infeasible solutions will be reduced significantly.

##### 4.2. Handling equality constraints

The MOEA/D algorithm is a population-based optimization method inspired by natural phenomena, finding optimal solutions by randomly searching with multi-design points at a time. Therefore, solving optimization problems by employing this method is often time-consuming. Recognizing this issue, in the recent version (Ho-Huu et al., 2017), we have developed a new adjustment on the settings of the optimization problem and the algorithm itself, which helps to significantly reduce the unnecessary computational cost. Compared to the original method, this variant has already shown to be very effective. However, this version only handles inequality constraints (*i.e.*, bank angle constraints), while the problem considered in this study contains both inequality and equality constraints. As seen in Eq. (1), the equality constraint ensures that the number of aircraft allocated to the two alternative departure routes must be equal to the total number of aircraft. However, it is obvious that many solutions created by the algorithm do not satisfy all constraints – especially the equality constraints. Consequently, if we approach this problem by using typical methods for constraint handling like the penalty method, the computational cost spent on the evaluation of infeasible solutions will be extremely high. Therefore, while keeping the same technique for coping with the inequality constraints as in the previous version, a new simple technique for handling equality constraints is introduced in this work.

A general procedure of the technique is presented in steps as follows:

- In the optimization problem in Eq. (1), each equality constraint  $i$  ( $i = 1, \dots, N_{at}$ ) is replaced by a new variable  $c_i$ .
- For each new variable  $c_i$ , the set of feasible combinations  $\mathbf{S}_i$  of the allocation of aircraft type  $i$  to all routes is defined. Note that a combination is feasible when the sum of the number of aircraft type  $i$  on all routes is equal to the total number of aircraft type  $i$  ( $T_{at,i}$ ).
- In set  $\mathbf{S}_i$ , the combinations are represented by integer values, which are numbered from 1 to the last combination. Then, the design

space as well as the boundaries of variables  $c_i$  are determined, which are integer values. The lower bound is set to 1, and the upper bound will be the length of set  $S_i$ .

In order to make the proposed approach more transparent, a simple example is considered here. It is assumed that there are 20 flights with only one aircraft type which need to be distributed over two departure routes. From Eq. (1), we have  $i = 1, j = 2$ , and the equality constraint is defined as  $a_{11} + a_{12} = 20$ , with  $a_{11}, a_{12} \in \{0, 1, 2, \dots, 20\}$ . From this constraint, it is obvious that there is only a set of twenty-one possible combinations between  $a_{11}$  and  $a_{12}$  which satisfy the constraint,  $S = \{\{0,20\},\{1,19\},\dots,\{10,10\},\dots,\{19,1\},\{20,0\}\}$ . This set can be represented by defining a new variable  $c$  ( $c \in \{1, 2, \dots, 21\}$ ), where 1, 2, ..., 21 are, respectively, the combinations of  $\{0,20\}, \{1,19\}, \dots, \{20,0\}$ . In addition, in this work the design of two alternative routes and the allocation of aircraft movements takes place simultaneously and flexibly, hence the set of  $S$  can be reduced from twenty-one to eleven combinations and denoted by  $S = \{\{0,20\},\{1,19\},\dots,\{10,10\}\}$ . Consequently, the search space of the variable  $c$  is decreased considerably. It should be noted that for this specific example – having only two design variables in the equality constraint – we can use only  $a_{11}$  as a design variable, and  $a_{12}$  can be derived from the definition of the equality constraint. This approach is, however, only valid for equality constraints with two design variables. In addition, it should be noted that the proposed technique may be limited for certain problems with limited numbers of design variables as the set of feasible combinations will increase significantly with larger numbers of design variables.

In summary, applying the above technique to all equality constraints for the aircraft allocation will help decrease the complexity of the optimization problem and reduce the search space of the problem. Hence, the optimization process will be much faster, and the computational cost can be diminished considerably.

## 5. Numerical results and discussions

To demonstrate the reliability and applicability of the proposed approach, two different case studies are carried out in this section. The first example is a scenario at Rotterdam The Hague Airport (RTM), where a standard instrument departure (SID) named WOODY is considered. The second example is set at Amsterdam Airport Schiphol (AAS), where a SID called LUNIX is investigated. In order to evaluate the influence of the third objective on the optimal routes, for each case study two different optimization problems are evaluated. In the first problem only the two objectives  $f_1(\mathbf{d})$  and  $f_2(\mathbf{d})$  are optimized, while the second problem considers all three objectives at the same time. Both SIDs are currently in use at the airports, and the existing SIDs are used as reference solutions in the next sections. To solve the optimization problems, the MOEA/D algorithm is used with a population size of 50 and a maximum number of iterations of 1000. The search process of the algorithm will be terminated when either the stopping criterion is met or the maximum number of iterations has been reached. All simulations are implemented in Matlab 2016b on an Intel Core i5, 8 GB RAM desktop.

### 5.1. Rotterdam the Hague airport case study

Rotterdam The Hague Airport is a regional airport located to the north of the city of Rotterdam in The Netherlands, and is surrounded by densely populated regions such as The Hague, Rotterdam, and Utrecht. The design of a new optimal departure route for the WOODY SID, in this example, is assumed to start at the end of runway 24 at an altitude of 35 ft and a take-off safety speed of  $V_2 + 10$  kts, and finishes at waypoint EH162 at an altitude of 6000 ft and an equivalent airspeed (EAS) of 250 kts. It is assumed that on a peak day, there are 40 flights following this SID. This assumption is based on the reference data at flightradar24<sup>§</sup> in the summer season, which also indicates that there are only three aircraft types commonly operating from RTM, viz. the Embraer 190 (E190), Boeing 737–700 (B737) and B737–800 (B738). Also, in an effort to avoid the noise computation burden associated with the noise impact assessment, these aircraft can be represented by one aircraft type (Hartjes et al., 2014). In this study, the B738 is selected as a representative aircraft for the noise calculations. It is also noted that for the allocation of aircraft, the real departure times are ignored, and hence all flights are assumed to count as a day-time flight in the determination of the noise impact.

By applying the parameterization technique described in Section 3 and allocation variables described in Section 4.2, the optimization problems have nineteen design variables: sixteen variables to describe the two alternative ground tracks, one for the aircraft allocation, and two to select the departure procedures. An area of  $22 \times 30.5$  km and a population grid cell size of  $500 \times 500$  m (based on data obtained from the Dutch Central Bureau of Statistics (CBS)) are used for the noise calculations, as shown in Fig. 3. The aircraft are modeled based on the Base of Aircraft Data (BADA) (Angela et al., 2010). The optimization takes 3.08 hours (h) with 562 iterations and 4.31 h with 942 iterations to achieve a full convergence for the first and second problems, respectively.

The comparison of Pareto solutions for fuel burn and number of people annoyed obtained by both approaches are presented in Fig. 4, in which the reference solutions are marked as well. The Pareto solutions acquired by solving the second problem (optimization with three objectives) are given in Fig. 5. As seen in Fig. 4, the solutions acquired by both approaches are quite close together, and most of the solutions obtained by the first approach dominate those of the second one. Nevertheless, if the third objective (essentially representing the spreading of the noise impact) is considered to evaluate the results of the first approach, all of their solutions are worse than those of the second approach. This is because the solutions obtained by the second approach have to balance between the three objectives, while those of the first problem only balance between the first two objectives. Moreover, as shown in

<sup>§</sup> <https://www.flightradar24.com/data/airports/rtm/departures>.

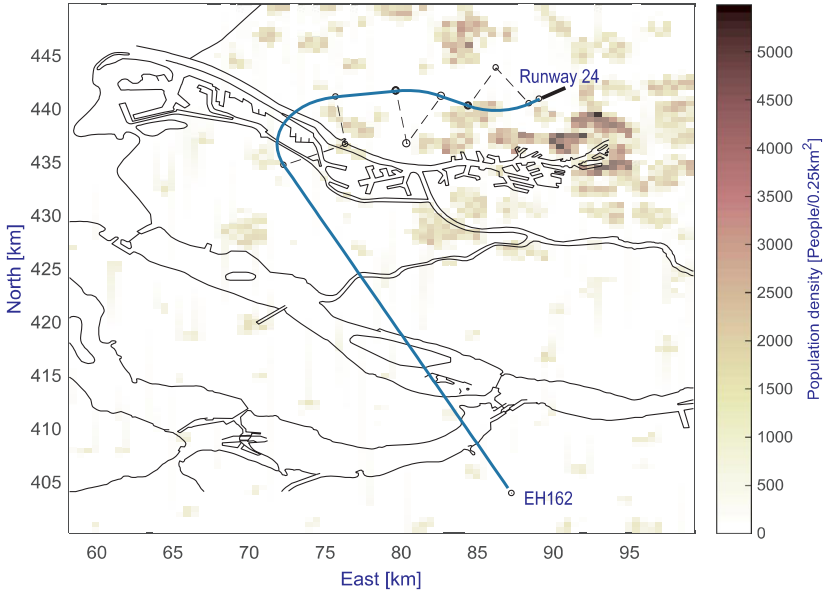


Fig. 3. Departure route WOODY.

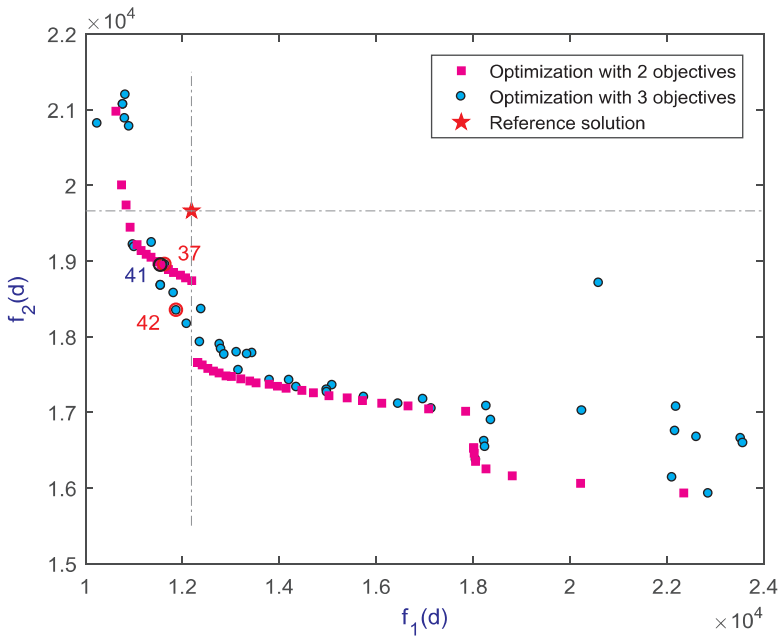


Fig. 4. Comparison of Pareto fronts obtained by the first and second problems and the reference case.

Fig. 4, the second approach can also provide some solutions which dominate some of the solutions found in the first problem. In a comparison with the reference solution, from the figure, it is observed that both approaches offer better solutions regarding both fuel burn and number of annoyed people.

The ground tracks corresponding to the solutions given in Figs. 4 and 5 are provided in Figs. 6 and 7, where the former shows

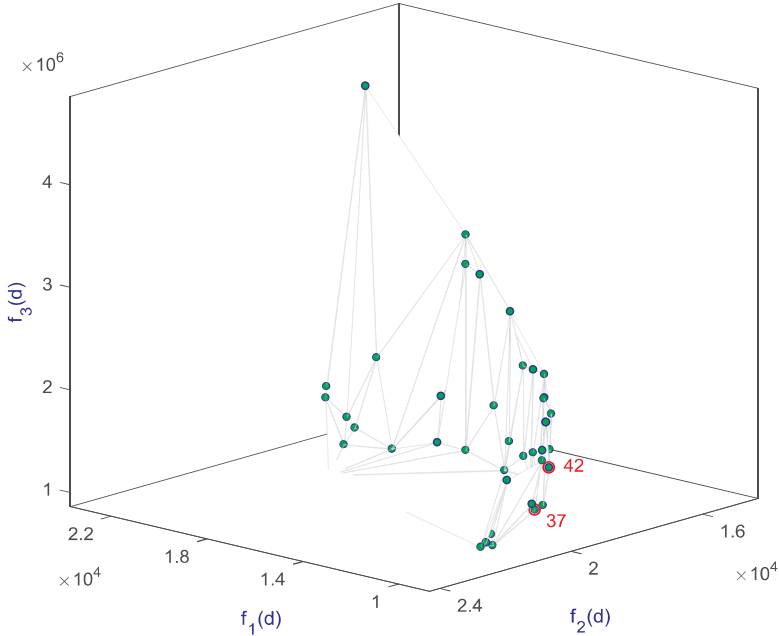


Fig. 5. Pareto fronts obtained by the second problem.

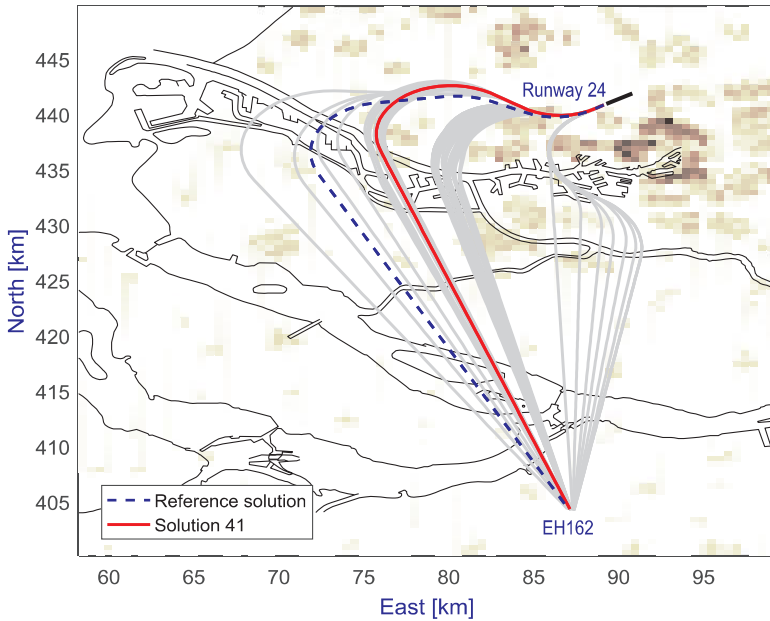


Fig. 6. Optimal ground tracks obtained by the first problem.

those of the first problem, and the latter shows those of the second one. Some routes have been highlighted corresponding to the solutions highlighted in Figs. 4 and 5. It should be noted that in all results the NADP2 departure procedure is selected as an optimal procedure for all obtained routes. For the first approach – only considering fuel burn and people annoyed – only one optimal route is

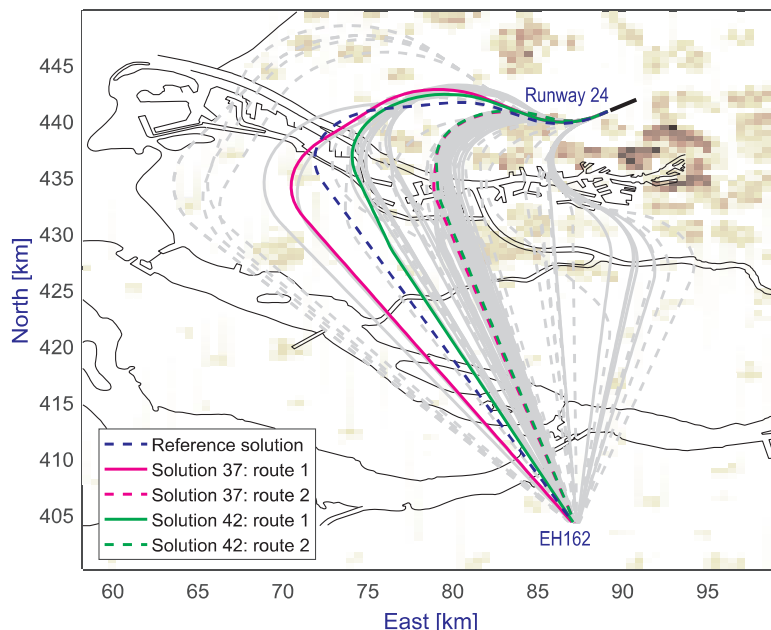


Fig. 7. Optimal ground tracks obtained by the second problem.

found for each solution, and all aircraft are allocated on the same route as can be seen in Fig. 6. On the other hand, when considering all three objectives, most of the solutions contain two distinct routes with different allocations of aircraft as shown in Fig. 7, where the alternative routes are indicated by solid and dashed lines. Looking at the figures, it can be seen that all the solutions tend to avoid the most densely populated areas.

In order to show the comparison between the two different approaches and the reference case more clearly, the ground tracks of the representative solutions as highlighted in Fig. 4, and that of the reference solution, are presented in Fig. 8, where the N65 and 37 dBA  $L_{den}$  contours (the threshold level for annoyance) are given as well. A comparison of the representative solution 41 of the first problem with the reference case indicates that route 41 takes a longer initial right turn to avoid the population close to the runway and turns towards the South sooner to reduce the total ground distance and hence the fuel burn. Therefore, its performance is better than the reference case for both objectives. Similarly, solutions 37 and 42 of the second approach show the same trend. Looking at solution 37, though the first route (red line) is longer than the reference route, the second one is much shorter, and owing to the distinct distribution of aircraft on each route (19 flights on the red route and 21 flights on the blue route), the total fuel burn is reduced significantly. This is similar for solution 42. Nevertheless, due to the spreading of the noise, the  $L_{den}$  contours of these solutions are larger than those of solution 41 and the reference solution, which may lead to a higher number of people annoyed. The numerical results presented in Table 1, however, show that the number of people annoyed has not significantly increased as compared to solution 41 optimized for only two objectives. The explanation for this can be seen in Fig. 9, where it can be seen that although the 37 dBA  $L_{den}$  contours are wider, the concentration of noise is lower, which limits the increase in the number of annoyed people as compared to solution 41. For the third objective, representing the spreading of noise, however, solutions 37 and 42 obviously provide a considerable reduction, while for the reference case and solution 41, this objective logically remains very high. In addition, the conflicting nature of the considered objectives can also be observed in these figures. While the conflict of the first two objectives is quite apparent in Fig. 4, the potential conflict between them and the third objective can be recognized in the comparison of solution 41 and solutions 37 and 42, as shown in Fig. 8. More specifically, in the case where all aircraft follow the same route as in solution 41, it is obvious that the number of annoyed people is reduced significantly owing to the narrow  $L_{den}$  contour. Nevertheless, all people living underneath the flight path will be exposed to all aircraft movements. Meanwhile, if there is a sharing of routes as in solutions 37 and 42, the number of annoyed people may be higher, but the number of people exposed to all flights is significantly lower. Based on these observations, it can be concluded that the optimization problem formulated in Section 2 is reasonable and basically satisfies the general requirements of a multi-objective optimization problem. From a practical point of view, however, it should be noted that since the distribution of optimal routes depends highly on the distribution of population around the airport, in some cases these objectives may or may not conflict.

The specific comparison of indicators estimated by the representative and reference cases is given in Table 1. The indicators contain number of people annoyed, fuel burn, number of people enclosed in the N65 contour and exposed more than 50% of the flights, the Person Event Index (PEI), and the Average Individual exposure (AIE) (which is the division of PEI and the total exposed

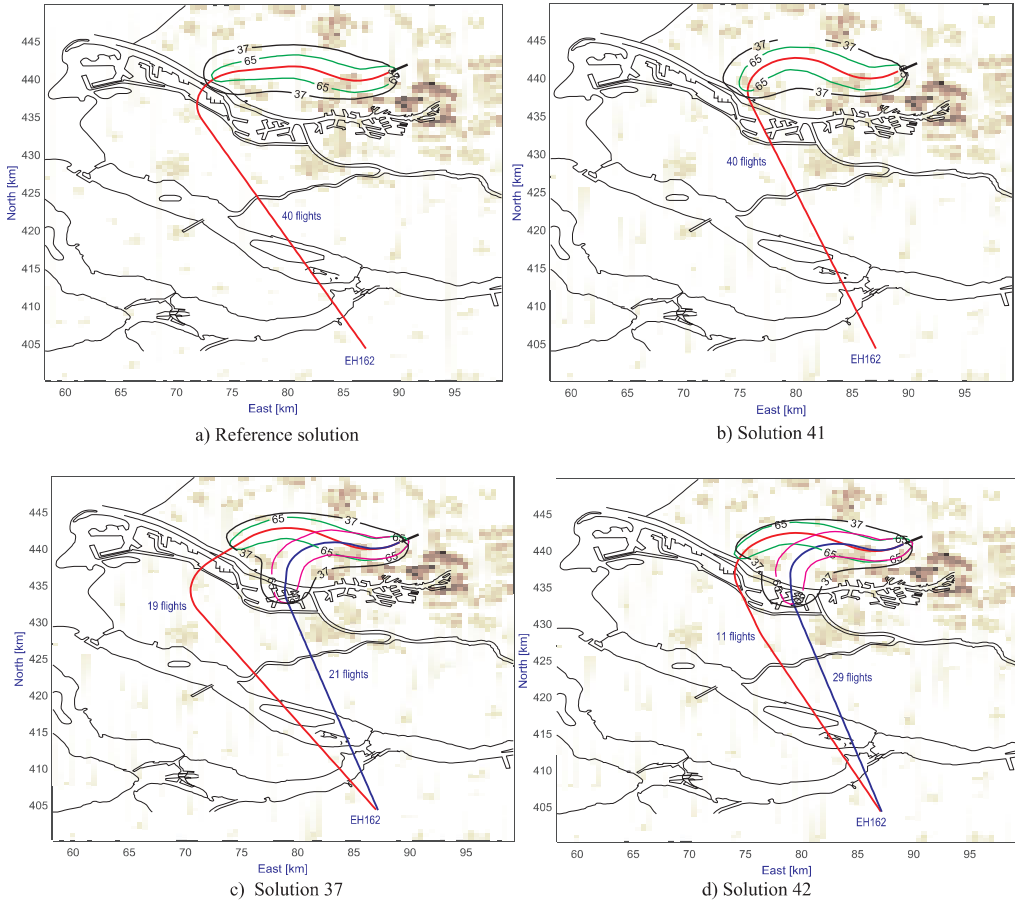


Fig. 8. Illustration of  $L_{den}$  and N65 contours of the representative routes and the reference case.

**Table 1**  
Comparison of the metrics of the representative solutions and the reference case.

Optimization approaches	Case number	No. of people annoyed	Fuel burn (kg)	No. of people living within N65 and exposed $\geq 50\%$ of flights	PEI (person event index)	AIE (average individual exposure)
2 objectives	Solution 41	11,476	18,993	54,340	2,173,600	40
	% reduction	-5.8	-3.4	+10.9	+10.9	0.0
3 objectives	Solution 37	11,642	18,952	46,295	1,811,140	34
	% reduction	-4.5	-3.6	-5.5	-7.6	-15.3
	Solution 42	11,879	18,347	45,385	1,840,865	32
	% reduction	-2.5	-6.7	-7.4	-6.1	-19.2
Reference solution		12,189	19,664	49,000	1,960,000	40

population). At first glance, compared with the reference solution, all the metrics obtained by solutions 37 and 42 are better, while solution 41 only performs better at two metrics and equal or worse in the other three metrics. Regarding the number of annoyed people, it can be seen from the table that solution 41 gives the best reduction of 5.8% with respect to the reference case, while those of solutions 37 and 42 obtain 4.5% and 2.5%, respectively. In contrast, solutions 42 and 37 outperform solution 41 for all other metrics. More specifically, solutions 42 and 37 result in a decrease of 6.7% and 3.6% in fuel burn, respectively, while that of solution 41 is only 3.4%. In terms of the number of people living within the N65 contour and exposed to more than 50% of all flights, solutions 42 and 37 yield a good reduction of 7.4% and 5.5%, respectively, whereas solution 41 results in a significant increase of 10.9% compared to the reference case. Similarly, the comparison of the PEI also shows the same trend, in which the PEI of solution 41

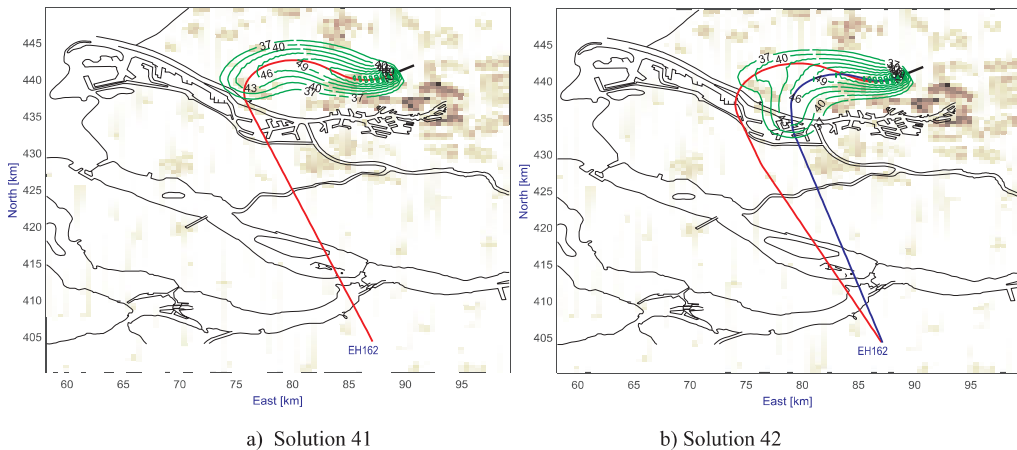


Fig. 9. Illustration of the concentration of  $L_{den}$  contours of solutions 41 and 42.

increases with 10.9%, while that of solutions 37 and 42 reduces by 7.6% and 6.1%, respectively. Finally, regarding the AIE metric, only those obtained by solutions 37 and 42 show a reduction of 19.2% and 15.3%, respectively.

In summary, based on the obtained results, it can be concluded that the proposed approach using three objectives can provide new optimal routes which result in a better spread of the noise impact, while still performing almost as good as routes optimized for traditional noise impact criteria such as annoyance.

### 5.2. Amsterdam Schiphol airport case study

In order to further evaluate the performance of the proposed approach, a case study at Amsterdam Schiphol Airport in The Netherlands is considered as well. The airport is an international airport and one of the busiest airports in the world, and is located to the southwest of the city of Amsterdam. In this example, the SID named LUNIX is investigated. The trajectory starts at the end of runway 24 and ends at the IVLUT intersection. The initial and final airspeed and altitudes are the same as in the previous case. Regarding the number of flights and aircraft types, it is assumed that there are 400 flights operating on this SID on a busy day with a highly diverse fleet mix. For this example, it is assumed that the fleet mix consists of 80% medium aircraft represented by the B738 and 20% heavy aircraft represented by the Boeing 777-300 (B773). As in the case study at RTM, the actual departure times of flights are ignored.

This optimization problem has sixteen design variables: ten to define the routes, two for the allocation of flights and four to select the departure procedure. An area of  $51.5 \times 23$  km and a population grid cell size of  $500 \times 500$  m as shown in Fig. 10 are used. To solve the optimization problems, the algorithm converges after 652 iterations in 9.18 h and 912 iterations in 12.06 h for the first and second problems, respectively. It should be noted that, compared with the previous example, the significant increase in the computational cost in this problem is due to the consideration of two different aircraft types at the same time. Moreover, the investigated area in this example is also larger than the area considered in the previous example.

Fig. 11 shows the comparison of Pareto solutions with the reference case for fuel burn and number of annoyed people obtained by both the approaches. The Pareto solutions gained by solving the optimization problem with three objectives (the second problem) are presented in Fig. 12. It can be seen in Fig. 12 that some solutions of the second approach are located on the Pareto front resulting from the bi-objective optimization. In these solutions, the first two objectives are dominant, and in fact these solutions share a common ground track rather than two alternative routes, resulting in a high value for the third objective. The figure also shows that some solutions (from both the approaches) dominate the reference case. However, these solutions again only have one common route, and hence they perform very poorly with respect to the third objective. In an effort to identify solutions which are good at distributing the noise impact over different communities while not significantly compromising the other two objectives, solutions 42 and 49 of the second approach are further evaluated as representative cases. Furthermore, to provide an alternative choice disregarding the third objective, solution 27 of the first approach, which dominates the reference case, is also selected for evaluation.

The ground tracks of the solutions obtained by the two approaches are shown in Figs. 13 and 14, respectively. From the figures, it can be seen that in all solutions noise-sensitive areas are avoided. Again, NADP2 is selected as the optimal departure procedure for all ground tracks and all aircraft types in both approaches. For the first problem, only one optimal route is found for each solution, and all aircraft follow the same route. On the other hand, the second approach comprises both kinds of solutions which have either one route or two different routes.

To make the comparison more explicit, the ground tracks of the representative solutions and that of the reference case are isolated in Fig. 15, in which again the 37 dB  $L_{den}$  and N65 contours (B738 in magenta and B773 in green) are provided. As can be seen in the

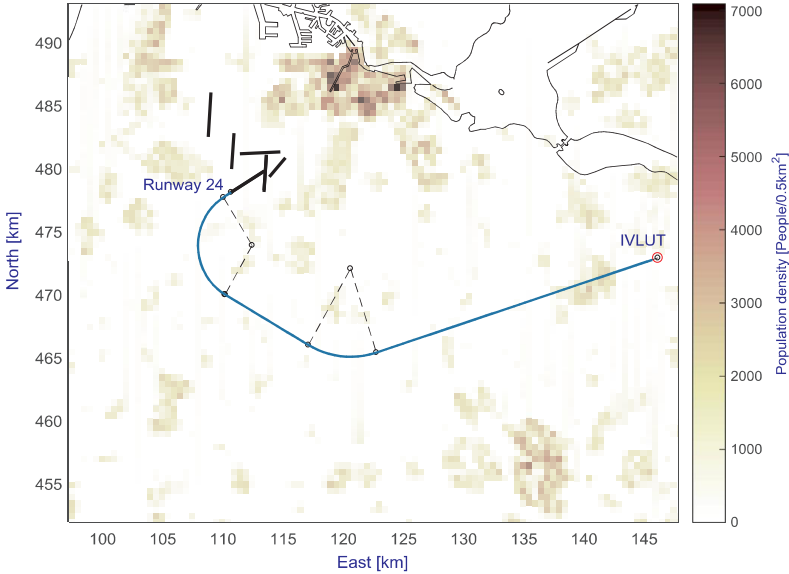


Fig. 10. Departure route LUNIX.

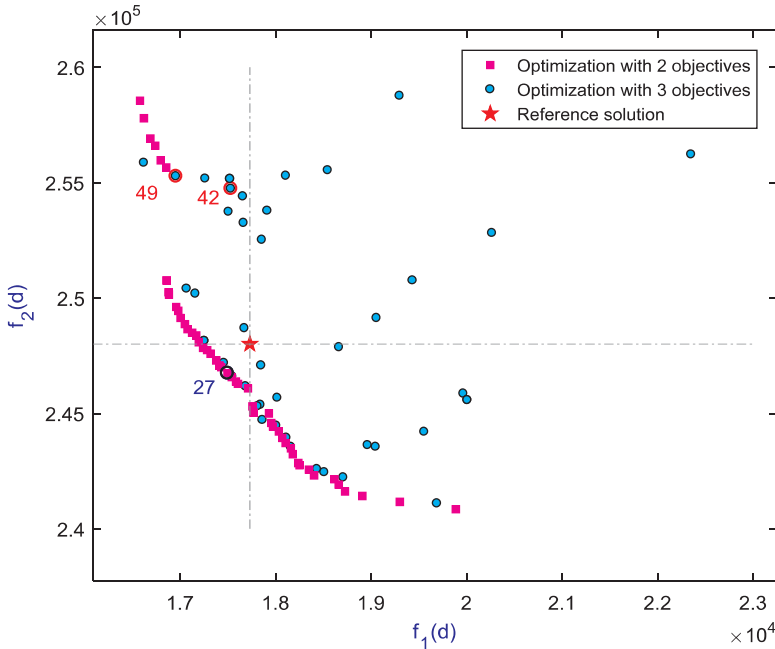


Fig. 11. Comparison of Pareto fronts obtained by the first and second problems and the reference case.

figure, compared to the reference case, solutions 42 and 49 have two distinct routes, while solution 27 has only one route. Regarding the share of aircraft noise, it can be seen that the number of people living within the N65 contour and exposed to more than 50% of all flights obtained by solutions 42 and 49 is reduced significantly compared with those of solution 27 and the reference case. This can be seen in the numerical results in Table 2 as well.

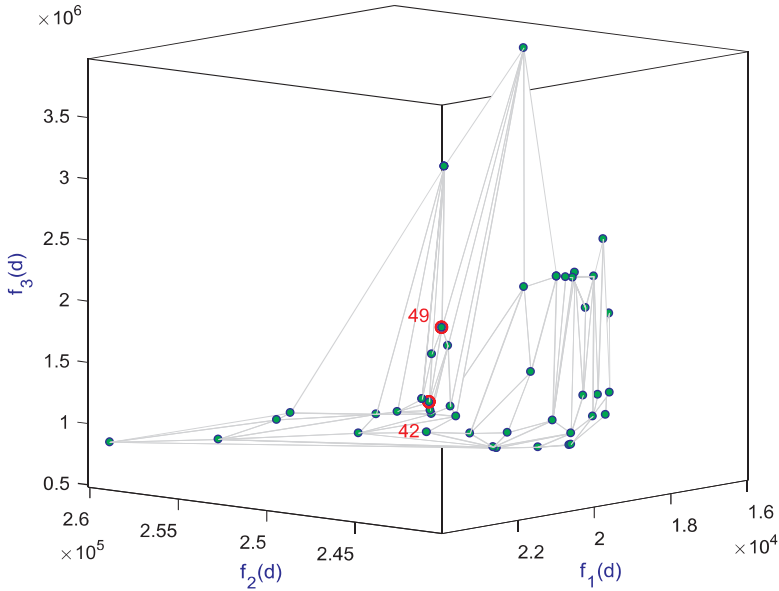


Fig. 12. Pareto fronts obtained by the second problem.

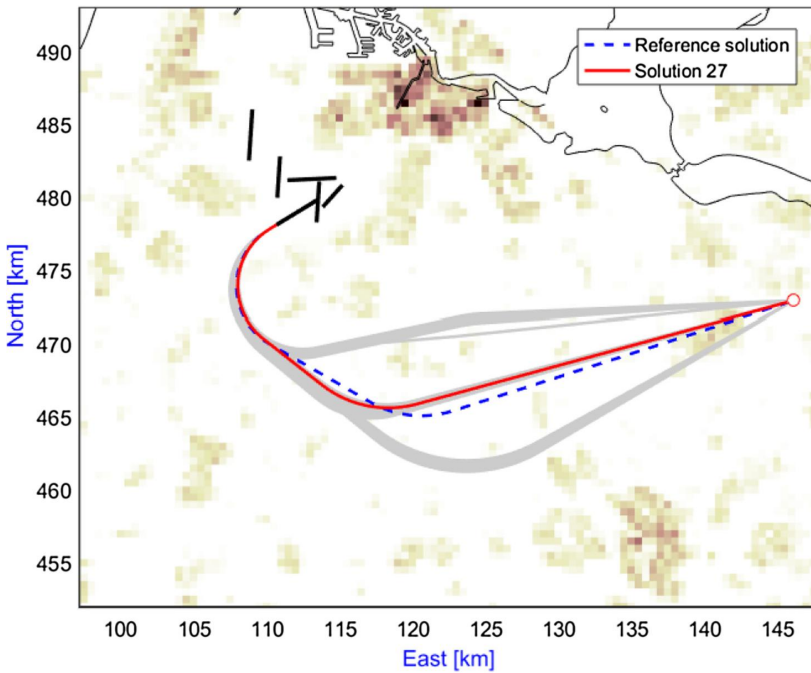


Fig. 13. Optimal ground tracks obtained by the first problem.

The table also shows that the three representative solutions show a small improvement in terms of the number of people annoyed, and a slight increase in fuel burn as compared to the reference case. However, especially solution 42 shows a large reduction in the third objective, indicating that the noise load – which is already slightly lower for the traditional annoyance criterion – is spread out

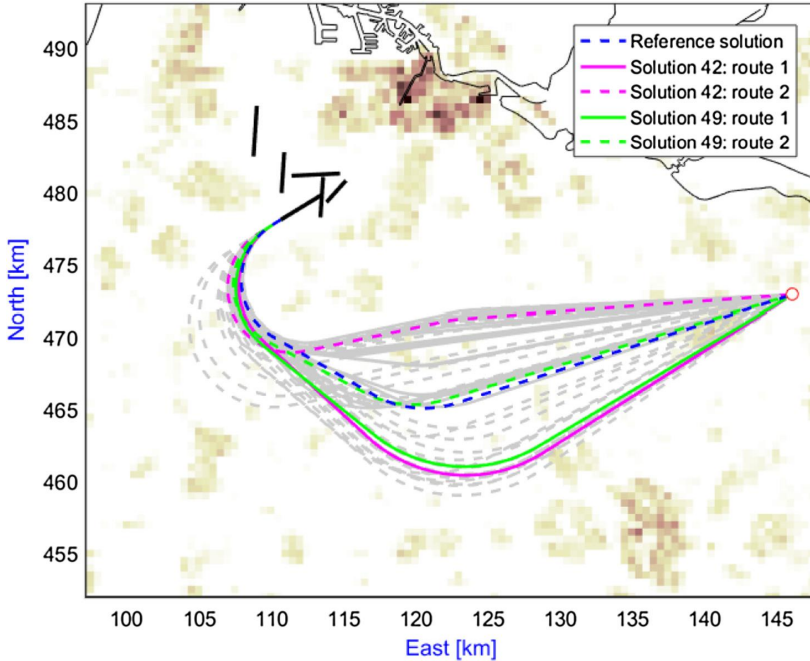


Fig. 14. Optimal ground tracks obtained by the second problem.

much better over different communities, indicating that the individual annoyance related to frequency could be lowered significantly.

In summary, the method discussed above shows potential to reduce the annoyance whilst at the same time improving the distribution of the noise load over different communities, at the cost of only a minor increase in the ground path length.

6. Conclusion

In an effort to effectively balance the concerns regarding the environmental impacts caused by aircraft and airport operations, a new formulation for the design of optimal departure routes and the allocation of flights to these routes has been developed in this paper. Apart from two conventional objectives, as a novel feature, a new objective has been developed and included in the optimization problem. This objective aims to take into account the frequency of noise events for individual people, and in essence ensures a fairer distribution of the noise impact over the communities surrounding an airport. In order to take advantage of the combination of designing new routes and allocating flights to these routes, two different routes have been considered, and the distribution of flights on these two routes is optimized simultaneously. Also, to solve the optimization problem, a new version of the MOEA/D algorithm has been developed, in which a new technique for handling equality constraints and a simple technique for dealing with mixed continuous-discrete design variables have been introduced. The reliability and applicability of the proposed approach are exemplified through two different case studies at Rotterdam The Hague Airport and at Amsterdam Airport Schiphol in The Netherlands. The obtained simulation results indicate that the proposed approach can provide solutions in which the fair distribution of the noise impact has improved significantly, whilst the traditional noise impact criterion based on annoyance is increasing only slightly or – in some cases – decreasing as compared to the reference case based on current-day operations.

However, the work presented in this paper has also led to the identification of further challenges. Firstly, the developed fairness metric relies on the assumption that the frequency of noise events is indeed a concern. Consequently, more research would be needed to identify the impact of exposure frequency on annoyance. In addition, by applying this approach each SID will have (at least) two different routes which may cause operational challenges and may increase the workload of air traffic controllers. Though this study is based on representative amounts of aircraft movements and hence departure capacity itself should not be an issue, the merging of two or more alternative routes at the final point may also negatively affect the controller’s workload. Therefore, these problems should be considered in the future.

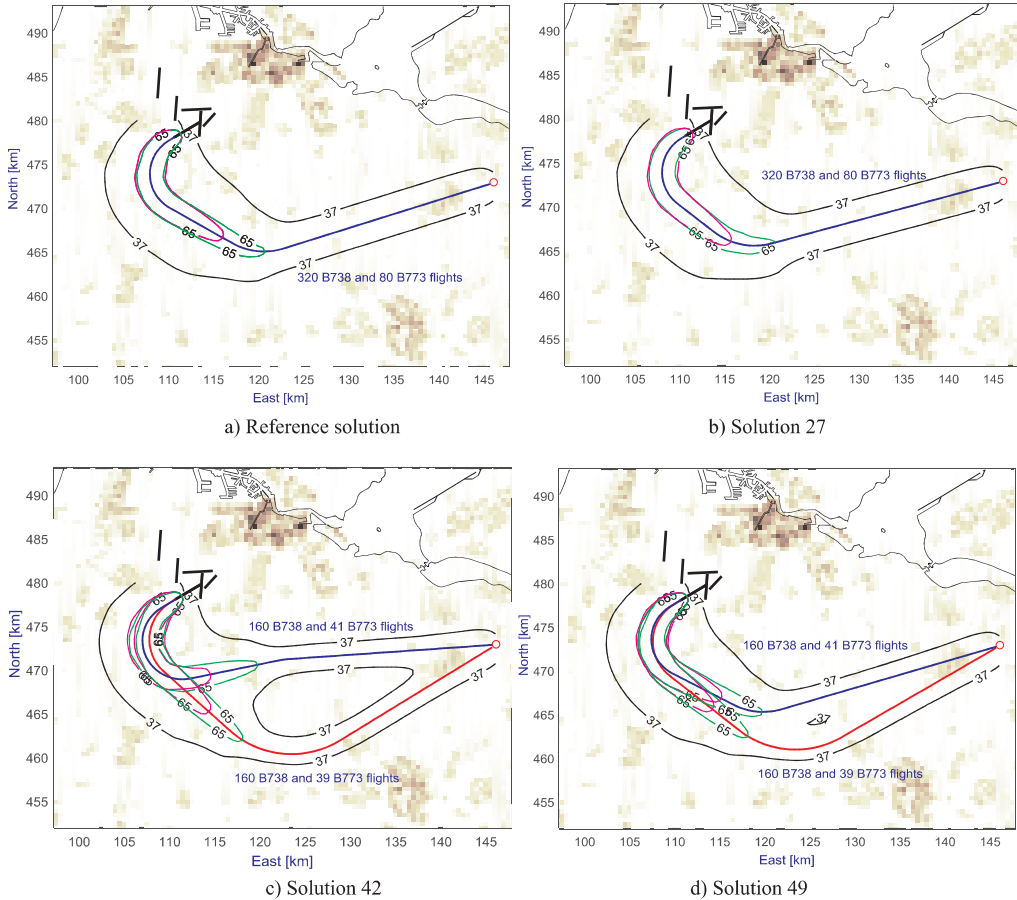


Fig. 15. Illustration of  $L_{den}$  and N65 contours of the representative routes and the reference case.

Table 2

Comparison of the metrics of the representative solutions and the reference case.

Optimization approaches	Case number	No. of people annoyed	Fuel burn (kg)	No. of people living within N65 and exposed $\geq 50\%$ of flights	PEI (person event index)	AIE (average individual exposure)
2 objectives	Solution 27	17,496	246,749	9785	4,031,600	340
	% reduction	-1.3	-0.5	+19.5	+19.7	+0.7
3 objectives	Solution 42	17,531	254,740	4575	3,420,575	233
	% reduction	-1.1	+2.7	-44.1	+1.6	-31.1
	Solution 49	16,956	255,278	7380	3,768,615	293
	% reduction	-4.4	+2.9	-9.8	+11.9	-13.4
Reference solution		17,729	248,006	8185	3,367,200	338

## Appendix A. Supplementary material

Supplementary data associated with this article can be found, in the online version, at <https://doi.org/10.1016/j.trd.2018.07.006>.

## References

Angela, N., Damir, P., Vincent, M., 2010. BADA: An advanced aircraft performance model for present and future ATM systems. *Int. J. Adapt. Control Signal Process.* 24, 850–866. <https://doi.org/10.1002/acs.1176>.

- ANSI/ASA, 2008. Quantities and Procedures for Description and Measurement of Environmental Sound - Part 6: Methods for Estimation of Awakenings Associated with Outdoor Noise Events Heard in Homes.
- Boeing, 2016. Current Market Outlook 2016–2035.
- Braakenburg, M.L., Hartjes, S., Visser, H.G., 2011. Development of a Multi-Event Trajectory Optimization Tool for Noise-Optimized Approach Route Design. *AIAA J.* 1–13. <https://doi.org/10.2514/6.2011-6929>.
- Brown, A.L., 2014. An overview of concepts and past findings on noise events and human response to surface transport noise. In: *Internoise 2014*. 16–19 November, Melbourne, Australia, pp. 1–8.
- Department of Transport and Regional Services, 2000. Expanding Ways to Describe and Assess Aircraft Noise.
- European Environment Agency (EEA), 2010. Good practice guide on noise exposure and potential health effects. In: EEA Technical Report.
- Federal Aviation Administration (FAA), Office of Environment and Energy, 2008. INM User's Guide, Integrated Noise Model, INM 7.0, Technical Manual, FAA-AEE-08-01.
- Federal Interagency Committee on Aviation Noise (FICAN), 1997. Effects of aviation noise on awakenings from sleep.
- Fields, J.M., 1984. The effect of numbers of noise events on people's reactions to noise: An analysis of existing survey data. *J. Acoust. Soc. Am.* 75, 447–467. <https://doi.org/10.1121/1.390469>.
- Frair, L., 1984. Airport noise modelling and aircraft scheduling so as to minimize community annoyance. *Appl. Math. Model.* 8, 271–281. [https://doi.org/10.1016/0307-904X\(84\)90162-8](https://doi.org/10.1016/0307-904X(84)90162-8).
- Green, J.E., 2005. Air travel – greener by design mitigating the environmental impact of aviation: Opportunities and priorities. *Aeronaut. J.* 109, 361–416. <https://doi.org/10.1017/S0001924000000841>.
- Hartjes, S., Dons, J., Visser, H.G., 2014. Optimization of area navigation arrival routes for cumulative noise exposure. *J. Aircr.* 51, 1432–1438. <https://doi.org/10.2514/1.C032302>.
- Hartjes, S., Visser, H., 2016. Efficient trajectory parameterization for environmental optimization of departure flight paths using a genetic algorithm. *Proc. Inst. Mech. Eng. Part G J. Aerosp. Eng.* 1–9. <https://doi.org/10.1177/0954410016648980>.
- Hartjes, S., Visser, H.G., Hebly, S.J., 2010. Optimisation of RNAV noise and emission abatement standard instrument departures. *Aeronaut. J.* 114, 757–767. <https://doi.org/10.1017/CBO9781107415324.004>.
- Ho-Huu, V., Hartjes, S., Geijselaers, L.H., Visser, H.G., Curran, R., 2018a. Optimization of noise abatement aircraft terminal routes using a multi-objective evolutionary algorithm based on decomposition. *Transp. Res. Procedia* 29, 157–168. <https://doi.org/10.1016/j.trpro.2018.02.014>.
- Ho-Huu, V., Hartjes, S., Visser, H., Curran, R., 2017. An efficient application of the MOEA/D algorithm for designing noise abatement departure trajectories. *Aerospace* 4, 54. <https://doi.org/10.3390/aerospace4040054>.
- Ho-Huu, V., Hartjes, S., Visser, H.G., Curran, R., 2018b. An improved MOEA/D algorithm for bi-objective optimization problems with complex Pareto fronts and its application to structural optimization. *Expert Syst. Appl.* 92, 430–446. <https://doi.org/10.1016/j.eswa.2017.09.051>.
- Hogenhuis, R.H., Hebly, S.J., Visser, H.G., 2011. Optimization of area navigation noise abatement approach trajectories. *Proc. Inst. Mech. Eng. Part G-J. Aerosp. Eng.* 225, 513–521. <https://doi.org/10.1177/09544100JAERO840>.
- International Civil Aviation Organization (ICAO), 2006. Procedures for air navigation services – Aircraft operations. Vol. I, Flight Procedures.
- Janssen, S.A., Centen, M.R., Vos, H., Van Kamp, I., 2014. The effect of the number of aircraft noise events on sleep quality. *Appl. Acoust.* 84, 9–16. <https://doi.org/10.1016/j.apacoust.2014.04.002>.
- Khadi, S., Abdallah, L., 2012. Optimization approaches of aircraft flight path reducing noise: Comparison of modeling methods. *Appl. Acoust.* 73, 291–301. <https://doi.org/10.1016/j.apacoust.2011.06.012>.
- Kim, B., Li, L., Clarke, J.-P., 2014. Runway assignments that minimize terminal airspace and airport surface emissions. *J. Guid. Control. Dyn.* 37, 789–798. <https://doi.org/10.2514/1.61829>.
- Kuiper, B.R., Visser, H.G., Heblj, S., 2012. Efficient use of an allotted airport annual noise budget through minimax optimization of runway allocations. *Proc. Inst. Mech. Eng. Part G J. Aerosp. Eng.* 227, 1021–1035. <https://doi.org/10.1177/0954410012447767>.
- Marais, K.B., Reynolds, T.G., Uday, P., Muller, D., Lovgren, J., Dumont, J.-M., Hansman, R.J., 2013. Evaluation of potential near-term operational changes to mitigate environmental impacts of aviation. *Proc. Inst. Mech. Eng. Part G J. Aerosp. Eng.* 227, 1277–1299. <https://doi.org/10.1177/0954410012454095>.
- Porter, N., Knowles, A., Fisher, N., Southgate, D., 2014. The next generation of supplementary aviation noise metrics and their use in managing aviation noise. In: *Internoise 2014*. 16–19 November, Melbourne, Australia, pp. 1–10.
- Prats, X., Puig, V., Quevedo, J., 2011. Equitable aircraft noise-abatement departure procedures. *J. Guid. Control. Dyn.* 34, 192–203. <https://doi.org/10.2514/1.49530>.
- Prats, X., Puig, V., Quevedo, J., Nejari, F., 2010a. Lexicographic optimisation for optimal departure aircraft trajectories. *Aerosp. Sci. Technol.* 14, 26–37. <https://doi.org/10.1016/j.ast.2009.11.003>.
- Prats, X., Puig, V., Quevedo, J., Nejari, F., 2010b. Multi-objective optimisation for aircraft departure trajectories minimising noise annoyance. *Transp. Res. Part C Emerg. Technol.* 18, 975–989. <https://doi.org/10.1016/j.trc.2010.03.001>.
- Southgate, D., 2011. The evolution of aircraft noise descriptors in Australia over the past decade. In: *Proceedings of Acoustics*. 2–4 November 2011, Gold Coast, Australia.
- Torres, R., Chaptal, J., Bès, C., Hiriart-Urruty, J.-B., 2011. Optimal, environmentally friendly departure procedures for civil aircraft. *J. Aircr.* 48, 11–23. <https://doi.org/10.2514/1.C031012>.
- Visser, H.G., Wijnen, R.A.A., 2003. Optimisation of noise abatement arrival trajectories. *Aeronaut. J.* 107, 607–615. <https://doi.org/10.1017/S0001924000013828>.
- Visser, H.G., Wijnen, R.A.A., 2001. Optimization of noise abatement departure trajectories. *J. Aircr.* 38, 620–627. <https://doi.org/10.2514/2.2838>.
- Zachary, D.S., Gervais, J., Leopold, U., 2010. Multi-impact optimization to reduce aviation noise and emissions. *Transp. Res. Part D Transp. Environ.* 15, 82–93. <https://doi.org/10.1016/j.trd.2009.09.005>.
- Zhang, M., Filippone, A., Bojdo, N., 2016. Multi-objective departure trajectory optimisation of commercial aircraft on environmental impacts. In: *Greener Aviation Conference*, At Brussels, Belgium. doi: 10.13140/RG.2.2.23283.32805.
- Zhang, Q., Li, H., 2007. MOEA/D: A multiobjective evolutionary algorithm based on decomposition. *IEEE Trans. Evol. Comput.* 11, 712–731. <https://doi.org/10.1109/TEVC.2007.892759>.



# 4

## FLIGHT ALLOCATION

*In the previous two chapters, the first main component of this research was presented, viz. the optimization of departure routes for noise impact and fuel consumption. The main aim of the study presented in this chapter is to develop a flight allocation problem formulation that allows to address noise impact and fuel consumption concurrently. Unlike models developed in previous research, the model developed here considers each flight operation as a design variable and optimizes both two potentially conflicting objectives, i.e., noise impact and fuel consumption, simultaneously. The model is applied to a case study at Belgrade Airport in Serbia. The obtained results are compared with those acquired in other previous research. The performance of the proposed approach is also tested on the same case study but at a larger scale and with a daily commuting population.*

---

The content of this chapter is based on the following research articles:

- [1]. Emir Ganić, **V. Ho-Huu**, Sander Hartjes, Obrad Babić, *Air traffic assignment to reduce population noise exposure and fuel consumption using multi-criteria optimization*, The 26th international conference on Noise and Vibration, 6-7 December 2018, Nis, Serbia. -> Paper 4.1.
- [2]. **V. Ho-Huu**, E. Ganić, S. Hartjes, O. Babić, and R. Curran, *Air traffic assignment based on daily population mobility to reduce aircraft noise effects and fuel consumption*, Transportation Research Part D: Transportation and Environment , vol. 72, pp. 127–147, 2019. -> Paper 4.2.

### 4.1. PROBLEM STATEMENT

In the field of aircraft and airport operations, proper allocation of flights to departure and arrival routes always plays a vital role. For example, sending aircraft to routes that are remote from populated regions can significantly reduce noise impact, or assigning flights to short routes can help to considerably reduce fuel burn. Hence, besides the design of optimal routes, research to develop suitable flight allocation models is also important.

Over the past decades, various models have been proposed for the flight assignment problem. Unfortunately, many of these were devoted to the reduction of either flight delay or fuel consumption. Meanwhile, studies focusing on reducing noise impact are limited. Also, the problems considered in these models were typically formulated as single-objective nonlinear programming models [23], and hence the problem size is normally large. Although such a model can be extended to multi-objective problems, it is difficult to obtain solutions that effectively balance potentially conflicting objectives [20].

In this chapter, a new air traffic assignment model is proposed. The model performance is first evaluated on a case study at Belgrade Airport in Serbia, which is presented in detail in Ganic et al. [39]. Later, the model is extended to solve a more complex problem at a larger scale with a daily commuting population. The details of this study are presented in Ho-Huu et al. [40].

### 4.2. CONTRIBUTIONS

The main contributions of this chapter are as follows:

1. In Ganic et al. [39], a new air traffic assignment model that is able to provide proper trade-off solutions between two potentially conflicting objectives is developed. Compared with the previous model in [23], the developed model does not only give reliable solutions, but also offers a range of solutions which can be a good reference base for users to refer to before making decisions. In addition, owing to considering each operation as a design variable, the size of the optimization problem is significantly reduced. As a result, the process of solving the optimization problem is improved considerably.
2. In Ho-Huu et al. [40], the capability of the method is demonstrated in a more complicated case study, in which a daily commuting population is considered. This research was also the first study on the influence of the daily commuting population on the evaluation of the aircraft noise impact. The research indicated that aircraft noise not only affects people living close to the airport, but also people living farther away the airport as a result of moving to places close to the airport for work, while the opposite site is also observed. Owing to the changes in population distribution at each location during the day, the study also reveals that there are differences in the optimal assignments obtained when using the static (census) data and mobility data. Although the obtained solutions are very promising, they are only conceptual results. Therefore, studies on the implementation of such results should also be considered in future work.



## AIR TRAFFIC ASSIGNMENT TO REDUCE POPULATION NOISE EXPOSURE AND FUEL CONSUMPTION USING MULTI-CRITERIA OPTIMISATION

Emir Ganić<sup>1</sup>, Vinh Ho-Huu<sup>2</sup>, Obrad Babić<sup>1</sup>, Sander Hartjes<sup>2</sup>

<sup>1</sup> University of Belgrade, Faculty of Transport and Traffic Engineering, Belgrade, Serbia, [e.ganic@sf.bg.ac.rs](mailto:e.ganic@sf.bg.ac.rs)

<sup>2</sup> Delft University of Technology, Faculty of Aerospace Engineering, Delft, The Netherlands

**Abstract** - Air traffic assignment to departure and arrival routes has a major impact on the population noise exposure in the vicinity of the airport. In some cases, by choosing the suitable air traffic assignment it is possible to avoid overflying populated areas and reduce number of people affected by noise. However, such an approach almost always leads to an increase in route length, and therefore an increase in fuel consumption and CO<sub>2</sub> emissions. Although aircraft noise and fuel consumption reduction are conflicting goals, they both represent pivotal aspects of air transport sustainable development. In this paper, the methods of multi-criteria optimisation are applied, which are generally used when it is necessary to make an optimal decision that requires a compromise (trade-off) solution between two or more conflicting goals. The aim of this research is to develop a mathematical model and to propose an algorithm for air traffic assignment to departure and arrival routes that will, through the Pareto optimality concept, find the approximation of a set of nondominated solutions that minimize population noise exposure and fuel consumption. The approach was demonstrated on Belgrade airport to show the benefits of the proposed model on a real data example. Since all Pareto optimal solutions are considered equally good, from all obtained air traffic assignments the three representative solutions were compared to the actual air traffic assignment (Base case). The obtained results indicate that the proposed approach can provide solutions which offer a good trade-off between the concerned metrics.

### 1. INTRODUCTION

Major commercial airports generate benefits to their neighbouring communities, providing more investment and employment, increasing mobility, as well as providing a strong stimulus to the globalization of the industry, business and long distance tourism. However, external costs are associated with these benefits and any increase in aircraft movement causes adverse environmental impacts. It is widely accepted that the most significant environmental impacts related to the operation of airports arise from the noise generated by aircraft and fuel consumption leading to global CO<sub>2</sub> emissions increase.

Considerable efforts have been invested in order to alleviate the noise nuisance and reduce fuel consumption. On the European level, the Environmental Noise Directive 2002/49/EC (END) relating to the assessment and management of environmental noise has been introduced [1]. In the framework of implementing the requirements set in

this Directive, many airports have developed strategic noise maps and noise action plans [2]–[4]. Numerous initiatives to reduce fuel consumption and emissions have been launched in recent years including Atlantic Interoperability Initiative to Reduce Emissions (AIRE), Asia and South Pacific Initiative to Reduce Emissions (ASPIRE), ACI Airport Carbon Accreditation, The European Advanced Biofuels Flightpath.

In addition to these initiatives that require enormous budgets and are more focused on the strategic level, on a practical level it was observed that the variation of aircraft/airport operational procedures could bring short-term improvements and could be less costly in comparison with the other options [5].

The literature shows that efforts to design optimal departure and arrival routes with less noise and fuel burn have been well studied over the past decades, and various strategies have been proposed. Besides the attempts to design environmentally friendly departure/arrival routes, the allocation of aircraft and operational procedures to specific routes could also help to considerably diminish the environmental impacts. For instance, Frair [6] proposed a nonlinear integer programming model to minimize community annoyance at an airport by allocating aircraft to the existing arrival and departure trajectories. Zachary et al. [7] investigated the optimization problem which aims at finding an optimal combination of approach and departure routes, operational procedures and fleet composition to optimize noise and pollutant emissions. Kim et al. [8] built an optimization model to minimize the total emissions on the airport surface and in the terminal area by allotting aircraft to runways and scheduling the arrival and departure operations on these runways concurrently.

Several air traffic assignment strategies have been proposed in order to allocate noise more wisely. Netjasov suggested the model that was based on the categorization of aircraft according to engine type and wake turbulence category and the assignment of specific runways for take-off and landing for each aircraft category [9]. Heblj et al. developed the Noise Allocation Planning Tool that maintained an equal noise level over a wider area, effectively reducing peak levels [10]. Zaporozhets and Tokarev formulated and solved several problems related to minimisation of aircraft noise impact, including a selection of optimum operations around an airport by distributing the aircraft between the routes [11]. On a tactical level, Nibourg et al. have developed Runway Allocation Advice System (RAAS) which is currently in

operation at Amsterdam Airport Schiphol (AAS) and Basel Euro Airport and which allows controllers to choose the optimal runway (combination) in any given situation with respect to noise preferential runway system in place [12]. Kuiper et al. proposed an optimization approach that aims to minimize the risk of exceeding the limit at any predefined location in the vicinity of the airport by distributing flights over different runways [13].

Each decision regarding the assignment of aircraft to routes should consider the number of people who will be exposed to adverse noise levels. Due to population daily migrations, number of people in some residential areas could significantly differ from census data. Ott was one of the first researchers to spot the drawback when relying to census data since it leads to overlooking the fact that some residents spend a long time far from the area, which is supposed to represent their exposure [14]. Ganić et al. [15] incorporated population daily migrations into air traffic assignment optimisation model with the aim to reduce the number of people exposed to noise but without taking into account fuel consumption. Although the importance of analysis of daily migrations has been recognized in many transportation studies [16]–[21], to the best of the authors' knowledge, none of the air traffic assignment strategies addressed trade-off between population noise exposure and fuel consumption in combination with temporal and spatial variations in population in an airport's vicinity.

The idea presented in this paper is to tailor air traffic assignment of aircraft to departure and arrival routes taking into account temporal and spatial variations in population in an airport's vicinity in order to reduce the number of people exposed to noise as well as fuel consumption. The approach was demonstrated on Belgrade airport to show the benefits of the proposed model on a real data example. The obtained results indicate that the proposed approach can provide solutions which offer a good trade-off between the concerned metrics.

The rest of the paper is organised as follows. Section 2 presents the formulation of the multi-objective optimization problem by defining the mathematical model, explaining the necessary input data as well as the proposed (used) NSGA-II algorithm. Section 3 describes the Belgrade airport case study which is used to assess the capability of the proposed air traffic assignment model. The results are presented in Section 4. Finally, Section 5 provides the conclusion and ideas for further research.

## 2. MULTI-OBJECTIVE OPTIMIZATION PROBLEM FORMULATION

To generate optimal air traffic assignment with respect to population daily migrations, the mathematical model of an optimization problem with two objectives is developed. As a continuation of the research done by Ganić et al. [15], besides population noise exposure, this research takes into account fuel consumption as the second objective.

### 2.1. Input data

Description of proposed air traffic assignment model requires following input data:

- air traffic data,
- departure and arrival routes for each runway,

- noise data for each location produced by each aircraft flying over routes,
- fuel consumption data for each aircraft flying over each route,
- population data,
- human mobility patterns based on daily migrations.

Air traffic data includes information about origin and destination, aircraft type, actual take-off time (ATOT), arrival time, runway in use, operation type (take-off or landing) and can be obtained from Air Traffic Control. Real radar data could be used to represent departure and arrival routes or they could be obtained from Aeronautical Information Publication (AIP).

Noise level for each location produced by each aircraft flying over routes could be either measured or calculated. In the first case, noise levels are measured at noise monitoring stations which represent locations. In the second case, noise levels are calculated using some noise prediction and mapping software, such as Predictor-LimA, SoundPlan, Integrated Noise Model (INM), etc. Even though the first approach gives the opportunity to work with real-time data, the second approach seems more appealing since there are no limitations regarding the number of locations and their position.

Selection of locations for which noise levels will be assessed together with the actual number of people exposed to those noise levels during the observed periods is crucial for the population noise exposure assessment. Low level of detail required for this research allows each settlement to be represented by a single point, i.e. location instead of observing each housing unit in particular.

Fuel consumption was calculated using the EMEP/EEA air pollutant emission inventory guidebook – 2016 [22]. Fuel burn for Landing and Take-Off (LTO) flight phases was assessed using information about origin and destination airports, aircraft type (engine type, number of engines), duration for each LTO phase (taxi, take off, climb out, approach) and rate of fuel burn (kg/s/engine). For Climb/Cruise/Descent (CCD) flight phases fuel consumption was calculated based on CCD stage length and aircraft type.

Population data are collected for each location which implies gathering the number of people living in each settlement based on census data. During some period of the day, especially when employees go to work and pupils and students go to schools and faculties, number of people at some residential areas could significantly differ from census data due to population daily migrations. Having that in mind, assessment of human mobility patterns based on daily migration gives an estimation of how many people will actually be present at some location during a defined period of time. Daily migrations presented in this paper include a special form of spatial mobility of economically active population performing an occupation, of pupils and students. This data can be obtained from the National Statistical Office for each municipality around the airport [23].

### 2.2. Mathematical model

To formulate this model, the following notations are used:

#### Parameters:

$P$  is the set of periods,  $t \in P$

$O_t$  is the set of operations during period  $t$ ,  $i \in O_t$ ,  $t \in P$

$L$  is the set of locations,  $k \in L$

$S_i$  is the set of feasible operational options of operation  $i$ ,  $i \in O_t$

$T_t$  is the duration of period  $t$ ,  $t \in P$

$p_{kt}$  is the number of population living at a location  $k$  during period  $t$

$k_{kt}$  is the legal noise limit at a location  $k$  during period  $t$

$fuel(x_i)$  is the fuel consumption that operation  $i$  costs when option  $x$  is selected

$nl(x_i)$  is the noise level that operation  $i$  cause when option  $x$  is selected

Design variables:

$\mathbf{x} = \{x_i, i \in O_t\}$  is the vector of optimal assignment of all operations to routes.

$x_i$  is an optimal option of operation  $i$ , which is selected from set of all feasible operational options  $S_i$ , ( $x_i \in S_i$ ).

The set of operational options  $S_i = \{1, 2, \dots, M\}$  is defined based on its operational type (departure/arrival) and navigation point, in which  $1, 2, \dots, M$  is the number of options that can be derived for aircraft operation  $i$ . For each option, noise level ( $nl(x_i)$ ) and fuel consumption ( $fuel(x_i)$ ) are predefined.

Objective functions:

$$\min(T_{fuel}(x), N_{pa}(x)) \quad (1)$$

- Fuel consumption:

$$T_{fuel}(x) = \sum_{i \in O_t} fuel(x_i) \quad (2)$$

- Number of people affected by noise:

$$N_{pa}(x) = \sum_{k \in L} p_k \cdot S_k(x) \quad (3)$$

$$S_k(x) = 2^{0.1 \cdot (N_k(x) - k_k)}, \forall k \quad (4)$$

$$N_k(x) = 10 \log \left( \frac{1}{t} \cdot \sum_{i \in O_t} 10^{0.1 \cdot nl(x_i)} \right), \forall k \quad (5)$$

It should be noted that besides the introduction of a new objective, i.e., fuel consumption, this model also contains a new promising feature in comparison with the model proposed in [15]. Particularly, in the model [15], for each operation, all feasible options it can be assigned to are considered as binary design variables, which means that only one of these options is equal to 1 if it is selected, and the rest of them will be equal to 0. Consequently, the size of optimization problem will be extremely enlarged when the number of operations increases. This may make the problem more difficult to solve by using evolutionary algorithms or even integer nonlinear programming models. On the contrary, in the paper, each operation is considered as a design variable, and all its feasible assignments will serve as its design space. As a result, the number of design variables of the problem will dramatically decrease, and hence the

problem can be effectively solved by using evolutionary algorithms.

### 2.3. NSGA-II algorithm

As described in Section 2.2, the formulated problem is an integer nonlinear optimization problem with two objective functions, which is hard to be solved by gradient-based optimization methods or linear/nonlinear programming models. Fortunately, in recent years, many evolutionary algorithms have been proposed that are capable of effectively solving such kind of problems. Among them, nondominated sorting genetic algorithm II (NSGA-II) proposed by K. Deb et al. [24] emerged as one of the most powerful methods, which has been widely used in many different engineering applications. In this paper, it is therefore utilized to deal with the optimization problem stated above. Since the details of the algorithm have been given in [24], interested readers are encouraged to refer to this reference.

### 3. BELGRADE AIRPORT CASE STUDY

To demonstrate the reliability and applicability of the proposed approach, a case study is carried out in this section. Belgrade airport Nikola Tesla (ANT), the largest and busiest international airport in Serbia, situated 18 km west of downtown Belgrade, has been chosen as the case study. In 2017, the airport handled more than 5 million passengers and approximately 60 thousand aircraft operations with single runway 3400 m long (direction 12/30).

The first step in this case study was to obtain detailed air traffic data for one day. September 16<sup>th</sup>, 2016 has been chosen since it was a summer day with relatively heavy traffic and some of the data was already available from the previous study [25] which also included measured noise levels at one location near Belgrade airport.

Daily traffic consisted of 220 operations, including 109 departures and 111 arrivals. Distribution of operations between runways was slightly in favour of runway 12 which handled 128 operations (58.2%), while the runway 30 was used for 92 operations (41.8%).

Departure and arrival routes for each runway were obtained from radar data since Standard Instrument Departure (SID) and Standard Arrival Routes (STAR) could not be considered accurate due to aircraft vectoring mostly in place at ANT. Taking into account that aircraft vectoring at ANT is usually done in a similar way, radar data could be regarded as constant since changes in departure/arrival routes derived from radar data from one day to another are minor.

From a bundle of radar tracks presented in Fig. 1a, a 27 different routes were selected to represent actual SID/STAR routes. There are seven departure routes and seven arrival routes from runway 12 (Fig. 1b) and six departure routes and seven arrival routes from runway 30 (Fig. 1c). Departure routes are marked in blue while red colour corresponds to arrival routes.

Noise and fuel data are in function of aircraft type. For the observed day, fleet mix consisted of 25 different aircraft types. However, for the purpose of simplifying the calculations, they were classified into 11 groups based on the similarity of aircraft types. In this way, 85% of the operations were presented by the aircraft types that were actually flown that day, while the remaining 15% were presented by aircraft

types that have approximately the same level of noise exposure and fuel consumption as their representative.

Table 1 shows the number of departure and arrival operations per each period per each aircraft type categorised as per the INM [26] and AzB [27] databases.

Before calculating the noise data, it is pivotal to choose the optimal number and position of locations for which the noise and population data will be obtained. Since ANT is surrounded by populated areas, 23 different municipalities were considered to be affected by aircraft noise: 17 Belgrade municipalities and the municipalities of Stara Pazova, Indjija, Irig, Ruma, Pecinci and Pancevo. In order to be certain that adequate locations would be selected, the conservative approach of calculating noise exposure of each location around the airport was applied in the following way: the most unfavourable case for a certain selected location is when all operations are assigned to departure and arrival routes that are closest to that location and when the noisiest aircraft type is overflying the location (in this study it is "Airbus A330-200"). From 306 locations (settlements) for which the noise exposure was calculated using a conservative approach, only 17 locations were selected since the noise levels at these locations were above legal noise limit values (above 55dB  $L_{den}$  and/or 45dB  $L_{night}$ ). Table 2 shows legal noise limits and population data for each selected location.

As it can be seen from Table 2, population data are presented in four different columns. Data in the first column represents 2011 census data [23]. In order to take into account human mobility patterns and to simulate the three-8h working shifts the day has been divided into three-8h periods: Period 1 from 8 am to 4 pm (90 operations), Period 2 from 4 pm to 12 am (79 operations) and Period 3 from 12 am to 8 am (51 operations). In order to obtain data on daily migrations of economically active persons who perform an occupation, pupils and students for each of the 23 municipalities around the airport it was necessary to make private request for special processing of data collected in the 2011 census to the Statistical Office of the Republic of Serbia since this data was not available publicly. Definition provided in 2011 Census methodology describes daily migrants as persons who work

or go to school/university outside the place of their usual residence, but who return on a daily basis or several times a week [23]. Data on daily migrations was the key to calculate the total daily inflow and outflow of inhabitants for each municipality. Based on that, the approximation of total daily inflows and outflows of the inhabitants for each settlement within the municipality was done in proportion to the number of inhabitants in the settlement.

Having in mind that in this way, human mobility patterns are obtained for the whole day only, and not for the separate periods of the day, some assumptions were needed to be made in order to assess how many people would actually be present at each location during a defined period of time. It was assumed that 50% of employees work first shift, 40% work second shift, and 10% work night shift, while pupils and students go to school in two shifts (Period 1 and 2) equally. In this way, for each period population data were calculated based on the census and daily migration data showing the difference in the number of people at the locations between periods. The total number of residents living near these 17 locations based on census data was 238,741.

Legal noise limit values for day, evening and night, given in Table 2, represent the limit values for EU common noise indicators  $L_{den}$  and  $L_{night}$  in the Republic of Serbia, for residential areas (see [28]). For Period 1 and 2, representing the day and evening, legal noise limit values in dB (A) were set to 55dB, while for Period 3 representing the night noise limit value of 45dB was used.

INM software was used to calculate the sound exposure levels (SEL) for each aircraft type in the fleet mix, flying over each route, for each location separately. This data was used as input for noise objective in optimization model. For each operation, standard INM profile settings were used taking into account the fact that different aircraft types overfly locations at different altitudes and thrust settings. In addition, different profile parameters for each aircraft type were assigned including take-off and landing masses, thrust and flaps settings, climb rate, descent angle,...

**Table 1** Flight statistics and aircraft classifications

Aircraft type	Assigned AzB class	INM airplane code	Departure			Arrival		
			Period	Period	Period	Period	Period	
			1	2	3	1	2	3
Boeing 737-300	S 5.2	737300	4	1	3	5	3	1
Boeing 737-800	S 5.2	737800	2	2	1	3	1	0
Airbus A319	S 5.2	A319-131	10	9	9	11	15	3
Airbus A320	S 5.2	A320-211	11	4	6	12	5	5
Airbus A330-200	S 6.1	A330-301	1	1	0	0	1	1
BE20	P 1.4	CNA441	1	0	1	1	0	0
Cessna 560 XL	S 5.1	CNA560XL	1	1	2	2	1	1
SW4	P 2.1	DHC6	1	2	1	3	1	0
ATR 42	P 2.1	DHC8	1	3	0	1	3	0
ATR 72	P 2.1	DO328	7	8	10	6	14	6
Embraer 190	S 5.2	EMB190	4	2	0	3	2	1
		Total	43	33	33	47	46	18

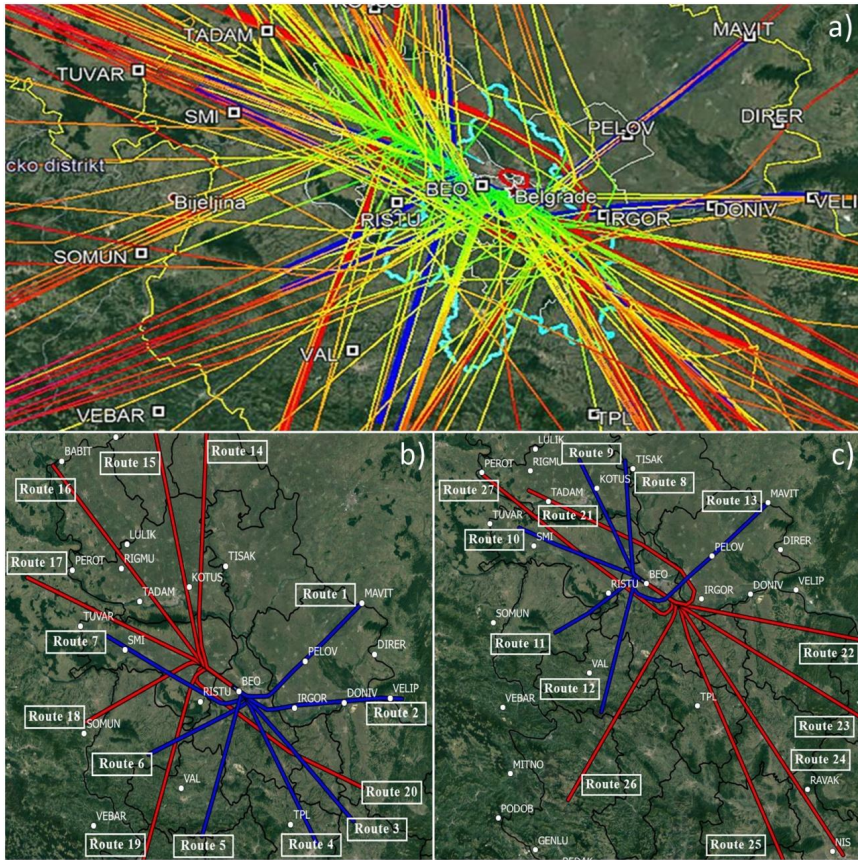


Fig. 1 Radar data and departure and arrival routes (source: Flightradar24.com, using Google Earth)

Table 2 Location and population data

No.	Municipality	Settlement	Legal noise limit (dB)		Population			
			Day and Evening	Night	2011 Census	Period 1	Period 2	Period 3
1	Cukarica	Banovo Brdo	55	45	44669	40098	40790	43978
2	Cukarica	Cerak	55	45	43993	39492	40172	43312
3	Cukarica	Zarkovo	55	45	30979	27809	28289	30500
4	Novi Beograd	Bezanijski blokovi	55	45	22455	22725	22610	22570
5	Novi Beograd	Ledine	55	45	6813	6895	6860	6848
6	Novi Beograd	Sava	55	45	18899	19126	19029	18996
7	Rakovica	Kanarevo Brdo	55	45	11389	9975	10194	11170
8	Rakovica	Kosutnjak	55	45	4944	4330	4425	4849
9	Rakovica	Miljakovac	55	45	7622	6676	6822	7476
10	Rakovica	Skojevska	55	45	4739	4151	4242	4648
11	Surcin	Dobanovci	55	45	8503	8055	8089	8469
12	Vozdovac	Jajinci	55	45	8876	8672	8733	8815
13	Vozdovac	Kumodraz	55	45	6064	5924	5966	6022
14	Vozdovac	Kumodraz 1	55	45	3852	3763	3790	3826
15	Vozdovac	Rakovica	55	45	3292	3216	3239	3269
16	Zemun	Ugrinovci	55	45	10807	10585	10616	10776
17	Stara Pazova	Krnjesevci	55	45	845	809	813	841
Total					238741	222301	224679	236365

#### 4. RESULTS AND DISCUSSION

The results obtained by the proposed approach for three different periods in comparison with those acquired by the base case and the model in [15] are depicted in Fig. 2. At first glance, it can be seen from Fig. 2 that the present approach offers a wide range of solutions (denoted as Pareto front), which try to make a good trade-off between the population noise exposure and fuel consumption. Another observation is that, for all three periods, the proposed model can provide solutions that dominate the base case, while compared with those obtained by [15], they are worse in terms of noise criterion and better regarding fuel burn.

In order to make the comparison more apparent, for each period, three different solutions are selected and highlighted, as shown in Fig. 2. With this selection, solution 1 represents for fuel optimization, solution 3 prefers to noise criterion, whereas solution 2 is one of solutions from the Pareto fronts which is close to the base case. All the metrics derived from these solutions are given in Table 3, where those obtained by the base case and the model in [15] are also provided.

From the table, a common trend for all the periods can be observed. Specifically, compared to base case, solution 1 offers a better performance in fuel burn, solution 2 performs better in noise criterion, while with almost the same amount of fuel consumption, solution 3 achieves a significant

reduction in population noise exposure. For example, in Period 1, solution 1 has a reduction of 0.7% and 0.5% in fuel burn and route length, respectively, and an increase of 3.3% in population noise exposure, compared with the base case. Solution 2 has a very good performance in noise criterion with a considerable decrease of 43.8% in comparison with the base case, which is almost the same with that of the model in [15]. However, it is worse than the base case in term of fuel burn and route length. For solution 3, there is a good trade-off between all the concerned metrics to be found. With the same amount of fuel burn, it gains a great reduction of 42.7% in noise metric, while the one acquired by Ganic et al. [15] has a reduction of 43.8%, but causes a significant increase up to 0.7% in fuel burn.

From the results obtained above, it can be concluded that the proposed approach is reliable and quite effective. It not only provides reliable solutions, but also offers a variety of options for interested users to choose with only one single run. This feature has made the proposed approach dominating other single objective approaches in previous studies. Moreover, with the new form of the optimization problem given in Section 2.2, the problem size is reduced significantly, which allows the proposed model to be capable of solving large scale problems.

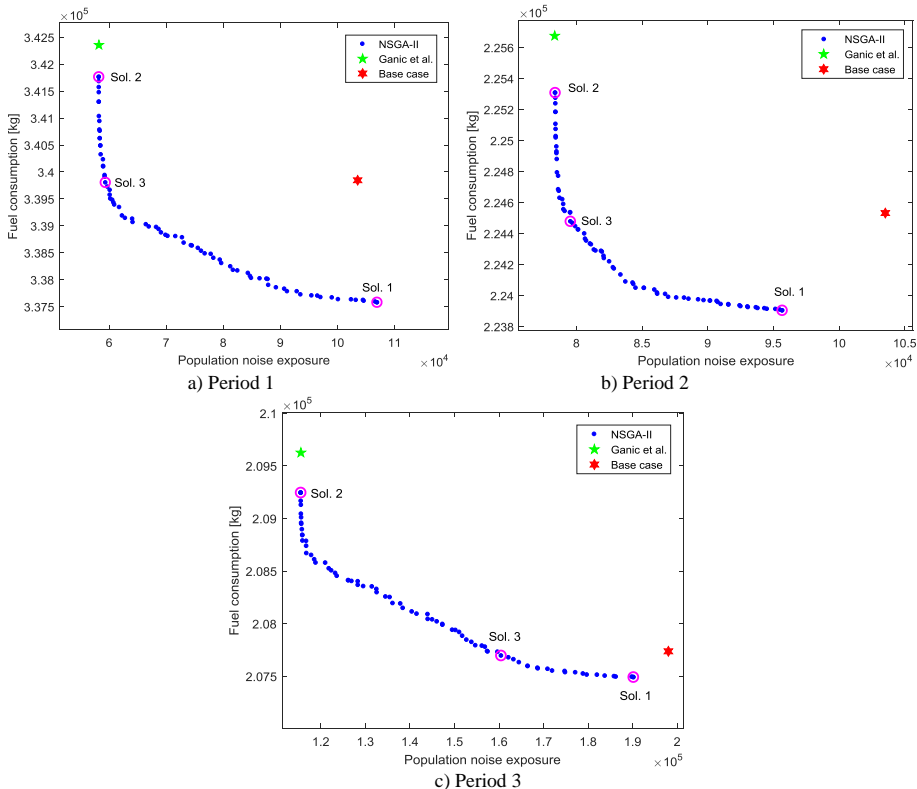


**Fig. 2** Pareto front obtained by the NSGA-II algorithm

**Table 3** Comparison of the metrics of the representative solutions and the reference case

Period	Metrics	Base case	Ganić et al. [15]		Solution 1		Solution 2		Solution 3	
			Absolute value	% reduction	Absolute value	% reduction	Absolute value	% reduction	Absolute value	% reduction
1	Population noise exposure	103541	58187	-43.8%	106974	3.3%	58211	-43.8%	59359	-42.7%
	Fuel consumption (kg)	339844	342358	0.7%	337567	-0.7%	341761	0.6%	339798	0.0%
	Route length (NM)	51459	52065	1.2%	51227	-0.5%	51923	0.9%	51647	0.4%
2	Population noise exposure	103506	78332	-24.3%	95643	-7.6%	78356	-24.3%	79518	-23.2%
	Fuel consumption (kg)	224527	225682	0.5%	223897	-0.3%	225315	0.4%	224477	0.0%
	Route length (NM)	38664	38924	0.7%	38515	-0.4%	38833	0.4%	38644	-0.1%
3	Population noise exposure	197999	115514	-41.7%	190204	-3.9%	115539	-41.6%	160493	-18.9%
	Fuel consumption (kg)	207735	209631	0.9%	207488	-0.1%	209248	0.7%	207695	0.0%
	Route length (NM)	33713	34279	1.7%	33639	-0.2%	34191	1.4%	33700	0.0%

**5. CONCLUSION**

In this paper, a new approach for air traffic assignment is developed. The proposed model is based on a new form of the optimization problem, in which two conflicting objective functions, including noise and fuel criteria, are taken into account simultaneously. The formulated problem is then solved by the well-known multi-objective optimization method, named NSGA-II. The reliability and applicability of the proposed approach are demonstrated through a case study at Belgrade Airport in Serbia. Through the evaluation and comparison of the obtained results with those of the base case and the model in [15], it reveals that the proposed method is reliable and quite effective. It does not only provide reliable solutions but also gives a wide range of solutions – featuring a good trade-off between the considered two objectives – which can be a good reference base for users to refer to before making decisions.

Furthermore, thanks to the new ways of formulating the optimization problem, the proposed approach is promising to be extended for solving large problems in busy airports.

**Acknowledgements**

This research is supported by the Ministry of Science and Technological Development of the Republic of Serbia and represents a part of the project named “A support to sustainable development of the Republic of Serbia’s air transport system” (TR36033).

**REFERENCES**

[1] EC, “Directive 2002/49/EC of the European parliament and the Council of 25 June 2002 relating to the assessment and management of environmental noise,” *Official Journal of the European Communities*, vol. 189, no. 12, pp. 12–25, 2002.

[2] K. Vogiatzis, “Airport environmental noise mapping and land use management as an environmental protection action policy tool. The case of the Larnaka International Airport (Cyprus),” *The Science of the total environment*, vol. 424, pp. 162–73, May 2012.

[3] I. Glekas, K. Vogiatzis, and C. Antoniadis, “Strategic noise mapping & action plans for the international airports of Larnaca & Pafos in Cyprus,” in *The 23rd International Congress on Sound and Vibration*, 2016.

[4] K. Vogiatzis, “Assessment of environmental noise due to aircraft operation at the Athens International Airport according to the 2002/49/EC Directive and the new Greek national legislation,” *Applied Acoustics*, vol. 84, pp. 37–46, Oct. 2014.

[5] V. Ho-Huu, S. Hartjes, H. G. Visser, and R. Curran, “Integrated design and allocation of optimal aircraft departure routes,” *Transportation Research Part D: Transport and Environment*, vol. 63, pp. 689–705, Aug. 2018.

[6] L. Frair, “Airport noise modelling and aircraft scheduling so as to minimize community annoyance,” *Applied Mathematical Modelling*, vol. 8, no. 4, pp. 271–281, Aug. 1984.

[7] D. S. Zachary, J. Gervais, and U. Leopold, “Multi-impact optimization to reduce aviation noise and emissions,” *Transportation Research Part D: Transport and Environment*, vol. 15, no. 2, pp. 82–93, Mar. 2010.

[8] B. Kim, L. Li, and J.-P. Clarke, “Runway Assignments That Minimize Terminal Airspace and Airport Surface Emissions,” *Journal of Guidance, Control, and Dynamics*, vol. 37, no. 3, pp. 789–798, May 2014.

[9] F. Netjasov, “A Model of Air Traffic Assignment as a Measure for Mitigating Noise at Airports: The Zurich Airport Case,” *Transportation Planning and Technology*, vol. 31, no. 5, pp. 487–508, Oct. 2008.

[10] S. J. Heblj, V. Hanenburg, R. A. A. Wijnen, and H. G. Visser, “Development of a Noise Allocation Planning Tool,” in *45th AIAA Aerospace Sciences Meeting and Exhibit*, 2007, pp. 1–7.

[11] O. I. Zaporozhets and V. I. Tokarev, “Predicted flight procedures for minimum noise impact,” *Applied Acoustics*, vol. 55, no. 2, pp. 129–143, Oct. 1998.

[12] J. M. Nibourg, H. H. Hesselink, and Y. A. J. R. van de Vijver, “Environment-Aware Runway Allocation Advice System,” Amsterdam, the Netherlands, NLR-

- TP-2008-506, 2012.
- [13] B. R. Kuiper, H. G. Visser, and S. J. Heblj, "Efficient use of an allotted airport annual noise budget through minimax optimization of runway allocations," *Proceedings of the Institution of Mechanical Engineers, Part G: Journal of Aerospace Engineering*, vol. 227, no. 6, pp. 1021–1035, Jun. 2013.
- [14] W. R. Ott, "Concepts of human exposure to air pollution," *Environment International*, vol. 7, no. 3, pp. 179–196, 1982.
- [15] E. Ganić, O. Babić, M. Čangalović, and M. Stanojević, "Air traffic assignment to reduce population noise exposure using activity-based approach," *Transportation Research Part D: Transport and Environment*, vol. 63, pp. 58–71, Aug. 2018.
- [16] M. Hatzopoulou and E. J. Miller, "Linking an activity-based travel demand model with traffic emission and dispersion models: Transport's contribution to air pollution in Toronto," *Transportation Research Part D: Transport and Environment*, vol. 15, no. 6, pp. 315–325, Aug. 2010.
- [17] I. Kaddoura, L. Kröger, and K. Nagel, "User-specific and Dynamic Internalization of Road Traffic Noise Exposures," *Networks and Spatial Economics*, Mar. 2016.
- [18] J. Hao, M. Hatzopoulou, and E. Miller, "Integrating an Activity-Based Travel Demand Model with Dynamic Traffic Assignment and Emission Models Implementation in the Greater Toronto, Canada, Area," *Transportation Research Record: Journal of the Transportation Research Board*, vol. 2176, pp. 1–13, 2010.
- [19] S. Jiang, J. Ferreira, and M. C. Gonzalez, "Activity-Based Human Mobility Patterns Inferred from Mobile Phone Data: A Case Study of Singapore," *IEEE Transactions on Big Data*, vol. 3, no. 2, pp. 208–219, Jun. 2017.
- [20] S. Jiang, J. Ferreira, and M. C. González, "Clustering daily patterns of human activities in the city," *Data Mining and Knowledge Discovery*, vol. 25, no. 3, pp. 478–510, Nov. 2012.
- [21] J. Novák and L. Sýkora, "A City in Motion: Time-Space Activity and Mobility Patterns of Suburban Inhabitants and the Structuration of the Spatial Organization of the Prague Metropolitan Area," *Geografiska Annaler, Series B: Human Geography*, vol. 89, no. 2, pp. 147–168, Jun. 2007.
- [22] M. Winther, K. Rypdal, L. Sørensen, M. Kalivoda, M. Bukovnik, N. Kilde, R. De Laurentis, R. Falk, D. Romano, R. Deransy, L. Box, L. Carbo, N. T. Meana, and M. Whiteley, *EMEP/EEA air pollutant emission inventory guidebook 2016 – Update July 2017 - 1.A.3.a, 1.A.5.b Aviation*, no. July. European Environment Agency, 2017.
- [23] Statistical Office of the Republic of Serbia, *2011 Census of Population, Households and Dwellings in the Republic of Serbia. Daily Migrants (data by municipalities/cities)*. Belgrade, Serbia: Statistical Office of the Republic of Serbia, 2013.
- [24] K. Deb, A. Pratap, S. Agarwal, and T. Meyarivan, "A fast and elitist multiobjective genetic algorithm: NSGA-II," *IEEE Transactions on Evolutionary Computation*, vol. 6, no. 2, pp. 182–197, Apr. 2002.
- [25] E. Ganić, M. Radojević, and O. Babić, "Influence of aircraft noise on quiet areas," in *25th International Conference Noise and Vibration Proceeding of papers*, 2016, pp. 47–53.
- [26] Federal Aviation Administration, "INM v7.0 User's Guide," 2007.
- [27] AzB-08, *Anleitung zur Berechnung von Lärmschutzbereichen nach dem Gesetz zum Schutz gegen Fluglärm vom 19. November 2008 in: 1. Verordnung zur Durchführung des Gesetzes zum Schutz gegen Fluglärm (1. FlugLSV) vom 27.12.2008*. 2008.
- [28] Government of Republic of Serbia, *Regulation on noise indicators, limit values, assessment methods for indicators of noise, disturbance and harmful effects of noise in the environment (in Serbian)*, vol. 75/2010. Republic of Serbia, 2010.



Contents lists available at ScienceDirect

## Transportation Research Part D

journal homepage: [www.elsevier.com/locate/trd](http://www.elsevier.com/locate/trd)



# Air traffic assignment based on daily population mobility to reduce aircraft noise effects and fuel consumption

Vinh Ho-Huu<sup>a,\*,1</sup>, Emir Ganić<sup>b,\*,1</sup>, Sander Hartjes<sup>a</sup>, Obrad Babić<sup>b</sup>, Richard Curran<sup>a</sup>

<sup>a</sup> Faculty of Aerospace Engineering, Delft University of Technology, P.O. Box 5058, 2600 GB Delft, the Netherlands

<sup>b</sup> Faculty of Transport and Traffic Engineering, University of Belgrade, 305 Vojvode Stepe Street, Belgrade, Serbia

4

### ARTICLE INFO

#### Keywords:

Air traffic noise  
 Airport noise  
 Aircraft noise  
 Noise annoyance  
 Fuel consumption  
 Multi-objective optimization

### ABSTRACT

The paper first investigates the influence of daily mobility of population on evaluation of aircraft noise effects. Then, a new air traffic assignment model that considers this activity is proposed. The main objective is to reduce the number of people affected by noise via lowering as much as possible the noise exposure level  $L_{den}$  of individuals or groups of people who commute to the same locations during the day. It is hereby intended to reduce the noise impact upon individuals rather than to reduce the impact in particular – typically densely populated – areas. However, sending aircraft farther away from populated regions to reduce noise impact may increase fuel burn, thus affecting airline costs and sustainability. Therefore, a multi-objective optimization approach is utilized to obtain reasonable solutions that comply with overall air transport sustainability. The method aims at generating a set of solutions that provide proper balance between noise annoyance and fuel consumption. The reliability and applicability of the proposed method are validated through a real case study at Belgrade airport in Serbia. The investigation shows that there is a difference between the number of people annoyed (NPA) evaluated based on the census data and the NPA evaluated based on the mobility data. In addition, these numbers differ significantly across residential locations. The optimal results show that the proposed model can offer a considerable reduction in the NPA, and in some cases, it can gain up to 77%, while maintaining the same level of fuel consumption compared with the reference case.

## 1. Introduction

Proper allocation of aircraft to departure and arrival routes may play an important role in reducing aircraft noise effects on communities located near airports, and this issue has attracted considerable attention of researchers and authorities over the years. Although this topic has been well studied, research is often conducted based on census data, and hence it is assumed that people remain at the same location throughout the day. In reality, however, people spend substantial portion of the day at school, work or other places outside their homes. Consequently, analyses of daily population mobility have been considered in many transportation studies (Hatzopoulou and Miller, 2010; Jiang et al., 2017; Kaddoura et al., 2016; Novák and Šýkora, 2007) as an important factor for a more precise estimation of noise effects. Nevertheless, there is a lack of this kind of research for air traffic assignment problems. This paper, therefore, first investigates the influence of population's daily mobility upon evaluation of aircraft noise effects. Then, a new

\* Corresponding authors.

E-mail addresses: [v.hohuu@tudelft.nl](mailto:v.hohuu@tudelft.nl) (V. Ho-Huu), [e.ganic@sf.bg.ac.rs](mailto:e.ganic@sf.bg.ac.rs) (E. Ganić), [s.hartjes@tudelft.nl](mailto:s.hartjes@tudelft.nl) (S. Hartjes), [o.babic@sf.bg.ac.rs](mailto:o.babic@sf.bg.ac.rs) (O. Babić), [r.curran@tudelft.nl](mailto:r.curran@tudelft.nl) (R. Curran).

<sup>1</sup> These authors contributed equally to this work.

<https://doi.org/10.1016/j.trd.2019.04.007>

air traffic assignment model that takes daily movement of population into account is proposed. In the proposed model, the main objective is to minimize the number of people affected by aircraft noise while maintaining fuel consumption as low as possible. In order to achieve this purpose, a multi-objective optimization approach is utilized herein. The method aims at producing a set of solutions that are able to deliver a proper balance between conflicting objectives, i.e., noise annoyance and fuel consumption. An extensive review of the literature that served as the background and that motivated the authors to conduct this research is presented below.

Over the years, significant efforts have been devoted to relieving the noise impact as well as to reducing fuel consumption and pollutant emissions. At the European level, a legislative framework has been introduced, namely the Environmental Noise Directive 2002/49/EC (END) (EC, 2002) for the assessment and management of environmental noise. The Directive regulated the obligation to develop strategic noise maps and noise action plans with the aim of avoiding, preventing and reducing the harmful effects of noise on public health, and these have been successfully implemented at many airports (Glekas et al., 2016; Vogiatzis, 2014, 2012). After more than 15 years of enforcement, both the implementation review and the evaluation of END have been done twice so far, addressing questions related to effectiveness, efficiency, coherence, relevance and EU added value (European Commission, 2016). In addition, common noise assessment methods (CNOSSOS-EU) for the determination of the noise indicators  $L_{den}$  and  $L_{night}$  have been adopted by the EC through the revision of Annex II of the END in 2015 (Coelho et al., 2011; Kephelopoulou et al., 2014; Vogiatzis and Remy, 2014). CNOSSOS-EU has been developed to improve the consistency and the comparability of noise assessment results across the EU member states, providing a harmonized framework for assessment of each noise source covered by END. Upon the release of the Directive, numerous initiatives to reduce fuel consumption and emissions have been launched in recent years, as well. The examples include the Atlantic Interoperability Initiative to Reduce Emissions (AIRE)<sup>2</sup>, Asia and South Pacific Initiative to Reduce Emissions (ASPIRE)<sup>3</sup>, ACI Airport Carbon Accreditation<sup>4</sup>, and the European Advanced Biofuels Flightpath<sup>5</sup>.

In addition to the above initiatives that require enormous budgets and focus more on strategical levels, at a practical level it has been observed that the variation of aircraft/airport operational procedures is one of the feasible options that could bring short-term improvements and could be less costly (Marais et al., 2013). From this perspective, literature shows that research efforts in designing optimal departure and arrival routes with less noise and fuel burn have been well studied over the past decades, and various strategies have been proposed (Prats et al., 2011; Visser, 2005; Visser and Wijnen, 2001). Recently, with the utilization of multi-objective optimization techniques, research has also demonstrated that the obtained optimal routes are beneficial not only from the noise perspective, but also in terms of fuel burn (Ho-Huu et al., 2017; Vinh Ho-Huu et al., 2018; Torres et al., 2011; Zhang et al., 2018). In addition to efforts invested to improve environmentally friendly departure and arrival routes, optimal distribution of aircraft and operational procedures to specific routes could also contribute significantly to environmental impact decrease (Frair, 1984; Heblj et al., 2007; Kuiper et al., 2013; Netjasov, 2008; Nibourg et al., 2012; Zachary et al., 2011, 2010).

In order to assess the impact of flight operations on communities located near airports, it is critical to include distribution data of populations in the vicinity of airports, as done in a number of previous studies. However, census data takes into account only the homes of people, whereas, in reality, people spend substantial portions of the day at work, school, university or other places away from their residential locations. Consequently, the population may experience noise exposures which are very different from the ones predicted when using only the census data. One of the first studies that has called attention to the drawback of relying on census data was carried out by Ott (1982). In this study, the author shows that employees and students usually spend a long time away from their residential locations, and this leads to a different overall impact of, in this case, air pollutants. The same observation is also recognized in a recent study by Kaddoura et al. (2017). In this work, the authors suggest that the evaluation of population's exposure to road traffic noise should take spatial and temporal variations in the population into account, because the use of static data would lead to an overassessment.

One of the first air traffic assignment studies that takes daily mobility of population into account was done by Ganić et al. (2018). In this study, however, the evaluation of noise effects is based only on the change of population at several locations through three different periods of day, and is hence treated as three separate optimization problems. Furthermore, the model of air traffic assignment developed in Ganić et al. (2018) has some limitations, as well. The problem was formulated as a binary nonlinear optimization problem, in which, for each operation, every feasible assignment of routes was considered a decision variable. Therefore, the size of the problem is rather large and hence it is difficult to solve the problem when the number of aircraft operations increases. In addition, only the noise objective is considered, while fuel consumption and local air quality are not considered, and these may very well be adversely affected.

Motivated by the above limitations, the authors of this paper considered the information on daily mobility of population in the air traffic assignment model. To evaluate whether the inclusion of mobility data is necessary or not, the influence of census and mobility data on evaluation of noise effects is investigated first. Then, a new air traffic assignment model that is capable of taking daily mobility of population into account is developed. In order to reduce the number of people affected by aircraft noise, the noise exposure level  $L_{den}$  is calculated for each individual or group of people who commute to the same locations during an entire day from 00:00 to 24:00 h. Afterwards, a noise annoyance criterion recommended by EEA (2010) is employed to obtain the number of people annoyed. Furthermore, to acquire optimal solutions which are able to balance between noise impact and fuel consumption

<sup>2</sup> [https://ec.europa.eu/transport/modes/air/environment/aire\\_en](https://ec.europa.eu/transport/modes/air/environment/aire_en) (assessed 9 September 2018)

<sup>3</sup> <https://aviationbenefits.org/case-studies/aspire/> (assessed 9 September 2018)

<sup>4</sup> <https://www.airportcarbonaccreditation.org/> (assessed 9 September 2018)

<sup>5</sup> <https://www.biofuelsflightpath.eu/about> (assessed 9 September 2018)

effectively, a bi-objective optimization problem is formulated. In addition, since the considered problem is an integer nonlinear multi-objective optimization problem, it is rather difficult to solve it by nonlinear optimization programming models as applied in Ganić et al. (2018). To allow the problem to be solved with a multi-objective evolutionary algorithm, a new problem formulation is proposed. In the proposed formulation, each operation is considered a decision variable, and its feasible assignments of routes, after taking into account wind conditions, runway configurations and separation minima, are considered its search space. With the application of this formulation, the size of the problem reduces significantly, and hence the problem can be solved effectively by employing an evolutionary algorithm. The proposed approach is then applied to a real case study at Belgrade airport in the Republic of Serbia.

The structure of the paper is as follows. In Section 2, first the problem definition is presented, and then the mathematical formulation and data preparation are described in detail. Section 3 provides a brief description of the optimization method, namely the non-dominated sorting genetic algorithm (NSGA-II) which is applied to solve the formulated problem. The Belgrade airport case study is presented in Section 4. The results and discussion are presented in Section 5. Finally, some conclusions, remarks and ideas for future work are presented in Section 6.

**2. Problem definition**

This section presents the model of the air traffic assignment problem in detail. The main idea of the formulated problem is to assign aircraft to suitable routes with the aim of minimizing noise impact on communities close to the airport and fuel consumption. First, the mathematical form is presented. Then, the preparation of the input data is described.

**2.1. Mathematical formulation**

The mathematical model of the optimization problem is formed based on several assumptions which are explained in detail in Section 2.2. The model is described through three components: notations, decision variables, and objective functions, as follows.

*Notations:*

- $O$  is the set of aircraft movements departing from and arriving at an airport during a considered day;
- $S_i$  is the set of feasible routes to which aircraft movement  $i$  can be assigned, and which takes into account runway configuration, wind conditions and separation minima,  $i \in O$ ;
- $L$  is the number of considered locations;
- $J$  is the set of individual persons or groups of people commuting to the same location during an entire day (from 00:00 to 24:00 h);
- $T$  is the number of time periods;
- $SEL_{itl}$  is the sound exposure noise level (SEL) generated by the movement  $i$  at the time  $t$  and the location  $l$ ,  $i \in O$ ,  $t \in T$ ,  $l \in L$ ;
- $p_j$  is the number of people in the group of people  $j$  who commute to the same location at the same time during the day,  $j \in J$ ;

*Decision variables:*

- $x_i$  is an integer design variable of route assignment of the movement  $i$ , which is selected from the set of feasible operational options  $S_i$  ( $x_i \in S_i$ ). It should be noted that the noise level  $SEL$  at all locations in  $L$  and the fuel consumption for an entire flight are predefined for each option within  $S_i$ .
- $\mathbf{x}$  is the vector of the design variable  $x_i$ , containing the optimal assignments of all movements to routes.

*Objective functions:*

With the aim of finding optimal solutions that are capable of balancing effectively between the number of people affected by aircraft noise and fuel consumption, an optimization problem with two objectives is considered. The first one is the total number of people annoyed (hereinafter referred to as NPA), which is defined as follows:

$$NPA(\mathbf{x}) = \sum_{j \in J} \%PA_j \cdot p_j \tag{1}$$

where  $\%PA_j$  is the percentage of people in the group of people  $j$  who are annoyed due to being exposed to a certain level of aircraft noise. According to EEA (2010), it is based on the  $L_{den}$  cumulative noise metric, and estimated as follows:

$$\%PA_j = 8.588 \times 10^{-6}(L_{denj} - 37)^3 + 1.777 \times 10^{-2}(L_{denj} - 37)^2 + 1.221(L_{denj} - 37) \tag{2}$$

where  $L_{denj}$  is the day-evening-night noise level to which the group of people  $j$  is exposed during the day, and it is determined as follows:

$$L_{denj} = 10 \log_{10} \left( \frac{1}{T_d} \left( \sum_{i \in O} \sum_{t \in T} 10^{\frac{SEL_{itl} + w_{den}}{10}} \right) \right), \forall j \tag{3}$$

where  $w_{den} = \{0, 5, 10\}$  is the weighting factor to account for day, evening and night time operations, and it is defined based on the time at which the movement  $i$  takes place.  $T_d$  is the considered time period of an entire day in seconds ( $T_d = 24 \times 3600$  s). It should

be noted that, for further analyses in the later sections, the number of people who are highly annoyed (hereinafter referred to as NPHA) is used as well. This criterion is also developed by [EEA \(2010\)](#) and defined as follows:

$$NPHA(\mathbf{x}) = \sum_{j \in J} \%PHA_j \cdot p_j \quad (4)$$

where  $\%PHA_j$  is the percentage of people in the group of people  $j$  who are highly annoyed due to their exposure to a certain level of aircraft noise, and it is calculated by:

$$\%PHA_j = 9.199 \times 10^{-5}(L_{denj} - 42)^3 + 3.932 \times 10^{-2}(L_{denj} - 42)^2 + 0.2939(L_{denj} - 42) \quad (5)$$

The second objective is the total fuel burn. The EMEP/EEA air pollutant emission inventory guidebook – 2016 (Part B: sectoral guidance chapters, 1.A.3.a Aviation 2016) ([Winther et al., 2017](#)) is used to calculate the fuel consumption for each operation. Particularly, the LTO and Master Emission calculators in Annex 5 of this document, which use the data from the ICAO Aircraft Engine Emissions Databank (ICAO, 2017), are applied. These calculations have been done in the previous study ([Ganić et al., 2018](#)), and they are again to be used in this research. Then, the fuel objective is defined as follows:

$$T_{fuel}(\mathbf{x}) = \sum_{i \in O} fuel(x_i) \quad (6)$$

where  $fuel(x_i)$  is the fuel consumption for the movement  $i$ .

## 2.2. Data requirements

As described in the notations, the model needs the following input data:

- air traffic data,
- departure and arrival routes for each runway with a predefined set of feasible routes,
- population locations,
- noise data for each location caused by all aircraft operating on all feasible routes,
- fuel consumption of all aircraft operating on all feasible routes,
- population data,
- daily mobility patterns.

The air traffic data includes information about origin and destination, aircraft type, actual take-off time, arrival time, and runway in use. This information can be obtained from Air Traffic Control. Real radar data can be used to represent departure and arrival routes, or the routes can be obtained from Aeronautical Information Publication (AIP). In this research radar data were used. Runway configuration, wind condition forecasts from METAR reports and separation minimum are taken into account to determine the set of feasible routes for each aircraft operation.

The noise levels caused by each aircraft movement on all feasible routes need to be determined a priori and stored in a database. The locations at which the noise is determined coincide with the census data and the data on population's daily mobility. Considering the low level of detail required for this research, each settlement can be represented as a single point, i.e., location since it is not required to observe each housing unit in particular.

The fuel consumption is calculated by using the EMEP/EEA air pollutant emission inventory guidebook – 2016 ([Winther et al., 2017](#)). Fuel burn for Landing and Take-Off (LTO) flight phases is assessed by using the origin and destination information of airports, as well as aircraft type (engine type, number of engines), duration for each LTO phase (taxi, take off, climb out, approach) and rate of fuel burn (kg/s/engine). For Climb/Cruise/Descent (CCD) flight phases fuel consumption is calculated based on CCD stage length and aircraft type.

Static population data are collected for each location based on the census data. Census data essentially represent home addresses of the population. To account for daily mobility patterns the population is divided into groups of people commuting to the same locations during the day at the same time period. Daily mobility presented in this paper includes a special form of spatial mobility of economically active populations (who perform an occupation), pupils and students. This data for each municipality around the airport is available at National Statistical Office ([Statistical Office of the Republic of Serbia, 2013](#)).

## 3. Optimization algorithm

As described in [Section 2](#), the formulated problem is an integer nonlinear optimization problem with two objective functions. Thus, it is rather challenging to solve it using gradient-based optimization methods or nonlinear programming models. The difficulties lie in two aspects. Firstly, the decision variables are options that do not link directly to the objective functions, and hence they are difficult to solve with gradient-based optimization methods and nonlinear programming models. Secondly, even under the assumption that these models can be applied, they need to be combined with other techniques, such as weight methods, to solve the multi-objective optimization problem. Nevertheless, it is still hard to decide which weight vectors should be used. In addition, it is challenging to obtain a well-distributed Pareto front by applying these approaches when the considered problem is nonlinear.

Fortunately, many evolutionary algorithms capable of effectively dealing with similar problem have been proposed in recent

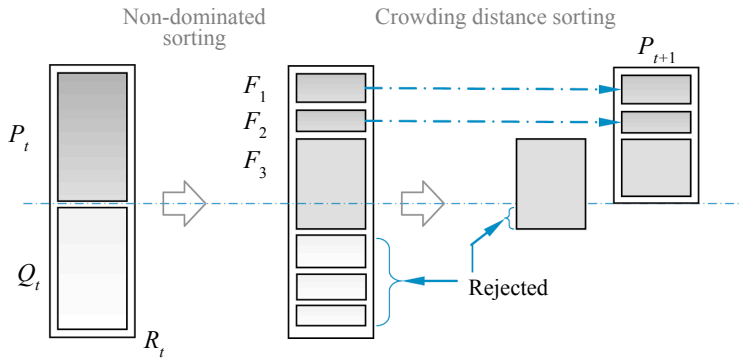


Fig. 1. Illustration of NSGA-II procedure.

years. Among them, the non-dominated sorting genetic algorithm II (NSGA-II) proposed by Deb et al. (2002) has emerged as one of the most powerful methods. The algorithm has been successfully applied in various engineering applications, for instance, structural optimization problems (Thang et al., 2018; Vo-Duy et al., 2017), scheduling problems (Martínez-Puras and Pacheco, 2016; Wang et al., 2017), allocation problems (Abouei and Taghi, 2018; Alikar et al., 2017), noise abatement departure trajectories (Hartjes and Visser, 2016), etc.

The NSGA-II algorithm is the improved version of NSGA developed earlier by Srinivas and Deb (1994) with a fast non-dominated sorting procedure and a crowded-comparison technique. Due to the outstanding features of these techniques, the performance of NSGA-II has been significantly enhanced in comparison to the previous version. In NSGA-II, the optimization process is started with a random number of solutions called the initial population  $P_0$ , in which  $t$  is the generation. Then, for each candidate solution in the population, the objective functions are evaluated. In order to gradually evolve the population towards the optimal solutions, from the previous (parent) population, an offspring population  $Q_t$  is generated by using genetic operators, such as tournament selection, crossover and mutation. Similarly, the objective function information of these solutions is also assessed. Next, both the parent population and the offspring population are combined and denoted as  $R_t$ . From the combined population  $R_t$ , the fast non-dominated sorting procedure and the crowded-comparison technique are applied to obtain a new population  $P_{t+1}$  for the next generation. The algorithm repeats the same procedures until the maximum generation or a stopping condition is reached. Once the search process of the algorithm is terminated, the set of optimal solutions called the Pareto front is obtained. They are non-dominated solutions that can provide a sound basis for users to make decisions. A brief description of NSGA-II for one generation is shown in Fig. 1 (Deb et al., 2002).

Due to its outstanding performance, NSGA-II has been implemented in various programming languages including MATLAB, which is used in this paper. However, this version handles only the optimization problem with continuous design variables. Therefore, to enable the algorithm to solve the presented problem with integer design variables, a rounding technique is applied. By using this technique, whenever the algorithm introduces new candidate solutions, these solutions are all rounded to their nearest integer values before their objective functions are evaluated. Although the technique is rather simple, it has been demonstrated to be effective when dealing with discrete and integer design variables in evolutionary algorithms (V. Ho-Huu et al., 2018).

#### 4. Case study: Belgrade Airport

In order to validate and demonstrate the reliability and applicability of the proposed approach, Belgrade Airport is selected as the case study in this paper. The airport is the largest and the busiest international airport in the Republic of Serbia, located 18 km west of the Belgrade capital. With a single runway 3,400 m long (direction 12/30), the airport handled more than 5 million passengers and approximately 60 thousand aircraft operations in 2018.

As presented in Section 2, detailed air traffic data is required to prepare the input data for the model. The operations on September 16<sup>th</sup>, 2016 were chosen as it was a summer day with relatively heavy traffic. In addition, some of the data have been already available from the previous study (Ganić et al., 2016), which included measured noise levels at locations near the airport as well. Daily traffic comprised of 220 operations, consisting of 109 departures and 111 arrivals. The distribution of operations between runways was slightly in favor of runway 12, which handled 128 operations (58.2%), while runway 30 was used for 92 operations (41.8%). Departure and arrival routes for each runway were obtained from the radar data (flightradar24.com) because the Standard Instrument Departure (SID) and Standard Arrival Routes (STAR) could be less accurate, as most aircraft are vectored at Belgrade Airport.

From the radar tracks presented in Fig. 2a, 27 representative routes were selected, each representing a SID or STAR route. There are seven departure routes and seven arrival routes from runway 12 (Fig. 2b), and six departure routes and seven arrival routes from runway 30 (Fig. 2c). Departure routes are marked blue, and arrival routes are marked red. Note that since operations in solutions obtained by the proposed model could be assigned to arrival/departure routes that are different from the ones assigned in the

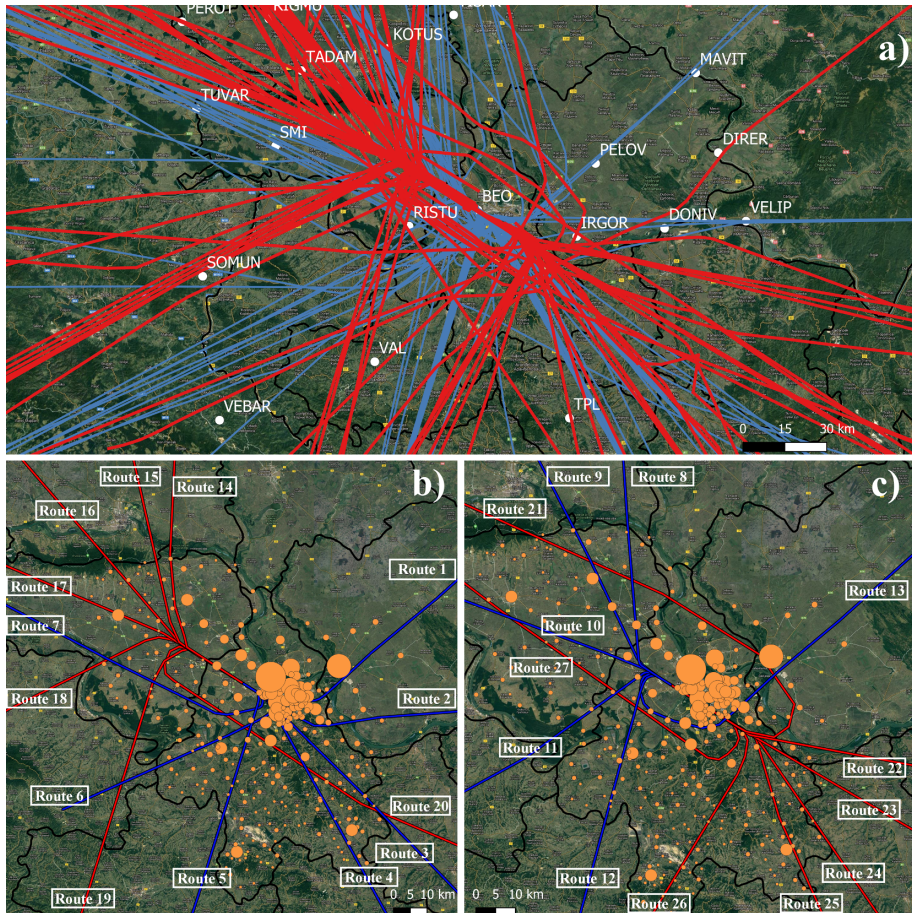


Fig. 2. Radar data and representative departure and arrival routes (source: [Flightradar24.com](http://Flightradar24.com) using QGIS).

reference case (the base-case scenario), the routes shown in Fig. 2b and Fig. 2c are complemented by parts of the route which connect them with border corridors applied in the reference case. For more details, interested readers may refer to [Ganić et al. \(2018\)](#). Noise and fuel data have to be defined for each aircraft type. For the observed day, the fleet mix consisted of 25 different aircraft types. However, in an effort to simplify the calculations, the aircraft were classified into 11 groups based on the similarity of aircraft types using principles of acoustic equivalency and noise significance ([ECAC, 2016](#)). Thereby, 85% of the operations are presented by the aircraft types that were actually operated that day, while the remaining 15% are presented by aircraft types that have approximately the same level of noise exposure and fuel consumption as their representative type. [Table 1](#) shows the number of departure and arrival operations for different periods with different aircraft types that are categorized based on the INM ([Federal Aviation Administration, 2007](#)). The classification of these aircraft types in AzB databases is also provided and it can be used as an alternative when the AzB noise model is applied ([AzB-08, 2008](#); [Isermann and Vogelsang, 2010](#)).

The sound exposure levels (SEL) at each location caused by each aircraft type on the different routes are calculated by the INM software, which is used as input for the noise objective in the optimization model. For each operation, the standard INM profile settings are used and the fact that different aircraft types overfly locations at different altitudes and thrust settings is taken into account. In addition, different profile parameters for each aircraft type are also assigned, including take-off and landing weights, thrust and flaps settings, climb rate, and descent angle.

Before calculating the noise data, it is crucial to choose reasonable numbers and positions of locations for which the noise data and the population data will be obtained. Since the airport is surrounded by populated areas, 23 different municipalities are considered to be affected by aircraft noise, viz. 17 municipalities of Belgrade and 5 municipalities of Stara Pazova, Indija, Irig, Ruma, Pećinci and Pančevo. In this case study, the SEL was calculated for 306 locations with each location representing one settlement in these 23 municipalities around the airport. [Table 2](#) shows the population data and the number of settlements/locations for each

**Table 1**  
Flight statistics and aircraft classifications.

Aircraft type	Assigned AzB class	INM airplane code	Departure			Arrival		
			Day	Evening	Night	Day	Evening	Night
Boeing 737-300	S 5.2	737300	6	1	1	5	2	2
Boeing 737-800	S 5.2	737800	2	2	1	3	0	1
Airbus A319	S 5.2	A319-131	18	5	5	19	2	8
Airbus A320	S 5.2	A320-211	15	3	3	14	3	5
Airbus A330-200	S 6.1	A330-301	1	1	0	0	1	1
Beechcraft King Air	P 1.4	CNA441	1	0	1	1	0	0
Cessna 560 XL	S 5.1	CNA560XL	3	0	1	2	1	1
Swearingen Metroliner	P 2.1	DHC6	3	1	0	3	0	1
ATR 42	P 2.1	DHC8	1	3	0	3	1	0
ATR 72	P 2.1	DO328	14	6	5	12	6	8
Embraer 190	S 5.2	EMB190	5	1	0	6	0	0
		Total	69	23	17	68	16	27

**Table 2**  
Population data and the number of settlements for municipalities around the airport.

Municipality	Number of settlements	Census population (2011)	Period				
			1	2	3	4	5
Barajevo	14	27,110	25,050	24,422	26,020	25,559	26,497
Čukarica	9	181,231	166,349	159,679	172,064	168,848	176,209
Grocka	15	83,907	76,011	73,679	78,942	78,573	81,748
Lazarevac	34	58,622	60,304	62,146	59,584	60,969	59,545
Mladenovac	22	53,096	51,297	51,024	52,022	52,108	52,752
Novi Beograd	16	214,506	222,238	226,900	218,799	222,321	217,613
Obrenovac	29	72,524	69,586	68,859	70,803	70,635	71,802
Palilula	13	173,521	176,540	174,006	175,343	172,061	172,950
Rakovica	13	108,641	96,108	90,980	100,827	98,808	104,699
Savski venac	1	39,122	75,290	88,058	61,474	65,749	49,778
Sopot	17	20,367	19,270	19,054	19,930	19,711	20,122
Stari grad	1	48,450	88,436	96,797	73,554	71,702	57,748
Surčin	7	43,819	41,546	41,638	42,342	43,130	43,544
Voždovac	24	158,213	160,242	155,406	159,370	153,766	156,380
Vračar	1	56,333	64,953	66,643	61,698	61,250	58,312
Zemun	5	168,170	170,663	169,291	169,851	167,703	167,986
Zvezdara	11	151,808	147,073	140,364	148,991	143,108	148,303
Pančevo	10	123,414	119,466	119,439	121,154	121,946	122,873
Indjija	11	47,433	45,032	44,657	46,029	46,160	46,930
Irig	12	10,866	10,336	10,328	10,533	10,669	10,786
Pećinci	15	19,720	18,965	19,155	19,447	19,579	19,670
Ruma	17	54,339	51,925	52,171	52,991	53,643	54,060
Stara Pazova	9	65,792	61,430	61,113	63,249	63,797	65,018
Total	306	1,981,004	2,018,110	2,015,809	2,005,017	1,991,795	1,985,325
People living in other municipalities, but commuting to these 23 municipalities or vice versa		88,942	51,836	54,137	64,929	78,151	84,621

municipality and for each period of time in accordance with human mobility patterns and 2011 census data (Statistical Office of the Republic of Serbia, 2013).

In order to take into account human mobility patterns and to simulate working shifts of employees, pupils and students, the day has been divided into five periods, as shown in Fig. 3. The periods are defined in such a way that the number of people at each location remains constant for the duration of the period. This data was made available by the Statistical Office of the Republic of Serbia.

The definition provided in the 2011 Census methodology describes daily migrants as persons who work or go to school/university outside the place of their usual residence, but they return on a daily basis or several times a week (Statistical Office of the Republic of Serbia, 2013). The daily mobility data is the key to calculate the total daily inflow and outflow of inhabitants for each settlement. This was used as the basis to calculate groups of people commuting to the same location at the same period of time during the day.

Having in mind that human mobility patterns are obtained for the whole day only, and not for separate periods of the day, some assumptions are needed in order to assess how many people would actually be present at each location during a defined period of time. Therefore, it has been assumed that 50% of employees work first shift, 30% work second shift, and 20% work night shift. Out of

Group Number	Period → Time of the day →	Period 1 08:00 - 14:00	Period 2 14:00 - 16:00	Period 3 16:00 - 20:00	Period 4 20:00 - 22:00	Period 5 22:00 - 08:00
1	Employees 1 <sup>st</sup> shift	Working location		Residential location		
2	Employees 2 <sup>nd</sup> shift	Residential location	Working location			Residential location
3	Employees 3 <sup>rd</sup> shift	Residential location		Working location		
4	Students 1 <sup>st</sup> shift	Studying location	Residential location			
5	Students 2 <sup>nd</sup> shift	Residential location	Studying location		Residential location	
6	Staying at home	Residential location				
Number of aircraft movements		76	14	51	13	66

Fig. 3. Groups of people and periods based on working shifts of employees, pupils and students.

4

the total pupils and students going to schools or universities, 60% follows the first shift, and 40% the second. Hereby, 76,423 groups of people were observed, and the population data calculated based on the census data and the daily mobility data show a difference in the number of people at each location in the pre-defined periods. The total number of residents living within these 306 locations based on the census data was 1,981,004. This research also includes the mobility of people living outside the 23 municipalities mentioned above, but working or studying in some of these municipalities, and vice versa.

By comparing the total number of people for different periods with the census population data, it can be seen that the highest absolute difference is 2% for Period 1. The reason behind is the fact that this study takes into account only the daily mobility of employees going to work and pupils and students going to schools and universities.

## 5. Results and discussions

As mentioned in Section 1, although the influence of the mobility data on evaluation of noise effects has been well recognized in previous transportation studies (Kaddoura et al., 2017, 2016), the investigation of mobility data influence in air traffic models is still limited. Therefore, before executing the optimization problem, the influence of the mobility patterns on evaluation of aircraft noise effects is assessed first. Afterwards, the optimal solutions based on the mobility data and derived from the proposed model are obtained and analyzed.

### 5.1. Influence of daily population mobility on evaluation of aircraft noise effects

In order to assess the influence of census data and mobility data on evaluation of aircraft noise effects, the real air traffic operations on 16 September 2016 are used, which is hereinafter referred to as the reference case. The  $L_{den}$  noise contours caused by all the operations are shown in Fig. 4, where the NPA at each (residential) location is also indicated. At first glance, it can be observed that there is a significant difference between the census data and the mobility data among noise-affected locations. In fact, with the census data (depicted by triangles), only people at locations enclosed in the noise contours are affected. Meanwhile, when using the mobility data (depicted by circles), the noise effects occur not only at these locations, but also at locations outside of the noise contours. This can be explained by considering that people who live outside the area affected by aircraft noise may work or study within these areas at some time during the day, and are therefore affected by aircraft noise.

For a specific evaluation, the NPA at the locations covered by  $L_{den}$  noise contours  $\geq 37$  dB ( $L_{den} \geq 37$  dB), as shown in Fig. 4, is estimated for both datasets and presented in Table 3. As seen from the table, the total NPA at these locations for the census data is 57,519, which is by 2.18% relatively higher (by 1228 in absolute numbers) than the NPA based on the mobility data. The same situation is observed for the NPHA, where the difference is even higher, 5.24%. These observations show that even though people live inside the noise contours, some of them are still not annoyed by aircraft noise due to their mobility for working or studying purposes to locations far away from the airport.

Furthermore, in order to see how many people live outside the noise contours, but still experience noise impact, the NPA based on the mobility data at all locations is evaluated and presented in Table 4. The table shows that the total NPA is 60,265, more than 7.05% of whom live outside the  $L_{den} \geq 37$  dB. The same trend is observed for the total NPHA as well. This is easily explained when considering that people who live farther away from the airport may still work or study in the areas affected by aircraft noise.

Apart from the observations in the above tables, it is also noted that although the absolute difference of the total NPA between the census data and the mobility data is relatively small, the difference in the NPA at each location is rather significant, as shown in Fig. 5. Summarizing the relative difference at all locations compared to the NPA obtained by the census data can add up to 52.9%. This number indicates that there is a significant change in the number of people at each location during the day. For example, for location 220, the NPA based on the census data is 0, while the NPA based on the mobility data is 307; and for location 15, the NPA based on the census data is 8286, whereas the NPA based on the mobility data is 7936.

For a better illustration of the daily mobility of population outside and inside the noise contours, movements at locations 15 and 220 are highlighted in Fig. 6 and Fig. 7, respectively. Fig. 6 shows that location 15 is located nearby the airport and enclosed in the

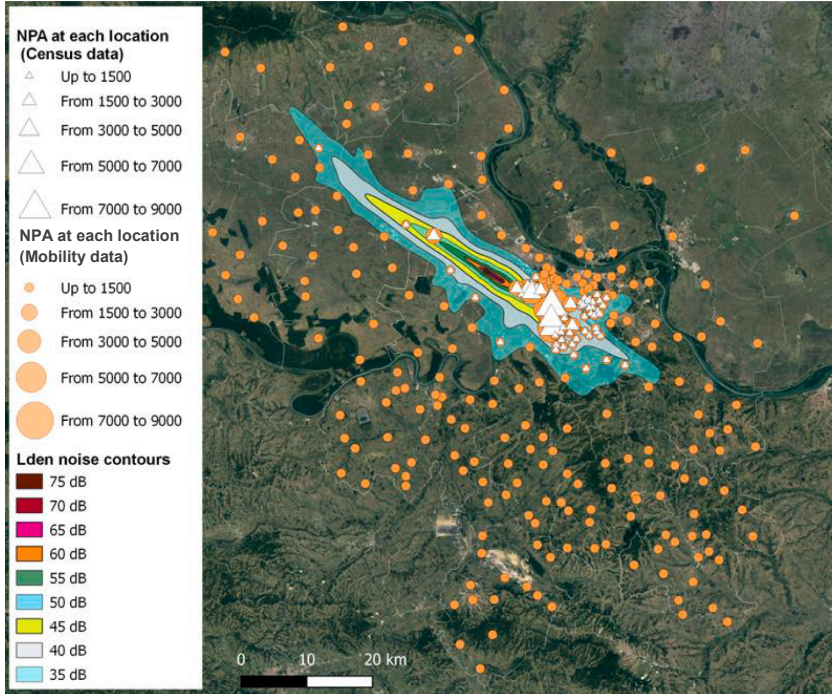


Fig. 4. Illustration of people at locations affected by noise with  $L_{den} \geq 37$  dB. (All the figures with the Google earth background are created using the open source software, QGIS (<https://qgis.org/en/site/>).

Table 3  
Number of people affected by noise at locations enclosed in  $L_{den} \geq 37$  dB.

Criterion	Census data	Mobility data	Absolute difference	Relative difference
NPA	57,519	56,291	1,228	2.18%
NPHA	10,583	10,056	527	5.24%

Table 4  
Number of people affected by noise based on mobility data ( $L_{den} \geq 37$  dB).

Criterion	All locations	Only locations enclosed in $L_{den} \geq 37$ dB	Absolute difference	Relative difference
NPA	60,265	56,291	3,974	7.05%
NPHA	10,499	10,056	443	4.40%

noise contours of  $L_{den} > 45$  dB. However, some of the people living at this location may experience less noise than others, as they work or study outside the area. Therefore, the total NPA calculated using the mobility data at this location is less than the NPA obtained by the census data. In contrast, an opposite situation can be observed for location 220 in Fig. 7. At this location, people who live outside the noise contours work or study at locations close to the airport, and hence they can experience significant noise impact. This explains the significant difference in the NPA at each location. In addition, the combined mobility at locations 15 and 220 explains why the difference in the total NPA between the census data and mobility data is relatively small.

To enable further examination of the influence that mobility data has on the number of people affected by aircraft noise during the night, the sleep disturbance criteria<sup>6</sup> based on  $L_{night}$  recommended by WHO (2009) are also evaluated. These evaluations are provided in Table 5 and Table 6. As can be seen in the tables, the results obtained by using  $L_{night}$  also have the same trend as those

<sup>6</sup> %SD =  $13.714 - 0.807 L_{night} + 0.01555 (L_{night})^2$ , and %HSD =  $18.147 - 0.956 L_{night} + 0.01482 (L_{night})^2$ , where %SD and %HSD are the percentages of people whose sleep is disturbed and highly disturbed, respectively (WHO, 2009).

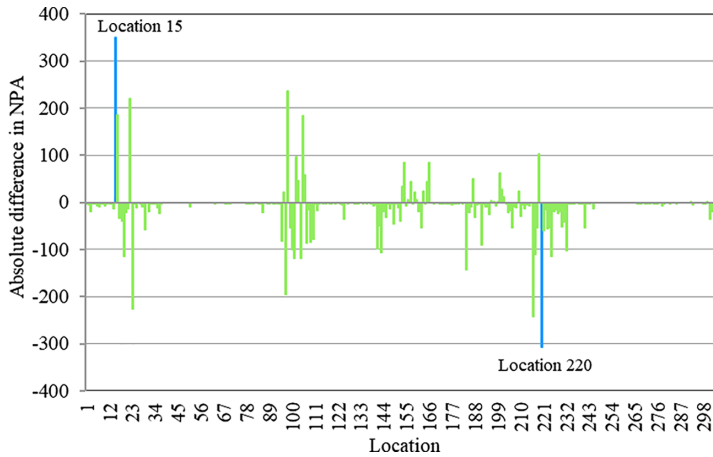


Fig. 5. Difference in the NPA between census data and daily mobility data at all locations.

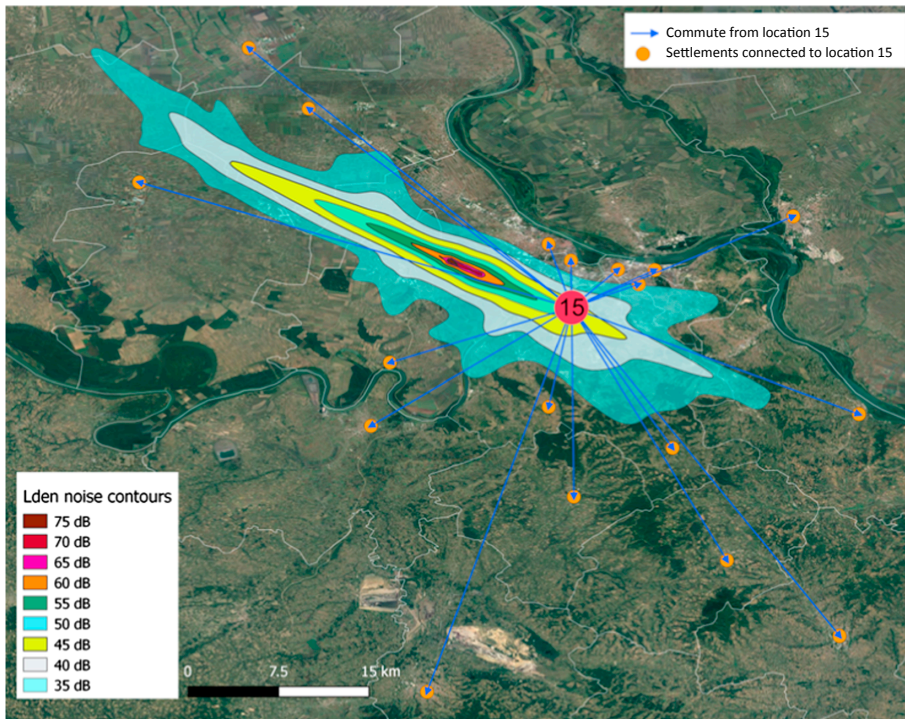


Fig. 6. Illustration of population at location 15 commuting outside  $L_{den} \geq 37$  dB.

obtained by using  $L_{den}$  even though during the night only the mobility of employees is considered. The explanation for this is that, according to the mobility data, groups of employees account for a significant portion in the mobility of the entire population, which is approximately twice as high as the groups of students. In addition, the noise impact during the night is more sensitive compared to the noise impact during the day and evening, and hence the percentage of disturbed people in each group is higher. Consequently, the mobility data also has a noticeable impact on the estimation of aircraft noise effects during the night.

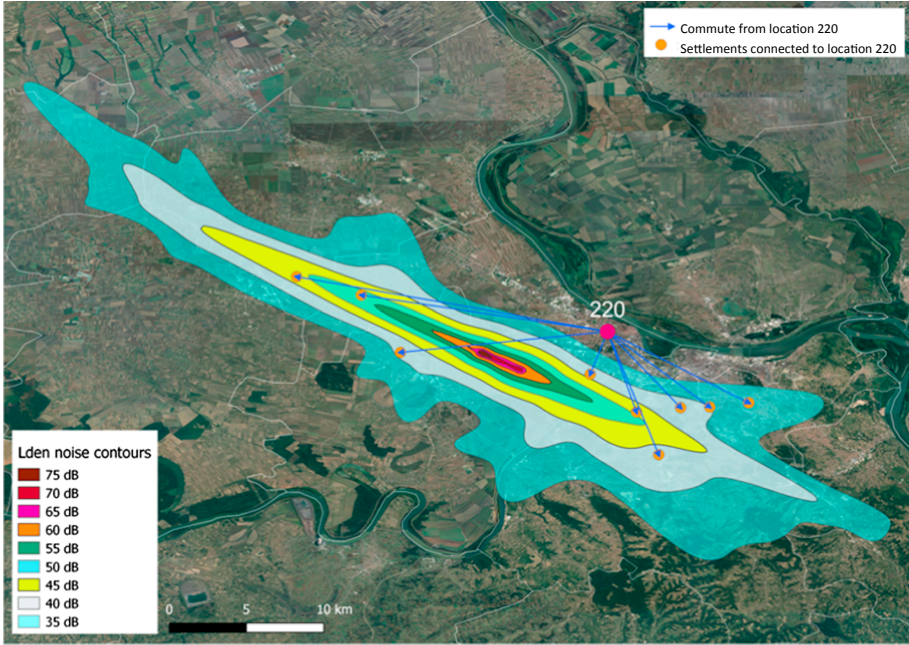


Fig. 7. Illustration of population at location 220 commuting inside  $L_{den} \geq 37$ .

**Table 5**  
Number of people affected by noise at locations enclosed in  $L_{night} \geq 30$  dB.

Criterion	Census data	Mobility data	Absolute difference	Relative difference
NSD	33,750	32,601	1149	3.52%
NHSD	21,103	20,381	722	3.54%

**Table 6**  
Number of people affected by noise based on mobility data ( $L_{night} > 30$  dB).

Criterion	All locations	Only locations enclosed in $L_{night} > 30$ dB	Absolute difference	Relative difference
NSD	33,809	32,601	1208	3.71%
NHSD	21,138	20,381	757	3.71%

Based on the above considerations, it can be concluded that evaluation of aircraft noise effects is significantly dependent on population data (i.e., the census data and the mobility data). Although the difference in the total NPA between these data is small, the difference in the NPA at each individual location is considerable as a result of the daily mobility. From the perspective of air traffic assignment, variations of population at each location may lead to different optimal assignments compared to the case when solely census data are used. This is because, in order to reduce the noise impact, optimal allocation of aircraft should avoid locations at which most people are present during the day, rather than just their home addresses. Consequently, developing a methodology that is capable of creating optimal air traffic assignments based on mobility data is important and necessary. In the following section, therefore, the methodology presented in the previous sections is applied to solve the optimization problem of the air traffic assignment. The obtained results are analyzed and compared to those obtained by the reference case. Since the main aim of the research is to find optimal air traffic assignments for an entire day, only the noise criteria based on  $L_{den}$  are employed for the optimization problems and further analyses as well.

5.2. Air traffic assignment based on daily population mobility

The NSGA-II algorithm with a population size of 70 and a maximum generation (Gen.) of 1500 is applied to solve the multi-objective optimization problem stated in Section 2. The method is set with an intermediate crossover rate of 1.5 and the Gaussian

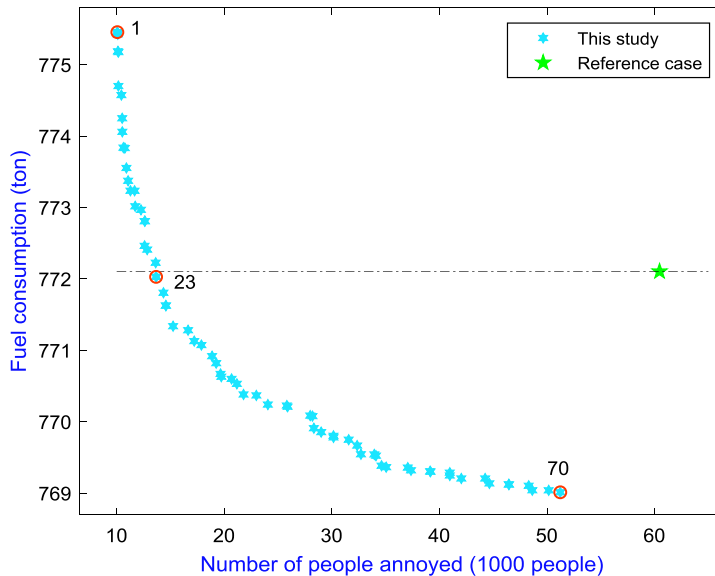


Fig. 8. Illustration of optimal solutions obtained by proposed method and reference case.

mutation technique with a scale of 0.8 and a shrink of 0.1. All the simulations are run on an Intel Core i5, 8 GB RAM desktop and MATLAB 2016b.

Fig. 8 presents the optimal solutions obtained in comparison with that of the reference case. Fig. 8 shows that the proposed approach generates solutions which are much better than that of the reference case. When a population size of 70 is used, the Pareto front contains 70 distinct non-dominated solutions, and all of them dominate the reference case. Generally, all solutions will have the same weight of advantages, which spread from noise to fuel preference. Basically, decision makers can, therefore, choose any of the solutions based on their specific needs. However, to arrive at acceptable trade-off solutions from all of them, systematic analyses which are not considered in this study are needed. Therefore, only some representative solutions are chosen for further analyses later on.

In terms of computational cost, Fig. 9 shows the convergence history of results after specific generations with a particular amount of computational time. As seen from Fig. 9, the results seem to converge faster after 800 generations, and there are no significant improvements after 1200 generations. The computational cost (CPU time) is also recorded after each generation. To reach the last generation, the method spends almost 24 h, mostly on calculating Eq. (3) for all 76,423 groups of people. Although the computation time is high, the algorithm is still applicable as the flight schedule can be obtained some days in advance. Moreover, with the development of powerful computers such as cluster and cloud computing, this issue can be addressed relatively easily.

For a better overview on the optimal solutions, three distinct solutions are selected, viz. 1, 23 and 70 as marked in Fig. 8, for further examinations. For these solutions, solutions 1 and 70 represent the minimum noise and fuel solutions, respectively, while solution 23 shows the same fuel consumption as the reference case, but has significantly better noise performance. Table 7 presents the objective values of the optimization problem (i.e., the total NPA and fuel consumption) and other concerned metrics obtained by the representative solutions and the reference case. At first glance, the table indicates that all the solutions have better NPA and NPHA in comparison with the reference case. Particularly, the total NPA of solutions 1, 23 and 70 are, respectively, 10,061, 13,663 and 51,234, and hence there is a reduction of 83.31%, 77.33% and 14.99%, respectively, compared to that of the reference case (with 60,265 people annoyed). Similar relative amounts of the reduction are observed for the NPHA as well.

Regarding the total fuel consumption and route length, due to focusing on the noise preference and hence assigning aircraft to routes which are farther away from the populated regions, solution 1 generates more fuel consumption than the reference case with an increase of 0.43%. However, even though it results in a significant reduction of the noise impact, solution 23 still keeps the total fuel consumption slightly lower than that of the reference case, whilst with a still smaller amount of noise impact reduction, solution 70 provides the best option for fuel preference. The same trend is also recognized for the total route length, except for solution 23. For this solution, although the total fuel burn is slightly less than that of the reference case, the total route length is still higher. This can

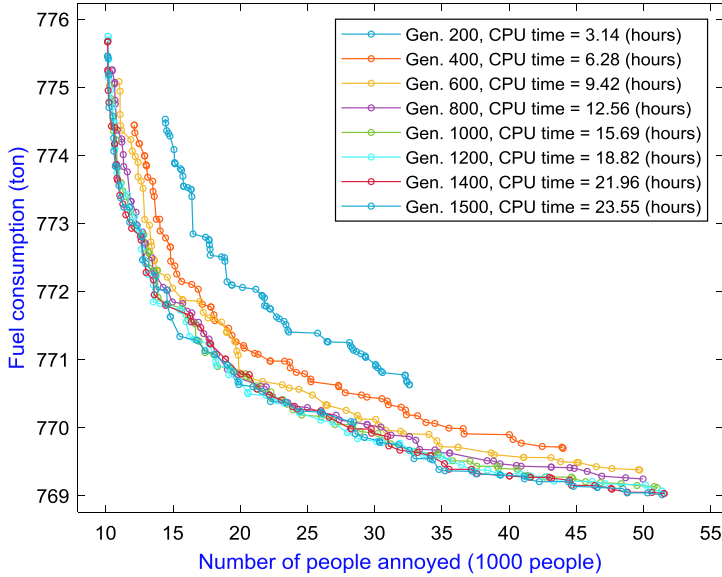


Fig. 9. Convergence history of optimal solutions.

Table 7  
Comparison of different metrics of representative solutions and reference case.

Method	Case number	NPA	NPHA	Fuel consumption (kg)	Route length (NM)
This study	Solution 1	10,061	2059	775,457	124,771
	Absolute reduction	-50,204*	-8440	+3351	+935
	% reduction	-83.31	-80.39	+0.43	+0.76
	Solution 23	13,663	2308	772,030	124,139
	Absolute reduction	-46,602	-8191	-76	+303
	% reduction	-77.33	-78.02	-0.01	+0.24
	Solution 70	51,234	8892	769,013	123,391
	Absolute reduction	-9031	-1607	-3093	-445
Reference case	% reduction	-14.99	-15.31	-0.40	-0.36
		60,265	10,499	772,106	123,836

\* The signs “+” and “-” indicate increase and reduction compared to reference case, respectively.

Table 8  
Comparison of the number of people enclosed in specific  $L_{den}$  noise contours.

Method		Noise band						
		< 40	[40–45]	[45–50]	[50–55]	[55–60]	[60–65]	≥ 65
This study	Solution 1	1,987,474	59,075	5326	10,860	7211	0	0
	Solution 23	1,970,373	72,420	7897	8891	10,365	0	0
	Solution 70	1,654,134	241,767	125,281	41,829	3684	3251	0
Reference case		1,595,717	253,308	156,340	57,587	1803	5191	0

**Table 9**  
Comparison of optimal route assignments of three representative solutions.

Route number	Number of operation			Route number (continued)	Number of operation		
	Solution 1	Solution 23	Solution 70		Solution 1	Solution 23	Solution 70
1	0	3	7	15	4	10	3
2	0	1	3	16	10	7	1
3	0	0	2	17	8	2	5
4	0	2	19	18	9	7	7
5	31	24	11	19	12	12	10
6	0	1	0	20	24	26	22
7	3	11	9	21	2	7	9
8	20	13	12	22	16	8	6
9	19	15	15	23	0	1	9
10	23	19	18	24	0	2	1
11	0	6	7	25	0	0	0
12	10	6	4	26	0	1	4
13	3	8	2	27	0	5	15
14	26	23	19				

4

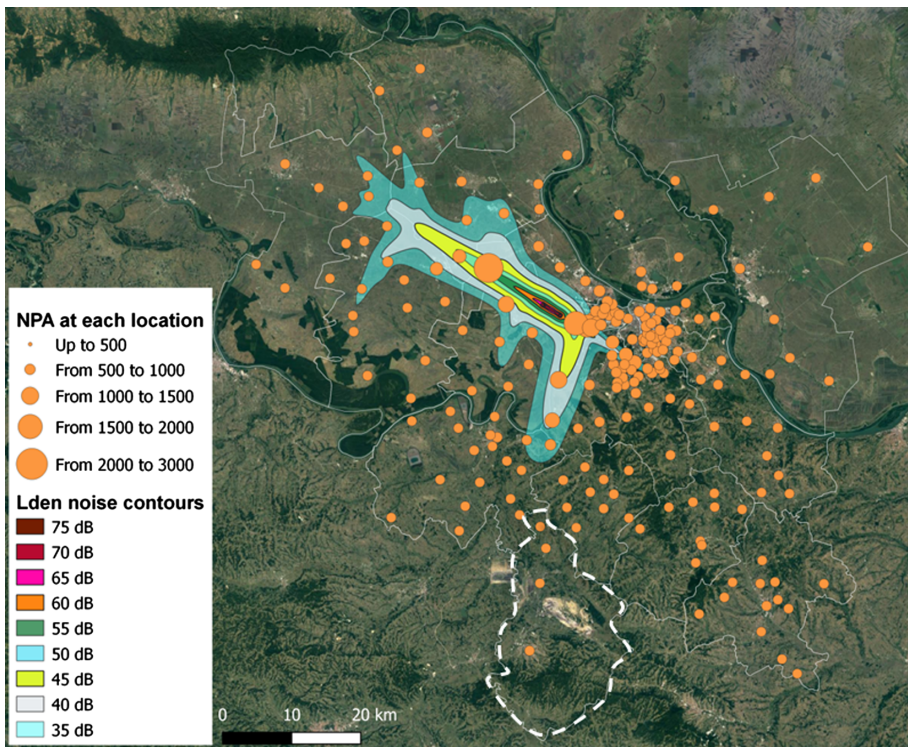


Fig. 10. Illustration of NPA at each location (solution 1).

be explained by considering the distribution of aircraft types. Even though the total route length has increased, the route length of aircraft with higher fuel burn has reduced, leading to an overall reduction in fuel consumption.

It is also worth noting that the reason for the relatively small difference in fuel burn between the solutions and the reference case is due to the fact that departure and arrival operations account only for a small part of the flight. Nevertheless, there is an identifiable effect when considering the absolute values. Specifically, for solution 70, 3093 kg can save airline companies around \$ 2327 per day

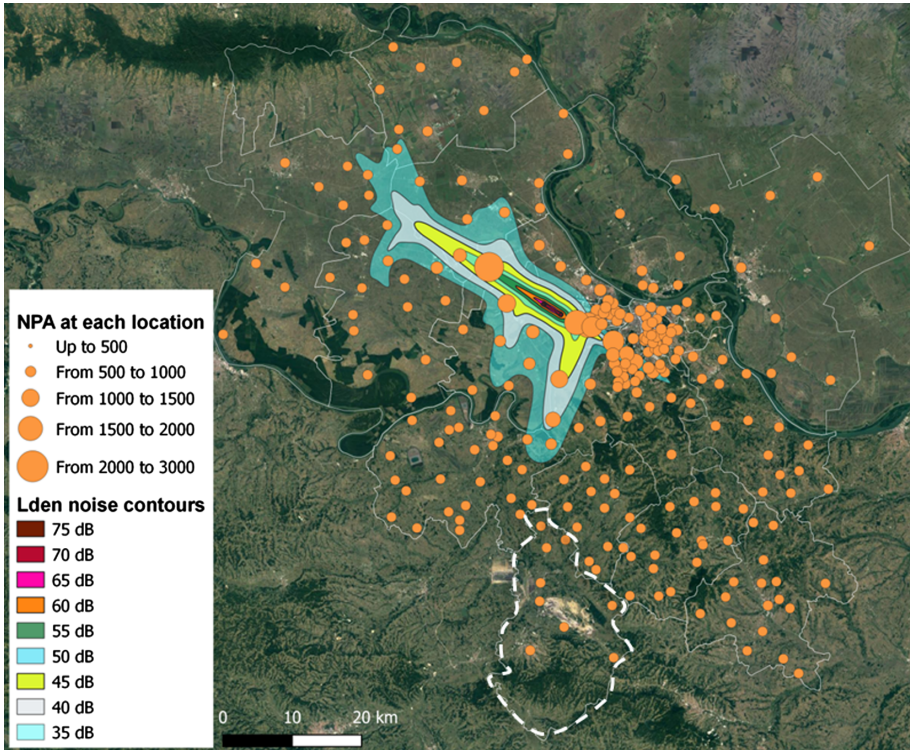


Fig. 11. Illustration of NPA at each location (solution 23).

(with an average cost of jet-A1 fuel of \$ 86.1 per barrel<sup>7</sup> in 2018), and generate roughly 9.7 ton of CO<sub>2</sub><sup>8</sup> emission less.

Besides the evaluation of the criteria as given in Table 7, the number of people enclosed in specific  $L_{den}$  noise contours is also evaluated and provided in Table 8. A comparison of the representative solutions and the reference case shows that the number of people enclosed in the higher noise contours reduces for solutions with more emphasis on noise. This behavior is expected, and it is comparable with the trends of the NPA and the NPHA in Table 7. According to the formula in Eq. (2), it is obvious that the higher the value  $L_{den}$  each group of people is subjected to, the greater the number of people annoyed that group has.

In order to perceive the difference between the optimal solutions in terms of air traffic assignments as well as the noise contours and the NPA at each location, the features of solutions 1, 23 and 70 are further analyzed. The optimal assignment of these solutions is shown in Table 9, which provides the number of aircraft assigned to each route, while their  $L_{den}$  noise contours and the NPA at each location are depicted in Fig. 10, Fig. 11 and Fig. 12, respectively.

Table 9 shows that the distribution of aircraft over the routes between the solutions is rather different. For example, for route 5, solution 1 has 31 operations, and solution 23 has 24 operations, while solution 70 has only 11 operations. On the other hand, for route 27, there is no operation from solution 1, but 5 operations from solution 23, and 15 operations from solution 70. More specifically, solution 1 tends to send more aircraft to route 5 as it is positioned farther away from the populated regions. However, this selection will result in longer routes for aircraft that have their final destination in a different direction, and it will consequently cost more fuel. Meanwhile, solution 70 tends to directly send aircraft along routes in the direction of their final destinations disregarding populated areas, and hence leading to an increase in the NPA. Solution 23 tends to balance between noise and fuel concerns, and hence its distribution falls in the middle of those of solutions 1 and 70.

The above examinations are even more apparent when looking at Fig. 10, Fig. 11 and Fig. 12. In these figures, the variation in the NPA between the solutions can be observed in the region that is highlighted by the white dotted line. In fact, for solution 1, there are only 3 locations which have people affected by noise due to their daily mobility, while 8 locations are recognized in solution 23, and

<sup>7</sup> <https://www.iata.org/publications/economics/fuel-monitor/Pages/index.aspx> (assessed 19 January 2019)

<sup>8</sup> <https://www.icao.int/environmental-protection/Carbonoffset/Pages/default.aspx> (assessed 19 January 2019)

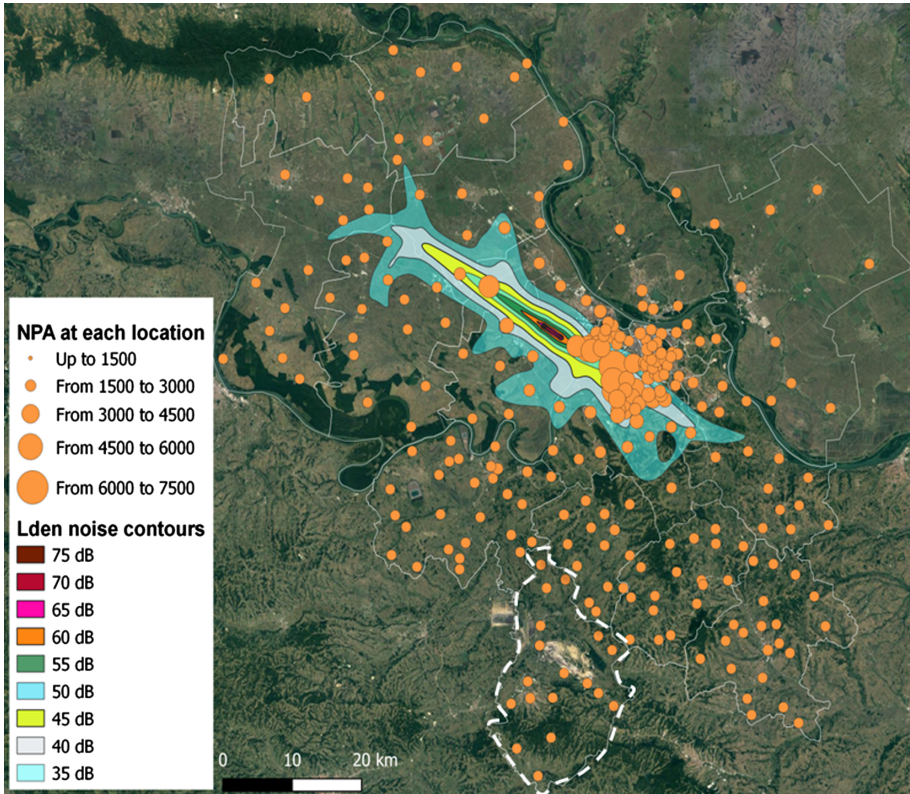


Fig. 12. Illustration of NPA at each location (solution 70).

up to 18 locations in solution 70. Moreover, upon a closer look at the legends on the figures, it is also noted that the scale of the NPA at each location of these solutions is rather different. A further distinction of this comparison can be clearly recognized in Fig. 13. It can be seen from the figure that the difference of the NPA occurs not only at the highlighted region, but also at other locations.

### 5.3. Evaluation of optimal assignments based on census data and mobility data

As noted earlier at the end of Section 5.1, the variation of population at each location between the census data and the mobility data during the day may lead to a change in the optimal assignments obtained by these data as well. Therefore, to estimate this concern for the applied case study, the air traffic assignment problem based on the census data is also performed. The obtained results are then compared with those based on the mobility data.

Fig. 14 and Fig. 15 compare the objective functions (i.e., the total NPA and fuel consumption) for both datasets. In Fig. 14, the comparison is made based on the optimal assignments using the census data, whereas the comparison in Fig. 15 is made based on the optimal assignments using the mobility data. Both figures indicate that there is a small difference in the NPA between solutions evaluated based on the difference of datasets. Note that since the assignments for each comparison in each figure are the same, consequently the fuel consumption will be the same regardless of the data used. The variation increases from solution 1 to solution 70. Therefore, there is a difference in their optimal assignments. The variation of the optimal assignments between both sets of solutions can be readily explained. As mentioned earlier in Section 5.1, due to the daily mobility, the population at each location changes at different times of the day. Therefore, to reduce the noise impact, the optimal assignments should be changed as well. It

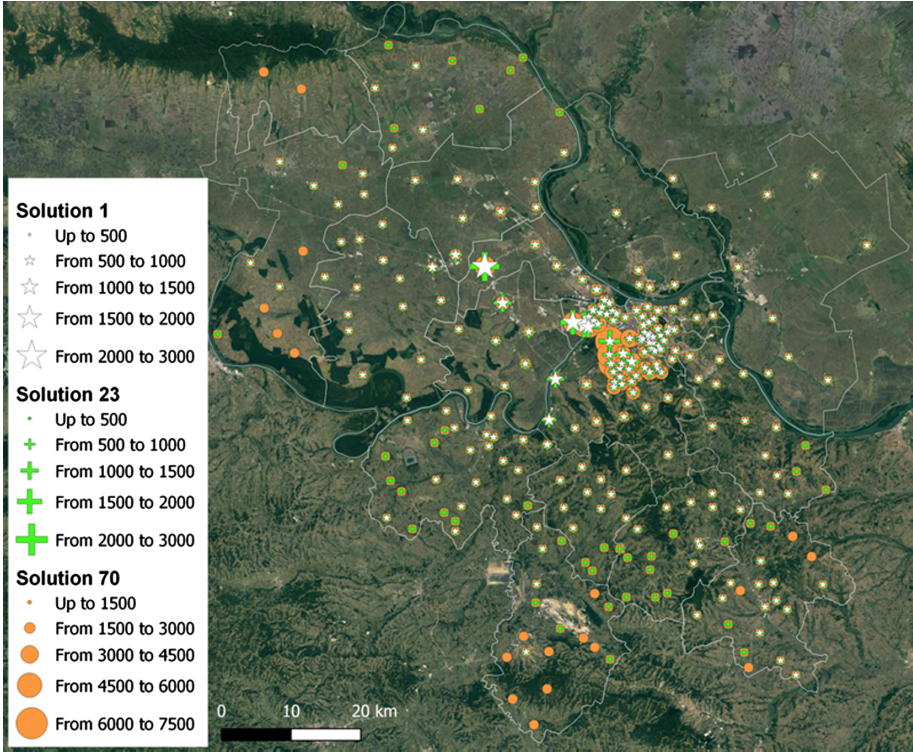


Fig. 13. Comparison of NPA between solutions 1, 23 and 70 at each location.

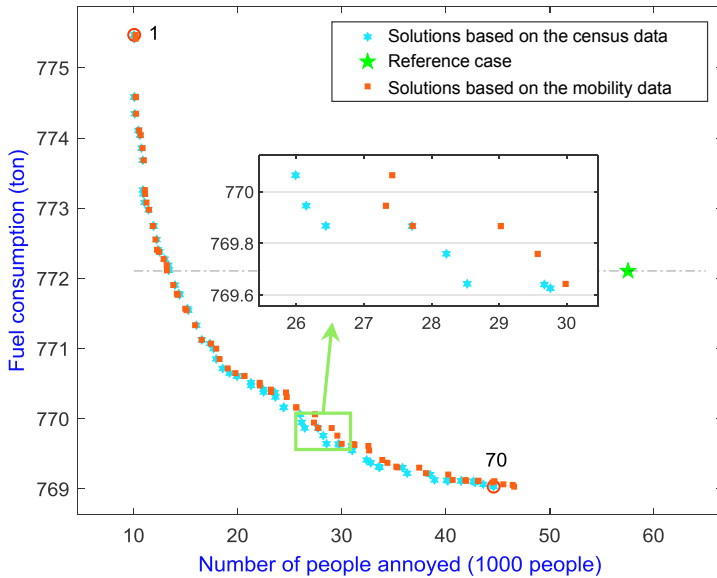


Fig. 14. Comparison based on the optimal assignments using the census data.

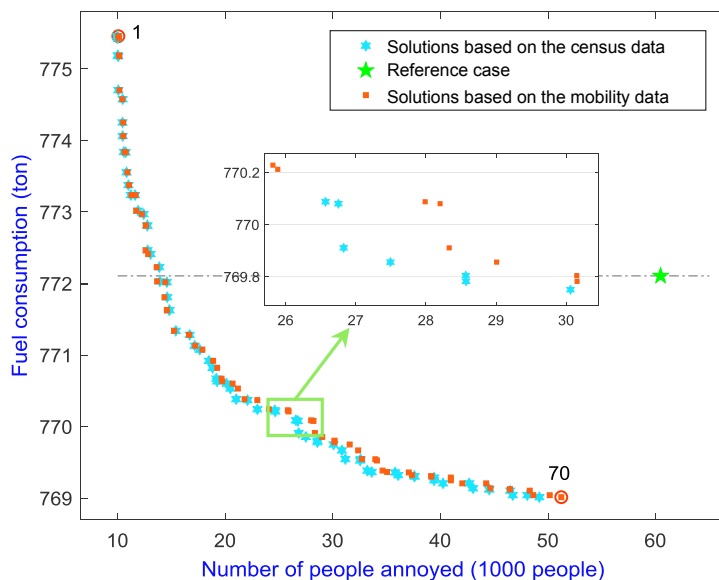


Fig. 15. Comparison based on the optimal assignments using the mobility data.

Table 10

Comparison of the optimal route assignments of solutions 1 and 70 based on both data.

Route number	Number of operation				Route number (continued)	Number of operation			
	Solution 1		Solution 70			Solution 1		Solution 70	
	Census data	Mobility data	Census data	Mobility data		Census data	Mobility data	Census data	Mobility data
1	0	0	6	7	15	5	4	0	3
2	0	0	5	3	16	14	10	2	1
3	0	0	1	2	17	5	8	2	5
4	0	0	16	19	18	10	9	10	7
5	28	31	12	11	19	10	12	10	10
6	0	0	0	0	20	21	24	21	22
7	6	3	8	9	21	3	2	7	9
8	17	20	12	12	22	15	16	9	6
9	25	19	14	15	23	0	0	6	9
10	22	23	17	18	24	0	0	3	1
11	0	0	9	7	25	0	0	0	0
12	8	10	7	4	26	0	0	3	4
13	3	3	2	2	27	0	0	16	15
14	28	26	22	19					

should also be noted that although the change in the total NPA between the census data and the mobility data is relatively small, the change of the NPA at each location can be rather large, which has been discussed earlier in Section 5 as well.

In order to further analyze the difference above, the optimal assignments of two representative solutions, viz. 1 and 70 obtained by using both datasets are extracted and presented in Table 10. This table shows that the optimal assignments are slightly different. For example, for route 9 of solution 1, the difference in the number of operations is 6, whilst for route 15 of solution 70 it is 3. It should be also noted that although the number of operations on each route for both datasets used is more or less the same, the distribution of aircraft types also contributes to the variation in the NPA.

To get a better insight into the effect of the change in the optimal assignments, the resulting  $L_{den}$  noise contours for these assignments are illustrated in Fig. 16 and Fig. 17, for solutions 1 and 70, respectively. As seen in the figures, the noise contours are rather different, especially for solution 70.

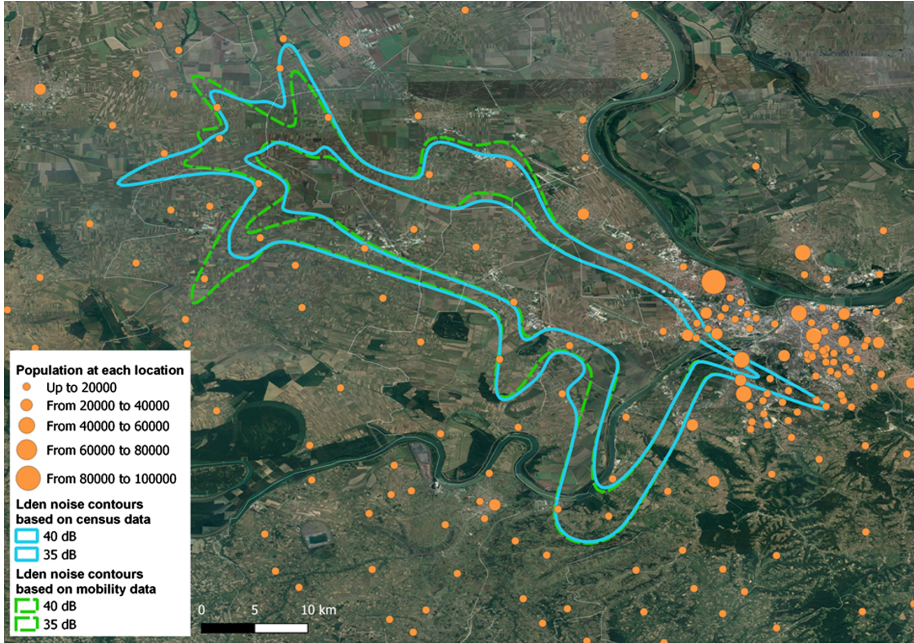


Fig. 16. Comparison of  $L_{den}$  noise contours based on census data and on daily mobility data (solution 1).

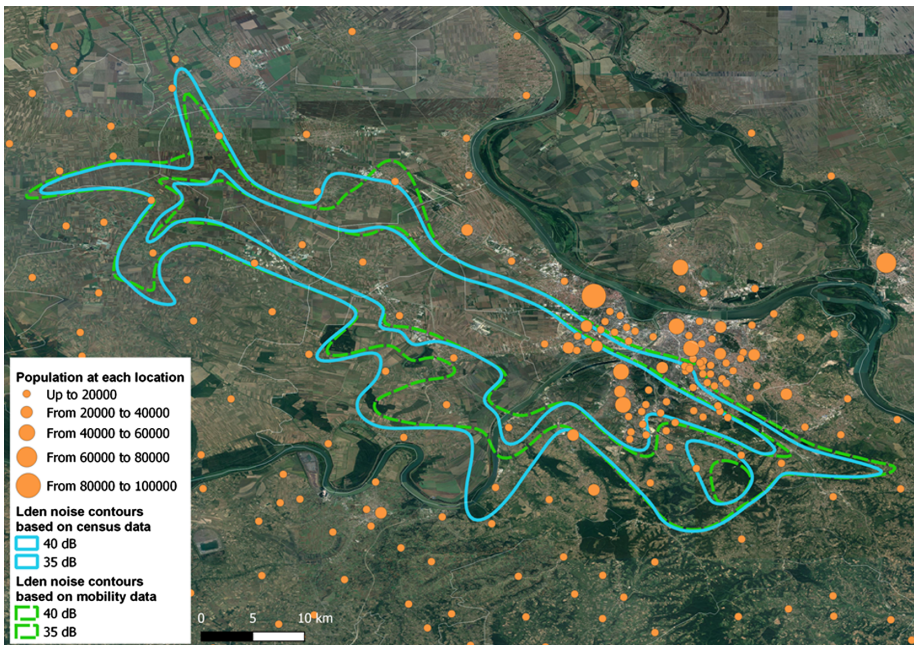


Fig. 17. Comparison of  $L_{den}$  noise contours based on census data and on daily mobility data (solution 70).

## 6. Conclusions and future work

This paper introduces a new air traffic assignment model which is capable of taking the daily mobility of a city's population into account, in addition to having a acceptable trade-off between conflicting objectives (i.e., the NPA and fuel consumption). Furthermore, substantial efforts have been invested to investigate the influence of the data used on the evaluation of aircraft noise effects. Then, the optimal solutions of the air traffic assignment based on the mobility data are obtained and compared with that of the reference case and those based on the census data. The following conclusions can be drawn from this work:

- (1) The evaluation of aircraft noise impact is influenced by the daily population mobility data used. Specifically, when the census data are used, only people who live inside the noise contours get annoyed, whereas it has been found that people living outside the noise contours could be annoyed when the mobility data are used. Moreover, not all of the annoyed people suggested from the census data will actually be annoyed if their daily mobility is taken into account. Although the total NPA obtained by using either census data or mobility data is very similar, the NPA at each location is significantly different.
- (2) Compared to the reference case herein, the proposed methodology can generate solutions that are much improved in terms of both the total NPA and fuel consumption. Even with a small change in the total fuel consumption, the method can still offer a solution which can reduce the total NPA up to 77%. Furthermore, the proposed approach also provides a wide range of solutions with different benefits to either noise or fuel burn, and these solutions can serve as a valuable input for authorities and policymakers in their decision making.
- (3) The optimal assignments obtained by both datasets are different since there is a significant difference in the number of people at each location during the day. The evaluation thereof also indicates that the difference in the optimal assignments is rather dependent on the case study under consideration, and on whether the variation of population at each location is significant or not, relative also to the population distribution and airport layout.

Some inherent limitations of the work which have not yet been considered in this study are also worth mentioning. First, the mobility data are considered only for three distinct groups of people, including students and pupils, employees and people staying at home. This assumption may lead to variations in optimal assignments as a result of the change of population at each location during the day if other types of mobility are also considered. Further research should also investigate to a larger extent the assumption regarding the allocation of employees, students and pupils to shifts. Second, for the air traffic assignment model, only the feasible options for each operation are considered, while the runway and airspace capacity (e.g., aircraft sequencing), which can lead to delay of flights, are not yet considered. This model could be regarded as pre-tactical and intended to be used for planning purposes since it takes into account forecasted data for the whole day and it is not resistant to any disruption in the pre-defined timetable. In order to render it suitable for tactical use in real-time operations, changes in runway in use, aircraft changes as well as delays should be included in the model. Therefore, these issues will be dealt with in further work. Furthermore, by using the mobility data, changes in population at sensitive regions such as schools and hospitals, can be recognized. These more detailed mobility data can help develop more realistic, applied solutions in terms of applying more complex fair weightings for each different category.

## Acknowledgments

This research is supported by the Ministry of Science and Technological Development of the Republic of Serbia and represents a part of the project named “A support to sustainable development of the Republic of Serbia's air transport system” (TR36033). The authors would like to express their gratitude to the Statistical Office of the Republic of Serbia for providing the data regarding daily mobility. The authors would also like to thank the editor and anonymous reviewers for their constructive, helpful and valuable comments and suggestions.

## Appendix A. Supplementary material

Supplementary data to this article can be found online at <https://doi.org/10.1016/j.trd.2019.04.007>.

## References

- Abouei, M., Taghi, M., 2018. Multi-objective optimization of reliability – redundancy allocation problem with cold-standby strategy using NSGA-II. *Reliab. Eng. Syst. Saf.* 172, 225–238. <https://doi.org/10.1016/j.res.2017.12.019>.
- Alikar, N., Mousavi, S.M., Raja Ghazilla, R.A., Tavana, M., Olugu, E.U., 2017. Application of the NSGA-II algorithm to a multi-period inventory-redundancy allocation problem in a series-parallel system. *Reliab. Eng. Syst. Safety* 160, 1–10. <https://doi.org/10.1016/j.res.2016.10.023>.
- AzB-08, 2008. Anleitung zur Berechnung von Lärmschutzbereichen nach dem Gesetz zum Schutz gegen Fluglärm vom 19. November 2008 in: 1. Verordnung zur Durchführung des Gesetzes zum Schutz gegen Fluglärm (1. FlugLSV) vom 27.12.2008, BGBl. I S.2980.
- Coelho, J.L.B., Vogiatzis, K., Licitra, G., 2011. The CNOSSOS-EU initiative: a framework for road, railway, aircraft and industrial noise modelling for strategic noise mapping in EU Member States. In: 18th International Congress on Sound and Vibration 2011. ICSV, pp. 789–795.
- Deb, K., Pratap, A., Agarwal, S., Meyarivan, T., 2002. A fast and elitist multiobjective genetic algorithm: NSGA-II. *IEEE Trans. Evol. Comput.* 6, 182–197. <https://doi.org/10.1109/4235.996017>.
- EC, 2002. Directive 2002/49/EC of the European parliament and the Council of 25 June 2002 relating to the assessment and management of environmental noise. *Off. J. Eur. Commun.*
- ECAC, 2016. ECAC/CEAC Doc 29 4th Edition Report on Standard Method of Computing Noise Contours around Civil Airports Volume 1: Applications Guide 1.
- European Commission, 2016. Evaluation of Directive 2002/49/EC relating to the assessment and management of environmental noise. Executive Summary. Brussels,

- Belgium.
- European Environment Agency (EEA), 2010. Good practice guide on noise exposure and potential health effects, n.d. EEA Technical Report.
- Federal Aviation Administration, 2007. INM v7.0 User's Guide.
- Frair, L., 1984. Airport noise modelling and aircraft scheduling so as to minimize community annoyance. *Appl. Math. Model.* 8, 271–281. [https://doi.org/10.1016/0307-904X\(84\)90162-8](https://doi.org/10.1016/0307-904X(84)90162-8).
- Ganić, E., Babić, O., Čangalović, M., Stanojević, M., 2018. Air traffic assignment to reduce population noise exposure using activity-based approach. *Transport. Res. Part D: Transport Environ.* 63, 58–71. <https://doi.org/10.1016/j.trd.2018.04.012>.
- Ganić, E., Radojević, M., Babić, O., 2016. Influence of aircraft noise on quiet areas. In: 25th International Conference Noise and Vibration Proceeding of Papers. University of Niš, Faculty of Occupational Safety, Tara, Serbia, pp. 47–53.
- Glekas, I., Vogiatzis, K., Antoniadis, C., 2016. Strategic noise mapping & action plans for the international airports of Larnaca & Pafos in Cyprus. The 23rd International Congress on Sound and Vibration, Athens, Greece.
- Hartjes, S., Visser, H., 2016. Efficient trajectory parameterization for environmental optimization of departure flight paths using a genetic algorithm. *Proc. Inst. Mech. Eng. Part G: J. Aerospace Eng.* 1–9. <https://doi.org/10.1177/0954410016648980>.
- Hatzopoulou, M., Miller, E.J., 2010. Linking an activity-based travel demand model with traffic emission and dispersion models: transport's contribution to air pollution in Toronto. *Transport. Res. Part D: Transport Environ.* 15, 315–325. <https://doi.org/10.1016/j.trd.2010.03.007>.
- Heblij, S.J., Hanenburg, V., Wijnen, R.A.A., Visser, H.G., 2007. Development of a noise allocation planning tool. In: 45th AIAA Aerospace Sciences Meeting and Exhibit. American Institute of Aeronautics and Astronautics, Reno, Nevada, pp. 1–7. <https://doi.org/10.2514/6.2007-1335>.
- Ho-Huu, Vinh, Hartjes, S., Geijselaers, L.H., Visser, H.G., Curran, R., 2018a. Optimization of noise abatement aircraft terminal routes using a multi-objective evolutionary algorithm based on decomposition. *Transport. Res. Procedia* 29, 157–168. <https://doi.org/10.1016/j.trpro.2018.02.014>.
- Ho-Huu, V., Hartjes, S., Visser, H., Curran, R., 2017. An efficient application of the MOEA/D algorithm for designing noise abatement departure trajectories. *Aerospace* 4, 54. <https://doi.org/10.3390/aerospace4040054>.
- Ho-Huu, V., Hartjes, S., Visser, H.G., Curran, R., 2018b. Integrated design and allocation of optimal aircraft departure routes. *Transport. Res. Part D: Transport Environ.* 63, 689–705. <https://doi.org/10.1016/j.trd.2018.07.006>.
- Isermann, U., Vogelsang, B., 2010. AzB and ECAC Doc. 29—Two best-practice European aircraft noise prediction models. *Noise Control Eng. J.* 58, 455–461. <https://doi.org/10.3397/1.3455442>.
- Jiang, S., Ferreira, J., Gonzalez, M.C., 2017. Activity-based human mobility patterns inferred from mobile phone data: a case study of Singapore. *IEEE Trans. Big Data* 3, 208–219. <https://doi.org/10.1109/TBDATA.2016.2631141>.
- Kaddoura, I., Kröger, L., Nagel, K., 2017. An activity-based and dynamic approach to calculate road traffic noise damages. *Transport. Res. Part D: Transport Environ.* 54, 333–347. <https://doi.org/10.1016/j.trd.2017.06.005>.
- Kaddoura, I., Kröger, L., Nagel, K., 2016. User-specific and dynamic internalization of road traffic noise exposures. *Netw. Spatial Econ.* <https://doi.org/10.1007/s11067-016-9321-2>.
- Kephalopoulos, S., Paviotti, M., Anfosso-lédée, F., Van Maerck, D., Shilton, S., Jones, N., 2014. Science of the total environment advances in the development of common noise assessment methods in Europe: the CNOSSOS-EU framework for strategic environmental noise mapping. *Sci. Total Environ.* 482–483, 400–410. <https://doi.org/10.1016/j.scitotenv.2014.02.031>.
- Kuiper, B.R., Visser, H.G., Heblij, S.J., 2013. Efficient use of an allotted airport annual noise budget through minimax optimization of runway allocations. *Proc. Inst. Mech. Eng. Part G: J. Aerospace Eng.* 227, 1021–1035. <https://doi.org/10.1177/0954410012447767>.
- Marais, K.B., Reynolds, T.G., Uday, P., Muller, D., Lovegren, J., Dumont, J.-M., Hansman, R.J., 2013. Evaluation of potential near-term operational changes to mitigate environmental impacts of aviation. *Proc. Inst. Mech. Eng. Part G: J. Aerospace Eng.* 227, 1277–1299. <https://doi.org/10.1177/0954410012454095>.
- Martínez-Puras, A., Pacheco, J., 2016. MOAMP-Tabu search and NSGA-II for a real Bi-objective scheduling-routing problem. *Knowl.-Based Syst.* 112, 92–104. <https://doi.org/10.1016/j.knsys.2016.09.001>.
- Netjasov, F., 2008. A model of air traffic assignment as a measure for mitigating noise at airports: the Zurich airport case. *Transport. Plan. Technol.* 31, 487–508. <https://doi.org/10.1080/03081060802364448>.
- Nibourg, J.M., Hesselink, H.H., van de Vijver, Y.A.J.R., 2012. Environment-Aware Runway Allocation Advice System (No. NLR-TP-2008-506). Amsterdam, the Netherlands.
- Novák, J., Šýkora, L., 2007. A city in Motion: time-space activity and mobility patterns of suburban inhabitants and the structuration of the spatial organization of the prague metropolitan area. *Geografica Ann. Ser. B: Hum. Geogr.* 89, 147–168. <https://doi.org/10.1111/j.1468-0467.2007.00245.x>.
- Ott, W.R., 1982. Concepts of human exposure to air pollution. *Environ. Int.* 7, 179–196. [https://doi.org/10.1016/0160-4120\(82\)90104-0](https://doi.org/10.1016/0160-4120(82)90104-0).
- Prats, X., Puig, V., Quevedo, J., 2011. A multi-objective optimization strategy for designing aircraft noise abatement procedures. Case study at Girona airport. *Transport. Res. Part D: Transport Environ.* 16, 31–41. <https://doi.org/10.1016/j.trd.2010.07.007>.
- Srinivas, N., Deb, K., 1994. Multiobjective optimization using nondominated sorting in genetic algorithms. *Evol. Comput.* 2, 221–248. <https://doi.org/10.1162/evco.1994.2.3.221>.
- Statistical Office of the Republic of Serbia, 2013. 2011 Census of Population, Households and Dwellings in the Republic of Serbia. Daily Migrants (data by municipalities/cities). Statistical Office of the Republic of Serbia, Belgrade, Serbia.
- Thang, L.-D., Ho-Huu, V., Hung, N.-Q., 2018. Multi-objective optimal design of magnetorheological brakes for motorcycling application considering thermal effect in working process. *Smart Mater. Struct.* 27, 75060.
- Torres, R., Chaptal, J., Bès, C., Hiriart-Urruty, J.-B., 2011. Optimal, environmentally friendly departure procedures for civil aircraft. *J. Aircraft* 48, 11–23. <https://doi.org/10.2514/1.C031012>.
- Visser, H.G., 2005. Generic and site-specific criteria in the optimization of noise abatement trajectories. *Transport. Res. Part D: Transport Environ.* 10, 405–419. <https://doi.org/10.1016/j.trd.2005.05.001>.
- Visser, H.G., Wijnen, R.A.A., 2001. Optimization of noise abatement departure trajectories. *J. Aircraft* 38, 620–627. <https://doi.org/10.2514/2.2838>.
- Vo-Duy, T., Duong-Gia, D., Ho-Huu, V., Vu-Do, H.C., Nguyen-Thoi, T., 2017. Multi-objective optimization of laminated composite beam structures using NSGA-II algorithm. *Compos. Struct.* 168, 498–509. <https://doi.org/10.1016/j.compstruct.2017.02.038>.
- Vogiatzis, K., 2014. Assessment of environmental noise due to aircraft operation at the Athens International Airport according to the 2002/49/EC Directive and the new Greek national legislation. *Appl. Acoust.* 84, 37–46. <https://doi.org/10.1016/j.apacoust.2014.02.019>.
- Vogiatzis, K., 2012. Airport environmental noise mapping and land use management as an environmental protection action policy tool. The case of the Larnaca International Airport (Cyprus). *Sci. Total Environ.* 424, 162–173. <https://doi.org/10.1016/j.scitotenv.2012.02.036>.
- Vogiatzis, K., Remy, N., 2014. Strategic Noise Mapping of Herakleion: The Aircraft Noise Impact as a factor of the Int. Airport relocation. *Noise Mapp.* 1, 15–31. <https://doi.org/10.2478/noise-2014-0003>.
- Wang, H., Fu, Y., Huang, M., Huang, G.-Q., Wang, J., 2017. Computers & Industrial Engineering A NSGA-II based memetic algorithm for multiobjective parallel flowshop scheduling problem. *Comput. Ind. Eng.* 113, 185–194. <https://doi.org/10.1016/j.cie.2017.09.009>.
- WHO, 2009. Night Noise Guidelines for Europe.
- Winther, M., Rypdal, K., Sørensen, L., Kalivoda, M., Bukovnik, M., Kilde, N., Lauretis, R. De, Falk, R., Romano, D., Deransy, R., Box, L., Carbo, L., Meana, N.T., Whiteley, M., 2017. EMEP/EEA air pollutant emission inventory guidebook 2016 – Update July 2017 – 1.A.3.a, 1.A.5.b Aviation. European Environment Agency.
- Zachary, D.S., Gervais, J., Leopold, U., 2010. Multi-impact optimization to reduce aviation noise and emissions. *Transport. Res. Part D: Transport Environ.* 15, 82–93. <https://doi.org/10.1016/j.trd.2009.09.005>.
- Zachary, D.S., Gervais, J., Leopold, U., Schutz, G., Huck, V.S.T., Braun, C., 2011. Strategic planning of aircraft movements with a three-cost objective. *J. Aircraft* 48, 256–264. <https://doi.org/10.2514/1.C031090>.
- Zhang, M., Filippone, A., Bojdo, N., 2018. Multi-objective optimisation of aircraft departure trajectories. *Aerosp. Sci. Technol.* 79, 37–47. <https://doi.org/10.1016/j.ast.2018.05.032>.



# 5

## LINKING AIRCRAFT ROUTE DESIGN AND FLIGHT ALLOCATION

*In the previous chapters, the development and application of methodologies addressing the two individual problems of route design and flight allocation have been presented. The chapter presents a study aiming to establish a suitable approach that can solve both problems in a linked manner. The developed framework features two consecutive steps. In the first step, multi-objective trajectory optimization is used to compute and store a set of routes for each given SID route. The obtained sets then serve as input to the optimization problem in the second step. In this second step, the selection of routes from the set of optimal routes and the optimal allocation of flights among these routes are conducted simultaneously. To validate the proposed framework, an analysis involving an integrated (one-step) approach, in which both trajectory optimization and flight allocation are formulated as a single integrated optimization problem, is also conducted. A comparison of both approaches is then performed, and their advantages and disadvantages are identified.*

---

The content of this chapter is based on the following research article:

**V. Ho-Huu**, S. Hartjes, H. G. Visser, and R. Curran, *An optimization framework for route design and allocation of aircraft to multiple departure routes*, Transportation Research Part D: Transportation and Environment, vol. 76, pp. 273-288, 2019. -> Paper 5

## 5.1. PROBLEM STATEMENT

As already observed in Chapters 3 and 4, various studies have been proposed to mitigate aircraft noise impact and fuel consumption over the years. However, these studies typically consider only a single problem of aircraft or airport operations at a time. Consequently, the potential reduction of environmental impact by formulating and solving problems that consider different problems (e.g., the design of optimal routes, the allocation of aircraft movements to routes and runways) in a linked manner has not yet been fully investigated.

In an attempt to address the above-mentioned research gap, an optimization framework, which is able to consider both strands of problem (i.e., route design and flight allocation) in a linked manner, is proposed in this chapter. The main aim of the framework is to minimize cumulative noise annoyance and fuel consumption. The performance and capabilities of the developed approach are demonstrated using a case study at Amsterdam Airport Schiphol in The Netherlands. The details of the study are presented in Ho-Huu et al. [41].

## 5

## 5.2. CONTRIBUTIONS

In this chapter, a two-step optimization framework has been developed, which is able to effectively solve both the problems of route design and flight allocation in a linked manner. The reliability of the framework has been validated through the analysis of an employed noise criterion and the solution of the integrated optimization problem in a single step. A case study at Amsterdam Airport Schiphol in The Netherlands, where 337 departure flights and 4 SID routes are considered, has been used to evaluate the efficiency and capability of the proposed framework. The obtained results show that the proposed framework can provide a trade-off solution which can gain a reduction in the number of people annoyed of up to 31% and a reduction in fuel consumption of 7.3% relative to the reference case solution. Furthermore, a comparison between the one- and two-step approaches indicates that the two-step approach is more flexible to adapt to the changes in the number of flights, when a reallocation of flights is demanded or new routes and runways are considered. It is worth mentioning that the obtained results in this chapter are based on a specific application at Amsterdam Airport Schiphol. Therefore, the overall potential of the developed method should be investigated for other types of airport architectures.



ELSEVIER

Contents lists available at ScienceDirect

## Transportation Research Part D

journal homepage: [www.elsevier.com/locate/trd](http://www.elsevier.com/locate/trd)

# An optimization framework for route design and allocation of aircraft to multiple departure routes

V. Ho-Huu\*, S. Hartjes, H.G. Visser, R. Curran

Faculty of Aerospace Engineering, Delft University of Technology, P.O. Box 5058, 2600 GB Delft, the Netherlands



## ARTICLE INFO

## Keywords:

Departure routes  
Trajectory optimization  
Aircraft allocation  
Noise abatement  
Aircraft noise  
Airport noise

## ABSTRACT

In this article, we present the development of a two-step optimization framework to deal with the design and selection of aircraft departure routes and the allocation of flights among these routes. The aim of the framework is to minimize cumulative noise annoyance and fuel burn. In the first step of the framework, multi-objective trajectory optimization is used to compute and store a set of routes that will serve as inputs in the second step. In the second step, the selection of routes from the sets of pre-computed optimal routes and the optimal allocation of flights to these routes are conducted simultaneously. To validate the proposed framework, we also conduct an analysis involving an integrated (one-step) approach, in which both trajectory optimization and route allocation are formulated as a single optimization problem. A comparison of both approaches is then performed, and their advantages and disadvantages are identified. The performance and capabilities of the present framework are demonstrated using a case study at Amsterdam Airport Schiphol in The Netherlands. The numerical results show that the proposed framework can generate solutions which can achieve a reduction in the number of people annoyed of up to 31% and a reduction in fuel consumption of 7.3% relative to the reference case solution.

5

## 1. Introduction

Over the past decades, aircraft noise and pollutant emissions have remained major issues in the aviation sector. These environmental issues do not only negatively affect the quality of life of communities surrounding airports and global climate change, but also hamper the expansion of flight and airport operations. Research efforts towards mitigating these negative impacts have received much attention, and some important achievements have been reported (Casalino et al., 2008; Lee et al., 2009). However, it appears that these attempts still remain insufficient to meet the need to accommodate the expected rapid growth in air traffic demand in the coming years (Girvin, 2009). In order to support the sustainable development of the aviation industry, more research on these topics is necessary. There are several possible strategies to achieve this objective; for example, adjusting operational procedures at airports, developing new aircraft technologies and using alternative fuels, or setting new rules and regulations (Marais et al., 2013). While new technologies and sustainable fuels may provide a significant reduction in environmental impact, they require more effort and time to develop and implement. In contrast, despite having smaller mitigation potential, operational changes can be carried out in the short-term period (Marais et al., 2013). As promising options in this category, the design of optimal aircraft routes and the assignment of aircraft to specific runways and routes have been well recognized and have shown promising results over the years (Frair, 1984; Visser, 2005).

\* Corresponding author.

E-mail addresses: [v.hohuu@tudelft.nl](mailto:v.hohuu@tudelft.nl), [vinh.ho.h@gmail.com](mailto:vinh.ho.h@gmail.com) (V. Ho-Huu), [s.hartjes@tudelft.nl](mailto:s.hartjes@tudelft.nl) (S. Hartjes), [h.g.visser@tudelft.nl](mailto:h.g.visser@tudelft.nl) (H.G. Visser), [r.curran@tudelft.nl](mailto:r.curran@tudelft.nl) (R. Curran).

<https://doi.org/10.1016/j.trd.2019.10.003>

Regarding the design of optimal aircraft routes, research has been typically aimed at minimizing community noise impact and fuel consumption or pollutant emissions such as nitrogen oxides (NO<sub>x</sub>) and carbon dioxides (CO<sub>2</sub>). Based on the use of noise criteria, studies can be classified into two groups. The first group includes research that employs noise criteria derived from a single fly-over noise event. For instance, the awakening criterion proposed by the Federal Interagency Committee on Aviation Noise (FICAN, 1997) was used in Hartjes et al. (2010), Hartjes and Visser (2016), Hogenhuis et al. (2011), and Visser and Wijnen (2001, 2003), while the more recent dose-response relationship developed by the American National Standards Institute (ANSI, 2008) was utilized in Ho-Huu et al. (2017), Yu et al. (2016), and Zhang et al. (2018). Also, noise nuisance criteria based on the maximum perceived sound level were applied by Prats et al. (2011, 2010a, 2010b) and Torres et al. (2011). The second group consists of studies in which the aggregation of multiple noise events is utilized as a noise criterion. For example, the annoyance criterion based on the  $L_{den}$  cumulative noise metric was used in Braakenburg et al. (2011), Ho-Huu et al. (2018a), and Song et al. (2014), whilst a sleep disturbance criterion based on the  $L_{night}$  cumulative noise metric was used by Hartjes et al. (2014).

In terms of research on the allocation of flights to specific routes and runways, Frair (1984) developed an integer optimization model to find the optimal allocation of aircraft among available approach and departure routes with the aim of minimizing community annoyance. Kuiper et al. (2012) maximized the number of aircraft movements operating at an airport within an allotted annual noise budget by optimally assigning annual flights to available routes and runways. Kim et al. (2014) minimized airport surface emissions by concurrently allocating aircraft among runways and scheduling departure and arrival flights on these runways. Zachary et al. (2010) formulated and solved an optimization problem to minimize noise and pollutant emissions by simultaneously considering operational procedures, arrival and departure routes, and fleet combination. In later research, with a similar approach, Zachary et al. (2011) evaluated the potential reduction in operational cost that could be gained by optimal solutions. Ganić et al. (2018) and Ho-Huu et al. (2019) developed integer optimization models to allocate flights among available departure and arrival routes with the aim of reducing population noise exposure, while taking into account daily migrating populations.

A review of the above literature reveals that the design of aircraft routes and the assignment of flights to available routes and runways have indeed been broadly studied. These studies were, however, typically carried out separately, while studies that consider both trajectory optimization and allocation problems together are lacking. In particular, with respect to the problem of designing aircraft routes, research has been aimed at finding the optimal flight trajectories for a given standard route. On the other hand, studies focusing on the allocation of aircraft movements generally only considered existing standard routes rather than optimized routes. Consequently, the potential reduction of environmental impact by formulating and solving an integrated optimization problem that consists of these two sub-problems has not yet been fully explored. It is important to note that the two sub-problems of route design and aircraft allocation are intrinsically coupled when a cumulative noise metric such as  $L_{den}$  is considered. This coupling is brought about by the fact that the optimal route obtained by the route design problem directly depends on the number of aircraft (of any given types) which is assigned to that route.

Although the problem of integrating both sub-problems could, in principle, be formulated and solved as a single integrated problem, it is likely to be prohibitively large and complicated due to high computational cost. In an attempt to fulfil the above research gaps and to overcome the aforementioned challenges, an optimization framework consisting of two sequential steps is developed in this paper. In the first step, the optimization problem of designing optimal routes is formulated and solved. The results obtained in this step contain sets of optimal routes which can effectively balance between noise annoyance and fuel consumption. Next, these data sets are used as the inputs for the allocation problem in the second step, in which the selection of optimized routes and the optimal allocation of aircraft movements among these routes are conducted concurrently.

In order to assess the reliability of the present approach, we also perform an integrated problem (here also referred to as the one-step approach), which combines both optimization sub-problems into a single integrated problem. A comparison between the one-step and two-step approaches is then presented, and the advantages and disadvantages of both approaches are discussed. Since only the ground tracks of routes were considered in previous research using annoyance criteria (Braakenburg et al., 2011; Hartjes et al., 2014; Ho-Huu et al., 2018a; Song et al., 2014), the potential of including optimized vertical profiles is also evaluated in the proposed framework. As a consequence, two different cases are investigated. In the first case, only the ground tracks are optimized, whilst in the second case, the ground tracks and the vertical profiles are optimized simultaneously. Furthermore, the consideration of these two case studies also aims to validate the reliability of the proposed two-step approach, as well as to highlight the drawbacks of the one-step approach. All computational experiments have been carried out in a case study involving Amsterdam Airport Schiphol (denoted as AMS) in The Netherlands.

The remainder of the paper is structured as follows. Theoretical backgrounds are provided in Section 2. Section 3 presents the proposed two-step optimization framework in detail, while numerical results and discussion are presented in Section 4. Finally, conclusions and future work are discussed in Section 5.

## 2. Theoretical background

### 2.1. Aircraft model

To evaluate aircraft performance, an intermediate point-mass dynamic model that has been widely utilized in previous research (Hartjes et al., 2014; Visser and Wijnen, 2001) is employed in this study. This dynamic model relies on the assumptions that: (1) no wind is present, (2) the Earth is flat and non-rotating, (3) flight is coordinated, and (4) the flight path angle is sufficiently small ( $\gamma < 15^\circ$ ). The equations of motion are then given by

$$\begin{aligned}
\dot{V}_{TAS} &= g_0 \left( \frac{T-D}{W} - \sin \gamma \right) \\
\dot{s} &= V_{TAS} \cos \gamma \\
\dot{h} &= V_{TAS} \sin \gamma \\
\dot{W} &= -\dot{m}_0 g_0
\end{aligned} \tag{1}$$

where  $\dot{V}_{TAS}$ ,  $\dot{s}$ ,  $\dot{h}$ ,  $\dot{W}$  are, respectively, the derivatives with respect to time of the true airspeed, ground distance flown, altitude and aircraft weight; and  $T$ ,  $D$ ,  $\dot{m}_0$ , and  $g_0$  are thrust, drag, fuel flow and the gravitational acceleration, respectively.

Since departure operations take place at low airspeeds and altitudes, the equivalent airspeed  $V_{EAS}$  can be used as a proxy for the indicated airspeed. Based on the relationship with the true airspeed,  $V_{EAS}$  can be defined as follows:

$$V_{EAS} = V_{TAS} \sqrt{\rho/\rho_0} \tag{2}$$

where  $\rho_0$  and  $\rho$  are, respectively, the air density at sea level and the ambient air density.

With the use of the relationship in Eq. (2), Eq. (1) can be redefined by:

$$\begin{aligned}
\dot{V}_{EAS} &= \left[ g_0 \left( \frac{T-D}{W} - \sin \gamma \right) + \frac{1}{2\rho^2} \frac{\partial \rho}{\partial h} V_{EAS}^2 \sin \gamma \right] \sqrt{\rho/\rho_0} \\
\dot{s} &= V_{EAS} \sqrt{\rho_0/\rho} \cos \gamma \\
\dot{h} &= V_{EAS} \sqrt{\rho_0/\rho} \sin \gamma \\
\dot{W} &= -\dot{m}_0 g_0
\end{aligned} \tag{3}$$

in which  $\frac{\partial \rho}{\partial h}$  is the derivative of the ambient air density  $\rho$  with respect to altitude  $h$ .

## 2.2. Trajectory parameterization

To parameterize the trajectory of a route, the method presented in [Hartjes and Visser \(2016\)](#) is utilized. This technique divides a trajectory into two different components: a horizontal and a vertical profile. In the horizontal profile, the flight path is constructed by employing Required Navigation Performance (RNP) based on flight legs, relying on two common leg types, i.e., track-to-a-fix (TF) and radius-to-a-fix (RF). This essentially results in a ground track that consists of an alternating sequence of straight segments and constant radius turns. For an example of how these leg types are used to create a route, interested readers can refer to [Ho-Huu et al. \(2017\)](#).

For the generation of the vertical profile, the flight procedures outlined in [ICAO \(2006\)](#) are applied. In the trajectory synthesis conducted in this study, a decrease in altitude and/or a deceleration in velocity during departure is not allowed, and similarly, an increase in altitude and/or acceleration in velocity is also prohibited during approach. The parameterization of the vertical profile has been based on splitting a trajectory into a number of segments. Depending on operational requirements, the two control inputs in each segment, viz. the throttle and flight path angle settings, are designated either as design (optimization) variables or their values are directly assigned. The vertical profile is then projected onto the ground track, yielding a complete 3-dimensional trajectory. For more details on the applied technique, interested readers can refer to [Hartjes and Visser \(2016\)](#) and [Ho-Huu et al. \(2017\)](#).

By using this technique, the design variables of a route comprise all parameters defining the ground track and vertical profile. However, in case the vertical profile is a priori fixed, the design variables only relate to the parameters defining the ground track.

## 2.3. Optimization criteria

In the field of design and allocation of optimal aircraft routes, two widely used objectives are fuel burn and noise annoyance. While the fuel-burn criterion can be readily assessed by estimating the change of aircraft gross weight during departure, the second criterion is significantly difficult to gauge due to the lack of consistency between single-event and multi-event noise metrics. Two noise criteria that have been broadly utilized in previous studies are the number of expected awakenings ([ANSI, 2008](#)) and annoyance ([EEA, 2010](#)). The awakening criterion is a single-event noise metric, which only considers a single noise event at a time and hence is only suitable for assessing the noise impact of a single movement of a single aircraft type. Although it might be used to design optimal routes in the first step of the framework, it is not suitable to be used for the allocation problem in the second step, as this step - by definition - considers the impact of multiple aircraft movements. Consequently, it does not represent a feasible option for the proposed framework. The annoyance criterion, however, is based on the accumulation of multiple noise events, and it can, therefore, be applied in both steps. For this reason, this particular criterion has been adopted within the optimization framework. Its implementation is described below.

As indicated by [EEA \(2010\)](#), the percentage of people annoyed (%PA) based on the  $L_{den}$  cumulative noise metric at a given location on the ground is given by

$$\%PA = 8.588 \times 10^{-6} (L_{den} - 37)^3 + 1.777 \times 10^{-2} (L_{den} - 37)^2 + 1.221 (L_{den} - 37) \tag{4}$$

where  $L_{den}$  is the day-evening-night noise level, determined as follows:

$$L_{\text{den}} = 10 \log_{10} \left[ \sum_{k \in N_r} \sum_{i \in N_{\text{at}}} a_{ki} 10^{\frac{SEL_{ki} + w_{\text{den}}}{10}} \right] - 10 \log_{10} T \quad (\text{dBA}) \quad (5)$$

where  $N_r$  is the total number of departure routes;  $N_{\text{at}}$  is the total number of aircraft types;  $SEL_{ki}$  is the sound exposure level resulted from aircraft type  $i$  on route  $k$ ;  $w_{\text{den}} = \{0, 5, 10\}$  is a weighting factor to account for day, evening and night time operations;  $a_{ki}$  is the number of aircraft type  $i$  operating on route  $k$ ; and  $T$  is the considered time period in seconds (in this case  $T = 24 \times 3600$  s). The  $SEL$  metric is calculated at each location on the ground by using a replication of the noise model given in the technical manual of the Integrated Noise Model (INM) (FFA, 2008).

It should be noted that, in order to evaluate this criterion, the total number of movements on each individual route within a given time period needs to be known in advance. However, given that the trajectory optimization process precedes the allocation of flights, the optimal number of flights is yet unknown. To overcome this, a strategy has been developed to identify appropriate estimates of the number of flights that are allocated to each route, allowing to generate a sufficiently comprehensive set of alternative routes in step one. This strategy will be further discussed in Section 4.1.

#### 2.4. Optimization method

To solve the optimization problems in two steps, a novel variant of the multi-objective evolutionary algorithm based on decomposition (MOEA/D), recently developed in Ho-Huu et al. (2018a), has been employed. The MOEA/D method was originally proposed by Zhang and Li (2007) and has been proven to be one of the most effective multi-objective evolutionary algorithms in recent years (Trivedi et al., 2016). In MOEA/D, decomposition approaches such as Tchebycheff decomposition are utilized to transform a multi-objective optimization problem into a set of scalar optimization sub-problems. Then, an evolutionary algorithm such as genetic algorithm (GA) or differential evolution (DE) is employed to solve the sub-problems concurrently. The performance of MOEA/D for solving the optimization problems of designing optimal aircraft routes has been clarified in Ho-Huu et al. (2017), demonstrating that MOEA/D performed much better than the non-dominated sorting genetic algorithm II (NSGA-II) proposed by Deb et al. (2002). Since the details of the algorithm have been given in Ho-Huu et al. (2017, 2018b), and Zhang and Li (2007) interested readers are encouraged to refer to these references.

### 3. A two-step optimization framework

Before the description of the proposed framework is presented in detail, it is worth mentioning that the first step in the optimization framework (i.e., the design of optimal routes) is a planning step which needs to be executed off-line based on a flight schedule and a variety of runway configurations. Indeed, due to the high computational cost, the first step cannot be executed on-line. Meanwhile, the second step (i.e., the allocation problem) can be performed within half an hour CPU time, and hence it might be quickly adapted to unplanned changes in flight schedules and runway configurations. The details of the two optimization steps are presented below.

#### Step 1: design of optimal routes

The main objective of the first step is to identify optimal routes for a given standard instrument departure route (hereafter referred as SID), in which a trade-off between the number of people annoyed and fuel burn is considered. The optimization problem is formulated as follows:

$$\begin{aligned} \min_{\mathbf{d}} \quad & (N_{\text{pa}}(\mathbf{d}), T_{\text{fuel}}(\mathbf{d})) \\ \text{s.t.} \quad & \mu_i(t) \leq \mu_{\text{max}}(h), \quad \forall i \in N_{\text{at}} \end{aligned} \quad (6)$$

where  $N_{\text{pa}}(\mathbf{d})$  and  $T_{\text{fuel}}(\mathbf{d})$  are the two objective functions which are, respectively, the total number of people annoyed and the total fuel burn of all aircraft following the SID, and  $\mathbf{d}$  is the vector of design variables that contains the parameters defining the route as described in Section 2. The index  $N_{\text{at}}$  is the number of aircraft types, and the variable  $\mu_i(t)$  is the bank angle of aircraft type  $i$  during a turn. With the use of the assumptions indicated in Section 2.1, the bank angle can be expressed as:  $\mu_i(t) = \pm \tan^{-1} \left( \frac{V_{\text{TAS},i}^2}{g_0 R} \right)$ , where  $V_{\text{TAS},i}$  is the true airspeed of aircraft type  $i$ , and  $R$  is the turn radius. The parameter  $\mu_{\text{max}}$  is the maximum permissible value of  $\mu$ , varying according to altitude  $h$  (ICAO, 2006).

In Eq. (6), the objective  $N_{\text{pa}}(\mathbf{d})$  is calculated by aggregating over all grid cells the product of %PA in Eq. (4) in each grid cell with the population in that cell. The population residing in each grid cell is retrieved from a Geographic Information System (GIS) containing population density data surrounding an airport. It is noted that  $N_r$  in Eq. (5) is equal to 1 in this case, since only one SID at a time is evaluated. The objective  $T_{\text{fuel}}(\mathbf{d})$  is the sum of the fuel burn of all aircraft during the specific departure period and is evaluated by

$$T_{\text{fuel}}(\mathbf{d}) = \sum_{i \in N_{\text{at}}} a_i \text{fuel}_i(\mathbf{d}) \quad (7)$$

where  $a_i$  is the number of aircraft type  $i$ ,  $\text{fuel}_i(\mathbf{d})$  is the fuel burn of aircraft type  $i$ .

By solving the problem defined in Eq. (6) for each SID, the sets of optimal routes and associated performances are found, which then serve as inputs to the optimization problem in the second step. It should be noted that the aircraft types selected when designing

optimal routes are assumed to be given. Also, to be able to adapt to different runway configurations, the optimal routes for all standard routes of each runway should be obtained.

### Step 2: selection of routes and allocation of aircraft to these routes

Based on the sets of optimal routes obtained in Step 1 for all SIDs, this step aims to define which routes from the sets are preferred, and how many movements of each aircraft type should be allocated to these preferred routes for different operational times. The answer to these questions can be obtained by solving the optimization problem stated as follows:

$$\begin{aligned} \min_{\mathbf{r}, \mathbf{a}} \quad & (N_{pa}(\mathbf{r}, \mathbf{a}), T_{fuel}(\mathbf{r}, \mathbf{a})) \\ \text{s.t.} \quad & \sum_{k \in SD_s} a_{itk} = T_{at,its}, \quad \forall i \in N_{at}, \quad \forall t \in (d,e,n), \quad \forall s \in T_p \\ & \sum_{t \in (d,e,n)} \sum_{i \in N_{at}} a_{itk} \leq \bar{N}_{t,k}, \quad \forall k \in N_r \\ & 0 \leq a_{itk} \leq \bar{a}_{itk} \end{aligned} \quad (8)$$

where  $\mathbf{r} = \{r_1, \dots, r_k, \dots, r_{N_r}\}$  is the vector of design variables of departure routes, in which the preferred route  $r_k$  is selected from the set of optimal routes  $O_k$  obtained in Step 1 for SID  $k$ , and  $N_r$  is the total number of considered SIDs. The vector  $\mathbf{a}$  is the design variable vector of aircraft allocation, in which  $a_{itk}$  is the number of aircraft type  $i$  at time  $t$  on route  $k$ . The index  $t$  is the operating time of aircraft (i.e. day (d), evening (e) or night (n)). The index  $s$  is the terminal point (i.e., the end point of departure procedure), and  $T_p$  is the set of terminal points. The vector  $SD_s$  is the vector that contains SIDs having the same terminal point  $s$ . The identification of SIDs with the same terminal point allows the algorithm to allocate aircraft movements on different SIDs originating from the same or different runways. The parameter  $T_{at,its}$  is the total number of aircraft type  $i$  at time  $t$  sent to departure routes having the same terminal point  $s$ . The parameter  $\bar{N}_{t,k}$  is the upper bound of the number of movements that route  $k$  can handle in a certain period of time. Finally, the parameter  $\bar{a}_{itk}$  is the upper bound of the number of aircraft type  $i$  on route  $k$  at time  $t$ . It should be noted that the exit point of each flight in a flight schedule can be specified in advance based on its destination airport.

In Eq. (8), the objectives  $N_{pa}(\mathbf{r}, \mathbf{a})$  and  $T_{fuel}(\mathbf{r}, \mathbf{a})$  are the same as the ones considered in Step 1, however, the design variables are different. Specifically, the design variables in this problem represent the selection of routes from the sets of optimal routes for each SID, and the distribution of aircraft on these routes. As in Step 1, the objective  $N_{pa}(\mathbf{r}, \mathbf{a})$  is evaluated by the sum of the multiplication of %PA in each grid cell with the population in that cell. However, the *SEL* metric for each route is now known in advance, as it was stored in Step 1. Consequently, both  $L_{den}$  and %PA can be determined directly from the *SEL*-data stored in the set of optimal routes by applying Eqs. (5) and (4). The objective  $T_{fuel}(\mathbf{r}, \mathbf{a})$  is defined as follows:

$$T_{fuel}(\mathbf{r}, \mathbf{a}) = \sum_{k \in N_r} \sum_{i \in N_{at}} a_{ik} fuel_{ik}(r_k) \quad (9)$$

where  $fuel_{ik}(r_k)$  is the fuel burn of aircraft type  $i$  on route  $r_k$ .

It should be noted that, in the problem stated in Eq. (8), airspace capacity and aircraft sequence are assumed to be satisfied via the constraint, in which each route can only accommodate a certain number of flights within the considered time frame (24 h in this case). The actual influence of optimal allocation solutions on the airspace capacity and aircraft sequence, which is a challenging problem, is not considered yet. This aspect will be explored in future work.

## 4. Numerical examples and discussion

In this section, a case study at AMS in The Netherlands, as shown in Fig. 1, is presented to exemplify the capabilities of the proposed framework. For this case study, four existing standard instrument departures (SIDs), viz. LEKKO, KUDAD, LUNIX and RENDI departing from two different runways, viz. RW18 and RW24, are considered. The SIDs LEKKO and KUDAD both end at the LEKKO intersection, whereas LUNIX and RENDI both terminate at IVLUT. On the selected reference day, 337 flights operating on these routes were recorded. These flights can be classified into three groups with different departure times, viz. 237 day flights (07h00-19h00) accounting for 70% of the total traffic volume, 43 evening flights (19h00-23h00) accounting for 13%, and 57 night flights (23h00-7h00) accounting for 17% (Dons, 2012). Although many different aircraft types operate on these routes, for the sake of simplicity all flight movements are assumed to be conducted by either of two aircraft types, namely the Boeing 737-800 (B738) and Boeing 777-300 (B773). It is assumed that the B738 represents all small and medium aircraft, accounting for 80% of the total number of flights, while the B773 represents heavy aircraft accounting for 20%. Both aircraft types are modelled based on the Base of Aircraft Data (BADA) (Nuic et al., 2010). The population data acquired from the Dutch Central Bureau of Statistics (CBS) with a grid cell size of  $500 \times 500$  m, as shown in Fig. 1, is utilized. The MOEA/D algorithm with a population size of 50 and a maximum number of iterations of 1000 is applied to solve all optimization problems. The simulations are performed on an Intel Core i5, 8 GB RAM desktop with the use of MATLAB 2016b.

### 4.1. Sensitivity analysis of noise criterion

As mentioned in Section 2.3, to use the noise annoyance criterion for the design of optimal routes, the number of aircraft movements on each SID has to be known a priori. However, this information is unknown within Step 1 of the framework. Therefore, to choose a representative number of movements that leads to a comprehensive set of alternative routes for the allocation problem in the second step, a brief analysis to determine a valid assumption for the number of movements is carried out in this section. For this

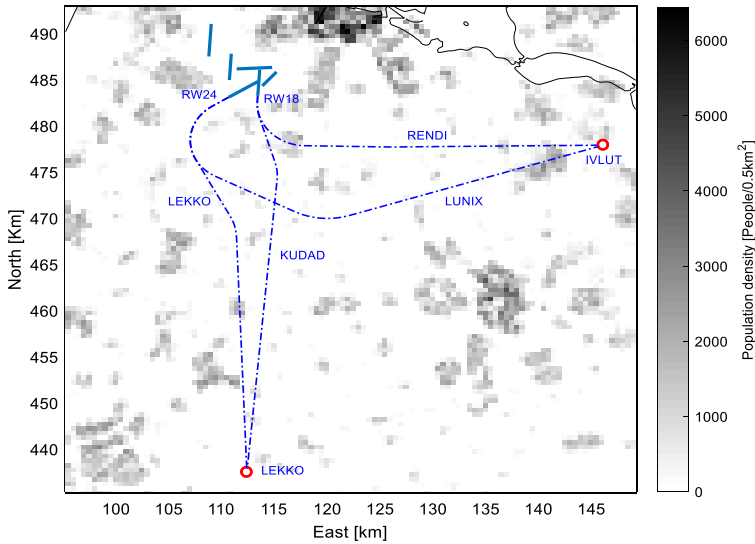


Fig. 1. Illustration of the case study at AMS.

analysis, the LUNIX SID and the B738 model are used. By considering the actual operational data, approximately 100 flights (including 66% day, 3% evening and 31% night) could be identified, and this number of flights might be used as a “representative” number. However, as the allocation algorithm may actually result in a totally different number of flights assigned to either SID, a significant variation (either positive or negative) to this number needs to be taken into account. Therefore, we assess the results for the assumed number of 50, 100 and 150 flight movements, using the percentages of 66%, 3% and 31% for day, evening and night, respectively.

The comparison of optimal ground tracks and vertical profiles corresponding to different assumed numbers of flights is illustrated in Fig. 2. At first glance, it can be seen from Fig. 2 that the number of flights has a significant influence on the optimal results. The reasons for this are due to the significant increase of  $L_{den}$  with increasing number of movements and the distribution of the population. An illustration of the  $L_{den}$  contours for different numbers of flights is given in Fig. 3. By taking a closer look at Fig. 2, however, it can be observed that the solutions obtained by assuming 150 flights include those acquired by assuming 50 and 100 flights. This can also be seen in Fig. 4, where most of the solutions obtained by assuming 50 and 100 flights are on the Pareto front obtained by 150 flights.

Consequently, assuming a large number of flights results in the most comprehensive set of alternative trajectories. Therefore, the maximum number of flights that can be allocated to a specific SID – based on the projected number of movements in the entire scenario – is considered as an acceptable assumption in Step 1. It should be noted that although only the analysis for the LUNIX SID with a B738 is presented here, the same behavior is also observed for different aircraft types (i.e., B773) and different SIDs.

#### 4.2. 2D optimization case

As mentioned before, the problem that integrates both sub-problems can theoretically be formulated and solved. Nevertheless, due to the high computational cost, it is likely to be prohibitively large and complex. To still be able to validate the proposed framework by comparing it with an integrated problem formulation, a relatively simple problem scenario is considered in this section. Specifically, for the optimization problems in the first step, only the ground tracks of routes are optimized, whilst the vertical profiles are fixed and derived from the noise abatement departure procedure 2 (NADP2)<sup>1</sup> (ICAO, 2006) and typical airline procedures.

As shown in Fig. 1, all SIDs are modelled by two turns and three straight legs, which results in 5 design variables for each optimal route design problem. The definition of these design variables can be found in Ho-Huu et al. (2017). It is noted that both B738 and B773 are assumed to follow the same route. The SIDs are assumed to start at the end of the runways at an altitude of 35 ft and a take-off safety speed of  $V_2 + 10$  kts, and to terminate at an altitude of 6000 ft and an equivalent airspeed (EAS) of 250 kts. To design

<sup>1</sup> In this study, the vertical profile is set as follows: from the start to an altitude of 800 ft, full take-off thrust is applied, and  $V_2 + 10$  kts is maintained. After reaching 800 ft, thrust is cut back to climb thrust, and the aircraft is accelerating to  $V_{clean}$  whilst continuing a moderate climb. After retracting the flaps, the aircraft maintains climb thrust at a moderate climb gradient until the final conditions are met. At that point, thrust is reduced to maintain these conditions.

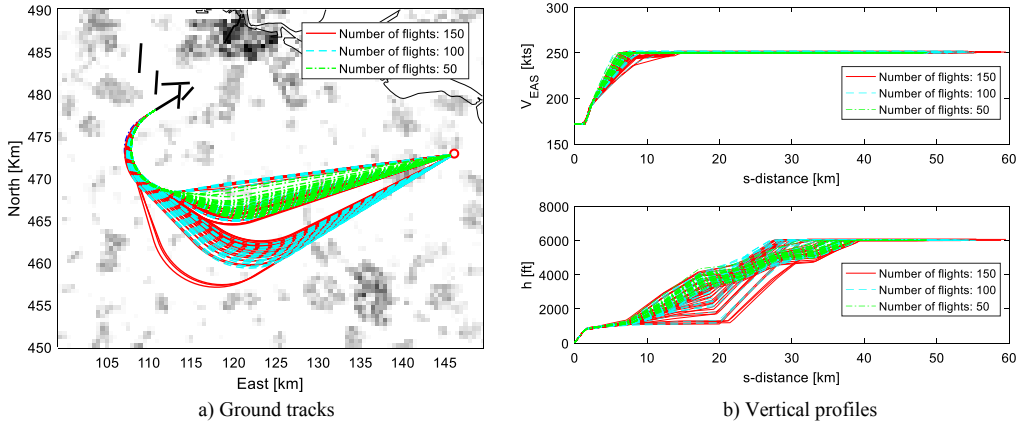


Fig. 2. Comparison of vertical profiles and ground tracks with different numbers of flights.

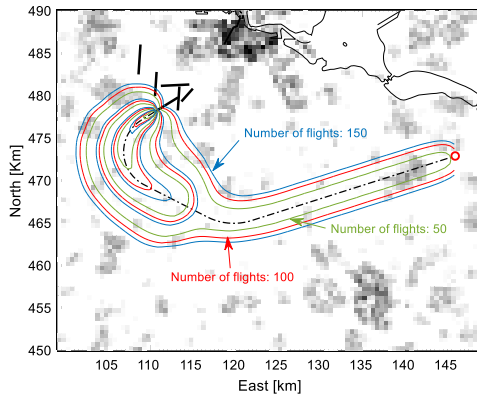


Fig. 3. Comparison of the  $L_{den}$  noise contours (37 dBA) caused by different numbers of flights.

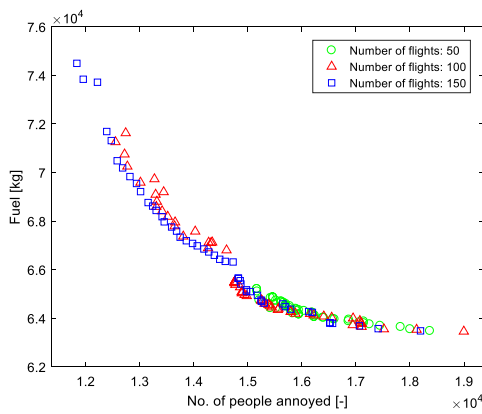


Fig. 4. Comparison of objectives with different numbers of flights.

**Table 1**  
Optimal aircraft allocation of the representative solutions and the reference case.

Aircraft allocation		One-step approach			Two-step approach			Reference case
		Sol. 3	Sol. 39	Sol. 51	Sol. 1	Sol. 34	Sol. 50	
B738	KUDAD	[34,0,0] *	[7,0,0]	[5,0,0]	[38,0,1]	[5,0,0]	[5,0,0]	[36,10,0]
	LEKKO	[32,10,21]	[59,10,21]	[61,10,21]	[28,10,20]	[61,10,21]	[61,10,21]	[30,0,21]
	LUNIX	[15,3,25]	[50,24,25]	[52,24,25]	[18,0,25]	[47,24,25]	[45,24, 25]	[53,2,25]
	RENDI	[108,21,0]	[73,0,0]	[71,0,0]	[105,24,0]	[76,0,0]	[78,0,0]	[70,21,0]
B773	KUDAD	[17,3,4]	[17,3,0]	[17,3,0]	[17,2,1]	[17,2,0]	[17,3,0]	[10,3,0]
	LEKKO	[0,0,1]	[0,0,5]	[0,0,5]	[0,1,4]	[0,1,5]	[0,0,5]	[7,0,5]
	LUNIX	[0,0,0]	[0,0,6]	[1,0,6]	[0,0,0]	[0,6,6]	[1,6,6]	[13,1,6]
	RENDI	[31,6,6]	[31,6,0]	[30,6,0]	[31,6,6]	[31,0,0]	[30,0,0]	[18,6,0]

[...]\*: Number of flights [day, evening, night].

5

optimal routes for each SID in step one, a number of 150 flights – which is representative for the maximum possible number of movements on any of the SIDs under consideration – is used. The percentage of day, evening and night flights and the distribution of aircraft types as stated in Section 4 are also applied to this number of movements. For the second step, the main objectives are to choose suitable routes for the four SIDs and to allocate all the 337 flights featuring two different aircraft types and flown in different time periods (day, night or evening) to these routes. The details of the 337 flights under consideration can be seen in the reference case in Table 1. The optimization problem in Step 2 features 28 design variables, viz. 4 variables for route selection and 24 variables for aircraft allocation (which are the result of the consideration of four SIDs, two aircraft types and three different operational time periods). By looking at the distribution of the population in Fig. 1, it can be seen that the LUNIX SID is the route that causes less annoyance simply because fewer people live in its direct vicinity. From an airport operational perspective, therefore, this route should accommodate as many flights as possible. However, based on the reference data in Table 1, only around 50% of the flights departing towards the IVLUT intersection are recorded on this route. This is the consequence of the fact that the LUNIX SID intersects the KUDAD SID, limiting the use of the LUNIX SID. Therefore, to include this issue in the allocation problem, we assume that the KUDAD and LUNIX SIDs can handle only 50% of the total number of movements, while RENDI and LEKKO can handle up to 80%. It should also be noted that this assumption can be easily adapted in the framework when the actual operational capacity becomes available. For the integrated optimization problem (the one-step approach), the design variables are the combined variables of both steps in the two-step approach, except for the 4 variables related to route selection. This leads to an optimization problem with 44 variables in total.

To evaluate the reliability and efficiency of both approaches, the results based on the reference case and those derived from the optimal allocation of aircraft movements based on the current SID routes are also estimated and provided. It should be noted that since the studies that address the problem as presented in this paper are not available in the literature, only the results derived from the reference case are used for comparison purposes. All results are shown in Fig. 5. At first glance, it can be seen that both approaches offer solutions that are significantly better than those derived from the reference cases in terms of both the number of people annoyed and fuel burn. A comparison of the result obtained by the reference case and those obtained by the optimal allocation based on the current SID routes indicates that the optimal allocation of flights has a positive influence on the reduction of noise annoyance and fuel burn. Once the optimized routes are also included, both one-step and two-step approaches produce

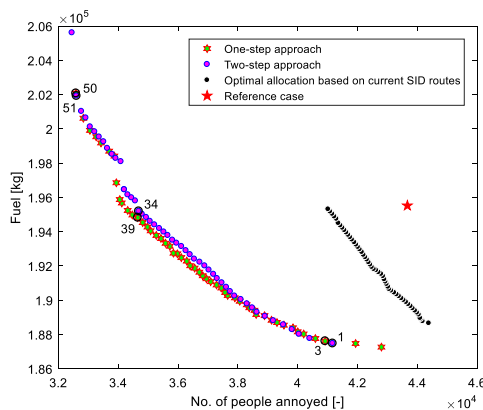


Fig. 5. Comparison of solutions obtained by the one- and two-step approaches and the reference case.

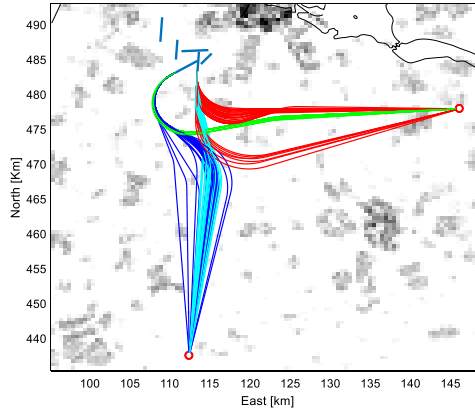


Fig. 6. Optimal ground tracks obtained by the one-step approach (the colors indicate the routes of different SIDs). (For interpretation of the references to colour in this figure legend, the reader is referred to the web version of this article.)

approximately the same solutions. It should be noted that the one-step approach will theoretically outperform the two-step approach. This is because the former approach allows the coupling between the generation of optimal routes for given SIDs and the flight allocation to take place directly in the same problem. However, there is no significant difference between the results from both approaches because of the following reason. The routes generated in Step 1 of the two-step approach are likely to cover most situations of flight allocations in Step 2, due to the nature of the applied noise criterion (see Section 4.1). Therefore, this approach can generate route selections that can lead to similar solutions as those from the one-step approach.

Regarding the computational cost, the two-step approach is far more efficient than the integrated approach. Specifically, to obtain these results, the one-step approach requires about 35 h (h) CPU time, while the calculation time of the two-step approach is only 18 h, mainly spent on the design of optimal routes in Step 1. Clearly, the computational cost is a major restriction of the integrated approach and may be limiting for large applications. Also, the obtained results are less flexible when in practice the number of flights is changed, and a reallocation of flights to the routes is required. Meanwhile, since the two-step approach solves the problem via separate steps, the complexity of the optimization problems has been decreased significantly. In addition, with the optimal routes obtained in the first step, the allocation of flights can be easily reevaluated at a computational cost of around 30 min CPU time when a reallocation of flights is requested. Furthermore, the computational cost of the allocation problem can also be further improved by using parallel computing with multiple cores or cluster computing. This is because the evaluation of objective functions in the optimization algorithm is independent.

Fig. 6 shows the optimal ground tracks obtained by the one-step approach, while those of the two-step approach are displayed in Fig. 7. A comparison of the ground tracks in Figs. 6 and 7b shows that they are quite similar for both SIDs. From Fig. 6, it can also be observed that the integrated approach creates more route options than the two-step approach. As can be seen in Fig. 5, however, the

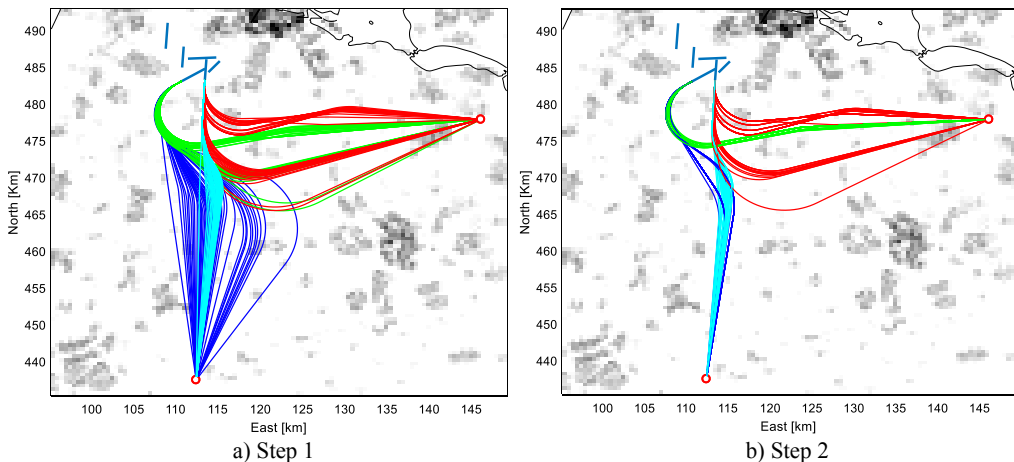


Fig. 7. Optimal ground tracks obtained by the two-step approach (2D optimization).

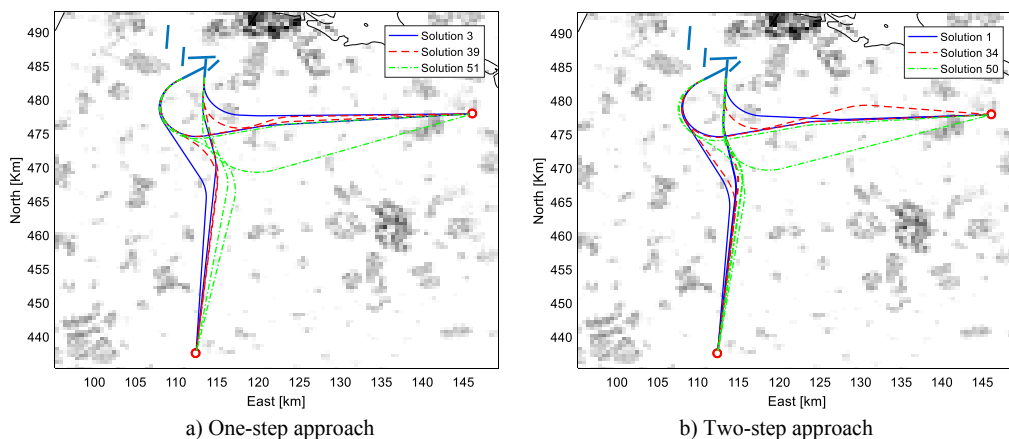


Fig. 8. Optimal ground tracks of the representative solutions obtained by the one-step and two-step approaches.

5

difference in objective functions between both approaches is moderate.

For a more detailed evaluation of the optimal results, the optimal routes of representative solutions (3, 39 and 51 for the one-step approach, and 1, 34 and 50 for the two-step approach) as labelled in Fig. 5 are presented in Fig. 8. The reason for selecting these solutions is that they effectively represent the different aspects of noise and fuel preference, while they are closely located on the Pareto fronts. The details of aircraft allocation of these solutions are provided in Table 1. From Fig. 8, it can be seen that all the routes tend to be close together, which reduces the width of the  $L_{den}$  contour areas, and consequently, may result in a narrow corridor of high noise exposure between major communities. It is also observed from the figure that the solutions acquired by both approaches exhibit the same trend. It should be noted that the aim of choosing these representative solutions is just to give an overview of the optimal solutions, and does not mean that they are solutions to be recommended for authorities or policymakers. The selection of solutions should be based on their preference, such as noise impact, fuel consumption or the trade-off between them. Also, other criteria associated with each solution, such as sleep disturbance, the fair distribution of noise over population and airspace capacity should be considered. Therefore, to select suitable solutions, deeper analyses and selection methods should be studied. However, they are not covered in this work and hence are left for further research.

In a comparison of the allocation of aircraft to the presented routes, Table 1 shows the difference in the distribution of aircraft types and the number of flights to the routes between the solutions and the reference case. From Table 1, it can be seen that the general distribution of movements is quite similar for both approaches. Solutions with a lower number of annoyed people (i.e. solutions 50 and 51) tend to prefer the LEKKO SID for the large number of B738s, whereas the B773s are mostly using the KUDAD SID. This is mostly because the limited number of B773s cause less noise, but more importantly, burn more fuel and as such prefer the shorter KUDAD route. Another observation from these results is that although the total number of aircraft using the LUNIX or RENDI SID is quite similar, the LUNIX SID is clearly preferred for evening and night flights, for either aircraft type. This is again due to the balance of fuel and noise. The LUNIX SID causes less annoyance but is a longer route than RENDI. As a result of the weighting factors in Eq. (5) for evening and night flights, moving specifically these flights to LUNIX has a significant positive influence on the noise impact, whereas the overall increase in fuel burn is limited. Table 2 presents the comparison of specific criteria obtained by these solutions and the reference case. It should be noted that while Table 1 displays the changes in the number of flights on each route, the associated changes in the flight schedule and flight delays are still unknown at this stage, due to the fact that the aircraft sequencing problem has not yet been taken into account. These evaluations will be further studied in future work.

As can be expected, the integrated approach, in general, provides the best solutions, as can be observed from Fig. 5. However, the differences with the two-step approach are very small indeed, and the latter approach clearly outperforms the former approach in terms of computational effort and flexibility. It can, therefore, be concluded that the two-step approach provides a valid mean to combine the optimal routing and allocation problems.

Table 2  
Comparison of the criteria of the representative solutions and the reference case.

Criteria	One-step approach			Two-step approach			Reference case
	Sol. 3	Sol. 39	Sol. 51	Sol. 1	Sol. 34	Sol. 50	
No. of people annoyed	40,918	34,654	32,588	41,167	34,687	32,606	43,759
Fuel (ton)	187.62	194.83	202.08	187.48	195.20	201.93	196.26
Distance (km)	13,372	14,412	15,394	13,359	14,414	15,378	14,327
Flight time (h)	28.82	30.81	32.76	28.79	30.82	32.78	30.66

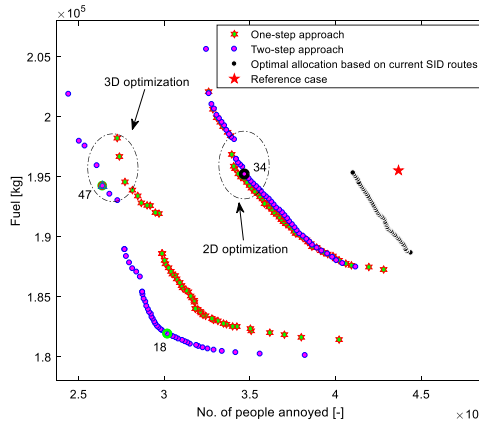


Fig. 9. Comparison of objectives obtained by the one-step and two-step approaches and the reference case.

4.3. 3D optimization case

In this section, the performance of both approaches is further evaluated for a more complicated optimization problem, where the vertical profile along the route is also considered in the trajectory optimization in Step 1. This case study is also used to assess the potential benefits of optimized vertical profiles in terms of reducing noise impact, which were not considered in previous studies (Braakenburg et al., 2011; Hartjes et al., 2014; Song et al., 2014).

By introducing new design variables for the vertical profile, the number of design variables of the optimization problem in Step 1 is increased significantly. While the ground track of the route is defined in the same way as in the previous section, the vertical part is subdivided into 10 segments and parameterized following the study in Hartjes and Visser (2016), resulting in an addition of 18 design variables. By optimizing the vertical profiles for two different aircraft types concurrently, the number of design variables for the optimization problem in this step now totals 41. Meanwhile, the optimization problem in Step 2 is kept the same as the one in the previous section. The number of design variables of the integrated optimization problem is now 186 in total.

Fig. 9 compares the solutions obtained by the two different approaches and the reference case. As can be seen in Fig. 9, there is a significant reduction in both fuel burn and the number of people annoyed when the vertical profiles are also optimized. This shows that the vertical profile has an important influence on the objective functions when minimizing for fuel burn and noise impact. Comparing the solutions obtained by both approaches reveals that the two-step approach provides solutions that are better than those of the one-step approach. It should be noted that to achieve these results, the two-step approach spent 26 h CPU time in total (of which only 0.58 h is used for the allocation problem with 443 iterations). Meanwhile, the one-step approach took 73 h CPU time after reaching the maximum number of iterations of 1000 that was set for the algorithm. This means that the solutions of the integrated problem still did not yet reach convergence. Although the integrated approach should theoretically always identify better results than the proposed two-step approach, it is clear from these results that the required computational effort is just too high. The results of the integrated solution in 3D are, therefore, not analyzed any further in this section.

In an effort to provide a more detailed analysis of these solutions, some representative solutions (as labelled in Fig. 9) for both 2D and 3D approaches and the reference case are selected. The specific performance metrics obtained by these solutions are presented in Table 3. With almost the same performance associated to fuel burn, it can be seen from Table 3 that the 3D solution 47 offers a reduction of up to 23.9% in the number of people annoyed compared to the 2D solution 34, and 39.6% compared to the reference case. Although there is a slight increase of 6.1% in the total distance as a result of avoiding populated regions, owing to the optimized vertical profile the fuel burn has still been reduced. Along the Pareto front of the 3D solutions, we can also identify solutions that outperform both the 2D solutions and the reference case regarding all defined metrics. An example of this is solution 18. Besides achieving a 7.3% reduction in fuel burn, solution 18 also provides good performance in the number of people annoyed, total distance

Table 3 Comparison of criteria of the 2D and 3D representative solutions and the reference case.

Criteria	Reference case	2D optimization	3D optimization	
		(solution 34)	(solution 47)	(solution 18)
No. of people annoyed	43,759	34,687	26,400	30,189
Fuel (ton)	196.26	195.20	194.23	181.90
Distance (km)	14,327	14,414	15,207	13,511
Flight time (h)	30.66	30.82	32.16	28.60

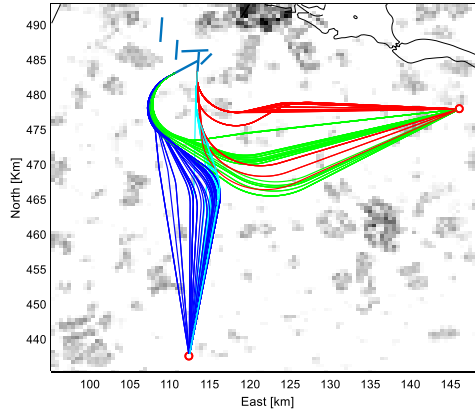


Fig. 10. Optimal ground tracks obtained by the two-step approach (3D optimization).

5

and flight time, showing a decrease of 31%, 5.7% and 6.7%, respectively, compared to the reference case.

Fig. 10 shows the ground tracks obtained by the two-step approach, while the ground tracks and the vertical profiles of the solutions 18, 34 and the reference case are given in Figs. 11 and 12, respectively. From Fig. 12, it can be seen that there is a significant difference between the optimized vertical profiles and the reference profile in the first part of the routes. In the optimized profiles, the emphasis lies more on acceleration in the initial part of the trajectory, whilst the standard profiles try to keep a balance between speed and altitude. The increased acceleration featured in the optimized profile allows for an earlier flap retraction and, in general, better performance in terms of fuel burn. In addition, the low altitude flight at a higher airspeed reduces the noise impact. The reason for this is twofold. Firstly, the higher airspeed leads to a lower exposure time and hence lower  $SEL$  and  $L_{den}$  values. In addition, the low altitude flight – although the noise exposure directly below the flight path is higher – leads to a lower noise exposure astride the trajectory, as the lateral attenuation losses are significantly higher. As a result, the number of annoyed people has significantly reduced. The illustration of this can be seen in Fig. 13, where the difference of  $L_{den}$  noise contour areas caused by solutions 18, 34 and the reference case, and the number of people annoyed on each grid cell are clearly illustrated.

## 5. Conclusion

In this paper, we have presented and validated a two-step optimization framework for the design of optimal aircraft departure routes and the distribution of aircraft movements over these routes. Firstly, to explore the potential of reducing noise and fuel burn for each standard instrument departure (SID), the multi-objective trajectory optimization problem is formulated and solved in the first step. Secondly, the obtained sets of optimal routes are then used as the inputs for the optimization problem in the second step, where the selection of optimal routes for SIDs and the assignment of flights among these routes are optimized simultaneously. The reliability of the framework has been validated through the analysis of the employed noise criterion and the solution of the integrated optimization problem in a single step. A case study at Amsterdam Airport Schiphol (AMS) in The Netherlands has been used to assess

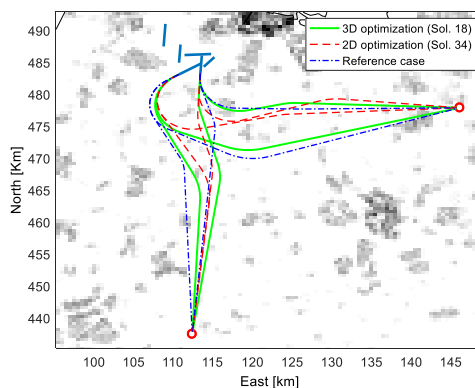
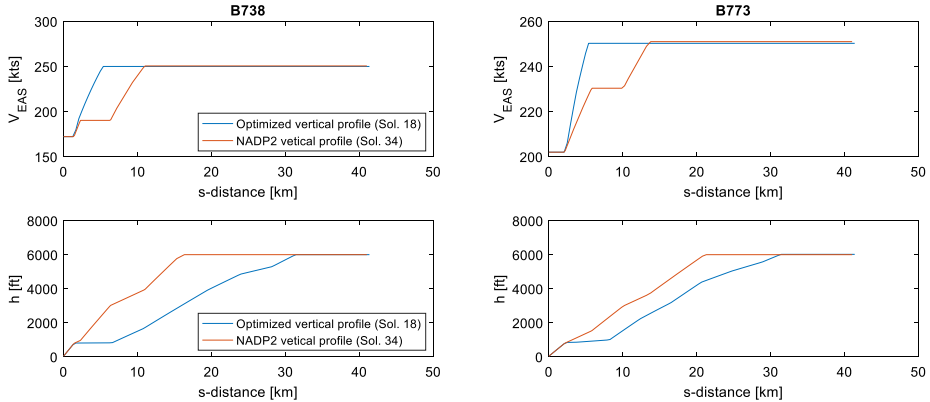
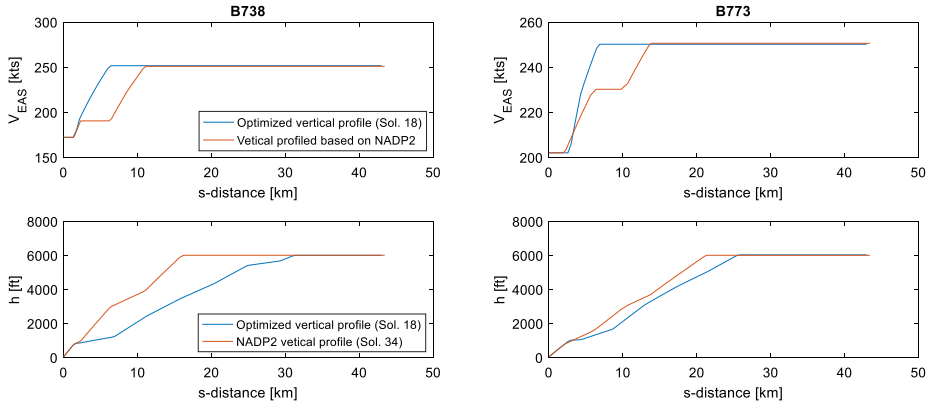


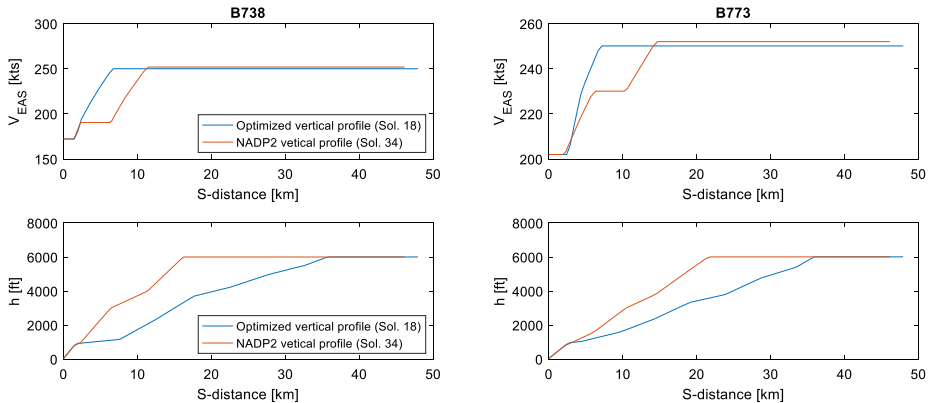
Fig. 11. Comparison of solutions obtained by the 2D and 3D optimization and the reference case.



a) Route KUDAD

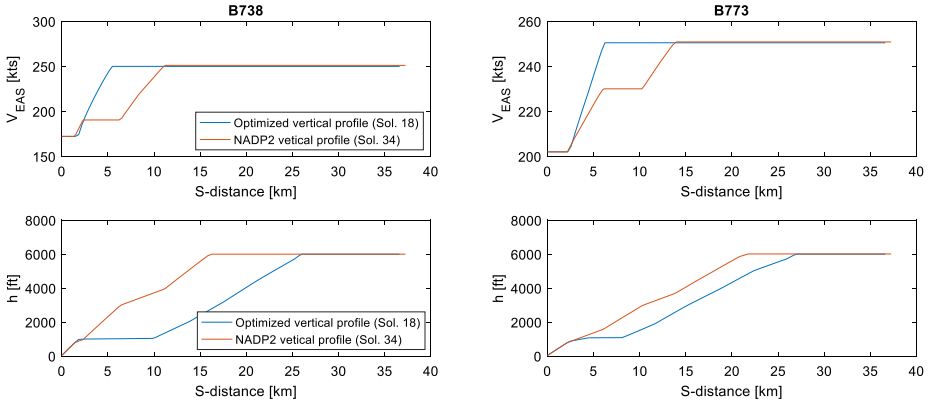


b) Route LEKKO



c) Route LUNIX

Fig. 12. Vertical profiles of the 3D solution (solution 18) and those based on the reference profile (solution 34).



d) Route RENDI

Fig. 12. (continued)

5

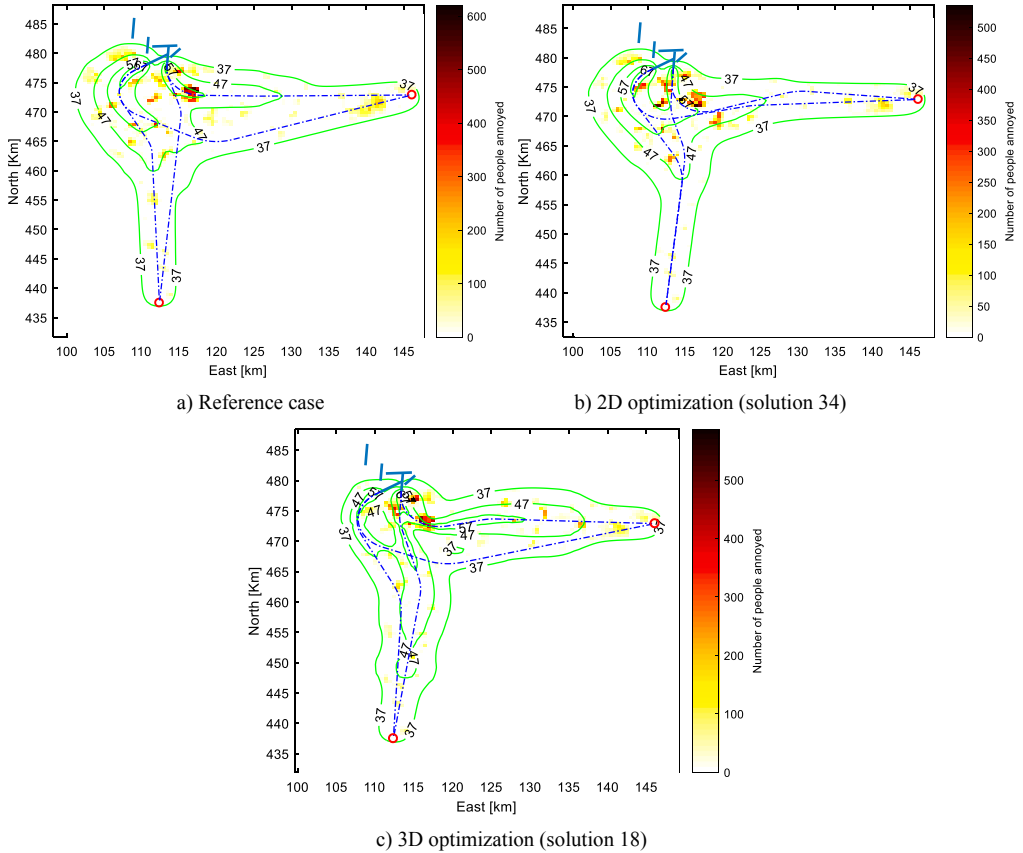


Fig. 13. Illustration of  $L_{den}$  and the number of people annoyed caused by the representative solutions and the reference case.

the efficiency and capability of the proposed framework.

The numerical results indicate that the two-step framework is reliable and able to provide solutions which can significantly reduce noise annoyance and fuel consumption. Moreover, the obtained results have shown that from a theoretical perspective, the one-step approach can, in principle, fully exploit the potential of noise and fuel reduction by solving the integrated optimization problem. However, the computational cost and the complexity associated to the integrated optimization problem are prohibitively large. Furthermore, this approach is also less flexible with respect to changes in the number of flights when a reallocation of flights is demanded or new routes or runways are considered. Although the integrated problem can theoretically lead to better results, the two-step framework proposed in this study has proven to be a valid and viable alternative, able to overcome the mentioned issues.

In view of the attained favorable results, the two-step framework appears to be suitable for extension to other applications such as the design and allocation of aircraft arrival routes, and the combined problem of departure and arrival routes. Moreover, an application with larger scale and scope, for instance, an entire airport, will also be considered in follow-on studies. In the current study, the actual influence of optimal allocation solutions on the airspace capacity and aircraft sequencing problem has not yet been considered. This issue will also be addressed in further research. Furthermore, since the results obtained by the proposed framework are Pareto solutions, it is a challenge for potential users to choose a suitable option from those solutions. Therefore, the development of selection methods and more in-depth analyses of the optimal results are necessary in future work.

### Acknowledgments

The authors would like to thank the editor and anonymous reviewers for their constructive, helpful and valuable comments and suggestions.

### Appendix A. Notation

---

$\dot{V}_{TAS}$	The derivative of the true airspeed with respect to time, $V_{TAS}$
$\dot{V}_{EAS}$	The derivative of the equivalent airspeed with respect to time, $V_{EAS}$
$\dot{s}$	The derivative of the ground distance flown with respect to time, $s$
$\dot{h}$	The derivative of the altitude with respect to time, $h$
$\dot{W}$	The derivative of the aircraft weight with respect to time, $W$
$\frac{\partial \rho}{\partial h}$	The derivative of the ambient air density $\rho$ with respect to altitude $h$
$\dot{m}_0$	Fuel flow
$T$	Thrust
$D$	Drag
$\gamma$	Flight path angle
$g_0$	Gravitational acceleration
$\rho$	Air density at sea level
$\rho_0$	Ambient air density
%PA	The percentage of people annoyed
$L_{den}$	Day-evening-night cumulative noise metric
$N_r$	Total number of departure routes (SIDs)
$N_{at}$	Total number of aircraft types
$SEL_{ki}$	Sound exposure level resulted from aircraft type $i$ on route $k$
$w_{den}$	Weighting factor
$a_{ki}$	Number of aircraft type $i$ operating on route $k$
$T$	Considered time period
$N_{pa}(\mathbf{d})$	Total number of people annoyed in Step 1
$T_{fuel}(\mathbf{d})$	Total fuel burn in Step 1
$\mathbf{d}$	Vector of design variables
$\mu_i(t)$	Bank angle of aircraft type $i$
$R$	Turn radius
$\mu_{max}$	Maximum permissible value of $\mu$
$a_i$	Number of aircraft type $i$
$fuel_i(\mathbf{d})$	Fuel burn of aircraft type $i$
$\mathbf{r}$	Design variable vector of departure routes
$O_k$	Set of optimal routes for the SID $k$
$\mathbf{a}$	Design variable vector of aircraft allocation
$a_{ik}$	Number of aircraft type $i$ at time $t$ on route $k$
$SD_s$	Vector containing SIDs having the same terminal point $s$
$T_{at,iss}$	Total number of aircraft type $i$ at time $t$ sent to departure routes having the same terminal point $s$
$N_{rk}$	Upper bound of the number of movements that route $k$ can handle in a certain period of time
$\bar{a}_{ik}$	Upper bound of the number of aircraft type $i$ on route $k$ at time $t$
$N_{pa}(\mathbf{r}, \mathbf{a})$	Total number of people annoyed in Step 2
$T_{fuel}(\mathbf{r}, \mathbf{a})$	Total fuel burn in Step 2
$fuel_{ik}(r_k)$	Fuel burn of aircraft type $i$ on route $r_k$

---

## Appendix B. Supplementary material

Supplementary data to this article can be found online at <https://doi.org/10.1016/j.trd.2019.10.003>.

## References

- ANSI/ASA, 2008. Quantities and Procedures for Description and Measurement of Environmental Sound - Part 6: Methods for Estimation of Awakenings Associated with Outdoor Noise Events Heard in Homes.
- Braakenburg, M.L., Hartjes, S., Visser, H.G., 2011. Development of a multi-event trajectory optimization tool for noise-optimized approach route design. *AIAA J.* 1–13. <https://doi.org/10.2514/6.2011-6929>.
- Casalino, D., Diozzi, F., Sannino, R., Paonessa, A., 2008. Aircraft noise reduction technologies: a bibliographic review. *Aerosp. Sci. Technol.* 12, 1–17. <https://doi.org/10.1016/j.ast.2007.10.004>.
- Deb, K., Pratap, A., Agarwal, S., Meyarivan, T., 2002. A fast and elitist multiobjective genetic algorithm: NSGA-II. *IEEE Trans. Evol. Comput.* 6, 182–197. <https://doi.org/10.1109/4235.996017>.
- Dons, J., 2012. Optimization of Departure and Arrival Routing for Amsterdam Airport Schiphol - A Noise Abatement Study. MSc thesis. Delft University of Technology.
- European Environment Agency (EEA), 2010. Good practice guide on noise exposure and potential health effects. In: EEA Technical Report.
- Federal Aviation Administration (FAA), Office of Environment and Energy, 2008. INM User's Guide, Integrated Noise Model, INM 7.0, Technical Manual, FAA-AEE-08-01.
- Federal Interagency Committee on Aviation Noise (FICAN), 1997. Effects of aviation noise on awakenings from sleep.
- Frair, L., 1984. Airport noise modelling and aircraft scheduling so as to minimize community annoyance. *Appl. Math. Model.* 8, 271–281. [https://doi.org/10.1016/0307-904X\(84\)90162-8](https://doi.org/10.1016/0307-904X(84)90162-8).
- Ganić, O., Babić, O., Čangalović, M., Stanojević, M., 2018. Air traffic assignment to reduce population noise exposure using activity-based approach. *Transp. Res. Part D Transp. Environ.* 63, 58–71. <https://doi.org/10.1016/j.trd.2018.04.012>.
- Girvin, R., 2009. Aircraft noise-abatement and mitigation strategies. *J. Air Transp. Manag.* 15, 14–22. <https://doi.org/10.1016/j.jairtraman.2008.09.012>.
- Hartjes, S., Dons, J., Visser, H.G., 2014. Optimization of area navigation arrival routes for cumulative noise exposure. *J. Aircr.* 51, 1432–1438. <https://doi.org/10.2514/1.C032302>.
- Hartjes, S., Visser, H., 2016. Efficient trajectory parameterization for environmental optimization of departure flight paths using a genetic algorithm. *Proc. Inst. Mech. Eng. Part G J. Aerosp. Eng.* 1–9. <https://doi.org/10.1177/0954410016648980>.
- Hartjes, S., Visser, H.G., Heblly, S.J., 2010. Optimisation of RNAV noise and emission abatement standard instrument departures. *Aeronaut. J.* 114, 757–767. <https://doi.org/10.1017/S0001924000004243>.
- Ho-Huu, V., Ganić, O., Hartjes, S., Babić, O., Curran, R., 2019. Air traff assignment based on daily population mobility to reduce aircraft noise effects and fuel consumption. *Transp. Res. Part D Transp. Environ.* 72, 127–147. <https://doi.org/10.1016/j.trd.2019.04.007>.
- Ho-Huu, V., Hartjes, S., Visser, H., Curran, R., 2017. An efficient application of the MOEA/D algorithm for designing noise abatement departure trajectories. *Aerospace* 4, 54. <https://doi.org/10.3390/aerospace4040054>.
- Ho-Huu, V., Hartjes, S., Visser, H.G., Curran, R., 2018a. Integrated design and allocation of optimal aircraft departure routes. *Transp. Res. Part D Transp. Environ.* 689–705. <https://doi.org/10.1016/j.trd.2018.07.006>.
- Ho-Huu, V., Hartjes, S., Visser, H.G., Curran, R., 2018b. An improved MOEA/D algorithm for bi-objective optimization problems with complex Pareto fronts and its application to structural optimization. *Exp. Syst. Appl.* 92, 430–446. <https://doi.org/10.1016/j.eswa.2017.09.051>.
- Hogenhuis, R.H., Heblly, S.J., Visser, H.G., 2011. Optimization of area navigation noise abatement approach trajectories. *Proc. Inst. Mech. Eng. Part G-J. Aerosp. Eng.* 225, 513–521. <https://doi.org/10.1177/0954410010AER0840>.
- International Civil Aviation Organization (ICAO), 2006. Procedures for air navigation services – Aircraft operations. Vol. I, Flight Procedures.
- Kim, B., Li, L., Clarke, J.-P., 2014. Runway assignments that minimize terminal airspace and airport surface emissions. *J. Guid. Control. Dyn.* 37, 789–798. <https://doi.org/10.2514/1.61829>.
- Kuiper, B.R., Visser, H.G., Heblly, S., 2012. Efficient use of an allotted airport annual noise budget through minimax optimization of runway allocations. *Proc. Inst. Mech. Eng. Part G J. Aerosp. Eng.* 227, 1021–1035. <https://doi.org/10.1177/0954410012447767>.
- Lee, D.S., Fahay, D.W., Forster, P.M., Newton, P.J., Wit, R.C.N., Lim, L.L., Owen, B., Sausen, R., 2009. Aviation and global climate change in the 21st century. *Atmos. Environ.* 43, 3520–3537. <https://doi.org/10.1016/j.atmosenv.2009.04.024>.
- Marais, K.B., Reynolds, T.G., Uday, P., Muller, D., Lovegren, J., Dumont, J.-M., Hansman, R.J., 2013. Evaluation of potential near-term operational changes to mitigate environmental impacts of aviation. *Proc. Inst. Mech. Eng. Part G J. Aerosp. Eng.* 227, 1277–1299. <https://doi.org/10.1177/0954410012454095>.
- Nuic, A., Poles, D., Mouillet, V., 2010. BADA: an advanced aircraft performance model for present and future ATM systems. *Int. J. Adapt. Control Signal Process.* 24, 850–866. <https://doi.org/10.1002/acs.1176>.
- Prats, X., Puig, V., Quevedo, J., 2011. Equitable aircraft noise-abatement departure procedures. *J. Guid. Control. Dyn.* 34, 192–203. <https://doi.org/10.2514/1.49530>.
- Prats, X., Puig, V., Quevedo, J., Nejari, F., 2010a. Lexicographic optimisation for optimal departure aircraft trajectories. *Aerosp. Sci. Technol.* 14, 26–37. <https://doi.org/10.1016/j.ast.2009.11.003>.
- Prats, X., Puig, V., Quevedo, J., Nejari, F., 2010b. Multi-objective optimisation for aircraft departure trajectories minimising noise annoyance. *Transp. Res. Part C Emerg. Technol.* 18, 975–989. <https://doi.org/10.1016/j.trc.2010.03.001>.
- Song, Z., Visser, H.G., Mingshan, H., Wei, C., 2014. Optimized multi-event simultaneous departure routes for Major Hub Airport. *Int. J. Model. Optim.* 4, 482–488. <https://doi.org/10.7763/LIMO.2014.V4.421>.
- Torres, R., Chaptal, J., Bès, C., Hiriart-Urruty, J.-B., 2011. Optimal, environmentally friendly departure procedures for civil aircraft. *J. Aircr.* 48, 11–23. <https://doi.org/10.2514/1.C031012>.
- Trivedi, A., Srinivasan, D., Sanyal, K., Ghosh, A., 2016. A survey of multiobjective evolutionary algorithms based on decomposition. *IEEE Trans. Evol. Comput.* 1–1. <https://doi.org/10.1109/TEVC.2016.2608507>.
- Visser, H.G., 2005. Generic and site-specific criteria in the optimization of noise abatement trajectories. *Transp. Res. Part D Transp. Environ.* 10, 405–419. <https://doi.org/10.1016/j.trd.2005.05.001>.
- Visser, H.G., Wijnen, R.A.A., 2003. Optimisation of noise abatement arrival trajectories. *Aeronaut. J.* 107, 607–615. <https://doi.org/10.1017/S0001924000013828>.
- Visser, H.G., Wijnen, R.A.A., 2001. Optimization of noise abatement departure trajectories. *J. Aircr.* 38, 620–627. <https://doi.org/10.2514/2.2838>.
- Yu, H., Van Kampen, E.-J., Mulder, J.A., 2016. An optimization paradigm for arrival trajectories using trajectory segmentation and state parameterization. *AIAA Guid. Navig. Control Conf.* 1–17. <https://doi.org/10.2514/6.2016-1872>.
- Zachary, D.S., Gervais, J., Leopold, U., 2010. Multi-impact optimization to reduce aviation noise and emissions. *Transp. Res. Part D Transp. Environ.* 15, 82–93. <https://doi.org/10.1016/j.trd.2009.09.005>.
- Zachary, D.S., Gervais, J., Leopold, U., Schutz, G., Huck, V.S.T., Braun, C., 2011. Strategic planning of aircraft movements with a three-cost objective. *J. Aircr.* 48, 256–264. <https://doi.org/10.2514/1.C031090>.
- Zhang, M., Filippone, A., Bojdo, N., 2018. Multi-objective optimisation of aircraft departure trajectories. *Aerosp. Sci. Technol.* 79, 37–47. <https://doi.org/10.1016/j.ast.2018.05.032>.
- Zhang, Q., Li, H., 2007. MOEA/D: a multiobjective evolutionary algorithm based on decomposition. *IEEE Trans. Evol. Comput.* 11, 712–731. <https://doi.org/10.1109/TEVC.2007.892759>.

# 6

## A MULTILEVEL OPTIMIZATION FRAMEWORK WITH INTEGRATED OPERATIONAL REQUIREMENTS

*In Chapter 5, a two-step optimization framework has been developed. However, operational conditions - mainly aircraft sequencing and separation - were not considered in this study. To take these issues into account, in this chapter three novel techniques are therefore proposed and added to the previously developed optimization framework. These techniques include a runway assignment model, a conflict detection algorithm, and a rerouting technique. Owing to the inclusion of these operational constraints, the formulation of the optimization problems has also been changed and reformulated. Finally, a completed multilevel optimization model is developed. The performance of the extended model is demonstrated through a realistic case study at Amsterdam Airport Schiphol in The Netherlands, in which 599 departure flights and 13 different standard instrument departures (SIDs) are considered.*

---

The content of this chapter is based on the following research article:

**V. Ho-Huu**, S. Hartjes, J. A. Perez-Castan, H. G. Visser, and R. Curran, *A multilevel optimization approach to route design and flight allocation taking aircraft sequencing and separation constraints into account*, Transportation Research Part C: Emerging Technologies, Under minor revision, 2019. -> Paper 6

## 6.1. PROBLEM STATEMENT

Thanks to the advantages inherited from the combination of route design and flight allocation problems, the two-step framework developed in Chapter 5 revealed the potential to considerably reduce noise impact and fuel consumption. Furthermore, the study indicated that the application of the two-step approach can help to significantly reduce the complexity of the combined problem, while keeping the quality of solutions at almost the same level as in the fully integrated (one-step) approach. Also, the framework proved to be sustainable and more efficient in terms of the computational cost and flexibility in adapting to changes in the flight schedules.

However, since the research mainly focused on the development and validation of an appropriate approach to cope with the complexity of the combined problem, some other operations-related constraints were ignored. Specifically, in the framework, the capacity limits of routes and runways were implicitly assumed to be satisfied by enforcing a constraint that limits the number of aircraft movements on each route. Moreover, because the sequencing and separation requirements for flights were essentially ignored, the results found were just simple distribution solutions that do not contain any information on individual aircraft movements.

As a continued development of the previous work, this chapter proposes three additional techniques and integrates them into the previous model to help overcome the above-mentioned research gaps. The first one is the development of a runway assignment model that is used to make sure that the separation requirements for all departing aircraft on runways are satisfied. The second additional component concerns a conflict detection algorithm that is included to check the separation requirements between aircraft along selected routes. Finally, a rerouting technique is proposed to resolve any separation violation between aircraft along the selected routes that might exist due to the assignment of flights. Furthermore, due to the inclusion of new operations-related constraints, the optimization problem in the second step of the framework has been reformulated. The details of this study are presented in Ho-Huu et al. [42].

## 6.2. CONTRIBUTIONS

The main contributions of this chapter are as follows:

1. A pure flight allocation model that takes aircraft sequencing and separation requirements at runways into account is formulated and solved. The obtained results reveal that the developed model is reliable and able to provide better options that can help significantly reduce the noise impact and fuel consumption compared with the reference case.
2. A completed multilevel optimization framework that is able to consider both the optimal route design and flight allocation problems, while taking operations-related constraints into account is proposed. The proposed framework is now able to fully address the main research objectives as stated in Chapter 1, in which for each given SID route, a suitable route and the number of movements of each aircraft type assigned to this route are defined, while taking aircraft sequencing and separation requirements for an entire operational day into account.

3. The performance of the proposed optimization framework has been demonstrated through a full case study, in which 599 departure flights and 13 different SIDs are considered. The optimization results show that the proposed model can offer conflict-free solutions which can lead to a reduction in the number of people annoyed of up to 21%, and a reduction in fuel consumption of 8% relative to the reference case solution.

## A multilevel optimization approach to route design and flight allocation taking aircraft sequencing and separation constraints into account

V. Ho-Huu<sup>†</sup>, S. Hartjes, J. A. Pérez-Castán, H. G. Visser, R. Curran

### Abstract

This paper presents the development of a multilevel optimization framework for the design and selection of departure routes, and the distribution of aircraft movements among these routes, while taking the sequence and separation requirements for aircraft on runways and along selected routes into account. The main aim of the framework is to minimize aircraft noise impact on communities around an airport, and the associated fuel consumption. The proposed framework features two consecutive steps. In the first step, for each given Standard Instrument Departure (SID), multi-objective trajectory optimization is utilized to generate a comprehensive set of possible alternative routes. The obtained set is subsequently used as input for the optimization problem in the second step. In this step, the selection of routes for each SID and the distribution of aircraft movements among these routes are optimized simultaneously. To ensure the feasibility of optimized solutions for an entire operational day, the sequence and separation requirements for aircraft on runways and along selected routes are included in this second phase. In order to address these issues, three novel techniques are developed and added to a previously developed multilevel optimization framework, *viz.*, a runway assignment model, a conflict detection algorithm, and a rerouting technique. The proposed framework is applied to a realistic case study at Amsterdam Airport Schiphol in the Netherlands, in which 599 departure flights and 13 different SIDs are considered. The optimization results show that the proposed model can offer conflict-free solutions, one of which can lead to a reduction in the number of people annoyed of up to 21%, and a reduction in fuel consumption of 8% relative to the reference case solution.

**Keywords:** trajectory optimization; aircraft allocation; aircraft noise; airport noise; aircraft separation; conflict detection.

---

<sup>†</sup> Corresponding author: V. Ho-Huu, [v.hohuu@tudelft.nl](mailto:v.hohuu@tudelft.nl); [vinh.ho.h@gmail.com](mailto:vinh.ho.h@gmail.com)  
E-mails: [s.hartjes@tudelft.nl](mailto:s.hartjes@tudelft.nl) (S. Hartjes), [javier.perez.castan@upm.es](mailto:javier.perez.castan@upm.es) (J. A. Pérez-Castán),  
[h.g.visser@tudelft.nl](mailto:h.g.visser@tudelft.nl) (H. G. Visser), [r.curran@tudelft.nl](mailto:r.curran@tudelft.nl) (R. Curran)

## 1. Introduction

Air transport is predicted to rapidly increase in the coming years due to its social and economic benefits (Boeing, 2016). The increase in air traffic volume may bring certain advantages to the development of society such as job creation, tourism, and industrial globalization. However, it also causes negative impacts on the quality of life of communities surrounding airports, especially as a result of aircraft noise nuisance and pollutant emissions (Asensio et al., 2017). Aircraft noise has been linked to various human health effects such as cardiovascular diseases, sleep disturbance, hearing loss, communication interference, and annoyance (Janssen et al., 2014; Morrell et al., 1997). Noise impact has been well recognized as one of the most significant factors leading to restrictions on the expansion of flight and airport operations (Rodríguez-Díaz et al., 2017).

In an effort to support the sustainable development of air transport, the International Civil Aviation Organization (ICAO) has provided the guideline for air traffic management (ICAO, 2016), and various approaches have been studied and proposed over the years (Casalino et al., 2008; Filippone, 2014; Gardi et al., 2015). In order to reduce noise impact caused by aircraft departure/arrival operations, noise abatement trajectory optimization has been applied to generate optimal trajectories, and a significant reduction in both the number of people affected by aircraft noise and fuel consumption has been reported (Zaporozhets and Tokare, 1998; Braakenburg et al., 2011; Hartjes et al., 2014, 2010, 2016; Ho-Huu et al., 2017, 2018; Hogenhuis et al., 2011; Prats et al., 2011, 2010b, 2010a; Song et al., 2014; Torres et al., 2011; Visser and Wijnen, 2003, 2001; Yu et al., 2016; Zhang et al., 2018). Furthermore, the development of allocation models to distribute aircraft movements over specific routes and runways have contributed to a significant reduction of aircraft noise effects (Chatelain and Van Vyve, 2018; Frair, 1984; Ganić et al., 2018; Ho-Huu et al., 2019a; Kuiper et al., 2012; Zachary et al., 2011, 2010). In addition to the research on aircraft noise reduction, research on improving airport capacity and fuel consumption has been widely conducted (D'Ariano et al. 2015; Sama et al. 2017a, 2017b, 2018, 2019).

Although a large effort has been made towards finding suitable options to support the continued growth of air transport, there is still a lack of studies that consider different aspects of flight and airport operations concurrently. In particular, research on the design of optimal routes typically considered only

one standard route at a time, while its interaction with other routes was not included, as evident from Refs. (Braakenburg et al., 2011; Hartjes et al., 2014, 2010, 2016; Ho-Huu et al., 2017, 2018; Prats et al., 2011, 2010a; Torres et al., 2011; Visser and Wijnen, 2001, 2003; Zhang et al., 2018). Although optimal routes can offer certain benefits, either in terms of noise impact or fuel burn, from an operational perspective, they might be rather difficult to apply when other factors, such as airspace capacity or aircraft separation, are not taken into account. Meanwhile, research on the allocation of aircraft to current-in-use runways and routes can provide more realistic solutions, as reported in Refs. (Chatelain and Van Vyve, 2018; Frair, 1984; Ganić et al., 2018; Kuiper et al., 2012; Zachary et al., 2011, 2010). However, these studies relied on the assumption that the optimal solutions satisfy operational requirements, such as aircraft sequence and separation. Therefore, the true influence of optimal allocation solutions on these issues has not yet adequately studied. Moreover, since these models only considered standard routes instead of optimized routes, the potential noise and fuel reduction benefits were not fully exploited. As a result, there is a need for the development of methodologies that can exploit the advantages of these two types of problems by considering them simultaneously or in a linked manner.

## 6

In recent work (Ho-Huu et al., 2019b), a two-step optimization framework was developed that can partly deal with the combination of the above two problems. Owing to the advantages inherited from the combination of optimal route design and the distribution of flights among these routes, the two-step framework revealed the potential to considerably reduce the number of people annoyed and fuel consumption. Furthermore, the study indicated that the application of the two-step approach can help to significantly reduce the complexity of the combined problem, while keeping the quality of solutions at almost the same level as in the fully integrated (one-step) approach. Also, the framework proved to be substantially more efficient in terms of the computational cost and flexibility to adapt to changes in the flight schedules. However, since this research mainly focused on the development and validation of an appropriate approach to cope with the complexity of the combined problem, some other operations-related issues were simplified. Specifically, the capacity limits of routes and runways in the framework were implicitly assumed to be satisfied by enforcing a constraint that limits the number of aircraft movements on each route. Moreover, because the sequence and separation requirements for flights were

essentially ignored, the results found were just simple distribution solutions that do not contain any information on individual aircraft movements, such as departure times.

As a continued development of the previous work, this paper proposes additional techniques and integrates them into the previous model to help overcome the above-mentioned research gaps. Similar to the previous model, the newly proposed framework also features two consecutive steps, in which Step 1 addresses the design of optimal routes, whilst Step 2 copes with the selection of routes and the distribution of flights among selected routes. Since the main research gaps of the previous work relate to Step 2, the problem model in Step 1 remains unchanged. In contrast, the optimization model in Step 2 has been reformulated as a result of the introduction of new constraints on the throughput capacity of runways and routes. In order to handle these new constraints, three new tool components are proposed. The first one is the development of a runway assignment model that is used to make sure that the safe separation requirements for all aircraft on runways are satisfied. The second additional component concerns a conflict detection algorithm that is included to check the separation requirements between aircraft along selected routes. Finally, a rerouting technique is proposed to resolve any separation violation between aircraft along the selected routes that still might exist after the conflict detection algorithm has been applied.

The proposed framework is demonstrated through a realistic case study at Amsterdam Airport Schiphol (denoted as AMS), in which a full operational day involving 599 flights and 13 different given standard instrument departure routes are considered. The obtained results are then analyzed and compared with those obtained from the reference case.

The remainder of the paper is organized as follows. Section 2 provides a brief introduction of the problem statement. Section 3 presents the proposed framework in detail, including a reformulated two-step optimization approach, a runway assignment model, a conflict detection algorithm, and a rerouting technique. Section 4 provides brief information on the optimization techniques that are used to solve optimization problems in the framework. The application of the proposed framework for a case study at AMS is presented in Section 5. Finally, conclusions are drawn in Section 6.

## 2. Problem statement

Before discussing the functioning of the proposed framework, an example of a representative problem at a generic airport is presented first. Fig. 1 shows a hypothetical example of four Standard Instrument Departure (SID) routes (hereafter referred to as SIDs<sup>‡</sup>) and the surrounding communities near an airport. Since noise caused by aircraft operations has significantly negative influences on the quality of life of communities surrounding the airport (in particular, those located near or underneath the routes), the design and selection of routes for each given SID (i.e., Question 1) should be made such as to avoid as many (highly) populated areas as possible. In addition, due to the accumulative nature of noise impact, the distribution of aircraft movements among these routes while guaranteeing aircraft sequence and separation requirements (i.e., Questions 2 and 3) is also an important factor that needs to be considered. Therefore, from a noise perspective, it is apparent that the design and use of noise-optimized routes and the optimal distribution of aircraft movements among these routes emerge as appropriate options that can help to reduce the aircraft noise impact on communities around the airport. However, due to the intricate coupling that exists between these two problems and the associated high computational cost, it is challenging to solve these problems integrally in a single step.

6

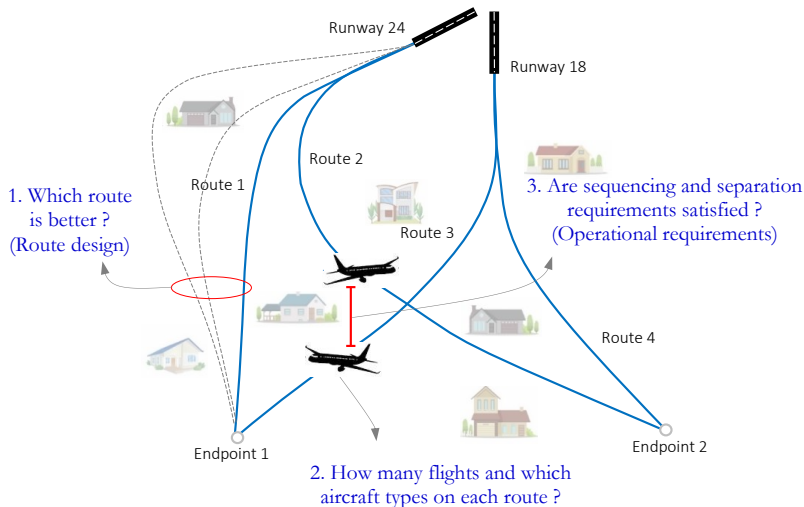


Fig. 1. An example of routes and communities around an airport.

<sup>‡</sup> Please note that the notation of SID is used to denote an existing published Standard Instrument Departure route that connects a given runway to a defined terminal endpoint, while “routes” are used in the context of this paper to represent the optimized ground tracks that are created for each SID by using an optimization algorithm.

In this work, a multilevel optimization framework is developed to overcome the complexity of the integrated problem, as well as the limitations of the computational burden. The main aim of the framework is to provide solutions that address all three questions together while minimizing the number of people affected by aircraft noise. Particularly, the final goal of the framework is to determine, for each given SID, which route is optimal, and how many movements of each aircraft type should be assigned to this route while taking aircraft sequence and separation requirements into account. Nevertheless, purely focusing on noise impact may lead to an increase in fuel burn as a result of aircraft seeking to circumnavigate populated areas. Therefore, fuel consumption is included as a second objective function in the formulation of the optimization problem. The two objectives are briefly described below.

To determine the Number of People Annoyed (hereafter defined as NPA), the  $L_{den}$ -based annoyance criterion, proposed by EEA (2010), is applied in this study. According to EEA (2010), the percentage of People Annoyed (%PA) at a given location on the ground is defined as

$$\%PA = 8.588 \times 10^{-6} (L_{den} - 37)^3 + 1.777 \times 10^{-2} (L_{den} - 37)^2 + 1.221 (L_{den} - 37) \quad (1)$$

where  $L_{den}$  is the day-evening-night noise level, determined by

$$L_{den} = 10 \log_{10} \left[ \sum_{k \in N_r} \sum_{i \in N_{at}} \sum_{j \in O_t} a_{ikj} 10^{\frac{SEL_{ik} + w_{den,j}}{10}} \right] - 10 \log_{10} T \text{ (dBA)}, \quad (2)$$

where  $N_r$  is the total number of given SIDs;  $N_{at}$  is the total number of aircraft types;  $O_t$  is the operational time, which includes day, evening and night time;  $SEL_{ik}$  is the sound exposure level caused by aircraft type  $i$  on route  $k$ ;  $w_{den,j}$  is a penalty weighting factor, which is either of 0, 5, or 10 dBA, accounting for day, evening and night time operations, respectively;  $a_{ikj}$  is the number of aircraft type  $i$  operating on route  $k$  at the time period  $j$ ; and  $T$  is the considered period of time in seconds ( $T = 24 \times 3600$  seconds in this case). In Eq. (2), the  $SEL$  metric is computed at each location on the ground by using a replication of the noise model laid down in the technical manual of ECAC (2016).

The fuel objective is determined as

$$T_{fuel} = \sum_{k \in N_r} \sum_{i \in N_{at}} a_{ik} fuel_{ik} \quad (3)$$

where  $fuel_{ik}$  is the fuel that aircraft type  $i$  consumes when operating on route  $k$ . The  $fuel_{ik}$  is calculated by using an intermediate point-mass model (Hartjes et al., 2016) and the Base of Aircraft Data (BADA) (EUROCONTROL, 2014b).

### 3. A multilevel optimization framework

In this section, the proposed multilevel optimization framework is presented in detail. The flowchart of the framework is illustrated in Fig. 2, while a description of the details will be given in the following subsections.

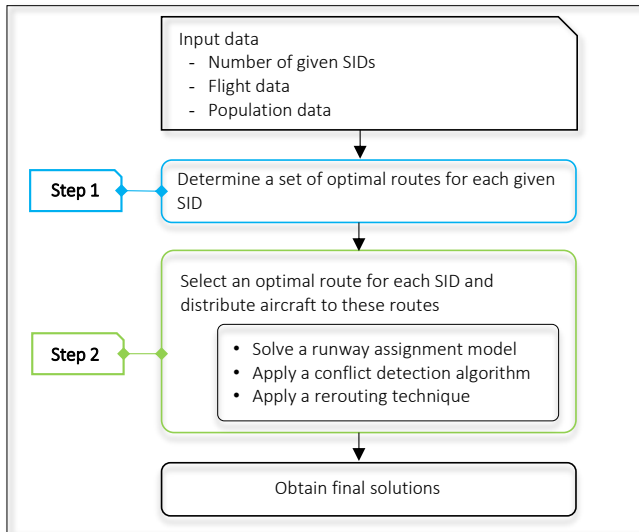


Fig. 2. Flowchart of the multilevel optimization framework.

### 3.1. A two-step approach

#### 3.1.1. Step 1: design of optimal routes

In order to generate, for each given SID, a set of optimal routes that effectively balances between NPA and fuel burn, a multi-objective trajectory optimization problem is formulated and solved. The optimization problem is defined as

$$\min_{\mathbf{p}} \quad (N_{pa}(\mathbf{p}), T_{fuel}(\mathbf{p})) \quad (4)$$

$$\text{s.t.} \quad \mu_i(t) \leq \mu_{\max}(h), \quad \forall i \in N_{at} \quad (5)$$

where  $N_{pa}(\mathbf{p})$  is the total NPA, and  $T_{fuel}(\mathbf{p})$  is the total fuel consumption of all aircraft following the SID. The design variables are the parameters that define a route; these parameters are collected in the vector  $\mathbf{p}$ . For more details about the definition of the vector  $\mathbf{p}$ , interested readers can refer to [Ho-Huu et al. \(2017; 2019b\)](#). The variable  $\mu_i(t)$  in [Eq.\(5\)](#) is the bank angle of aircraft type  $i$  during a turn at time  $t$ , and  $\mu_{max}$  is the maximum permissible value of  $\mu$ , varying according to altitude  $h$  ([ICAO, 2006](#)).

In [Eq. \(4\)](#), the objective  $N_{pa}(\mathbf{p})$  is calculated by considering the multiplication of %PA in [Eq. \(1\)](#) in each grid cell with the population in that cell and subsequent aggregation over all cells. The population density data surrounding an airport is retrieved from a Geographic Information System (GIS). The objective  $T_{fuel}(\mathbf{p})$  in [Eq. \(4\)](#) is defined similarly as in [Eq. \(3\)](#). It is noted that  $N_r$  is now by default equal to 1 since only one SID at a time is evaluated.

The optimization problem is applied for all considered SIDs. The obtained sets of optimal routes and their associated performances for all SIDs are then utilized as inputs for the optimization problem in Step 2. It should be noted that to be able to adapt to different runway configurations, the optimal routes for all given SIDs originating from each runway should be obtained.

**3.1.2. Step 2: selection of routes and distribution of flight among these routes**

Before going to the formulation of an optimization problem, it is assumed that the terminal point for each flight listed in the flight schedule is assumed to be specified in advance, based on its destination airport. From the sets of optimal routes obtained in Step 1, this step aims to determine, for each given SID, which route from the set should be selected, as well as to determine how many movements of each aircraft type should be assigned to this route for an entire day. The formulation of the flight distribution optimization problem is mathematically formulated as follows.

$$\begin{aligned} \min_{\mathbf{a}, \mathbf{r}} \quad & (N_{pa}(\mathbf{a}, \mathbf{r}), T_{fuel}(\mathbf{a}, \mathbf{r})) & (6) \\ \text{s.t.} \quad & \sum_{k \in SD_s} a_{ik} = T_{a, is}, \quad \forall i \in N_{at}, \forall s \in T_p & (7) \\ & f_d(\mathbf{a}, \mathbf{r}) = 0 & (8) \\ & f_{sr}(\mathbf{a}, \mathbf{r}) \leq 0 & (9) \\ & 0 \leq a_{ik} \leq \bar{a}_{ik}, \quad \forall k \in SD_s, \forall i \in N_{at} & (10) \end{aligned}$$

where  $\mathbf{a}$  is the design variable vector of flight distribution, in which  $a_{ik}$  is the number of aircraft type  $i$  on route  $k$ . The vector  $\mathbf{r} = \{r_1, \dots, r_k, \dots, r_{N_r}\}$  is the design variable vector of route selection, where the preferred route  $r_k$  is chosen from the set of optimal routes  $\mathbf{O}_k$  obtained in Step 1 for SID  $k$ . The index  $s$  relates to the terminal point (defined as the endpoint of each departure procedure), and  $T_p$  is the set of terminal points,  $s \in T_p$ . The vector  $SD_s$  is the vector that collects the SIDs which share the same terminal point  $s$ . The parameter  $T_{a, is}$  is the total number of aircraft type  $i$  assigned to SIDs having the same terminal point  $s$ . Eq. (10) represents the set of boundary constraints on the design variables, where the parameter  $\bar{a}_{ik}$  is the upper bound of the number of aircraft type  $i$  on route  $k$ , and it can be extracted from the flight schedule as the total number of aircraft type  $i$  assigned to SIDs having the same terminal point. The function  $f_d(\mathbf{a}, \mathbf{r})$  is a constraint imposing the separation requirements between aircraft on the runways and is defined in the runway assignment model presented in Section 3.2. Similarly, the function  $f_{sr}(\mathbf{a}, \mathbf{r})$  is related to safeguarding the separation requirements between aircraft along the selected routes and is defined in the conflict detection algorithm presented in Section 3.3.

## 6

In the above optimization problem (Eqs. (6-10)), the objectives  $N_{pa}(\mathbf{a}, \mathbf{r})$  and  $T_{fuel}(\mathbf{a}, \mathbf{r})$  are defined in a similar fashion as in Step 1. However, the design variables considered here are different. Particularly, the design variables in this step represent the routes selected from the sets of available optimal routes for each SID, and the distribution of flight among these routes. Meanwhile, the design variables in Step 1 are the geometric parameters that are used to construct a SID route. Note that the two objective functions in Eq. (6) are only calculated if the constraint in Eq. (8) is satisfied; otherwise, large numbers are assigned to the criteria, representing penalties on an infeasible solution. This avoids the computationally expensive calculation of the objective values when infeasible solutions are considered. Also, all the information associated with routes and aircraft types is known a priori in Step 2, as this information has been stored in Step 1.

### 3.2. Runway assignment model

The main objective of the model is to find, for any given instance of  $(\mathbf{a}, \mathbf{r})$  considered in Step 2, a suitable conflict-free solution for the assignment of individual flights to specific routes and runways, while

minimizing the total departure delay (relative to the departure times listed in the flight schedule) at runways. It is noted that the original objectives in Eq. (6) – NPA and fuel – are the focus of the main distribution algorithm, which determines which share of the total movements (for each aircraft type) are assigned to a specific route. In other words, the flight distribution optimization problem only considers the flows of aircraft movements. The flight to runway assignment model, on the other hand, merely determines how individual flights are assigned to runways, essentially looking for a conflict-free realization at the runways of the flow solution generated by the flight distribution optimization algorithm, taking departure times into account. Therefore, the flight to runway assignment has no impact on the original objectives NPA and fuel. It is important to note that although the runway assignment model yields solutions that are free of conflict at the departure runway, separation conflicts might still occur down-route. The handling of potential down-route conflicts is discussed in Section 3.3. It is also important to note that when a flight is assigned to a runway, its route is automatically determined. The flight to runway assignment model is mathematically written as follows.

$$\min_{\mathbf{x}, \mathbf{d}} \quad \sum_{j \in J} d_j \tag{11}$$

$$\text{s.t.} \quad (t_{j+1} + d_{j+1}) - (t_j + d_j) - Mx_{j+1}^r - Mx_j^r \geq t_s - 2M, \forall j \in J, \forall r \in R \tag{12}$$

$$(t_{j+1} + d_{j+1}) \geq (t_j + d_j), \forall j \in J \tag{13}$$

$$\sum_{r \in R} x_j^r = 1, \forall j \in J \tag{14}$$

$$\sum_{j \in J} c_{jis} x_j^r = N_{is}^r, \forall i \in N_{at}, \forall s \in T_p, \forall r \in R \tag{15}$$

where  $\mathbf{x}$  is the vector of binary design variables  $x_j^r$ , in which  $x_j^r$  represents the assignment of flight  $j$  to runway  $r$ ,  $x_j^r \in \{0,1\}$ . The vector  $\mathbf{d}$  is the vector of delay variables  $d_j$ , where  $d_j$  ( $d_j \geq 0$ ) represents the departure delay of flight  $j$  at the runway. The parameters  $J$  and  $R$  are, respectively, the set of flights in the flight schedule and the set of runways. The parameter  $t_j$  is the scheduled departure time of flight  $j$ , and  $t_s$  is the required time separation, which depends on the weight classes of following and leading aircraft, as indicated in EUROCONTROL (2018) (see Table 1). Note that the empty fields in Table 1 indicate a minimum departure interval of 60 seconds (Delsen, 2016). The parameter  $c_{jis}$  is the constraint coefficient of flight  $j$  that is associated with aircraft type  $i$  and terminal point  $s$ . The coefficient  $c_{jis}$  will

be equal to 1 if flight  $j$  of aircraft type  $i$  flies to terminal point  $s$ , otherwise it will be equal to 0. The parameter  $N_{is}^r$  is the total number of aircraft type  $i$  departing from runway  $r$  to terminal point  $s$ . It is noted that, for any instance of  $(\mathbf{a}, \mathbf{r})$  produced by the aircraft distribution optimization algorithm, the parameters  $N_{is}^r$  can be determined up front from the flight schedule information.

**Table 1.** RECAT-EU wake turbulence time-based separation minima on departure (EUROCONTROL, 2018).

RECAT-EU scheme		"SUPER HEAVY"	"UPPER HEAVY"	"LOWER HEAVY"	"UPPER MEDIUM"	"LOWER MEDIUM"	"LIGHT"
Leader / Follower		"A"	"B"	"C"	"D"	"E"	"F"
"SUPER HEAVY"	"A"		100s	120s	140s	160s	180s
"UPPER HEAVY"	"B"				100s	120s	140s
"LOWER HEAVY"	"C"				80s	100s	120s
"UPPER MEDIUM"	"D"						120s
"LOWER MEDIUM"	"E"						100s
"LIGHT"	"F"						80s

In the optimization problem (Eqs. (11-15)), the objective function represents the minimization of the total departure delay. The first constraint aims to ensure that the separation requirement between two consecutive aircraft on the same runway is always satisfied. The parameter  $M$  in the constraint is a large number (e.g.,  $10^6$ ) that helps to render the constraint inactive in the case that two consecutive aircraft are assigned to two different runways. For example, if two consecutive aircraft are assigned to two different runways (i.e.,  $x_j^r = 1$  and  $x_{j+1}^r = 0$  or  $x_j^r = 0$  and  $x_{j+1}^r = 1$ ), and the separation time between them is smaller than  $t_s$ , the constraint is still satisfied, which can be readily inferred from Eq. (12). In contrast, if two consecutive aircraft are assigned to the same runway, the separation between them has to be larger than  $t_s$ ; otherwise, the allocation solution is infeasible. The second constraint Eq. (13) ensures that the sequence of flights listed in the flight schedule is kept unchanged when departure delays are introduced. The third constraint guarantees that each flight is assigned to one runway only. Finally, the last constraint aims to ensure that the assignment of aircraft on each runway always matches the

information of the distribution variables in the main optimization problem in Step 2 and complies with the flight information and aircraft sequence as given in the flight schedule.

In order to determine the constraint Eq. (8) in Step 2, the function  $f_d(\mathbf{a}, \mathbf{r})$  is defined as

$$f_d(\mathbf{a}, \mathbf{r}) = \sum_{j \in J} d_j - \bar{D} \tag{16}$$

where  $\bar{D}$  is the total delay at the runways, which is derived from the runway assignment problem without considering the distribution constraint Eq. (15). Therefore, the delay  $\bar{D}$  is independent from the solution  $(\mathbf{r}, \mathbf{a})$  and can be calculated up front by solving the optimization problem in Eqs. (11-14) based on a given flight schedule and set of available runways. Meanwhile, the delay  $\sum d_j$  in Eq. (16) associated to a solution instance  $(\mathbf{r}, \mathbf{a})$  might be influenced by the inclusion of the constraint Eq. (15). Since the problem in Eqs. (11-14) represents a relaxation of the problem in Eqs. (11-15), the value of  $\bar{D}$  will not exceed that of  $\sum d_j$ . Therefore, the constraint  $f_d(\mathbf{a}, \mathbf{r}) = 0$  enforced in Eq.(8) makes sure that the solutions obtained by the optimization problem in Step 2 do not cause a delay compared with the delay  $\bar{D}$ , and hence the runway capacity is kept at the maximum level.

### 3.3. Conflict detection algorithm

Once the result of the runway assignment model has been returned, an additional check is carried out with respect to the satisfaction of constraint Eq. (9) along the routes. If the returned result does not satisfy the delay constraint Eq. (8), the check is no longer needed, and a large penalty number is assigned to this constraint. Otherwise, a conflict detection algorithm will be evoked to check the separation requirement of aircraft along the selected routes.

From the flight schedule and the assignment solution returned by the assignment model, the route information and associated performance can be obtained for each flight. This information comprises the flight trajectory (i.e., position coordinates, velocity, altitude, time), fuel burn and noise value (i.e., SEL). After the trajectories for all flights in the flight schedule have been defined, a simulation process is carried out for all flights contained in the schedule, using an iteration time step of 10 seconds (as suggested by Isaacson and Erzberger (1997)). In order to check the aircraft separation requirements in both vertical and horizontal dimensions, the distance separation minima suggested by ICAO (2016) and

EUROCONTROL (2018) is applied. The vertical separation is set to 1,000 ft (ICAO, 2016), while the horizontal separation standards are given in Table 2 (EUROCONTROL, 2018). The horizontal separation is defined here as the Euclidean distance in the horizontal plane between the aircraft in each pair (Isaacson and Erzberger, 1997; Visser, 2008). It is noted that the separation minima indicated in Table 2 are applied to flights operating on the same routes, while for those operating on different routes, a minimum radar separation of 3 NM is enforced. It should also be noted that only the wake vortex separation minima are enforced and that all runways are assumed to be operated independently, i.e., departures can take place simultaneously at all runways. The main procedure of the algorithm is described in Algorithm 1.

Table 2. RECAT-EU wake turbulence distance-based separation minima on approach and departure. (EUROCONTROL, 2018).

RECAT-EU scheme		"SUPER HEAVY"	"UPPER HEAVY"	"LOWER HEAVY"	"UPPER MEDIUM"	"LOWER MEDIUM"	"LIGHT"
Leader / Follower		"A"	"B"	"C"	"D"	"E"	"F"
"SUPER HEAVY"	"A"	3 NM	4 NM	5 NM	5 NM	6 NM	8 NM
"UPPER HEAVY"	"B"		3 NM	4 NM	4 NM	5 NM	7 NM
"LOWER HEAVY"	"C"		(*)	3 NM	3 NM	4 NM	6 NM
"UPPER MEDIUM"	"D"						5 NM
"LOWER MEDIUM"	"E"						4 NM
"LIGHT"	"F"						3 NM

(\*) means minimum radar separation (MRS), set at 2.5 nautical mile (NM), is applicable as per current ICAO doc 4444 provisions.

Algorithm 1. Conflict detection algorithm.

---

**Input:**  
 - Flight data;  
 - Route trajectories;  
 - Time step; starting time, ending time;  
 - Set the couple of flights violating the required distance separation ( $VS$ ) to 0,  $VS = 0$ ;

---

**For** each time step  
     Define flights entering into the time window;  
     Extract the flight trajectories for these flights;  
     Calculate the vertical distance for each couple of flights;  
     **For** each couple of flight  
         **If** the vertical separation is violated  
             Calculate the horizontal distance  
             **If** the horizontal separation is violated  
                 Set  $VS = VS + 1$ ;  
         **End**  
     **End**  
**End**

---

**Output:** A set of couple of flights violating the required separation,  $VS$ .

---

Once the algorithm has terminated, the number of instances of flights violating the required distance separation standards is stored in the parameter  $VS$ . If  $VS$  is equal to 0, the constraint in Eq. (9) is satisfied, and hence the allocation solution is feasible. Otherwise, the allocation solution is infeasible.

It should be noted that the resolution of the runway assignment problem in Section 3.2 may lead to a situation in which multiple (non-unique) optimal solutions are found. Since the assignments of aircraft on runways for the various optimal solutions may lead to different conflict situations down-route, the conflict algorithm will be applied for each optimal solution obtained by the runway assignment model. Subsequently, the solution without any conflicts or that with the smallest number of conflict cases is selected. In the latter case, the rerouting technique will be subsequently applied to the identified conflicting flights and will be presented in detail in the following section.

### 3.4. Rerouting technique

The conflict detection algorithm is applied to every distribution solution obtained for the optimization problem in Eqs. (6-10). If any couple of flights in these solutions violate separation minima which is discovered by the conflict detection algorithm, a rerouting technique is used. The idea behind the rerouting method is similar to that of the vectoring solutions as currently issued by Air Traffic Controllers (ATC), which is used to resolve the conflict between flights listed in the schedule when they fly along the selected routes. In the rerouting method, alternative routes are assigned to each pair of

flights whose separation distances violate the specified minima while still optimizing noise impact and fuel consumption. To this end, an optimization problem is formulated and solved for each pair of conflicting flights in the flight distribution solution. The associated optimization problem is written as follows.

$$\min_{\mathbf{r}_{ac}} w_1 \frac{N_{pa}(\mathbf{r}_{ac})}{N_{pa}(\mathbf{a}, \mathbf{r})} + w_2 \frac{T_{fuel}(\mathbf{r}_{ac})}{T_{fuel}(\mathbf{a}, \mathbf{r})} \quad (17)$$

$$\text{s.t.} \quad f_{sr}(\mathbf{r}) = 0 \quad (18)$$

where  $\mathbf{r}_{ac}$  is the design variable vector of alternative routes for the pair of conflicting flights whose separation violates the separation standard; the alternative routes are again selected from the sets of optimal routes obtained in Step 1. The objective function is the normalization of the NPA and fuel consumption, in which  $N_{pa}(\mathbf{r}_{ac})$  and  $T_{fuel}(\mathbf{r}_{ac})$  are the NPA and the total fuel burn associated with new alternative routes for conflicting flights, respectively; and  $N_{pa}(\mathbf{a}, \mathbf{r})$  and  $T_{fuel}(\mathbf{a}, \mathbf{r})$  are, respectively, the NPA and the total fuel burn associated with the design variables of the optimization problem in Eqs. (6-10). Note that  $N_{pa}(\mathbf{a}, \mathbf{r})$  and  $T_{fuel}(\mathbf{a}, \mathbf{r})$  are known at this stage. The parameters  $w_1$  and  $w_2$  are the weighting factors, which are used to transfer a bi-objective optimization problem into a single objective one. In this case,  $w_1$  and  $w_2$  are set to 0.5 with the aim of giving an equal priority to both the NPA and fuel consumption. This setting also aims to retain the diversity of solutions in the original Pareto front. As illustrated in Fig. 3, due to the use of the equivalent weight of 0.5 for both objectives, the solution obtained by the optimization problem in this section is expected to be located along the dotted diagonal line, which is the line having an angle of 45 degrees relative to the horizontal axis.

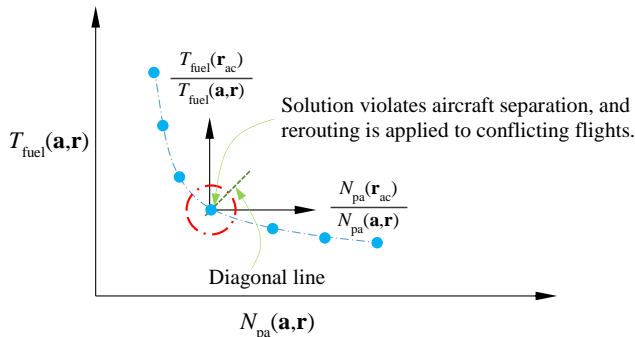


Fig. 3. Illustration of the optimal solution of the optimization problem in Eqs. (17-18).

The evaluation of the constraint is performed by evoking the conflict detection algorithm in Section 3.3. In this case, however, only flights involved in a time interval, within which conflict between flights take place, are taken into account. The time interval is determined by the total travel time of the pair of conflicting flights from the runways to the endpoints. To make sure the selection of new routes for the conflicting flights do not cause any conflicts to other flights outside of the time interval, the travel time of the conflicting flights is estimated based on the longest route stored in the set of available routes for each SID. The determination of the time interval and the identification of flights within this interval is illustrated in Fig. 4. In the figure, the two conflicting flights are  $f_3$  and  $f_4$ ; the time interval is delimited by the starting time of flight  $f_3$  and the ending time of flight  $f_4$ ; and the flights involved in this time interval are  $f_1, f_2$ , and  $f_5$ . Since only flights operating within the time interval are considered, the rerouting of conflicting flights does not influence flights outside this time interval. Furthermore, since typically only a few flights in the flight schedule are involved, the computational cost of solving the problem in this step is relatively small, just a few seconds of CPU time.

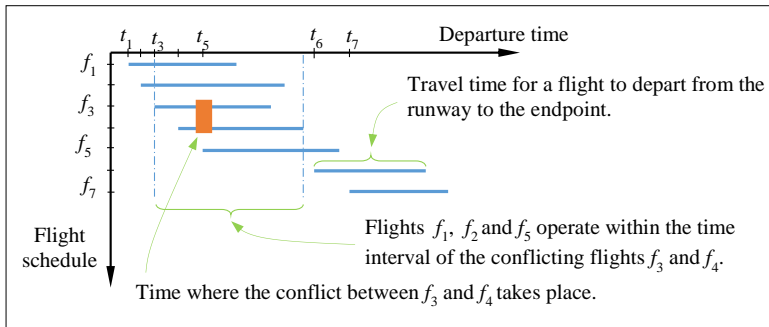


Fig. 4. Illustration of the number of flights involved in the time interval within which the conflict takes place.

When the conflict detection tool identifies more than one pair of conflicting aircraft, the rerouting algorithm is sequentially applied to each conflicting pair. Note that the rerouting technique is applied to every distribution solution obtained for the optimization problem in Eqs. (6-10) if the solution contains any couple of flights violating the separation standard.

#### 4. Optimization techniques

As can be seen in Section 3, four different optimization problems have been established. The first two problems are nonlinear multi-objective parameter optimization problems. The third problem is a mixed integer linear programming problem (MILP) which is nested in the second problem, and the last one is a nonlinear single-objective parameter optimization problem. To solve these four problems, four different optimization methods are used. For the first problem (Eqs. (4-5)), the Multi-objective Optimization Evolutionary Algorithm based on Decomposition (MOEA/D), as proposed by Zhang and Li (2007) and improved by Ho-Huu et al. (2017), is applied. This choice is motivated by the fact that MOEA/D has been demonstrated to be an efficient method to deal with this type of problems (Ho-Huu et al., 2017). Meanwhile, the Non-dominated Sorting Genetic Algorithm (NSGA-II) (Deb et al., 2002) is utilized to solve the second problem (Eqs. (6-10)). The preference for this method is, in this case, because the design space of this problem is very restricted, and hence the solutions easily violate the constraints. Therefore, NSGA-II is more suitable than MOEA/D in this case. A mixed integer linear solver from the CPLEX optimization suite/library<sup>§</sup> is applied to solve the linear optimization problem (Eqs. (11-15)). Finally, the last problem (Eq. (17-18)) is solved by using the Differential Evolution (DE) algorithm (Storn and Price, 1997). For more details on MOEA/D, NSGA-II, and DE, interested readers are referred to Refs. (Ho-Huu et al., 2017; Zhang and Li, 2007), (Storn and Price, 1997), and (Deb et al., 2002), respectively. It should be noted that, in order to deal with the equality constraint in Eq. (7), a constraint handling technique developed in (Ho-Huu et al., 2018) has been applied and coupled to the NSGA-II algorithm. Please note that since some of the applied optimization methods, including MOEA/D, NSGA-II and DE, are heuristic methods, the solutions obtained by these methods are only approximate or nearly optimal solutions.

#### 5. Numerical results and discussion

In this section, the reliability and efficiency of the proposed framework are evaluated using a realistic case study at Amsterdam Airport Schiphol (denoted as AMS) in The Netherlands. On the selected

<sup>§</sup>[https://www.ibm.com/support/knowledgecenter/SSSA5P\\_12.9.0/ilog.odms.cplex.help/CPLEX/MATLAB/topics/cplex\\_matlab\\_overview.html](https://www.ibm.com/support/knowledgecenter/SSSA5P_12.9.0/ilog.odms.cplex.help/CPLEX/MATLAB/topics/cplex_matlab_overview.html) (accessed 6 January 2020).

reference day, 599 departure flights were recorded, that operated on two runways, viz., RWs 24 and 18L (Dons, 2012), as shown in Fig. 5.



Fig. 5. Illustration of real departure operations at AMS.

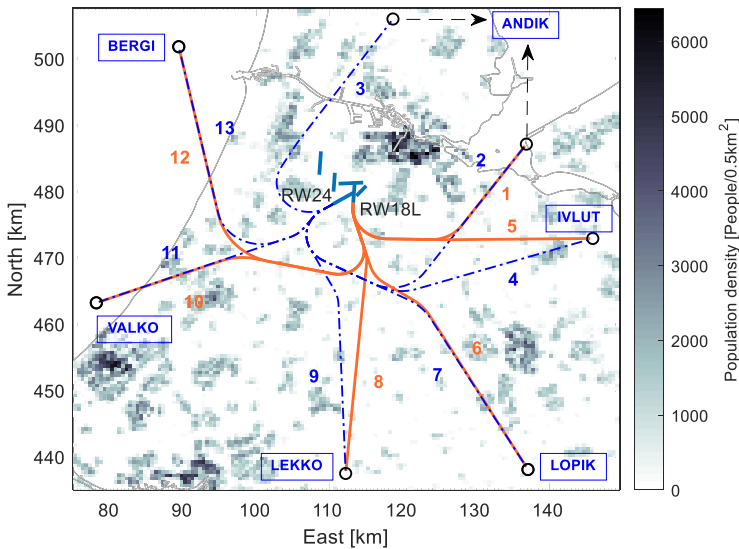


Fig. 6. Illustration of departure routes at AMS.

According to the flight data and the Aeronautical Information Publication (AIP)\*\*, 13 distinct SIDs were in use on the reference day, as shown in Fig. 6. In the figure, the solid routes originating from RW18L are highlighted and numbered in orange, while the dashed routes originating from RW24 are highlighted and numbered in blue. There are 6 terminal points (defined as the endpoints of departure

\*\* <https://www.lvn.nl/eaip/2019-12-19-AIRAC/html/index-en-GB.html> (accessed 2 January 2020).

procedures in this study), *viz.* ANDIK, IVLUT, LOPIK, LEKKO, VALKO and BERGI. Each terminal point is connected by two routes originating from either RW24 or RW18L, except for ANDIK that is connected by three routes, consisting of route 1 from RW18L and routes 2 and 3 from RW24. Note that, from the assignment solution produced by the runway assignment model, the assignment of flights to routes for the terminal points IVLUT, LOPIK, LEKKO, VALKO, and BERGI is automatically known, as there is only a single route available from each runway.

However, for the terminal point ANDIK, two different routes are available from RW24 runway, and hence an additional step is needed. To determine which flight is assigned to either route 2 or 3 from RW24, the following heuristic rule is applied. In order to reduce the number of potential crossing conflicts between flights during the peak hours, flights operating in this time period are assigned to route 3 until its capacity limit is reached; the remainder of the flights are assigned to route 2.

Though many different aircraft types operate on these routes, for the sake of simplicity, all flight movements are represented here by either of three aircraft types, namely, Fokker 100 (F100), Boeing 737-800 (B738), and Boeing 777-300 (B773). It is assumed that the F100, B738, and B773, respectively, represent lower medium (LM), upper medium (UM) and upper heavy (UH) aircraft, as classified by EUROCONTROL (2015). The population data provided by the Dutch Central Bureau of Statistics (CBS) (Centraal Bureau voor de Statistiek) with a grid cell size of 500 x 500 m, as shown in Fig. 6, is used. The detailed data of aircraft movements is provided in Table 3. All the simulations are carried out in MATLAB 2018b on an Intel Core i5 and 8GB RAM desktop.

Table 3. The detailed data for aircraft operations.

Terminal point	Number of aircraft movements			
	Entire day [LM, UM, UH]	Day (7h00-19h00) [LM, UM, UH]	Evening (19h00-23h00) [LM, UM, UH]	Night (23h00-7h00) [LM, UM, UH]
ANDIK	[45, 22, 8]	[32, 14, 3]	[6, 6, 5]	[7, 2, 0]
IVLUT	[74, 98, 43]	[57, 69, 28]	[9, 10, 12]	[8, 19, 3]
LOPIK	[7, 11, 2]	[4, 9, 2]	[2, 1, 0]	[1, 1, 0]
LEKKO	[35, 76, 3]	[30, 46, 3]	[3, 8, 0]	[2, 22, 0]
VALKO	[36, 31, 12]	[27, 24, 10]	[4, 4, 1]	[5, 3, 1]
BERGI	[34, 26, 36]	[27, 18, 35]	[4, 7, 0]	[3, 1, 1]
Total	[231, 264, 104]	[177, 180, 81]	[28, 36, 18]	[26, 48, 5]

### 5.1. Evaluation of the distribution model in Step 2

Since the aircraft sequence and separation requirements are considered and integrated into the distribution model in Step 2, it is important to investigate the performance of this model independently.

The main aim of this investigation is to see whether, based on the current SIDs, the model can provide better distribution options to reduce noise impact and fuel consumption compared with the reference case.

Before executing the model, the reference case is determined first. The reference case considers the 599 flights, as shown in Fig. 5. It is noted that due to capacity reasons, the flights in Fig. 5 have been vectored by Air Traffic Controllers (ATC). In order to make the calculation of the reference case simpler, it is assumed here that all vectored flights are simply assigned to one of the fixed routes as shown in Fig. 6. By recreating the traffic flow based on the reference data (which include the actual departure times) and the standard routes as defined in Fig. 6, the number of people annoyed and the total fuel burn in ton are 75,800 and 332.20, respectively, and there is no delay at the runways, i.e.,  $\bar{D}=0$ . The result also shows that 8 cases of flights which violate the required separation minima emerge. Nevertheless, the number of conflicting flights remains small, representing less than 2% of the total traffic volume. For comparison purposes, therefore, it is assumed that all distribution solutions derived from the distribution model are deemed acceptable if they feature less than 8 violations.

To solve the problem defined by Eqs. (6-10), the NSGA-II algorithm with a population size of 70 and a maximum number of 1500 generations (Gen.), as used in Ho-Huu et al. (2019a), is applied. Fig. 7 shows the optimal results obtained by the distribution model and the solution to the reference case. As expected, it can be seen from Fig. 7 that all the solutions from the model dominate that of the reference case and are much better in both the NPA and fuel consumption. In addition, only 7 violations are recorded for solutions obtained by the proposed model, which is one case less compared with that of the reference scenario. Note that in this section the rerouting technique is not yet applied.

Regarding the performance of the optimization algorithm, it can be seen from Fig. 8 that the algorithm has a good convergence rate. After 1200 generations, the solutions start to converge, and there are no significant changes after 1300 generations. The total time for the algorithm to reach the final generation is 7.39 hours. It should be noted that because the flight schedule can be obtained some days in advance, the model can be used as a planning tool to deliver reasonable solutions for the assignment of flights a priori. Furthermore, owing to the independent evaluation of objective functions in the

optimization algorithm, the computational cost of the distribution problem can be further improved by using parallel computing with multiple cores or cluster computing.

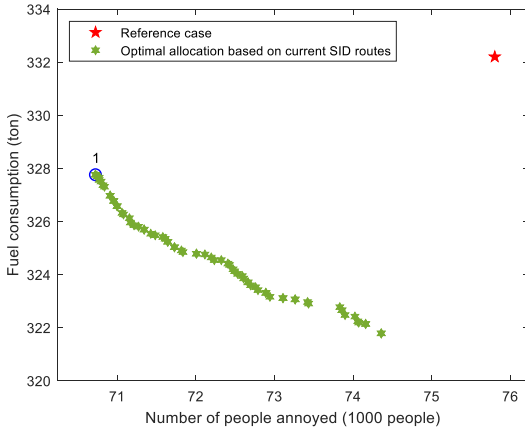


Fig. 7. Comparison of the NPA and fuel consumption obtained for the reference case and the optimized distribution solutions based on the current SID routes.

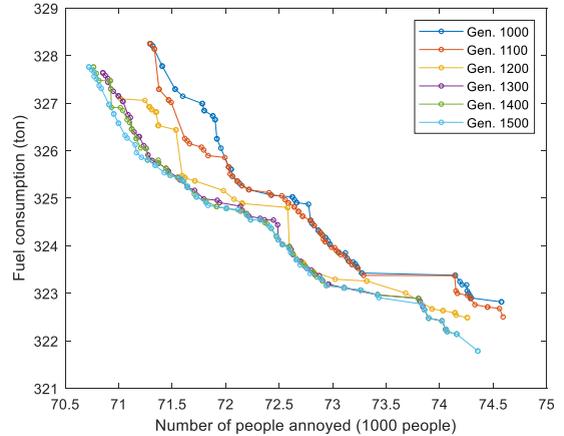


Fig. 8. Convergence history of the optimized distribution solutions based on the current SID routes.

## 6

To further examine the advantage of the model, a single representative solution, i.e., solution 1 as highlighted in Fig. 7, is selected for further analyses. The  $L_{\text{den}}$  noise contours associated to this solution are illustrated in Fig. 9, along with those resulting from the reference case. As can be seen from the figure, there is a distinct difference in the size of the  $L_{\text{den}}$  contours between the two solutions. Indeed, the contours associated with solution 1 appear to avoid populated regions better than those associated to the reference case, hence leading to a reduction in the NPA.

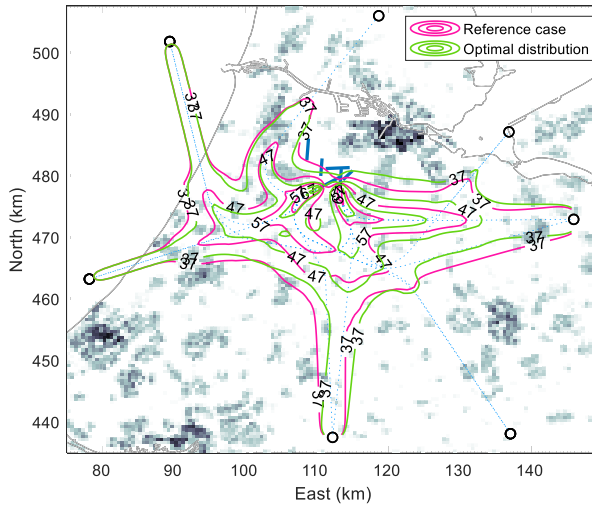


Fig. 9. Comparison of the  $L_{den}$  noise contours caused by the reference case and the optimized distribution solution (solution 1) based on current SIDs.

To provide a better understanding of the reason leading to the change of the contours in Fig. 9, the distribution of flights among the routes obtained in solution 1 is also provided numerically in Table 4. At first glance, it can be noted in Table 4 that there is a large shift of aircraft movements between routes 8 and 9. Specifically, on route 8 in the reference case, there are 44 daytime flights (21 F100s, 20 B738s and 3 B773s), 11 evening flights (3 F100 and 8 B738s), and no night flights, whilst in solution 1 there are 74 daytime flights (27 F100s, 44 B738s and 3 B773s), 10 evening flights (2 F100s and 8 B738s), and up to 24 night flights (2 F100s and 22 B738s). This redistribution of movements explains why in Fig. 9 the contours shift to the right of routes 8 and 9, which, evidently, results in a reduction in the NPA. Moreover, since the track along route 8 is shorter than that of route 9, more aircraft are assigned to route 8, and more fuel can be saved. The same situation can also be observed in the distribution of flights among routes 4 and 5, contributing to a significant reduction in fuel burn as a result of aircraft flying on a shorter route.

Table 4. Comparison of flight distribution obtained by the reference case and the optimized distribution solution (solution 1) based on current SIDs.

Route number	Approach	Day			Evening			Night		
		F100	B738	B773	F100	B738	B773	F100	B738	B773
1	RC*	0	0	0	2	2	2	0	0	0
	OD#	11	10	2	2	4	3	7	2	0
2	RC	3	5	2	0	1	1	7	2	0
	OD	0	0	0	0	0	0	0	0	0
3	RC	29	9	1	4	3	2	0	0	0
	OA	21	4	1	4	2	2	0	0	0
4	RC	20	31	15	1	2	1	8	19	3

	OD	3	2	3	0	0	3	0	0	0
	RC	37	38	13	8	8	11	0	0	0
5	OD	54	67	25	9	10	9	8	19	3
	RC	3	6	0	2	1	0	0	0	0
	OD	3	9	2	2	1	0	1	1	0
6	RC	1	3	2	0	0	0	1	1	0
	OD	1	0	0	0	0	0	0	0	0
	RC	21	20	3	3	8	0	0	0	0
	OD	27	44	3	2	8	0	2	22	0
7	RC	9	26	0	0	0	0	2	22	0
	OD	3	2	0	1	0	0	0	0	0
	RC	0	0	0	0	2	0	0	0	0
	OD	13	17	4	0	1	1	5	3	1
8	RC	27	24	10	4	2	1	5	3	1
	OD	14	7	6	4	3	0	0	0	0
	RC	0	0	0	0	3	0	0	0	0
	OD	2	7	13	1	3	0	1	1	1
9	RC	27	18	35	4	4	0	3	1	1
	OD	25	11	22	3	4	0	2	0	0

RC<sup>\*</sup>: Reference Case; OD<sup>#</sup>: Optimized Distribution

Based on the results obtained above, it can be concluded that the distribution model in Step 2 is reliable and effective. The proposed model can provide better distribution options in terms of both noise impact and fuel consumption.

## 6

### 5.2. Evaluation of the entire framework

In this section, the performance of the framework in its entirety is evaluated. However, in Step 1 of the framework, the set of optimized routes for each given SID can be obtained by using either 2D optimization or 3D optimization. For the 2D optimization, only ground tracks are optimized while vertical profiles comply with standard departure procedures, such as Noise Abatement Departure Procedures 1 and 2 (NADP1, NADP2) (ICAO, 2006). For the 3D optimization, both ground tracks and vertical profiles are optimized simultaneously. Therefore, before generating the optimized solutions, a comparison of these two approaches is first carried out in the next subsection. This comparison also aims to provide a better understanding of the final optimized solutions for the complete problem, which will be considered in Section 5.2.2.

#### 5.2.1. A comparison of optimized routes based on the different settings of vertical profiles

In order to evaluate the influence of the vertical profiles, including NADP1, NADP2, and optimized vertical profiles, on the noise impact and fuel consumption, three distinct optimization problems corresponding to three different vertical profile scenarios are performed for an example route. For this

comparison, route 3 is used. The evaluation is also a first study that compares the two different settings of vertical profiles in the field of the aircraft route design problem. To determine optimized solutions, the number of aircraft, as indicated in [Table 3](#) for the terminal point ANDIK with an additional 30% of traffic (which accounts for a potential increase in the number of movements due to the application of the distribution algorithm), is applied. For further details on the motivation to add 30% extra traffic, interested readers are encouraged to read [Ho-Huu et al. \(2019b\)](#). For each optimization problem, aircraft of all types follow a shared ground track, but each with its own distinct vertical profile, which is either a standard procedure or an optimized vertical profile. A SID is assumed to start at the end of the runway at an altitude of 35 ft AGL and at a take-off safety speed  $V_2+10$  kts, and to terminate at an altitude of 6,000 ft and an equivalent airspeed of 250 kts. To solve the three optimization problems, the MOEA/D algorithm with a population size of 50 and a maximum of 1,000 generations, as used in [Ho-Huu et al. \(2017\)](#), is applied. To generate optimized routes for each SID in Step 1 of the framework, the same approach is also applied to all the 13 SIDs.

The optimized solutions are shown in [Fig. 10](#). It can be seen in [Fig. 10](#) that, as expected, the optimized vertical profile is the best approach and significantly outperforms NADP1 and NADP2, while NADP2 generally performs better than NADP1. A closer look at [Fig. 10](#) shows that there are still two NADP1-based solutions that dominate some of the NADP2-based solutions. The reason for this is that, due to the focus on climbing in the initial phase of the departure, the airspeed in a NADP1 is lower than for a NADP2. The lower airspeed allows aircraft to make tighter turns over less populated regions while still satisfying the bank angle constraints, as defined by [Eq. \(5\)](#).

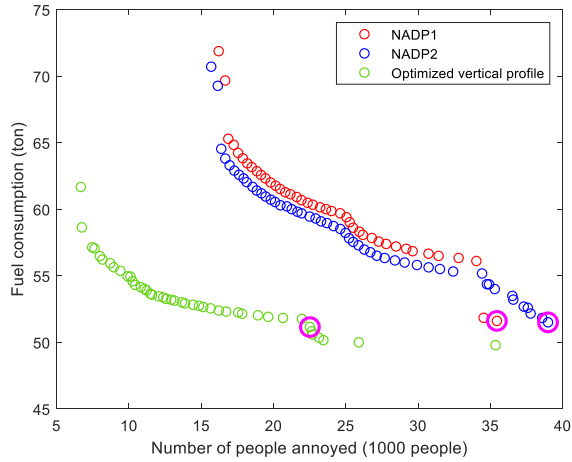


Fig. 10. Comparison of the optimized solutions obtained by NADP1, NADP2 and optimized vertical profiles.

Fig. 11 illustrates the optimized ground tracks obtained for three different optimization problems. It can be observed in Fig. 11 that all ground tracks attempt to avoid populated areas as far as possible. While the differences between the ground tracks obtained by using NADP1 and NADP2 are small, they are quite significant between those obtained by 3D optimization and 2D optimization. For a better understanding of the combination of ground tracks and vertical profiles, some representative solutions of each case, as highlighted in Fig. 11 in yellow, are selected. The vertical profiles derived from a B738 for each approach are depicted in Fig. 12. It is seen in Fig. 12 that there is a significant difference in the airspeed profile between the approaches.

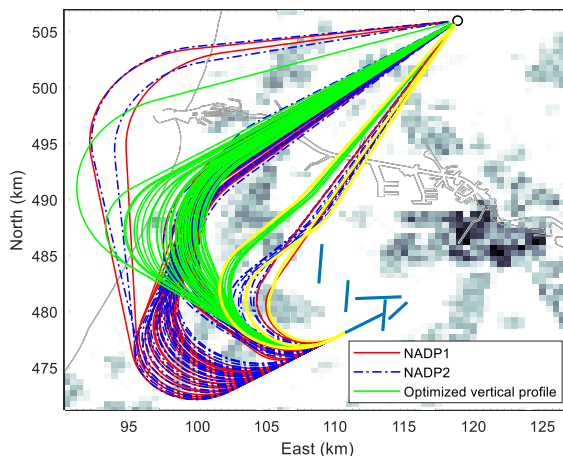


Fig. 11. Comparison of optimized ground tracks obtained by NADP1, NADP2 and optimized vertical profiles.

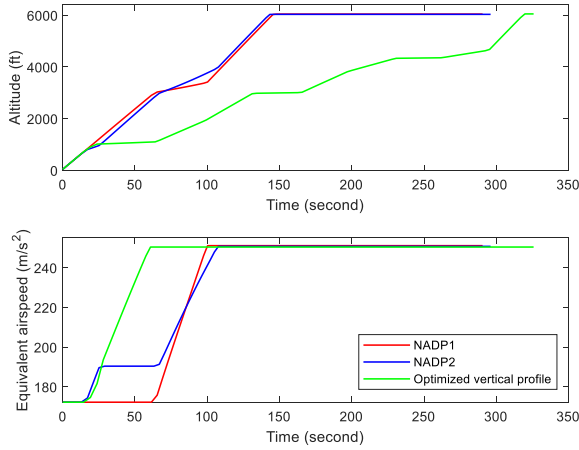


Fig. 12. Comparison of vertical profiles obtained by the representative solutions.

From noise and fuel perspectives, the optimized routes obtained by the 3D optimization approach are the best candidates and should be used in the set of alternative route options for the distribution problem in the second step. From a practical point of view, however, the implementation of the optimized vertical profiles may prove significantly more difficult. In contrast, NADP1 and NADP2 are the current standard procedures that are widely used. Also, compared with NADP1, NADP2 is generally a better option; however, the difference is small. The differences between their vertical profiles, however, may prove useful in dealing with separation conflicts between aircraft. Therefore, to obtain a better understanding from both a theoretical and a practical perspective, two different scenarios in input data are defined for the optimization problem in the second step. In the first scenario, only the routes obtained by NADP1 and NADP2 are applied, while in the second scenario the routes obtained by all the three types of vertical profiles are used. An overview of ground tracks obtained for all the SIDs originating from RW24 and RW18L in both 2D and 3D optimization scenarios is given in Fig. 13.

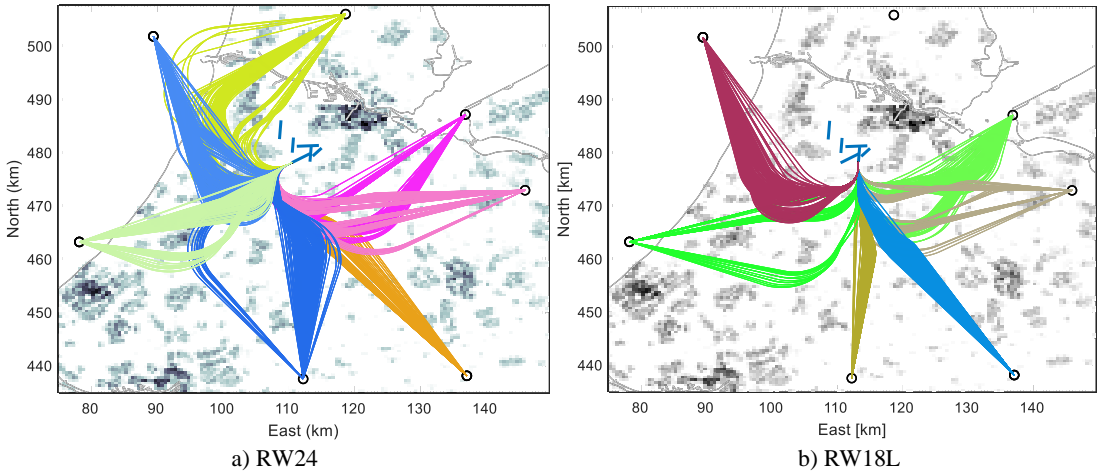


Fig. 13. Illustration of optimized routes for each SID obtained after Step 1.

### 5.2.2. Optimized solutions derived from the entire problem

6

As mentioned earlier, two different sets of input data are considered for the distribution problems in the second step. Therefore, two distinct optimization problems need to be solved in this section. These problems are again referred to as 2D and 3D optimization scenarios, respectively. To solve these problems, the NSGA-II algorithm with a population size of 70 and a maximum number of generations of 1500, as used in [Ho-Huu et al. \(2019a\)](#), is applied.

A closer look at the results obtained for both scenarios reveals that all the solutions obtained by the 3D optimization scenario have a unique route for each SID, while for the solutions obtained by the 2D optimization scenario, some SIDs require two routes to avoid potential conflicts. In addition, there is no delay at the runways for all solutions obtained by both approaches. [Fig. 14](#) shows the Pareto-optimized solutions obtained for the 2D and 3D optimization problems and compares them with the reference case solution, presented previously in [Section 5.1](#). As expected, the 3D optimization approach provides the best solutions (denoted as 3D solutions), that significantly outperform the solutions obtained by the 2D optimization approach (denoted as 2D solutions), as well as those obtained for the reference case, in terms of both the NPA and fuel consumption.

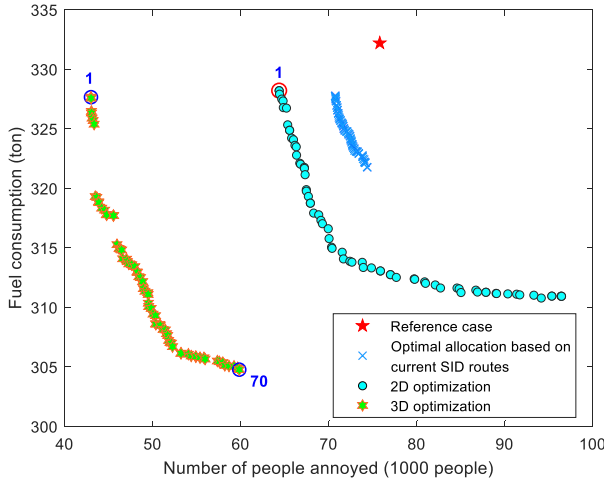


Fig. 14. Comparison of the optimized solutions obtained by the reference case, 2D and 3D optimization.

To further analyze the optimized results, three representative solutions, including solution 1 of the 2D optimization scenario and solutions 1 and 70 of the 3D optimization scenario, as highlighted in Fig. 14, are selected. Table 5 provides a comparison of specific criteria extracted for these solutions. From Table 5, it can be seen that all the compared metrics obtained by solution 1 (2D optimization) and solution 70 are better than those found for the reference case. Specifically, solution 1 offers, respectively, 15.08%, 1.20%, 0.96%, and 0.75% reduction in the NPA, fuel consumption, flight distance and flight time, while the corresponding reductions obtained for solution 70 are, respectively, 21.06%, 8.26%, 8.22% and 8.98%. In a comparison of solution 1 (3D optimization) with the reference case, solution 1 results in a significant decrease in the NPA of about 43.29%, while still saving 1.3% on fuel. Although there is an increase in the flight distance and elapsed time as a result of longer routes to avoid populated regions, the use of optimized vertical profiles results in a fuel burn that is still less than that of the reference case. Note that the purpose of selecting these representative solutions is to merely give insight into the solution behavior; it does not necessarily imply that the selected solutions should be recommended to authorities or policymakers. Essentially, the trade-off between criteria and the subsequent selection of the most desirable solution from the Pareto front is left to the authorities or policymakers.

Table 5. Comparison of the criteria of the representative solutions and the reference case.

Criteria	Solution 1 (2D optimization)	Solution 1 (3D optimization)	Solution 70 (3D optimization)	Reference case
Number of people annoyed	64,367	42,985	59,834	75,800
Fuel consumption (ton)	328.21	327.66	304.77	332.20
Flight distance (km)	25,240.57	27,357.49	23,388.53	25,484.13
Flight time (h)	56.71	59.80	52.01	57.14

The explanations provided for the comparisons in Table 5 are confirmed by the results shown in Figs. 15- 17, where the optimized routes, the  $L_{den}$  noise contours, and the NPA obtained by the three solutions are illustrated. A closer look at the optimized routes shows that although the optimized routes selected by these solutions are different, all of them seek to avoid high-density residential areas and tend to be close to each other. This results in narrower  $L_{den}$  contours and hence a reduced number of people affected by noise. Another observation is that the routes selected in solutions 1 (both 2D and 3D optimization) are longer than those selected by solution 70. This is according to expectations, as both solutions for 1 are noise-preferred solutions, and hence their routes tend to be longer to avoid populated regions. In contrast, solution 70 is a fuel-preferred solution and therefore prefers to choose shorter routes to reduce the fuel burn. Note that the red routes in Fig. 15 (solution 1 of 2D problem) are two alternative routes that are only used by some conflicting flights, whilst the remainder of the scheduled flights make use of one of the blue routes for each SID.

6

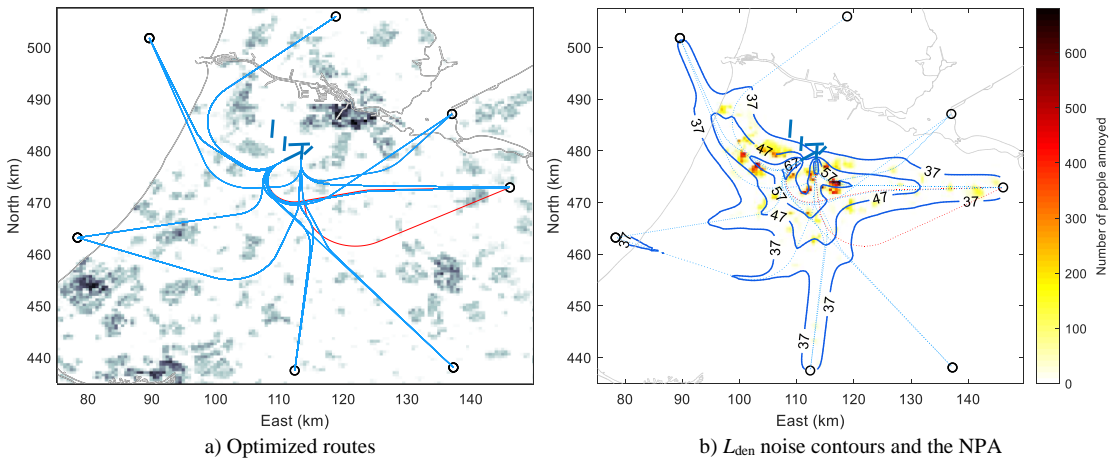


Fig. 15. Illustration of the optimized routes, the  $L_{den}$  noise contours, and the NPA (solution 1 – 2D optimization).

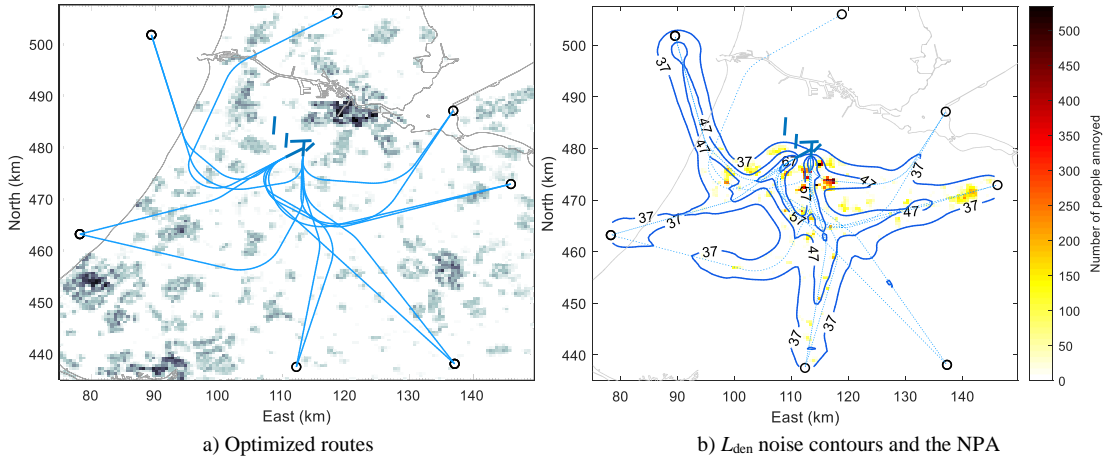


Fig. 16. Illustration of the optimized routes, the  $L_{den}$  noise contours, and the NPA (solution 1 – 3D optimization).

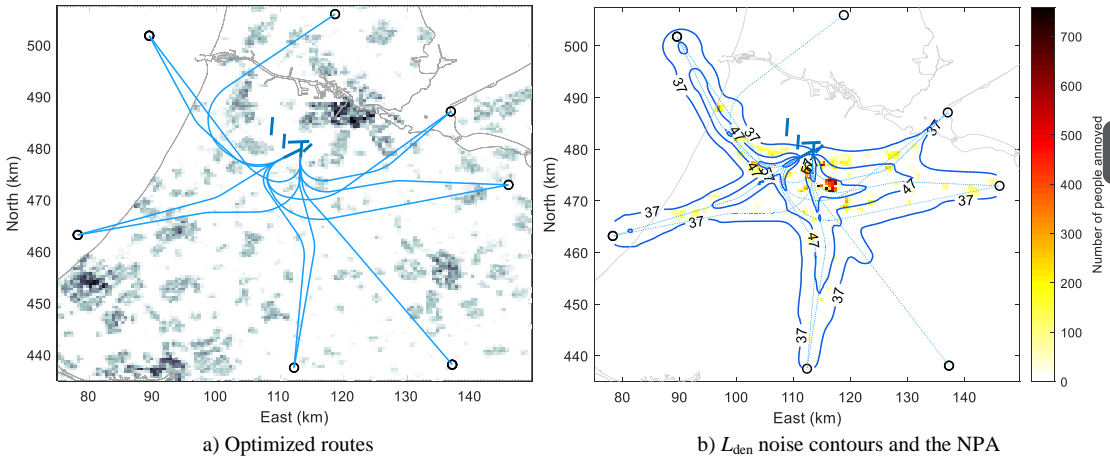


Fig. 17. Illustration of the optimized routes, the  $L_{den}$  noise contours, and the NPA (solution 70 – 3D optimization).

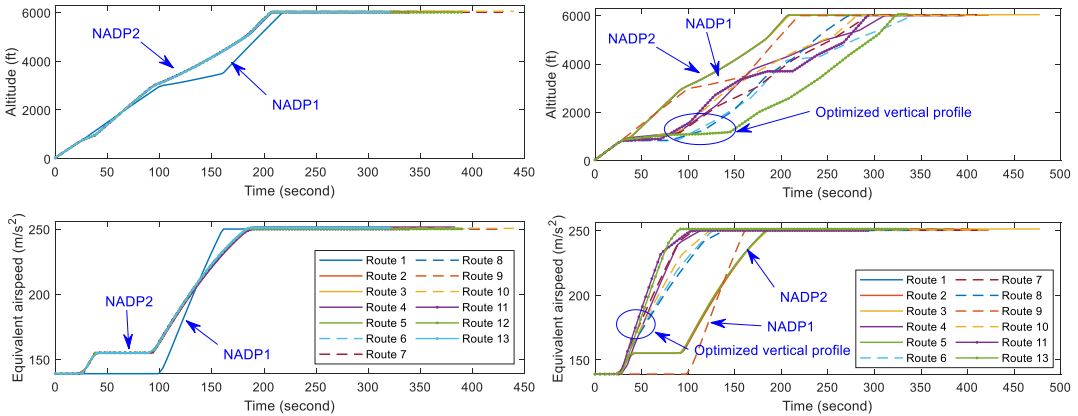
Table 6 provides the detailed distribution of flights among the optimized routes obtained in the selected solutions. It should be noted that as the selection of routes and the distribution of flights among these routes are optimized simultaneously, each solution will have its own optimal combination of selected routes and flight distribution. Therefore, it is difficult to make a direct comparison regarding the aircraft distribution between them, especially the comparison between 2D and 3D solutions. As a result, Table 6 merely aims to give insight into the optimized solution behavior, rather than serving as a basis for comparison.

Table 6. Distribution of flights to the optimized routes obtained by the 2D and 3D representative solutions.

Route number	Solution	Day			Evening			Night		
		F100	B738	B773	F100	B738	B773	F100	B738	B773
1	1 (2D)	6	0	0	0	0	0	0	0	0
	1 (3D)	4	11	0	0	4	1	0	2	0
	70 (3D)	12	11	2	1	4	3	5	2	0
2	1 (2D)	3	1	0	0	0	0	7	2	0
	1 (3D)	0	0	3	0	0	4	6	0	0
	70 (3D)	0	0	1	0	0	2	2	0	0
3	1 (2D)	23	13	3	6	6	5	0	0	0
	1 (3D)	28	3	0	6	2	0	1	0	0
	70 (3D)	20	3	0	5	2	0	0	0	0
4	1 (2D)	5	38	9	1	5	8	0	19	3
	1 (3D)	30	37	15	4	4	10	8	19	2
	70 (3D)	4	11	4	0	1	6	0	1	0
5	1 (2D)	52	31	19	8	5	4	8	0	0
	1 (3D)	27	32	13	5	6	2	0	0	1
	70 (3D)	53	58	24	9	9	6	8	18	3
6	1 (2D)	2	7	2	2	1	0	0	1	0
	1 (3D)	2	9	1	2	1	0	0	1	0
	70 (3D)	4	9	2	2	1	0	1	1	0
7	1 (2D)	2	2	0	0	0	0	1	0	0
	1 (3D)	2	0	1	0	0	0	1	0	0
	70 (3D)	0	0	0	0	0	0	0	0	0
8	1 (2D)	25	16	3	2	5	0	2	0	0
	1 (3D)	28	44	3	2	7	0	2	22	0
	70 (3D)	28	44	3	2	7	0	2	22	0
9	1 (2D)	5	30	0	1	3	0	0	22	0
	1 (3D)	2	2	0	1	1	0	0	0	0
	70 (3D)	2	2	0	1	1	0	0	0	0
10	1 (2D)	12	19	4	0	2	1	5	3	1
	1 (3D)	9	17	1	0	2	1	5	3	1
	70 (3D)	3	9	0	0	0	0	1	1	0
11	1 (2D)	15	5	6	4	2	0	0	0	0
	1 (3D)	18	7	9	4	2	0	0	0	0
	70 (3D)	24	15	10	4	4	1	4	2	1
12	1 (2D)	0	7	0	0	2	0	1	1	0
	1 (3D)	0	2	0	0	1	0	0	0	0
	70 (3D)	0	3	0	0	0	0	0	0	0
13	1 (2D)	27	11	35	4	5	0	2	0	1
	1 (3D)	27	16	35	4	6	0	3	1	1
	70 (3D)	27	15	35	4	7	0	3	1	1

In order to make the comparison regarding the vertical profiles more transparent, the representative vertical profiles of a Fokker 100 obtained for solutions 1 (both 2D and 3D optimization) are depicted in Fig. 18. As expected, despite not having the best performance in terms of either noise or fuel burn, NADP1 is still selected in both the 2D and 3D solutions, merely because it helps avoid conflicts. However, due to its poor performance, it is rarely used. More specifically, for both the 2D and 3D solutions, only 1 route selects NADP1 as the optimal option, while the remainder chooses either NADP2 or the optimized vertical profiles. The selection of NADP1 has shown that the separation requirement is an important and challenging issue that will be very difficult to solve if only one type of vertical profiles is available for all aircraft movements, especially for operations at peak hours. This issue again can be

seen in the 3D solution. In this solution, even though the optimized vertical profile offers the best performance in both criteria, only 7 routes use it as the optimal option, while there are still 4 routes using NADP2 and 1 route using NADP1. Thanks to the combination of all three different vertical profiles, the 3D optimized solutions are the only ones that offer conflict-free solutions by using only one route for each SID for the entire flight schedule.



a) Solution 1 (2D optimization)      b) Solution 1 (3D optimization)  
 Fig. 18. Comparison of the vertical profiles of Fokker 100 obtained by 2D and 3D optimization.

**6. Conclusions**

In this paper, we have presented a multilevel optimization framework for the design of optimal departure routes and the distribution of aircraft movements among these routes, while taking the sequence and separation constraints of aircraft into account. The proposed framework consists of two successive steps: 1) the design of optimal routes for each SID, and 2) the selection and distribution of flights among these routes. In order to deal with the sequence and separation requirements for aircraft, a runway assignment model, a conflict detection algorithm, and a rerouting technique have also been developed.

The performance and applicability of the proposed framework have been demonstrated through a case study at Amsterdam Airport Schiphol (AMS) in The Netherlands. In this case study, the departure operations for an entire day, featuring 599 flights and 13 distinct routes, have been considered. First, to validate the integration of the runway assignment model and the conflict detection algorithm into the allocation model in Step 2, a pure allocation problem based on the current SIDs has been executed. The

obtained results reveal that the distribution model is reliable and able to provide better options that help significantly reduce the noise impact and fuel consumption compared with the reference case. Subsequently, optimized solutions have been generated using the fully integrated framework. In order to provide a better view from both theoretical and practical perspectives, two different settings of input data for the distribution model in Step 2 have also been assessed. The numerical results have revealed that both problems can provide solutions that are much better in terms of both noise and fuel, relative to the reference case. Also, the 3D optimization approach significantly outperforms the 2D optimization approach.

In view of the attained favorable results, the framework appears to be suitable for expansion to other applications such as the design of arrival routes and the allocation of flights among these routes, and the problem that considers both departure and arrival operations concurrently. Moreover, instead of using the rerouting technique in the developed framework, at some occasions, Air Traffic Controllers could implement small delays on the ground or slow down or speed up one of the conflicting flights without changing the given SIDs to avoid conflict in the air. These considerations can also be integrated into the developed framework in future research. In addition, since the results obtained by the framework are Pareto solutions, it is a challenge for potential users to choose a suitable solution from a given Pareto front. Therefore, the development of selection methods and more in-depth analyses of the optimal results are necessary in future work.

## References

- Asensio, C., Gasco, L., de Arcas, G., 2017. A Review of Non-Acoustic Measures to Handle Community Response to Noise around Airports. *Curr. Pollut. Reports* 230–244. <https://doi.org/10.1007/s40726-017-0060-x>
- Boeing, 2016. Current Market Outlook 2016–2035.
- Braakenburg, M.L., Hartjes, S., Visser, H.G., 2011. Development of a Multi-Event Trajectory Optimization Tool for Noise-Optimized Approach Route Design. *AIAA J.* 1–13. <https://doi.org/10.2514/6.2011-6929>
- Casalino, D., D'iozzi, F., Sannino, R., Paonessa, A., 2008. Aircraft noise reduction technologies: A bibliographic review. *Aerosp. Sci. Technol.* 12, 1–17. <https://doi.org/10.1016/j.ast.2007.10.004>
- Centraal Bureau voor de Statistiek. Dataset bevolkingsdichtheid. <https://www.cbs.nl/nl-nl/dossier/nederland-regionaal/geografische-data>. Online, accessed 2016-10-20.
- Chatelain, P., Van Vyve, M., 2018. Modeling fair air traffic assignment in the vicinity of airports. *Transp. Res. Part D Transp. Environ.* 65, 213–228. <https://doi.org/10.1016/j.trd.2018.08.016>
- D'Ariano, A., Pacciarelli, D., Pistelli, M., Pranzo, M., 2015. Real-time scheduling of aircraft arrivals and departures in a terminal maneuvering area. *Networks*, 65(3) 212–227. <https://doi.org/10.1002/net.21599>
- Deb, K., Pratap, A., Agarwal, S., Meyarivan, T., 2002. A fast and elitist multiobjective genetic algorithm: NSGA-II. *IEEE Trans. Evol. Comput.* 6, 182–197. <https://doi.org/10.1109/4235.996017>
- J.G. Delsen., 2016. Flexible Arrival & Departure Runway Allocation Using Mixed-Integer Linear Programming:

- A Schiphol Airport Case Study, MSc. thesis, Delft University of Technology.
- Dons, J., 2012. Optimization of Departure and Arrival Routing for Amsterdam Airport Schiphol- A Noise Abatement Study. MSc. thesis, Delft University of Technology.
- ECAC, 2016. ECAC/CEAC Doc 29 4th Edition Report on Standard Method of Computing Noise Contours around Civil Airports Volume 1: Applications Guide 1.
- EUROCONTROL, 2014b. User Manual for the Base of Aircraft Data (BADA) Rev. 3.12, EEC Technical/Scientific Report No. 12/11/22-58.
- EUROCONTROL, 2018. RECAT-EU - European Wake Turbulence Categorisation and Separation Minima on Approach and Departure. Brussels. [http://www.recat-project.eu/sites/default/files/20180214\\_recat-eu\\_presentation\\_brochure\\_v1.2.pdf](http://www.recat-project.eu/sites/default/files/20180214_recat-eu_presentation_brochure_v1.2.pdf)
- European Environment Agency (EEA), 2010. Good practice guide on noise exposure and potential health effects, n.d. , in: EEA Technical Report.
- Filippone, A., 2014. Aircraft noise prediction. *Prog. Aerosp. Sci.* 68, 27–63. <https://doi.org/10.1016/j.paerosci.2014.02.001>
- Frair, L., 1984. Airport noise modelling and aircraft scheduling so as to minimize community annoyance. *Appl. Math. Model.* 8, 271–281. [https://doi.org/10.1016/0307-904X\(84\)90162-8](https://doi.org/10.1016/0307-904X(84)90162-8)
- Ganić, E., Babić, O., Čangalović, M., Stanojević, M., 2018. Air traffic assignment to reduce population noise exposure using activity-based approach. *Transp. Res. Part D Transp. Environ.* 63, 58–71. <https://doi.org/10.1016/j.trd.2018.04.012>
- Gardi, A., Sabatini, R., Ramasamy, S., 2015. Multi-objective optimisation of aircraft flight trajectories in the ATM and avionics context. *Prog. Aerosp. Sci.* 83, 1–36. <https://doi.org/10.1016/j.paerosci.2015.11.006>
- Hartjes, S., Dons, J., Visser, H.G., 2014. Optimization of Area Navigation Arrival Routes for Cumulative Noise Exposure. *J. Aircr.* 51, 1432–1438. <https://doi.org/10.2514/1.C032302>
- Hartjes, S., Visser, H., 2016. Efficient trajectory parameterization for environmental optimization of departure flight paths using a genetic algorithm. *Proc. Inst. Mech. Eng. Part G J. Aerosp. Eng.* 0, 1–9. <https://doi.org/10.1177/0954410016648980>
- Hartjes, S., Visser, H.G., Hebly, S.J., 2010. Optimisation of RNAV noise and emission abatement standard instrument departures. *Aeronaut. J.* 114, 757–767. <https://doi.org/10.1017/CBO9781107415324.004>
- Ho-Huu, V., Ganić, E., Hartjes, S., Babić, O., Curran, R., 2019a. Air traff assignment based on daily population mobility to reduce aircraft noise effects and fuel consumption. *Transp. Res. Part D Transp. Environ.* 72, 127–147. <https://doi.org/10.1016/j.trd.2019.04.007>
- Ho-Huu, V., Hartjes, S., Visser, H., Curran, R., 2017. An Efficient Application of the MOEA/D Algorithm for Designing Noise Abatement Departure Trajectories. *Aerospace* 4, 54. <https://doi.org/10.3390/aerospace4040054>
- Ho-Huu, V., Hartjes, S., Visser, H.G., Curran, R., 2019b. An optimization framework for the design and allocation of aircraft to multiple departure routes. *Transp. Res. Part D Transp. Environ.* 76, 273–288. <https://doi.org/10.1016/j.trd.2019.10.003>
- Ho-Huu, V., Hartjes, S., Visser, H.G., Curran, R., 2018. Integrated design and allocation of optimal aircraft departure routes. *Transp. Res. Part D Transp. Environ.* 63, 689–705. <https://doi.org/10.1016/j.trd.2018.07.006>
- Hogenhuis, R.H., Hebly, S.J., Visser, H.G., 2011. Optimization of area navigation noise abatement approach trajectories. *Proc. Inst. Mech. Eng. Part G-Journal Aerosp. Eng.* 225, 513–521. <https://doi.org/10.1177/09544100JAERO840>
- International Civil Aviation Organization (ICAO), 2006a. Procedures for air navigation services – Aircraft operations. Vol. I, Flight Procedures.
- International Civil Aviation Organization (ICAO), 2016b. Doc 4444 – Procedures for air navigation services – Air traffic management. Sixteenth Edition. Montreal, QC, Canada.
- Isaacson, D.R., Erzberger, H., 1997. Design of a conflict detection algorithm for the Center/TRACON automation system, in: 16th DASC. AIAA/IEEE Digital Avionics Systems Conference. Reflections to the Future. Proceedings. pp. 9.3–1. <https://doi.org/10.1109/DASC.1997.637306>
- Janssen, S.A., Centen, M.R., Vos, H., Van Kamp, I., 2014. The effect of the number of aircraft noise events on sleep quality. *Appl. Acoust.* 84, 9–16. <https://doi.org/10.1016/j.apacoust.2014.04.002>
- Kuiper, B.R., Visser, H.G., Hebli, S., 2012. Efficient use of an allotted airport annual noise budget through minimax optimization of runway allocations. *Proc. Inst. Mech. Eng. Part G J. Aerosp. Eng.* 227, 1021–1035. <https://doi.org/10.1177/0954410012447767>
- Morrell, S., Taylor, R., Lyle, D., 1997. A review of health effects of aircraft noise. *Aust. N. Z. J. Public Health* 21, 221–236. <https://doi.org/10.1111/j.1467-842X.1997.tb01690.x>
- Prats, X., Puig, V., Quevedo, J., 2011. Equitable Aircraft Noise-Abatement Departure Procedures. *J. Guid. Control. Dyn.* 34, 192–203. <https://doi.org/10.2514/1.49530>
- Prats, X., Puig, V., Quevedo, J., Nejjar, F., 2010a. Lexicographic optimisation for optimal departure aircraft

- trajectories. *Aerosp. Sci. Technol.* 14, 26–37. <https://doi.org/10.1016/j.ast.2009.11.003>
- Prats, X., Puig, V., Quevedo, J., Nejari, F., 2010b. Multi-objective optimisation for aircraft departure trajectories minimising noise annoyance. *Transp. Res. Part C Emerg. Technol.* 18, 975–989. <https://doi.org/10.1016/j.trc.2010.03.001>
- Rodríguez-Díaz, A., Adenso-Díaz, B., González-Torre, P.L., 2017. A review of the impact of noise restrictions at airports. *Transp. Res. Part D Transp. Environ.* 50, 144–153. <https://doi.org/10.1016/j.trd.2016.10.025>
- Samà, M., D'Ariano, A., D'Ariano, P., Pacciarelli, D., 2017a. Scheduling models for optimal aircraft traffic control at busy airports: tardiness, priorities, equity and violations considerations. *Omega* 67(1), 81–98. <https://doi.org/10.1016/j.omega.2016.04.003>
- Samà, M., D'Ariano, A., Corman, F., Pacciarelli, D., 2017b. Metaheuristics for efficient aircraft scheduling and re-routing at busy terminal control areas. *Transp. Res. Part C* 80 (1), 485–511. <https://doi.org/10.1016/j.trc.2016.08.012>
- Samà, M., D'Ariano, A., Corman, F., Pacciarelli, D., 2018. Coordination of scheduling decisions in the management of airport airspace and taxiway operations, *Transp. Res. Proce.* 23, 246–262. <https://doi.org/10.1016/j.trpro.2017.05.015>
- Samà, M., D'Ariano, A., Palagachev, K., Gerdt, M., 2019. Integration methods for aircraft scheduling and trajectory optimization at a busy terminal manoeuvring area. *OR Spec.* 41, 641–681. <https://doi.org/10.1007/s00291-019-00560-1>
- Song, Z., Visser, H.G., Mingshan, H., Wei, C., 2014. Optimized Multi-Event Simultaneous Departure Routes for Major Hub Airport. *Int. J. Model. Optim.* 4, 482–488. <https://doi.org/10.7763/IJMO.2014.V4.421>
- Storn, R., Price, K., 1997. Differential Evolution – A Simple and Efficient Heuristic for global Optimization over Continuous Spaces. *J. Glob. Optim.* 11, 341–359. <https://doi.org/10.1023/A:1008202821328>
- Torres, R., Chaptal, J., Bès, C., Hiriart-Urruty, J.-B., 2011. Optimal, Environmentally Friendly Departure Procedures for Civil Aircraft. *J. Aircr.* 48, 11–23. <https://doi.org/10.2514/1.C031012>
- Visser, H.G., 2008. Environmentally optimized resolutions of in-trail separation conflicts for arrival flights. *J. Aircr.* 45, 1198–1205. <https://doi.org/10.2514/1.34090>
- Visser, H.G., Wijnen, R.A.A., 2003. Optimisation of noise abatement arrival trajectories. *Aeronaut. J.* 107, 607–615. <https://doi.org/10.1017/S0001924000013828>
- Visser, H.G., Wijnen, R.A.A., 2001. Optimization of Noise Abatement Departure Trajectories. *J. Aircr.* 38, 620–627. <https://doi.org/10.2514/2.2838>
- Yu, H., Van Kampen, E.-J., Mulder, J.A., 2016. An Optimization Paradigm for Arrival Trajectories using Trajectory Segmentation and State Parameterization. *AIAA Guid. Navig. Control Conf.* 1–17. <https://doi.org/10.2514/6.2016-1872>
- Zachary, D.S., Gervais, J., Leopold, U., 2010. Multi-impact optimization to reduce aviation noise and emissions. *Transp. Res. Part D Transp. Environ.* 15, 82–93. <https://doi.org/10.1016/j.trd.2009.09.005>
- Zachary, D.S., Gervais, J., Leopold, U., Schutz, G., Huck, V.S.T., Braun, C., 2011. Strategic Planning of Aircraft Movements with a Three-Cost Objective. *J. Aircr.* 48, 256–264. <https://doi.org/10.2514/1.C031090>
- Zaporozhets, O.I., Tokarev, V.I., 1998. Predicted flight procedures for minimum noise impact. *Appl. Acoust.* 55, 129–143. [http://dx.doi.org/10.1016/S0003-682X\(97\)00108-4](http://dx.doi.org/10.1016/S0003-682X(97)00108-4)
- Zhang, M., Filippone, A., Bojdo, N., 2018. Multi-objective optimisation of aircraft departure trajectories. *Aerosp. Sci. Technol.* 79, 37–47. <https://doi.org/10.1016/j.ast.2018.05.032>
- Zhang, Q., Li, H., 2007. MOEA/D: A Multiobjective Evolutionary Algorithm Based on Decomposition. *IEEE Trans. Evol. Comput.* 11, 712–731. <https://doi.org/10.1109/TEVC.2007.892759>

# 7

## CONCLUSIONS

### 7.1. REVIEW OF OBJECTIVES

Along the course of the thesis, five objectives have been introduced and addressed. In this section, these objectives and key conclusions obtained from the research are reviewed.

1. To select or develop (a) suitable and efficient optimization method(s) capable of addressing the specific problems of route design and flight allocation for multiple objectives.

In **Chapter 2**, a new version of the MOEA/D algorithm was developed, which is capable of effectively handling multi-objective optimization problems. The performance of the developed method was tested on well-known benchmark test functions and structural optimization problems. The obtained results indicated that the developed method outperforms other approaches both in terms of convergence rate and solution quality. The method was then tested on route design problems with noise impact and fuel consumption as objective criteria. The obtained results also revealed that the method is suitable for and applicable to such a problem.

2. To improve the performance of solving aircraft route design problems based on the application of the developed method.

In **Chapter 3**, the selected MOEA/D algorithm was applied to more complex route design problems. This has given valuable insights into the characteristics of the problem, which has allowed for a further improvement in terms of algorithm performance. Specifically, computational cost has gone down by more than a factor 10. The performance of the developed approach was also demonstrated for a more complicated problem, where both problems of route design and flight allocation are addressed simultaneously. This study also considered a new criterion that aims to fairly distribute noise events over communities. With the introduction of the new noise criterion, the obtained results did not

only create good options for routes with less noise impact and fuel consumption, but also offer a fair distribution of noise among communities.

3. To develop a flight allocation problem formulation that allows to address noise impact and fuel consumption concurrently.

In **Chapter 4**, a new air traffic assignment model was proposed, in which both aircraft noise impact and fuel consumption are optimized concurrently. The model has been demonstrated to be efficient and able to provide proper trade-off solutions between two potentially conflicting objectives. Compared with a comparable model in [23], the developed model does not only give reliable solutions but also offers a range of solutions that can be a good reference base for users to refer to before making decisions. In addition, due to the consideration of each operation as a design variable, the size of the optimization problem, as well as the computational cost have been significantly reduced. The capability of the method has also been demonstrated in a more complicated case study with the consideration of a daily commuting population. The study showed that aircraft noise not only affects people living close to the airport, but also people living farther away the airport as a result of commuting to places close to the airport for work, while the opposite site is also observed. Due to the changes in population distribution at each location during the day, the research also indicated that the optimal assignments obtained by using the static (census) data and mobility data are different.

4. To establish a suitable approach that is capable of solving the problems of aircraft route design and flight allocation in a linked manner.

In **Chapter 5**, a two-step optimization framework that is able to cope with the consideration of both types of problems in a linked manner was developed. The reliability of the framework has been validated through the analysis of the employed noise criterion and the solution of the integrated optimization problem in a single step. A case study at Amsterdam Airport Schiphol in The Netherlands, including 337 departure flights and 4 SIDs, has been used to evaluate the efficiency and capability of the proposed framework. The obtained simulation results showed that the proposed framework can provide solutions which can gain a reduction in the number of people annoyed of up to 31% and a reduction in fuel consumption of 7% relative to the reference case solution. The obtained results also indicated that, besides the difference in routes, the allocation of flights obtained by the proposed framework and the reference case is also significantly different. As a result, the combination of route design and flight allocation has a positive impact on the reduction of noise and fuel. Furthermore, a comparison between the one- and two-step approaches indicated that the two-step approach is more flexible to adapt to changes in the number of flights when the reallocation of flights is demanded or new routes and runways are considered.

5. To develop an optimization framework that can effectively address the former points simultaneously.

In **Chapter 6**, a completed multilevel optimization model that is able to deal with the link between route design and flight allocation while taking aircraft sequencing and

separation into account was proposed. The reliability and applicability of the proposed model have been demonstrated through a realistic case study at Amsterdam Airport Schiphol, in which 599 departure flights and 13 different SIDs are considered. The optimization results showed that the proposed model can offer conflict-free solutions which can lead to a reduction in the number of people annoyed of up to 21%, and a reduction in fuel consumption of 8% relative to the reference case solution. Furthermore, the research indicated that the resolving of the conflict between flights has been the most difficult part which is to make sure that all flights in the flight schedule going to the same terminal points are operated on the same indicated routes. This has been a reason that some solutions in the Pareto front obtained by the 2D optimization approach use two different routes instead of one route for a given SID route to handle the conflict between flights for different periods of time during the day. The comparison of the results obtained by the 2D and 3D optimization approaches showed that the consideration of different vertical profiles in route design problems has a positive impact on resolving the conflict between flights. Due to the diversity of vertical profiles, i.e., the differences in speed and altitude between aircraft types on different routes, the chance of obtaining suitable routes which are able to handle the conflict is greater. Consequently, all solutions in the Pareto front obtained by the 3D optimization approach use only one route for a given SID route.

The five objectives mentioned here together address the main objective presented in **Chapter 1**, which is to determine for each given SID route, which route is optimal, and how many movements of each aircraft type should be assigned to this route while taking into account operational constraints related to aircraft sequencing and separation requirements.

## 7.2. RESEARCH NOVELTY AND CONTRIBUTION

This thesis has contributed to the field of aircraft and airport operations through the development of an efficient tool that can improve the operations of aircraft at an airport to become more efficient in terms of noise impact and fuel consumption. The research methodology has been established to deal with the problems of route design and flight allocation in a linked manner effectively. The reliability and capability of the proposed approach has been validated through many case studies along the thesis. To the best of the authors' knowledge, there is no work properly coping with the link between these two problems.

The main novelty of the research lies in the development of a multilevel optimization framework to address the problems of route design and flight allocation in conjunction. In addition to providing good options of route and flight allocation with less noise and fuel, the proposed framework also guarantees that the obtained solutions comply with operational requirements related to the sequencing of and separation between aircraft on runways and along routes. Furthermore, along the way to the successful development of the framework, the thesis has addressed certain limitations that existed in each research category, i.e., optimization techniques, aircraft route design, and flight allocation.

Firstly, a new version of the MOEA/D algorithm is developed. The developed method does not only provide fast solutions, but also offers a range of well-distributed Pareto solutions for multi-objective optimization problems featuring complex Pareto fronts. Sec-

only, an efficient optimization procedure that can significantly reduce the computational cost of solving aircraft route design problems is proposed. The proposed procedure can reduce up to two thirds the computational cost compared with traditional approaches. Thirdly, a new model for aircraft assignment problems is developed. With the simultaneous optimization of two potentially conflicting objectives, i.e., noise impact and fuel consumption, the proposed model is able to provide trade-off solutions between these objectives. Furthermore, the size and the complexity of the optimization problem are significantly reduced as a result of considering each aircraft operation as a single decision variable.

Lastly, a generic optimization framework is developed, which can support the operations of aircraft at an airport more efficiently in terms of noise impact and fuel burn. The model is able to consider the route design and flight allocation problems in a linked manner while taking aircraft sequencing and separation requirements into account. The model has been demonstrated to be sufficiently efficient and able to offer conflict-free and trade-off solutions between potentially conflicting objectives, which can reduce in the number of people annoyed up to 21%, and 8% in fuel consumption relative to the reference case solution. The proposed framework may be a promising approach for noise management at airports not only in the short-term but also for a long-term outlook.

### 7.3. LIMITATIONS AND RECOMMENDATIONS FOR FUTURE RESEARCH

The research in the thesis has been carried out based on some assumptions. Therefore, there will be a need for further research. Firstly, the operations of aircraft at airports are assumed to take place in standard weather conditions. This assumption implies that the effects of wind, temperature and precipitation on aircraft and airport operations, aircraft performance and aircraft noise have not been taken into account. Although the model can theoretically account for these effects, their inclusion may affect the final results and the performance of the framework, especially in terms of computational cost. Therefore, research to include these effects into the proposed framework is recommended in future work.

Secondly, the developed framework relies upon a specific noise criterion, i.e., noise annoyance, and hence optimality can only be guaranteed for this criterion. Therefore, the performance evaluation of the obtained solutions on other criteria and metrics should be considered. Moreover, due to the nature of the employed criterion, the link between two different problems (i.e., route design and flight allocation) at two steps of the framework is guaranteed. Although the employed noise criterion is one of the common criteria currently in use for the assessment of cumulative noise impact, there may be new criteria and metrics that can be considered to apply in the near future. To make the proposed framework still applicable, the analysis and investigation of these criteria and metrics should be considered.

Thirdly, the model developed in the thesis is mainly applied in the context of departure operations. Although the model can theoretically be extended to arrival operations, the formulation of operational constraints will be different due to the distinct nature in operations between arrivals and departures. In addition, the separation be-

tween arrival and departure flows needs to be guaranteed. Furthermore, only main operational requirements related to aircraft sequencing and separation are taken into account, depending on airport and airline policies there will be other operational requirements which also need to be considered.

Regarding the computational cost, although the performance of the methods developed in the thesis has been improved significantly, the computational cost of solving the optimization problems is still high. This limits the developed framework to be used as an operational tool. The computational cost of the framework can be divided into two parts corresponding to two separate steps. However, the optimization problems in Step 1 can be executed early in advance, and the computational cost of solving the route design problem has also been considerably improved. Therefore, to enable the proposed framework to work as an operational tool, the improvements should focus on Step 2, where the optimization problem may need to be resolved for every change in daily flight schedules. For this improvement, the development and application of new optimization methods should also be considered.

Last but not least, the results obtained by the proposed framework are non-dominated solutions due to the application of the multi-objective optimization approach. It is, therefore, a challenge for potential users to choose a suitable option from those solutions. Consequently, the development of selection methods and more in-depth analyses of the obtained optimal results are necessary in future work. Furthermore, the development of a tool based on the framework would also be interesting for airport stakeholders.



## REFERENCES

- [1] S. A. Janssen, M. R. Centen, H. Vos, and I. van Kamp, *The effect of the number of aircraft noise events on sleep quality*, *Applied Acoustics* **84**, 9 (2014).
- [2] A. Rodríguez-Díaz, B. Adenso-Díaz, and P. L. González-Torre, *A review of the impact of noise restrictions at airports*, *Transportation Research Part D: Transport and Environment* **50**, 144 (2017).
- [3] K. B. Marais, T. G. Reynolds, P. Uday, D. Muller, J. Lovegren, J.-M. Dumont, and R. J. Hansman, *Evaluation of potential near-term operational changes to mitigate environmental impacts of aviation*, *Proceedings of the Institution of Mechanical Engineers, Part G: Journal of Aerospace Engineering* **227**, 1277 (2013).
- [4] *Air travel – greener by design mitigating the environmental impact of aviation: Opportunities and priorities*, *The Aeronautical Journal* **109**, 361–416 (2005).
- [5] H. Visser, *Generic and site-specific criteria in the optimization of noise abatement trajectories*, *Transportation Research Part D: Transport and Environment* **10**, 405 (2005).
- [6] M. Braakenburg, S. Hartjes, H. Visser, and S. Heblj, *Development of a multi-event trajectory optimization tool for noise-optimized approach route design*, in *11th AIAA Aviation Technology, Integration, and Operations (ATIO) Conference, including the AIAA Balloon Systems Conference and 19th AIAA Lighter-Than* (2011) p. 6929.
- [7] S. Hartjes, J. Dons, and H. Visser, *Optimization of area navigation arrival routes for cumulative noise exposure*, *Journal of Aircraft* **51**, 1432 (2014).
- [8] S. Hartjes and H. Visser, *Efficient trajectory parameterization for environmental optimization of departure flight paths using a genetic algorithm*, *Proceedings of the Institution of Mechanical Engineers, Part G: Journal of Aerospace Engineering* **231**, 1115 (2017).
- [9] R. Hogenhuis, S. Heblj, and H. Visser, *Optimization of area navigation noise abatement approach trajectories*, *Proceedings of the Institution of Mechanical Engineers, Part G: Journal of Aerospace Engineering* **225**, 513 (2011).
- [10] X. Prats, V. Puig, J. Quevedo, and F. Nejjari, *Multi-objective optimisation for aircraft departure trajectories minimising noise annoyance*, *Transportation Research Part C: Emerging Technologies* **18**, 975 (2010).
- [11] X. Prats, V. Puig, J. Quevedo, and F. Nejjari, *Lexicographic optimisation for optimal departure aircraft trajectories*, *Aerospace science and technology* **14**, 26 (2010).

- [12] X. Prats, V. Puig, and J. Quevedo, *Equitable aircraft noise-abatement departure procedures*, Journal of guidance, control, and dynamics **34**, 192 (2011).
- [13] R. Torres, J. Chaptal, C. Bès, and J.-B. Hiriart-Urruty, *Optimal, environmentally friendly departure procedures for civil aircraft*, Journal of Aircraft **48**, 11 (2011).
- [14] Z. Song, H. Visser, H. Mingshan, and C. Wei, *Optimized multi-event simultaneous departure routes for major hub airport*, International Journal of Modeling and Optimization **4**, 482 (2014).
- [15] H. G. Visser and R. A. Wijnen, *Optimization of noise abatement departure trajectories*, Journal of Aircraft **38**, 620 (2001).
- [16] H. G. Visser and R. A. Wijnen, *Optimisation of noise abatement arrival trajectories*, The aeronautical journal **107**, 607 (2003).
- [17] H. Yu, E.-J. Van Kampen, and J. A. Mulder, *An optimization paradigm for arrival trajectories using trajectory segmentation and state parameterization*, in *AIAA Guidance, Navigation, and Control Conference* (2016) p. 1872.
- [18] M. Zhang, A. Filippone, and N. Bojdo, *Multi-objective optimisation of aircraft departure trajectories*, Aerospace Science and Technology **79**, 37 (2018).
- [19] L. Frair, *Airport noise modelling and aircraft scheduling so as to minimize community annoyance*, Applied Mathematical Modelling **8**, 271 (1984).
- [20] D. S. Zachary, J. Gervais, and U. Leopold, *Multi-impact optimization to reduce aviation noise and emissions*, Transportation Research Part D: Transport and Environment **15**, 82 (2010).
- [21] D. S. Zachary, J. Gervais, U. Leopold, G. Schutz, V. S. T. Huck, and C. Braun, *Strategic planning of aircraft movements with a three-cost objective*, Journal of Aircraft **48**, 256 (2011).
- [22] B. R. Kuiper, H. G. Visser, and S. Heblj, *Efficient use of an allotted airport annual noise budget through minimax optimization of runway allocations*, Proceedings of the Institution of Mechanical Engineers, Part G: Journal of Aerospace Engineering **227**, 1021 (2013).
- [23] E. Ganić, O. Babić, M. Čangalović, and M. Stanojević, *Air traffic assignment to reduce population noise exposure using activity-based approach*, Transportation Research Part D: Transport and Environment **63**, 58 (2018).
- [24] P. Chatelain and M. Van Vyve, *Modeling fair air traffic assignment in the vicinity of airports*, Transportation research part D: transport and environment **65**, 213 (2018).
- [25] S. Hartjes, H. Visser, and S. Hebly, *Optimisation of rnav noise and emission abatement standard instrument departures*, The Aeronautical Journal **114**, 757 (2010).
- [26] S. Khardi and L. Abdallah, *Optimization approaches of aircraft flight path reducing noise: comparison of modeling methods*, Applied acoustics **73**, 291 (2012).

- [27] S. Matthes, V. Grewe, K. Dahlmann, C. Frömming, E. Irvine, L. Lim, F. Linke, B. Lühns, B. Owen, K. Shine, *et al.*, *A concept for multi-criteria environmental assessment of aircraft trajectories*, *Aerospace* **4**, 42 (2017).
- [28] J. Kim, D. Lim, D. J. Monteiro, M. Kirby, and D. Mavris, *Multi-objective optimization of departure procedures at gimpo international airport*, *International Journal of Aeronautical and Space Sciences* **19**, 534 (2018).
- [29] Q. McEntegart and J. F. Whidborne, *Multiobjective environmental departure procedure optimization*, *Journal of Aircraft* **55**, 905 (2018).
- [30] B. Kim, L. Li, and J.-P. Clarke, *Runway assignments that minimize terminal airspace and airport surface emissions*, *Journal of Guidance, Control, and Dynamics* **37**, 789 (2014).
- [31] S. J. Heblj, *An integrated approach to optimised airport environmental management*, (2017).
- [32] Q. Zhang and H. Li, *Moea/d: A multiobjective evolutionary algorithm based on decomposition*, *IEEE Transactions on evolutionary computation* **11**, 712 (2007).
- [33] A. Trivedi, D. Srinivasan, K. Sanyal, and A. Ghosh, *A survey of multiobjective evolutionary algorithms based on decomposition*, *IEEE Transactions on Evolutionary Computation* **21**, 440 (2016).
- [34] H. Li and Q. Zhang, *Multiobjective optimization problems with complicated pareto sets, moea/d and nsga-ii*, *IEEE transactions on evolutionary computation* **13**, 284 (2008).
- [35] V. Ho-Huu, S. Hartjes, H. G. Visser, and R. Curran, *An improved moea/d algorithm for bi-objective optimization problems with complex pareto fronts and its application to structural optimization*, *Expert Systems with Applications* **92**, 430 (2018).
- [36] V. Ho-Huu, S. Hartjes, L. Geijselaers, H. Visser, and R. Curran, *Optimization of noise abatement aircraft terminal routes using a multi-objective evolutionary algorithm based on decomposition*, *Transportation Research Procedia* **29**, 157 (2018).
- [37] V. Ho-Huu, S. Hartjes, H. Visser, and R. Curran, *An efficient application of the moea/d algorithm for designing noise abatement departure trajectories*, *Aerospace* **4**, 54 (2017).
- [38] V. Ho-Huu, S. Hartjes, H. Visser, and R. Curran, *Integrated design and allocation of optimal aircraft departure routes*, *Transportation Research Part D: Transport and Environment* **63**, 689 (2018).
- [39] E. Ganić, V. Ho Huu, O. Babić, and S. Hartjes, *Air traffic assignment to reduce population noise exposure and fuel consumption using multi-criteria optimisation*, in *The 26th international conference on Noise and Vibration, 6-7 December 2018, Nis, Serbia* (2018).

- [40] V. Ho-Huu, E. Ganić, S. Hartjes, O. Babić, and R. Curran, *Air traffic assignment based on daily population mobility to reduce aircraft noise effects and fuel consumption*, Transportation Research Part D: Transport and Environment **72**, 127 (2019).
- [41] V. Ho-Huu, S. Hartjes, H. Visser, and R. Curran, *An optimization framework for route design and allocation of aircraft to multiple departure routes*, Transportation Research Part D: Transport and Environment **76**, 273 (2019).
- [42] V. Ho-Huu, S. Hartjes, J. Perez-Castan, H. Visser, and R. Curran, *A multilevel optimization approach to route design and flight allocation taking aircraft sequencing and separation constraints into account*, Transportation Research Part D: Transport and Environment, Under minor revision (2019).

# CURRICULUM VITÆ



**Vinh Ho-Huu\*** was born on 16 May 1990 in Binh Dinh, Vietnam. He received his B.E. degree in Engineering Mechanics from Ho Chi Minh City University of Technology and Education in 2012. After his B.E. graduation, he worked as a research assistant at the Division of Computational Mathematics and Engineering (CME), the Institute for Computational Science (INCOS), Ton Duc Thang University. During this period, he also participated a M.Sc. program in Computational Science at Ho Chi Minh City University of Technology and graduated after two years.

In August 2016, he got an offer to work as a PhD researcher at the group of Air Transport and Operations (ATO), Faculty of Aerospace Engineering, Delft University of Technology, Delft, The Netherlands. His PhD research was to develop a multilevel optimization framework for aircraft operations on near-airport communities to minimize noise impact and fuel consumption. His research interests include aircraft and airport operations, structural analysis and optimization, reliability-based design optimization, numerical methods (i.e., finite element method (FEM), smooth finite element method (SFEM), isogeometric analysis (IGA)), optimization algorithms, and intelligent computation (i.e., data mining, artificial neural network, machine learning).

---

\*Google scholar: [https://scholar.google.com.vn/citations?user=AxKDs\\_oAAAAJ&hl=nl&oi=ao](https://scholar.google.com.vn/citations?user=AxKDs_oAAAAJ&hl=nl&oi=ao)



# LIST OF PUBLICATIONS

## PUBLICATIONS RELATED TO THE THESIS

### Peer-reviewed journals

6. **V. Ho-Huu**, S. Hartjes, J. A. Pérez-Castán, H. G. Visser, and R. Curran, *A multilevel optimization approach to route design and flight allocation taking aircraft sequencing and separation into account*, Transportation Research Part C: Emerging Technologies, Under minor revision, 2019.
5. **V. Ho-Huu**, S. Hartjes, H. G. Visser, and R. Curran, *An optimization framework for route design and allocation of aircraft to multiple departure routes*, Transportation Research Part D: Transport and Environment, vol. 76, pp. 273–288, 2019.
4. **V. Ho-Huu**, E. Ganić, S. Hartjes, O. Babić, and R. Curran, *Air traffic assignment based on daily population mobility to reduce aircraft noise effects and fuel consumption*, Transportation Research Part D: Transport and Environment, vol. 72, pp. 127–147, 2019.
3. **V. Ho-Huu**, S. Hartjes, H. G. Visser, and R. Curran, *Integrated design and allocation of optimal aircraft departure routes*, Transportation Research Part D: Transport and Environment, vol. 63, pp. 689–705, 2018.
2. **V. Ho-Huu**, S. Hartjes, H. G. Visser, and R. Curran, *An improved MOEA/D algorithm for bi-objective optimization problems with complex Pareto fronts and its application to structural optimization*, Expert Systems with Applications, vol. 92, pp. 430–446, 2018.
1. **V. Ho-Huu**, S. Hartjes, H. Visser, and R. Curran, *An Efficient Application of the MOEA/D Algorithm for Designing Noise Abatement Departure Trajectories*, Aerospace, vol. 4, no. 4, p. 54, 2017.

### International Conferences

3. **V. Ho-Huu**, S. Hartjes, H. G. Visser, R. Curran, *Simultaneous design of different aircraft departure routes taking community noise exposure events into account*, The 48th International Congress and Exhibition on Noise Control Engineering, 16-19 June 2019, Madrid, Spain.
2. E. Ganić, **V. Ho-Huu**, S. Hartjes, O. Babić, *Air traffic assignment to reduce population noise exposure and fuel consumption using multi-criteria optimization*, The 26th international conference on Noise and Vibration, 6-7 December 2018, Nis, Serbia.

1. **V. Ho-Huu**, S. Hartjes, L.H. Geijselaers, H. G. Visser, R. Curran, *Optimization of noise abatement aircraft terminal routes using a multi-objective evolutionary algorithm based on decomposition*, Transp. Res. Procedia, vol. 29, pp. 157–168, 2018. The aerospace Europe 6th CEAS conference, 16-20 October 2017, Bucharest, Romania.

## OTHER PUBLICATIONS IN PEER-REVIEWED ISI JOURNALS

34. T. Vo-Duy, D. Duong-Gia, **V. Ho-Huu**, and T. Nguyen-Thoi, *An Effective Couple Method for Reliability-Based Multi-Objective Optimization of Truss Structures with Static and Dynamic Constraints*, Int. J. Comput. Methods, p. 1950016, Apr. 2019.
33. **V. Ho-Huu**, D. Duong-Gia, T. Vo-Duy, T. Le-Duc, and T. Nguyen-Thoi, *An efficient combination of multi-objective evolutionary optimization and reliability analysis for reliability-based design optimization of truss structures*, Expert Syst. Appl., vol. 102, pp. 262–272, 2018.
32. **V. Ho-Huu**, T. Le-Duc, L. Le-Anh, T. Vo-Duy, and T. Nguyen-Thoi, *A global single-loop deterministic algorithm for reliability-based design optimization of truss structures with continuous and discrete design variables*, Eng. Optim., vol. 50, no. 12, pp. 2071-2090, 2018.
31. **V. Ho-Huu**, T. Vo-Duy, D. Duong-Gia, and T. Nguyen-Thoi, *An efficient procedure for lightweight optimal design of composite laminated beams*, Steel Compos. Struct., vol. 3, pp. 297–310, 2018.
30. L.-D. Thang, **V. Ho-Huu**, and N.-Q. Hung, *Multi-objective optimal design of magnetorheological brakes for motorcycling application considering thermal effect in working process*, Smart Mater. Struct., vol. 27, no. 7, p. 75060, 2018.
29. T. Vo-Duy, **V. Ho-Huu**, and T. Nguyen-Thoi, *Free vibration analysis of laminated FG-CNT reinforced composite beams using finite element method*, Front. Struct. Civ. Eng., 2018.
28. H. P. H. Anh, N. N. Son, C. Van Kien, and **V. Ho-Huu**, *Parameter identification using adaptive differential evolution algorithm applied to robust control of uncertain nonlinear systems*, Appl. Soft Comput., vol. 71, pp. 672–684, 2018.
27. M. Y. A. Jamalabadi, **V. Ho-Huu**, and T. K. Nguyen, *Optimal design of circular baffles on sloshing in a rectangular tank horizontally coupled by structure*, Water (Switzerland), vol. 10, no. 11, pp. 1–18, 2018.
26. S. D. Nguyen, **V. Ho-Huu**, T.-T. Nguyen, N. T. Truong, and T.-I. Seo, *Novel fuzzy sliding controller for MRD suspensions subjected to uncertainty and disturbance*, Eng. Appl. Artif. Intell., vol. 61, no. February, pp. 65–76, 2017.
25. C. Le-Quoc, L. A. Le, **V. Ho-Huu**, P. D. Huynh, and T. Nguyen-Thoi, *An Immersed Boundary Proper Generalized Decomposition (IB-PGD) for Fluid–Structure Interaction Problems*, Int. J. Comput. Methods, vol. 15, no. 06, p. 1850045, Nov. 2017.

24. T. Vo-Duy, D. Duong-Gia, **V. Ho-Huu**, H. C. Vu-Do, and T. Nguyen-Thoi, *Multi-objective optimization of laminated composite beam structures using NSGA-II algorithm*, Compos. Struct., vol. 168, p. , 2017.
23. T. Banh-Thien, H. Dang-Trung, L. Le-Anh, **V. Ho-Huu**, and T. Nguyen-Thoi, *Buckling analysis of non-uniform thickness nanoplates in an elastic medium using the isogeometric analysis*, Compos. Struct., vol. 162, pp. 182–193, 2017.
22. T. Vo-Duy, **V. Ho-Huu**, T. D. Do-Thi, H. Dang-Trung, and T. Nguyen-Thoi, *A global numerical approach for lightweight design optimization of laminated composite plates subjected to frequency constraints*, Compos. Struct., vol. 159, pp. 646–655, Jan. 2017.
21. L. A. Le, T. Bui-Vinh, **V. Ho-Huu**, and T. Nguyen-Thoi, *An efficient coupled numerical method for reliability-based design optimization of steel frames*, J. Constr. Steel Res., vol. 138, pp. 389–400, 2017.
20. T. Vo-Duy, T. Truong-Thi, **V. Ho-Huu**, and T. Nguyen-Thoi, *Frequency optimization of laminated functionally graded carbon nanotube reinforced composite quadrilateral plates using smoothed FEM and evolution algorithm*, J. Compos. Mater., p. 002199831773783, 2017.
19. D.-C. Du, **V. Ho-Huu**, V.-D. Trung, N.-T. Hong Quyen, and N.-T. Trung, *Efficiency of Jaya algorithm for solving the optimization-based structural damage identification problem based on a hybrid objective function*, Eng. Optim., vol. 0273, no. September, pp. 1–19, 2017.
18. S. N. Nguyen, **V. Ho-Huu**, and A. P. H. Ho, *A neural differential evolution identification approach to nonlinear systems and modelling of shape memory alloy actuator*, Asian J. Control, vol. 20, no. 1, pp. 1–14, 2017.
17. D. Dinh-Cong, T. Vo-Duy, N. Nguyen-Minh, **V. Ho-Huu**, and T. Nguyen-Thoi, *A two-stage assessment method using damage locating vector method and differential evolution algorithm for damage identification of cross-ply laminated composite beams*, Adv. Struct. Eng., 2017.
16. T. Vo-Van, T. Nguyen-Thoi, T. Vo-Duy, **V. Ho-Huu**, and T. Nguyen-Trang, *Modified genetic algorithm-based clustering for probability density functions*, J. Stat. Comput. Simul., vol. 9655, no. March, pp. 1–16, 2017.
15. D. Dinh-Cong, T. Vo-Duy, **V. Ho-Huu**, H. Dang-Trung, and T. Nguyen-Thoi, *An efficient multi-stage optimization approach for damage detection in plate structures*, Adv. Eng. Softw., vol. 112, 2017.
14. T. Vo-duy, **V. Ho-Huu**, H. Dang-trung, D. Dinh-cong, and T. Nguyen-Thoi, *Damage Detection in Laminated Composite Plates Using Modal Strain Energy and Improved Differential Evolution Algorithm*, Procedia Eng., vol. 142, pp. 182–189, 2016.

13. H. Ao, T. N. Thoi, **V. Ho-Huu**, L. Anh-le, and T. Nguyen, *Backtracking Search Optimization Algorithm and its Application to Roller Bearing Fault Diagnosis*, Int. J. Acoust. Vib., vol. 21, no. 4, p. 445-452, 2016.
12. T. Nguyen-Thoi, T. Rabczuk, **V. Ho-Huu**, L. Le-Anh, H. Dang-Trung, and T. Vo-Duy, *An Extended Cell-Based Smoothed Three-Node Mindlin Plate Element (XCS-MIN3) for Free Vibration Analysis of Cracked FGM Plates*, Int. J. Comput. Methods, p. 1750011, Jun. 2016.
11. **V. Ho-Huu**, T. Nguyen-Thoi, T. Truong-Khac, L. Le-Anh, and T. Vo-Duy, *An improved differential evolution based on roulette wheel selection for shape and size optimization of truss structures with frequency constraints*, Neural Comput. Appl., pp. 1–19, 2016.
10. **V. Ho-Huu**, T. Vo-Duy, T. Luu-Van, L. Le-Anh, and T. Nguyen-Thoi, *Optimal design of truss structures with frequency constraints using improved differential evolution algorithm based on an adaptive mutation scheme*, Autom. Constr., vol. 68, pp. 81–94, 2016.
9. **V. Ho-Huu**, T. Nguyen-Thoi, T. Vo-Duy, and T. Nguyen-Trang, *An adaptive elitist differential evolution for truss optimization with discrete variables*, Comput. Struct., vol. 165, pp. 59–75, 2016.
8. **V. Ho-Huu**, T. Nguyen-Thoi, L. Le-Anh, and T. Nguyen-Trang, *An effective reliability-based improved constrained differential evolution for reliability-based design optimization of truss structures*, Adv. Eng. Softw., vol. 92, pp. 48–56, 2016.
7. **V. Ho-Huu**, D. Do-Thi, H. Dang-Trung, T. Vo-Duy, and T. Nguyen-Thoi, *Optimization of laminated composite plates for maximizing buckling load using improved differential evolution and smoothed finite element method*, Compos. Struct., vol. 146, pp. 132–147, Jun. 2016.
6. T. Vo-Duy, **V. Ho-Huu**, H. Dang-Trung, and T. Nguyen-Thoi, *A two-step approach for damage detection in laminated composite structures using modal strain energy method and an improved differential evolution algorithm*, Compos. Struct., vol. 147, pp. 42–53, Jul. 2016.
5. M. H. Nguyen-Thoi, L. Le-Anh, **V. Ho-Huu**, H. Dang-Trung, and T. Nguyen-Thoi, *An extended cell-based smoothed discrete shear gap method (XCS-FEM-DSG3) for free vibration analysis of cracked Reissner-Mindlin shells*, Front. Struct. Civ. Eng., pp. 1–18, 2015.
4. **V. Ho-Huu**, T. Nguyen-Thoi, M. H. Nguyen-Thoi, and L. Le-Anh, *An improved constrained differential evolution using discrete variables (D-ICDE) for layout optimization of truss structures*, Expert Syst. Appl., vol. 42, no. 20, pp. 7057–7069, 2015.

3. L. Le-Anh, T. Nguyen-Thoi, **V. Ho-Huu**, H. Dang-Trung, and T. Bui-Xuan, *Static and frequency optimization of folded laminated composite plates using an adjusted Differential Evolution algorithm and a smoothed triangular plate element*, *Compos. Struct.*, vol. 127, pp. 382–394, 2015.
2. T. Nguyen-Thoi, P. Phung-Van, **V. Ho-Huu**, and L. Le-Anh, *An edge-based smoothed finite element method (ES-FEM) for dynamic analysis of 2D Fluid-Solid interaction problems*, *KSCE J. Civ. Eng.*, vol. 19, no. 3, pp. 641–650, 2015.
1. T. Nguyen-Thoi, T. Rabczuk, T. Lam-Phat, **V. Ho-Huu**, and P. Phung-Van, *Free vibration analysis of cracked Mindlin plate using an extended cell-based smoothed discrete shear gap method (XCS-DSG3)*, *Theor. Appl. Fract. Mech.*, vol. 72, pp. 150–163, 2014.